

General Disclaimer

One or more of the Following Statements may affect this Document

- This document has been reproduced from the best copy furnished by the organizational source. It is being released in the interest of making available as much information as possible.
- This document may contain data, which exceeds the sheet parameters. It was furnished in this condition by the organizational source and is the best copy available.
- This document may contain tone-on-tone or color graphs, charts and/or pictures, which have been reproduced in black and white.
- This document is paginated as submitted by the original source.
- Portions of this document are not fully legible due to the historical nature of some of the material. However, it is the best reproduction available from the original submission.

AD-760 311

OMEGA VLF TIMING. REVISION 1

E. R. Swanson, et al

Naval Electronics Laboratory Center
San Diego, California

29 June 1972

DISTRIBUTED BY:

NTIS

National Technical Information Service
U. S. DEPARTMENT OF COMMERCE
5285 Port Royal Road, Springfield Va. 22151

NASA S-51743A-G
-Revision 1
NELC TR 1740
-Revision 1

760311

OMEGA VLF TIMING

Revision 1

E. R. Swanson and C. P. Kugel

Research and Development

29 June 1972

(Original Issue 5 November 1970)

DDC
RECEIVED
MAY 23 1973
B

Reproduced by
NATIONAL TECHNICAL
INFORMATION SERVICE
U S Department of Commerce
Springfield VA 22151

DISTRIBUTION STATEMENT A

Approved for public release;
Distribution Unlimited

Prepared for

NASA

Goddard Space Flight Center
Greenbelt, Maryland
under Defense Purchase
Request Number S-51743A-G

NAVAL ELECTRONICS LABORATORY CENTER
SAN DIEGO, CALIFORNIA 92152

UNCLASSIFIED

Security Classification

DOCUMENT CONTROL DATA - R & D		
<i>(Security classification of title, body of abstract and indexing annotation must be entered when the overall report is classified)</i>		
1. ORIGINATING ACTIVITY (Corporate author) Naval Electronics Laboratory Center San Diego, California 92152		2a. REPORT SECURITY CLASSIFICATION UNCLASSIFIED 2b. GROUP
3. REPORT TITLE OMEGA VLF TIMING		
4. DESCRIPTIVE NOTES (Type of report and inclusive dates) Research and Development, May 1970 to June 1972		
5. AUTHOR(S) (First name, middle initial, last name) E. R. Swanson and C. P. Kugel		
6. REPORT DATE 29 June 1972	7a. TOTAL NO. OF PAGES 192	7b. NO. OF REFS 72
8a. CONTRACT OR GRANT NO. S-51743A-G	9a. ORIGINATOR'S REPORT NUMBER(S) TR 1740 (Revision 1)	
b. PROJECT NO. NELC A105	9b. OTHER REPORT NO(S) (Any other numbers that may be assigned this report)	
c.		
d.		
10. DISTRIBUTION STATEMENT Approved for public release; distribution unlimited.		
11. SUPPLEMENTARY NOTES	12. SPONSORING MILITARY ACTIVITY GSFC J. Lavery	
13. ABSTRACT <p>'Omega' is a vlf navigation system described here and in several other NELC reports. This report specifically discusses time dissemination techniques, including epoch determination, frequency determination, and ambiguity resolution. It also discusses operational considerations including equipment, path selection, and adjustment procedure.</p> <p>'Epoch' (the actual location or timing of periodic events) is shown to be both maintainable and calibratable by the techniques described to better than 3-microsecond accuracy; and 'frequency' (the uniformity of the time scale) to about one part in 10¹².</p>		

DD FORM 1 NOV 65 1473

(PAGE 1)

0102-014-6600

UNCLASSIFIED

Security Classification

I

14. KEY WORDS	LINK A		LINK B		LINK C	
	ROLE	WT	ROLE	WT	ROLE	WT
Navigation systems OMEGA Operations research Systems analysis						

II

1. Report No. NASA S-51743A-G		2. Government Accession No.		3. Recipient's Catalog No.	
4. Title and Subtitle OMEGA VLF TIMING				5. Report Date 29 June 1972	
				6. Performing Organization Code	
7. Author(s) E. R. Swanson and C. P. Kugel				8. Performing Organization Report No. 1740-Revision 1	
9. Performing Organization Name and Address Naval Electronics Laboratory Center San Diego, California 92152				10. Work Unit No.	
				11. Contract or Grant No. S-51743A-G	
12. Sponsoring Agency Name and Address GSFC J. Lavery				13. Type of Report and Period Covered R&D May 1970 to June 1972	
				14. Sponsoring Agency Code	
15. Supplementary Notes Original issue published 5 November 1970. Revision 1 differs primarily in addition of appendices D, E, and F.					
16. Abstract <p>'Omega' is a vlf navigation system described here and in several other NELC reports.</p> <p>This report specifically discusses time dissemination techniques, including epoch determination, frequency determination, and ambiguity resolution. It also discusses operational considerations including equipment, path selection, and adjustment procedure.</p> <p>'Epoch' (the actual location or timing of periodic events) is shown to be both maintainable and calibratable by the techniques described to better than 3-micro-second accuracy; and 'frequency' (the uniformity of the time scale) to about one part in 10^{12}.</p>					
17. Key Words (Selected by Author(s)) Navigation systems OMEGA Operations research Systems analysis				18. Distribution Statement Approved for public release; distribution unlimited	
19. Security Classif. (of this report) UNCLASSIFIED		20. Security Classif. (of this page) UNCLASSIFIED		21. No. of Pages 192	22. Price*

* For sale by the Clearinghouse for Federal Scientific and Technical Information, Springfield, Virginia 22151.

III

PREFACE TO REVISION 1

To maintain coherence, recent developments in vlf timing have been incorporated into an existing comprehensive report on Omega vlf timing and issued as this first revision. New material principally is included in additional appendices. Appendix D shows that present global prediction theory is sufficient to calibrate a timing site to about 1 microsecond without need for flying clock trips. Appendix E investigates in detail periodicities in Omega measurements, while appendix F applies results of appendix E to show that typical temporal stability on more stable paths at optimum times and in the absence of disturbances is less than 1 microsecond. These results are more accurate than indicated in the original issue, which emphasized nominal 24-hour stability and predictability.

Revision 1 is thus principally an extension rather than a true "revision" of the original issue. Page, figure, table, equation, and reference numbers have been preserved, where possible, to avoid ambiguity in referencing. However, it was found necessary to include a new figure 5 to emphasize the importance of modal interference to dual frequency timing using closely spaced frequencies. New references 28 and 40 were also added. *Therefore, figures numbered 5 through 8 in the original issue of this document are renumbered 6 through 9, respectively, in this revision; and previous references 28 through 38 are now references 29 through 39, respectively.* In addition, minor errata have been corrected and references to the new appendices inserted as appropriate. Little editorial change has been required to insert these references. For example, on p. 68, the original issue noted that "If . . . 20 paths were used for calibration, then the epoch might be refined to 1 μ sec," while this revision reads "Appendix D shows existing prediction errors to be such that measurements over several paths may be synthesized to calibrate epoch to 1 μ sec."

General preservation of literature references from the original issue insures that only material originally pertinent to its development is included. More recent bibliographies may be of interest, however, and can be found in the following:

Swanson, E.R., and Kugel, C.P., "VLF Timing: Conventional and Modern Techniques Including Omega," Proceedings of the IEEE, v. 60, no. 5, p. 540-551, May 1972

Swanson, E. R., "VLF Phase Prediction," VLF Propagation: Proceedings from the VLF Symposium, Sandefjord, Norway, 27-29 October 1971, G. Bjøntegaard, ed., p. 8-1 to 8-36 (Norwegian Institute of Cosmic Physics Report 7201, January 1972)

PROBLEM

Determine time dissemination capabilities of Omega to fixed sites of known location. Develop associated information processing techniques suitable for fixed site time determination.

RESULTS

1. A useful timing capability is presently available from the existing four Omega stations—prior to implementation of a complete global system in the early 1970's—although at reduced accuracy in remote areas.
2. Techniques are described which have been employed in synchronizing Omega for the past 6 years and may be recommended as practicable for immediate implementation.
3. By means of Omega transmissions and the techniques described, epoch at timing sites may be deduced and maintained to better than 3 microseconds and frequency can be maintained to about 1 part in 10^{12} .

RECOMMENDATION

Continue research in pulse timing, receiver installation design, propagation prediction, interpath cross correlation and signal autocorrelation, adjustment procedure optimization, and autocorrelation of the frequency variations of quality standards.

ADMINISTRATIVE INFORMATION

Work was done by the Propagation Technology Division for NASA under Defense Purchase Request Number S-51743A-G and NELC A105 from May 1970 to June 1972. The original issue of this report was approved for publication 5 November 1970; this revision is the final report and was approved 29 June 1972.

CONTENTS

INTRODUCTION . . .	Page 5
Discussion of Time . . .	5
Omega Format Discussion . . .	6
Interrelation of Navigation and Timing . . .	8
SIMPLIFIED TIME DETERMINATION TECHNIQUES . . .	9
Epoch Determination . . .	9
Frequency Determination . . .	17
Ambiguity Resolution . . .	21
ACCURACY OF TIME DETERMINATION TECHNIQUES . . .	26
Pulse Techniques . . .	26
Phase Techniques . . .	29
Frequency Estimation Techniques . . .	47
Ambiguity Resolution Probabilities . . .	52
PROBLEM ANALYSIS . . .	54
OPERATIONAL CONSIDERATIONS. . .	59
Equipment . . .	59
Path Selection . . .	64
Additional Refinements . . .	68
Adjustment Procedures . . .	74
SUMMARY OF PROCEDURES . . .	78
CONCLUSIONS AND RECOMMENDATIONS . . .	79
REFERENCES . . .	80
APPENDIX A: RADIO TIMING . . .	83
APPENDIX B: OMEGA . . .	99
APPENDIX C: ADJUSTMENT PROCEDURE . . .	125
APPENDIX D: PATH CALIBRATION . . .	144
APPENDIX E: PERIODIC VARIATIONS . . .	157
APPENDIX F: EFFECTS OF TEMPORAL VARIATIONS AND DISTURBANCES ON PRECISE TIMING . . .	182

ILLUSTRATIONS

- 1 Suggested circuit for pulse epoch determination . . . *page 10*
- 2 Haiku leading edge as received at NELC . . . 26
- 3 Frequency offset of cesium 112 from Naval Observatory master clock . . . 50
- 4 Omega transmissions from Hawaii to Santiago, Chile . . . 67
- 5 Relative phase of daytime Omega difference frequency, North Dakota to Goddard . . . 67
- 6 Effect of X-ray absorption on a long-path phase track . . . 71
- 7 Recovery of Haiku-Norway path from PCA of 2 September 1966 . . . 72
- 8 Schematic diagram of clock . . . 74
- 9 Control procedure analysis results . . . 78

TABLES

- 1 Results of lead-edge experiments . . . *page 28*
- 2 Summary of phase measurements 1-8 . . . 46
- 3 Accuracy of frequency estimated from repeated Omega epoch measurements . . . 48
- 4 Frequency estimation over selected periods . . . 49
- 5 Interrelationship between oscillator stability and reset interval . . . 57

SAMPLE PROCEDURES

- 1 Pulse epoch determination . . . *page 10, 11*
- 2 Phase epoch determination . . . 14, 15
- 3 Frequency determination . . . 18, 19
- 4 Three-frequency ambiguity resolution . . . 22, 23
- 5 Two-frequency ambiguity resolution . . . 24, 25

MEASUREMENT LISTINGS

- 1 Rome, N. Y., June 1969 . . . *page 30*
- 2 Wales, Alaska, August 1969 . . . 32
- 3 Wales, Alaska, May 1969 . . . 34
- 4 Wales, Alaska, October 1969 . . . 36
- 5 San Diego, California, December 1969 . . . 38
- 6 Pyramid Rock, Hawaii, May 1969 . . . 40
- 7 Rome, N. Y., October 1969 . . . 42
- 8 Wales, Alaska, October 1969 . . . 44

INTRODUCTION

DISCUSSION OF TIME

Time is one of the most tenuous concepts employed by man for precise measurements. One unique feature distinguishing time from other units is the conceptual impossibility of building and maintaining a self-sufficient permanent standard. Hence, while most standards can be manufactured and stored without subsequent intercomparisons of the quantities represented, clocks must be periodically intercompared to maintain precise time. Maintenance of precise time is as much a problem of techniques for time dissemination¹ and adjustment as it is a problem of construction of clocks.

Time: frequency and epoch

The concept of time includes two major subdivisions—frequency and epoch. *Frequency* refers to the uniformity or periodicity of the time scale; *epoch* refers to the actual location or timing of periodic events. The concepts are developed more clearly in appendix A, where epoch is shown to be equivalent to the phase of a periodic function while frequency is the derivative of phase measured in cycles. Frequency or frequency stability always can be determined by periodic phase measurements or knowledge of phase stability and relevant autocorrelation processes for the medium. Appropriate relations are derived in appendix A.²

Epoch ambiguity resolution

Good time scales are based on regularly repeatable phenomena which are as periodic as practicable. However, *periodic* implies that each cycle of the event is indistinguishable from every other cycle. Hence, the epoch deduced from any periodic process is necessarily ambiguous by some unknown multiple of the period of the process. Any time determination thus also implies some method for *epoch ambiguity resolution*. As timing becomes more precise, ambiguity resolution problems may become more severe, particularly if the clocks are separated. For example, the period of a 10-kHz vlf carrier transmission is 100 μ sec. Hence, any time determination restricted to such a transmission would have an ambiguity of 100 n μ sec where n is any integer. This ambiguity must be resolved by some other technique, such as comparison with a second periodic process of longer period—say, 300 μ sec—but which will differ in epoch from the original 10-kHz determination by less than 50 μ sec. The ambiguity is thus resolved to an uncertainty of some integral multiple of the longer period; e.g., 300 m μ sec. The process may be repeated as often as necessary to resolve the coarsest time scale required; e.g., hours, days, or years. It is noteworthy that ambiguity resolution need not be performed with every epoch determination. Normally, some method is provided by which a count of the fine periods may be maintained, thus obviating the need for ambiguity resolution. However, even if epoch is resolved properly initially, there is some inherent

¹ See *REFERENCES*, p. 80.

probability that improper counting will occur and hence a need for a method of ambiguity resolution. Further, there is an inherent probability of error in resolving epoch ambiguity and hence a need for careful, if occasional, attention to coarse epoch. Appendix A discusses epoch ambiguity resolution more thoroughly and stresses that ambiguity resolution errors are failures in the sense that a gross error will occur. That is, the accuracy of the system or technique is unaffected by ambiguity errors although the reliability may be critically dependent on ambiguity resolution.

Dissemination of precise time thus implies a periodic process or processes and associated ability for measurement. One such process is the phase of the electric vector of a cw radio signal. If the transmissions are properly controlled and if frequencies and propagation paths are suitably chosen, properly interpreted phase measurements may be used for precise timing. Although carrier phase measurements will be ambiguous by some integral multiple of the carrier period, the associated uncertainties may be resolved by other methods³ or by additional transmissions at different frequencies.⁴

OMEGA FORMAT DISCUSSION

**Omega: VLF navigation;
global coverage early 1970's**

**All stations equivalent sources
of precise time**

Omega is a vlf navigation system scheduled for global implementation in the early 1970's. The worldwide network will employ eight fixed ground stations to provide continuous redundant coverage anywhere in the world. Each station will develop the radiated epoch from a bank of four cesium frequency standards so that each station may be considered an equivalent source of precise time. Since hyperbolic navigation requires signals from a minimum of three stations, more information will be available than required for time dissemination to a known fixed location. Indeed, the four stations now operating provide global coverage for time dissemination although not for navigation.

The basic navigational frequency of Omega is 10.2 kHz. Transmissions of approximately 1-second duration are time-shared by each station within a 10-second commutation pattern. Navigation receivers are equipped with a commutator which, when properly set initially, can separate the transmissions from the various stations. Phase tracking of the 10.2-kHz transmission from each selected station is performed within the receiver. Typically, hyperbolic navigation is employed so that the phase tracks are paired and differenced in various ways to read out fractional cycle difference. Lane counters accumulate integral cycle crossings, or, alternatively, cycle count can be maintained by annotation on continuously operating strip-chart recorders. After the application of propagation corrections, two or more hyperbolic lines of position are plotted on specially prepared navigation charts. Intersection of the LOP's forms the fix. Normally, a fix may be obtained in under 3 minutes. Since the integral lane count is maintained rather than measured, a problem of lane identification may arise as a result of receiver malfunction, power failure, station outage, etc. Although lane resolution problems

seldom occur and usually can be resolved by other means such as dead reckoning or independent fix, transmissions at two additional frequencies have been included so as to provide a method for lane identification. Omega is described in detail in appendix B.

Multiple frequencies available

Each station thus will transmit three frequencies on a time-shared basis every 10 seconds. The frequencies are 10.2, 11-1/3, and 13.6 kHz, any one of which may be used for navigation or timing. Of the available frequencies, 10.2 kHz has the longest period and greatest spacing between LOP's and hence presents the least problem from the viewpoint of possible navigational lane ambiguity or timing epoch ambiguity. 10.2 kHz is also the best calibrated of the Omega frequencies. However, 13.6 kHz will generally have the best signal-to-noise ratio and the greatest repeatability.

Control frequencies

In addition to the three frequencies transmitted from each station primarily for navigation, two additional frequencies are being considered for intrasystem control transmissions of synchronization information. These two frequencies will be unique to each station, and hence they may be received without commutation. As presently envisioned, these control transmissions will be generated from the same timing equipment used to develop the navigational frequencies. They will range from 12 to 13 kHz, and each station will be assigned two frequencies 250 Hz apart; e.g., Trinidad might transmit 12.0 and 12.25 kHz. Unlike the navigational frequencies, the control frequencies will not be assigned specific segments but may vary within a commutation cycle for transmission of synchronization information. However, during each commutation cycle, each transmission will occur on at least one segment, and the control frequency divisible by 100 Hz will occur on the segment immediately following the navigational transmissions. Possible formats are shown in appendix B, together with a more complete system description.

Omega transmissions will be almost ideal sources of precise time. Advantages include:

Advantages for timing

- Nearly continuous operation of each station
- Eight stations located conveniently around the world
- System synchronization procedures so that each station will be continuously held to agreed international time
- Extreme range from each station, providing redundancy
- Precise control of transmitted signals
- Stability of the propagation medium
- Transmissions of five related frequencies from each station
- Availability of propagation corrections

The primary disadvantage is that repeated measurements at various frequencies may be necessary to initially set or to periodically verify the coarse epoch. However, the necessary information is available from the transmitted carrier frequencies, the beat frequencies, and the commutation pattern.

INTERRELATION OF NAVIGATION AND TIMING

Using a system such as Omega, navigation and timing are inextricably interrelated. The navigation fixing problem using three stations may be viewed as the reduction of three navigation variates (signals) to deduce three unknowns — latitude, longitude, and time. In conventional navigation the time determination is disregarded. However, time is necessarily determined and, indeed, the time determination from the resultant fix position to any of the three stations must be identical. For example, the NELC synchronized Omega monitor at Cape Prince of Wales, Alaska, was being synchronized by a Naval Observatory 'flying clock' on 272100Z August 1969. The monitor position can be deduced from the actual Omega phase measurements of Norway, Hawaii, and New York as:

65° 37.2'N
168° 4.7'W

This indicates a position error of 0.6 nautical mile at a bearing of 34 degrees. The associated fractional cycle epoch error of the local clock is found to be a delay of 0.56 cycle. Simultaneous observatory measurement indicated a fractional cycle clock delay of 0.49 cycle, a discrepancy of 7 μ sec. Note that although the velocity of light is 6 μ sec per nautical mile, the fix error was 0.6 mile while the timing error was 7 μ sec. It is often erroneously assumed that timing accuracy is directly proportional to fixing accuracy; actually, the fix error can be large while the time error is zero.

Distinctions between Omega navigation and timing are thus not fundamental but only variations in application. For example, if time were precisely known, then a navigation fix could be used to obtain a more precise position estimate. Conversely, in the case of time dissemination to a fixed location, the position ordinarily would be known precisely and all available signals could be used to refine the time estimate. Although there is not a fundamental difference between navigation and timing applications, there are numerous practical differences. A receiver suitable for navigation is not necessarily suitable for timing nor, indeed, is a receiver suitable for timing necessarily suitable for navigation. Further, propagation corrections and accuracy estimates for navigation are not necessarily applicable for time dissemination or for estimating the accuracy of disseminated time. It makes no better sense to attempt to estimate practical timing accuracy from practical navigational accuracy than it does to attempt to estimate probable uncertainties in longitude knowing probable uncertainty in latitude but not the prevailing physics or geometry. However, valid estimates of timing capability can be made from proper application of knowledge of navigational signal predictability, stability, and correlation.

SIMPLIFIED TIME DETERMINATION TECHNIQUES

EPOCH DETERMINATION

PULSE TECHNIQUES

Precisely timed pulses

The proposed Omega signal format provides the user with several methods for estimating the coarse local epoch from the characteristics of the transmitted pulses. Because the pulses are turned on and off at precisely timed intervals, either lead- or trail-edge techniques may be used to estimate the time delay between the received signals and the local clock pulses.

Simple instrumentation;
adjustable delays

LEAD-EDGE TECHNIQUES. A simple lead-edge measuring technique uses an oscilloscope triggered with a pulse from the local clock to observe the time delay of a received signal. Because this delay may be so great as to preclude the use of the smaller time-base scales on the scope, some auxiliary measurement of a shorter time interval is required. The most obvious solution is to delay the local epoch a known amount sufficient to reduce the received delay to a few milliseconds, at most. An even more efficient solution is to delay the local epoch until it occurs *during* the received pulse rise-time. If the scope is then triggered with a pulse occurring a few msec *before* the delayed local epoch, both the received signal and the delayed epoch, or 'reference' pulse, can be observed simultaneously on the scope. The time interval of interest is now that between the start of the received pulse rise-time and the reference pulse and is independent of the triggering time.

Figure 1 shows a possible circuit configuration for implementing the foregoing procedure. The blocks depicting the delay circuitry for the reference and trigger pulses have been left unspecified and will be determined by equipment available at a particular monitor site. The trigger delay is readily available from the commutator gating pulses in the Omega receiver. As these pulses normally are adjusted to coincide with the received signals and are easily adjustable over msec ranges, mis-synchronizing the commutator slightly will provide a trigger pulse slightly advanced from the received pulse lead-edge. The reference pulse delay may or may not be needed depending upon the user's purpose in performing this epoch determination. If a total timing failure has occurred, there can be no objection to adjusting the local epoch until it occurs during the received pulse rise-time, as specified for the reference pulse. If the local epoch cannot be moved for these measurements, then some additional circuitry (e.g., General Radio clock type 1123) must be used to produce the proper reference.

See sample procedure 1.

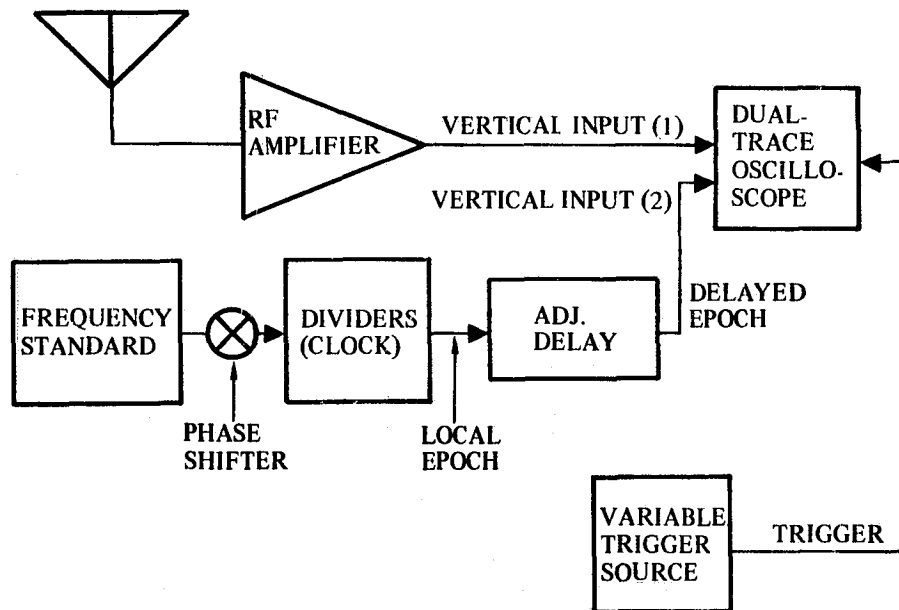


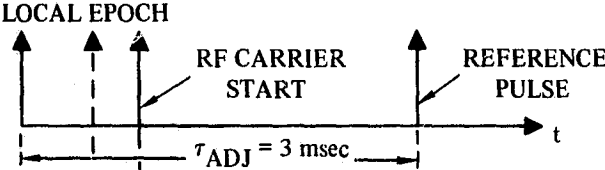
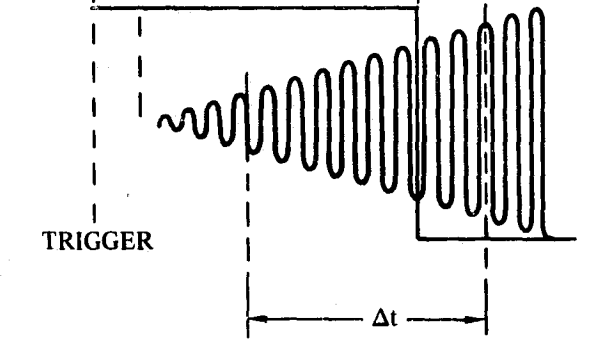
Figure 1. Suggested circuit for pulse epoch determination.

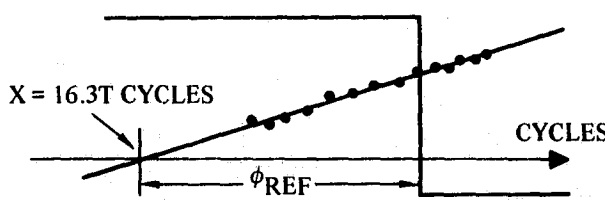
A. OBSERVED AND MEASURED VALUES

1. Arrange and adjust the experimental apparatus so as to permit the viewing of both the received pulse and the local 'reference' pulse on a dual-trace oscilloscope. Trigger the scope with a pulse advanced a few msec from the reference.
2. Obtain an oscillograph of the scope display. Photo integration over about an 8-minute period should produce suitable results. Maximum advantage of the 'gamma curve' of the film can be taken by deliberately misfocusing the oscilloscope slightly.
3. Select the time interval of the received pulse to be studied. The interval should begin as soon as the signal has emerged from the noise and terminate before significant nonlinearity develops in the envelope. Ordinarily, about 20 to 30 rf cycles will be included in an interval of 2-msec duration.
4. Measure and tabulate the *peak-to-peak* amplitude of the selected carrier cycles, indexing by cycle number with respect to the reference pulse. (Use of peak-to-peak measurements eliminates the effects of horizontal alignment error in the oscilloscope and provides for a larger unit of measurement.)

B. CALCULATED LOCAL EPOCH ERROR

1. Using the data tabulated in (A2), perform a linear least-squares regression to obtain the intercept of the lead-edge with the horizontal time axis. This value represents the number of carrier cycles from the start of the lead-edge to the reference pulse ϕ_{REF} .
2. Divide the intercept value by the carrier frequency to obtain the delay τ_{REF} , in time units, of the reference from the lead-edge.
3. Subtract this observed delay from any known delay τ_{ADJ} inserted to produce the reference pulse, and obtain the observed delay τ_{L} of the lead-edge from the local epoch.
4. Compute the predicted propagation delay τ_{d} for the specific Omega signal being observed.
5. Subtract the predicted from the observed delay to obtain the local clock error E_{T} . If all delays are given positive signs, a positive result indicates that the local clock is advanced from the proper time.

A. OBSERVED AND MEASURED VALUES	ARRANGE APPARATUS TO DISPLAY LEAD-EDGE AND REFERENCE	LOCAL EPOCH 	
	OBTAIN OSCILLOGRAPH		
	SELECT TIME INTERVAL	CYCLE NUMBER FROM REFERENCE	PEAK-TO-PEAK AMP. (ARBITRARY UNITS)
	MEASURE AND TABULATE CARRIER AMPLITUDE	1 2 3 . . . n	12 13 15 . . . 20

B. CALCULATED LOCAL EPOCH ERROR	PERFORM LINEAR LEAST-SQUARES REGRESSION FOR HORIZONTAL INTERCEPT (REFERENCE PHASE DELAY)	
	REFERENCE TIME DELAY	$\tau_{REF} = \frac{\phi_{REF}}{f} = \frac{16.3T}{10.2 \text{ kHz}} = 1600 \mu\text{sec}$
	OBSERVED EPOCH DELAY	$\tau_L = \tau_{ADJ} - \tau_{REF} = 3000 - 1600 = 1400 \mu\text{sec}$
	PROPAGATION DELAY	$\tau_d = d/\lambda = 1750 \mu\text{sec}$
	LOCAL EPOCH ERROR	$E_T = \tau_L - \tau_d = -350 \mu\text{sec}$

Sample procedure 1. Pulse epoch determination (refer to text on facing page).

TRAIL-EDGE TECHNIQUES. Methods for using the trailing edge of the received pulse for epoch determinations are similar to those for using the leading edge except that the portion of the waveform to be observed is in a region of higher signal-to-noise ratio. Calculation procedures are as described in *Lead-Edge Techniques* except that the peak (not peak-to-peak) carrier is measured and that additional scaling is needed prior to the fall to insure that the oscilloscope is properly aligned. Even so, instrumentation is more difficult, as only the immediate region of the start of the fall is of interest, and appropriate biasing circuits should be used. If biasing circuits are not used, then the apparent change in slope will be slight, and scaling uncertainties will contribute significant error. Because the times of interest are now almost a full second delayed from the lead-edge, the facility for controlling the trigger time and delaying or advancing the reference pulse is even more important than for the lead-edge measurements.

PHASE TECHNIQUES

**Carrier phase: predictable;
accurate**

The attribute which permits use of the Omega system format for timing as well as navigation purposes is the predictable behavior of the radiated carrier phase. Because vlf phase prediction techniques now approach accuracies of a few μsec even over long paths, a user possessing the appropriate equipment and procedures for observing and resolving the ambiguities in these signals also should be able to determine and maintain time to approximately these same accuracies. This section describes how to convert the raw measurement of remote versus local phase into an accurate estimate of the timing discrepancy between a local clock and the clock generating the remote signal. Single carrier measurements are considered here; composite phase is discussed in *Ambiguity Resolution*.

Sign conventions

Before entering into a step-by-step procedure for epoch estimation, a brief discussion of ambiguity and sign conventions is necessary. Because the remote signal must travel a definite distance from transmitter to receiver, it always will be *delayed* with respect to a local clock which is synchronized to the signal generating clock. However, as the receiver does not distinguish between separate cycles of the received periodic signal, and cannot count the total number of cycles of delay, the remote signal may appear either advanced or retarded with respect to the local clock. Standard procedure at Omega stations has been to arrange monitoring equipment so that an upscale reading of a phase difference track indicates *increasing delay* for the remote signal; i.e., the phase track would behave similarly to the effective ionospheric reflecting height by showing less delay during the day than at night. This same configuration is appropriate for local timing applications, as the upscale indication is now to be considered as an *advance* of the local clock with the remote signal as the reference. With these thoughts in mind, consider the procedure for epoch determination from single carrier phase measurements (sample procedure 2).

A. PREDICTED VALUE CALCULATIONS

1. From the known propagation path length d and the wavelength λ of the specific carrier being observed, compute the reference path delay or 'geodesic' G_R :

$$G_R = -0.9974/\lambda_f$$

2. Look up the expected diurnal correction SWC_R in the skywave correction tables provided. Select the value for the appropriate transmitter, frequency, year, month, day, and fraction of an hour:

$$SWC_R = \text{tabulated value}$$

3. Add the reference path delay to the diurnal correction to compute the predicted phase for the E-field vector ϕ_{P_E} :

$$\phi_{P_E} = G_R + SWC_R$$

4. If a loop antenna is used to observe the H-field vector, *reduce* the predicted E-field delay by $\frac{1}{4}$ cycle to compensate for the 90° lag of the E-field from the H-field:

$$\phi_{P_H} = \phi_{P_E} + 0.25$$

B. OBSERVED VALUE CALCULATIONS

1. Record the measured fractional cycle delay ϕ_O of the remote versus the local phase:

$$\phi_O = (\phi_R - \phi_L) = \text{data}$$

2. Assume that no ambiguity exists and assign a whole cycle count ϕ_N to adjust the measured fraction to within $\frac{1}{2}$ cycle of the predicted value:

$$\phi_{O'} = \phi_O + \phi_N$$

where $\phi_{O'}$ is defined as the 'observed phase.'

C. CLOCK PHASE AND TIME ERROR CALCULATIONS

1. Subtract the 'observed' from the 'predicted' phase to compute the *phase* error of the local clock:

$$E_\phi = (\phi_{P(H \text{ or } E)} - \phi_{O'}) \pm \phi_T = \Delta\phi \pm \phi_T$$

where ϕ_T represents the ambiguity as an integral number of carrier frequency cycles.

2. Divide the clock phase error by the carrier frequency to compute the clock *time* or epoch error:

$$E_T = \frac{E_\phi}{f} = \Delta t \pm t_T$$

where t_T represents the ambiguity as an integral number of carrier frequency periods.

A. PREDICTED VALUES	PATH LENGTH	d	7772.487 km		
	WAVELENGTH	$\lambda_{13.6}$	22.04 km/CYCLE		
	REFERENCE PATH DELAY	G_R	$-0.9974 d/\lambda_{13.6}$ kHz	-351.679 CYCLES	
	DIURNAL CORRECTION	SWC_R	published table	- 0.950 CYCLES	
	E-FIELD PHASE	ϕ_{P_E}	$G_R + SWC_R$	-352.629 CYCLES	
	LOOP ANTENNA ADJUSTMENT	ϕ_A	¼ CYCLE, IF APPLICABLE	+ 0.250 CYCLES	
	H-FIELD PHASE	ϕ_{P_H}	$\phi_{P_E} + \phi_A$	-352.379 CYCLES	-352.379 CYCLES

B. OBSERVED VALUES	MEASURED FRACTION	ϕ_O	$(\phi_{REMOTE} - \phi_{LOCAL})$	- 0.389 CYCLES	
	CYCLE IDENTIFICATION	ϕ_N	$\phi_{P_H} - \phi_O < 0.5$ cycle	-352.0 CYCLES	
	OBSERVED PHASE	ϕ_O'	$\phi_O + \phi_N$	-352.389 CYCLES	-352.389 CYCLES

C. CLOCK PHASE	ERROR	E_ϕ	PREDICTED-OBSERVED, $\phi_{P_H} - \phi_O'$	+ 0.010 CYCLE
	AMBIGUITY	ϕ_T	CARRIER FREQUENCY CYCLES	$\pm N$ CYCLES

C. CLOCK TIME	ERROR	E_T	PHASE \div FREQUENCY, $\frac{E_\phi}{f}$	+ 0.7 μ SEC
	AMBIGUITY	t_T	CARRIER FREQUENCY PERIODS	$\pm NT$ μ SEC

Sample procedure 2. Phase epoch determination. Done for Hawaii signal observed at Naval Observatory on 13.6 kHz on 112000Z Nov 1969--loop antenna (refer to text on facing page).

FREQUENCY DETERMINATION

Frequency estimated from periodic phase measurements

In ongoing operations, a monitor site periodically will be estimating the epoch error between the local clock and the received radio signals. If the local oscillator is characterized by accuracy and stability figures of the same magnitude as the transmitted signals, successive epoch errors eventually will indicate the approximate frequency offset between the local standard and the Omega system frequency. When Omega is being maintained on Universal Time (UTC), the indicated local offset is with respect to UTC also. Therefore, knowledge of this offset permits the site to predict future epoch errors and to compute the approximate 'time' without having to perform as many rf measurements as initially.

The uncertainty in the time estimate is determined by both the uncertainty of the estimate of the standard's past history and its ability to maintain a stable frequency. Although cesium standards are specified as having no long-term drift in frequency, experience with Omega station standards over the past 4 years indicates that significant drifts over periods of weeks can occur. By 'significant' is meant a change of more than 1×10^{-12} , or about $0.5 \mu\text{sec}$ in 1 week of operation. Such drifts may not be observable to the user for several weeks and may or may not be serious depending upon the tolerances for local timing errors and the spectrum of the standard's behavior. The behavior of cesium standards is discussed further in *OPERATIONAL CONSIDERATIONS, Equipment, Oscillator*. This section is concerned primarily with procedures for computing the standard frequency from the epoch measurements. See sample procedure 3.

Least-squares regression

Assuming the oscillator has a basically linear frequency offset from the universal reference, a least-squares regression of successive phase errors between the oscillator and the reference gives the required estimate of this frequency offset.

The following procedure uses equation (A4) from appendix A to calculate the frequency offset from the successive epoch errors which are available from the previous section on phase techniques.

A. OBSERVED EPOCH ERRORS

1. Using any convenient format, tabulate successive epoch error estimates over the total time interval for which the frequency offset is to be estimated:

$$E_{T_i} = E_{T_1}, E_{T_2}, E_{T_3}, \dots, E_{T_n}$$

2. Similarly, tabulate the product of the epoch errors and the multiplier index i:

$$iE_{T_i} = E_{T_1}, 2E_{T_2}, 3E_{T_3}, \dots, nE_{T_n}$$

B. COMPUTED REGRESSION SLOPE

1. Compute the summation term ΣE_{T_i} :

$$\Sigma E_{T_i} = E_{T_1} + E_{T_2} + E_{T_3} + \dots + E_{T_n}$$

2. Compute the product summation term ΣiE_{T_i} :

$$\Sigma iE_{T_i} = E_{T_1} + 2E_{T_2} + 3E_{T_3} + \dots + nE_{T_n}$$

3. Note the values for the number of data points n and the time between points T:

$$n = \text{data sample, } T = \text{sampling time}$$

4. Compute the regression constants A and B:

$$A = \frac{Tn(n^2-1)}{12} \quad B = \frac{Tn(n-1)}{6}$$

5. Compute the least-squares frequency offset Δf :

$$\Delta f = \frac{\Sigma iE_{T_i}}{A} - \frac{\Sigma E_{T_i}}{B} \quad (1)$$

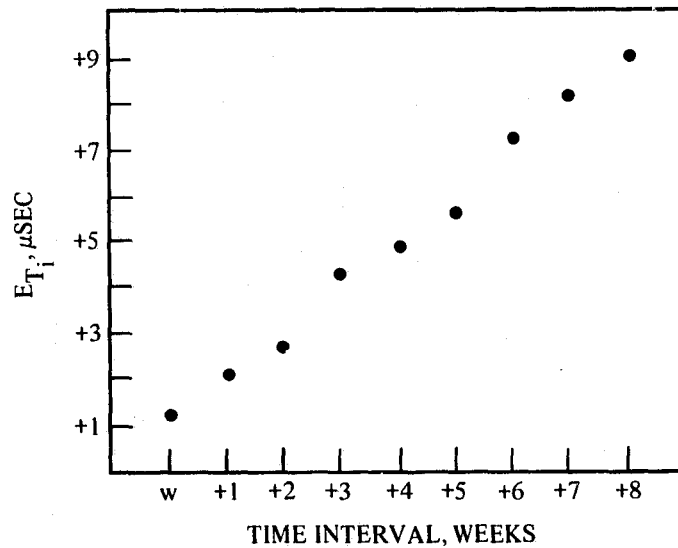
C. FREQUENCY CONVERSION

1. The units of E_{T_i} and T determine the units of Δf . When the E_{T_i} are in μsec , and T is in days, the frequency offset estimate has units of $\mu\text{sec/day}$. To convert to sec/sec^* or parts in 10^{12} :

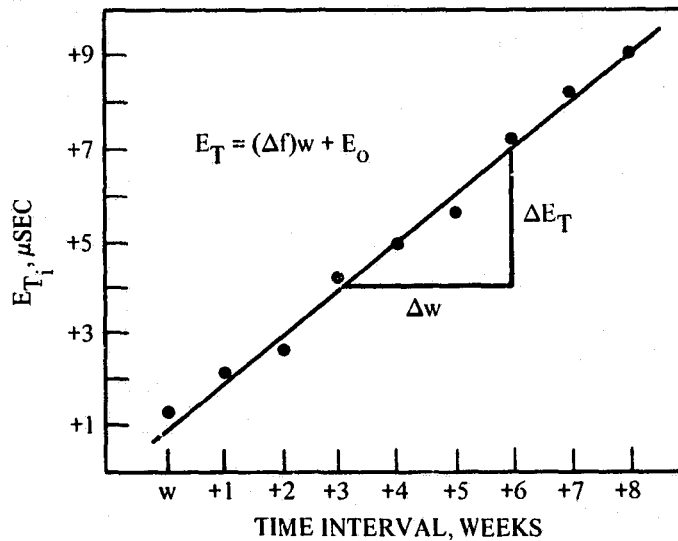
$$\Delta f \left(\frac{\text{sec}}{\text{sec}} \right) = \Delta f \left(\frac{\mu\text{sec}}{\text{day}} \right) \times \frac{10^{-12}}{0.0864}$$

*or any other common time period

A. OBSERVED EPOCH ERRORS	TIME INTER-VAL	EPOCH ERROR E_{T_i}	i	iE_{T_i}
	w	+1.2	1	1.2
	w+1	+2.1	2	4.2
	w+2	+2.7	3	8.1
	w+3	+4.3	4	17.2
	w+4	+4.8	5	24.0
	w+5	+5.6	6	33.6
	w+6	+7.2	7	50.4
	w+7	+8.1	8	64.8
w+8	+9.0	9	81.0	



B. COMPUTED REGRESSION SLOPE	$\Sigma E_{T_i} = 45.0$
	$\Sigma iE_{T_i} = 284.5$
	FOR T = 7, n = 9
	$A = \frac{12}{Tn(n^2-1)} = \frac{1}{420}$
	$B = \frac{6}{Tn(n-1)} = \frac{1}{84}$
	$\Delta f = \frac{\Sigma iE_{T_i}}{A} - \frac{\Sigma E_{T_i}}{B}$
	$\Delta f = +0.14 \frac{\mu\text{SEC}}{\text{DAY}}$



C. FREQUENCY CONVERSION	FREQUENCY OFFSET IN $\mu\text{SEC}/\text{DAY}$	$\Delta f = +0.14 \mu\text{SEC}/\text{DAY}$
	CONVERSION FACTOR IN $\text{DAY}/\mu\text{SEC}$	$\text{DAY}/\mu\text{SEC} = \frac{10^{-12}}{0.0864}$
	FREQUENCY OFFSET IN PARTS IN 10^{12}	$\Delta f' = \frac{\Delta f \times 10^{-12}}{0.0864} = 1.6 \times 10^{-12}$

Sample procedure 3. Frequency determination (refer to text on facing page).

UPDATING PROCEDURES

Provided the user revises the frequency estimate each time an epoch estimate is made, equation (1) has the advantage of being updated easily to obtain continuing estimates. The updated summation terms can be shown to be given by:

$$\sum_{i=j+1}^{n+1} E_{T_i} = \sum_{i=j}^n E_{T_i} + (E_{T_{n+1}} - E_{T_j})$$

Simple updating in continuous operation

$$\sum_{i=j+1}^{n+1} iE_{T_i} = \sum_{i=j}^n iE_{T_i} - \sum_{i=j}^n E_{T_i} + nE_{T_{n+1}} \quad (2)$$

The procedures described above may be used to develop long- or short-term frequency offset estimates; i.e., T and n may be varied over any range of interest. Depending upon the resulting magnitude and variability of the calculated estimates, the user may wish to consider the confidence on the estimates and the possibility of controlling the local clock time so as to remove or minimize the estimated drifts. These aspects are considered more completely in *ACCURACY OF TIME DETERMINATION TECHNIQUES* and *OPERATIONAL CONSIDERATIONS*, respectively.

If the local clock time is controlled to approximate synchronism with the external reference signals, successive epoch errors no longer represent the oscillator frequency offset but instead indicate any error in the applied clock adjustment rate. However, successive movements of the phase shifter *will* represent the approximate oscillator offset and are to be used to obtain ongoing estimates of future behavior. In other words, if a consistent epoch adjustment rate is evidenced by the phase shifter movements, and this rate has succeeded in maintaining past time correct to within the specified tolerances, this same rate should apply to future operation as well.

AMBIGUITY RESOLUTION

Many possible 'beat' frequencies

The multifrequency format of Omega provides a unique method for the determination of the crude epoch error of a local clock. The numerous possible phase comparisons may be combined in a variety of ways to yield 'composite' phase values which represent the epochs of frequencies with periods greater than any of the transmitted carriers. Appendix B tabulates some of the more useful 'beat frequency' combinations and gives the periods of the effective frequency of these combinations. For example, the minimum time between zero crossings of the 10.2, 11.33, and 13.6 kHz is 882 μ sec (or 1.133 kHz), while addition of the 12.0 kHz reduces the effective frequency to 66-2/3 cycles with a period of 15 msec. Evidently, a monitor capable of receiving the entire Omega spectrum is also capable of running through the full ambiguity resolution operation until an epoch correct to within some multiple of 30 seconds is established. Hopefully, some external information will permit resolution of the 30-second epoch. This section does not consider the entire resolution problem but presents two different approaches to the simple two- and three-frequency ambiguity cases noted previously. See sample procedures 4 and 5.

Algebraic and graphic methods

The first approach is entirely algebraic and presents formulas which convert observed phase errors and frequency ratios into the clock time \pm an integral number of periods of the unresolved 1.133 epoch. The second approach is more graphic and empirical in nature and is intended to demonstrate the simplification produced by equivalent prediction accuracy at all frequencies. Both approaches are meant to be applied to signals from only one Omega station at a time, but local prediction accuracies will determine whether combining signals from several stations will improve results. Both approaches are also readily extrapolated to additional frequencies.

A. OBSERVED VALUE CALCULATIONS

- Using the procedures of *SIMPLIFIED TIME DETERMINATION TECHNIQUES, Epoch Determination, Phase Techniques*, compute the indicated *phase errors* of the local clock with respect to signals on frequencies f_1 , f_2 , and f_3 from one specific Omega station. Assign an arbitrary number of integral cycles to represent the ambiguity in each estimate:

$$E_{\phi_1} = \Delta\phi_1 \pm K \quad E_{\phi_2} = \Delta\phi_2 \pm L \quad E_{\phi_3} = \Delta\phi_3 \pm M \quad (\text{cycles})$$

- Write the expressions for the clock *time errors* in terms of the respective carrier frequencies:

$$E_{T_1} = \frac{\Delta\phi_1 \pm K}{f_1} \quad E_{T_2} = \frac{\Delta\phi_2 \pm L}{f_2} \quad E_{T_3} = \frac{\Delta\phi_3 \pm M}{f_3} \quad (\mu\text{sec})$$

B. AMBIGUITY RESOLUTION CALCULATIONS

- As the clock can have only one epoch, the errors given in (A2) must be identical and can be equated to yield two equations in the three unknowns K, L, and M:

$$E_{T_1} = E_{T_2} = E_{T_3}$$

$$\frac{\Delta\phi_1 \pm K}{f_1} = \frac{\Delta\phi_2 \pm L}{f_2} = \frac{\Delta\phi_3 \pm M}{f_3}$$

$$L = \left(\frac{f_2}{f_1} \Delta\phi_1 - \Delta\phi_2 \right) \pm K \frac{f_2}{f_1} \quad M = \left(\frac{f_3}{f_1} \Delta\phi_1 - \Delta\phi_3 \right) \pm K \frac{f_3}{f_1}$$

- Using trial and error, find the integral values of K which yield integral values for L and M. The solutions will involve a minimum value and an ambiguous number of composite frequency periods:

$$K = K_0 \pm N \frac{f_1}{f_2 - f_1} \quad L = L_0 \pm N \frac{f_2}{f_2 - f_1} \quad M = M_0 \pm N \frac{f_3}{f_2 - f_1}$$

C. CLOCK EPOCH AND AMBIGUITY CALCULATIONS

- Substitute the solutions for K, L, and M into (A2) and compute the local clock epoch at each frequency:

$$E_{T_1} = \frac{\Delta\phi_1 \pm K_0}{f_1} \pm \frac{N}{f_2 - f_1} \quad E_{T_2} = \frac{\Delta\phi_2 \pm L_0}{f_2} \pm \frac{N}{f_2 - f_1} \quad E_{T_3} = \frac{\Delta\phi_3 \pm M_0}{f_3} \pm \frac{N}{f_2 - f_1}$$

- The answers in (C1) should be nearly identical, depending upon prediction accuracies, and should agree with similar calculations done for signals from other Omega stations.

A. OBSERVED VALUES	FREQUENCY	f	$f_1 = 10.2, f_2 = 11-1/3, f_3 = 13.6$		kHz
	CLOCK PHASE ERRORS	E_{ϕ_1}	$\Delta\phi_1 \pm K$	$+0.41 \pm K$	CYCLES
		E_{ϕ_2}	$\Delta\phi_2 \pm L$	$-0.43 \pm L$	CYCLES
		E_{ϕ_3}	$\Delta\phi_3 \pm M$	$-0.12 \pm M$	CYCLES
	CLOCK TIME ERRORS	E_{T_1}	$\frac{\Delta\phi_1 \pm K}{f_1}$	$\frac{0.41 \pm K}{f_1}$	μSEC
		E_{T_2}	$\frac{\Delta\phi_2 \pm L}{f_2}$	$\frac{-0.43 \pm L}{f_2}$	μSEC
E_{T_3}		$\frac{\Delta\phi_3 \pm M}{f_3}$	$\frac{-0.12 \pm M}{f_3}$	μSEC	

B. AMBIGUITY RESOLUTION	CYCLE RELATIONS	L	$\left(\frac{f_2}{f_1} \Delta\phi_1 - \Delta\phi_2\right) \pm K \frac{f_2}{f_1}$	$0.46 + 0.43 \pm \frac{10K}{9} = \frac{8 \pm 10K}{9}$
		M	$\left(\frac{f_3}{f_1} \Delta\phi_1 - \Delta\phi_3\right) \pm K \frac{f_3}{f_1}$	$0.55 + 0.12 \pm \frac{4K}{3} = \frac{2 \pm 10K}{3}$
	CYCLE RESOLUTION	K	$K_0 \pm N \frac{f_1}{f_2 - f_1}$	$1 \pm 9N$
		L	$L_0 \pm N \frac{f_2}{f_2 - f_1}$	$2 \pm 10N$
		M	$M_0 \pm N \frac{f_3}{f_2 - f_1}$	$2 \pm 12N$

C. CLOCK EPOCH AND AMBIGUITY	LOCAL	E_{T_1}	$\frac{\Delta\phi_1 \pm K_0}{f_1} \pm \frac{N}{f_2 - f_1}$	$+138 \pm 882N$	μSEC
	CLOCK	E_{T_2}	$\frac{\Delta\phi_2 \pm L_0}{f_2} \pm \frac{N}{f_2 - f_1}$	$+138 \pm 882N$	μSEC
	TIMES	E_{T_3}	$\frac{\Delta\phi_3 \pm M_0}{f_3} \pm \frac{N}{f_2 - f_1}$	$+138 \pm 882N$	μSEC

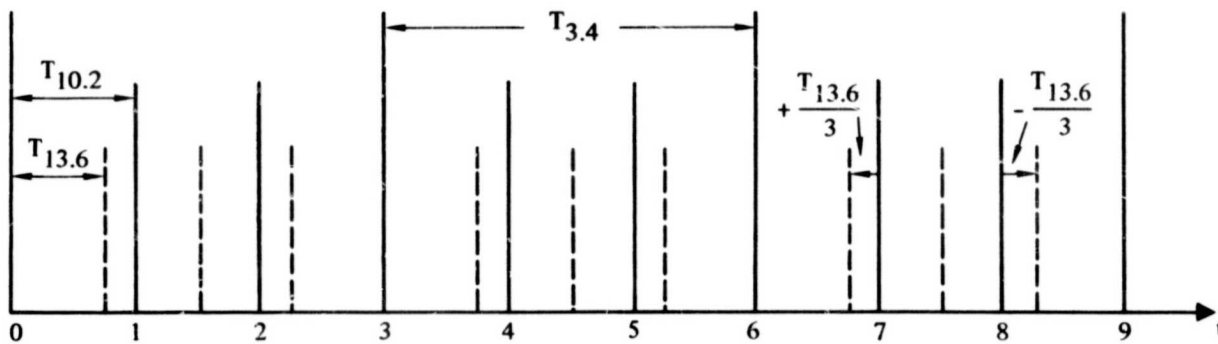
Sample procedure 4. Three-frequency ambiguity resolution (refer to text on facing page).

A. 3.4-kHz EPOCH RESOLUTION

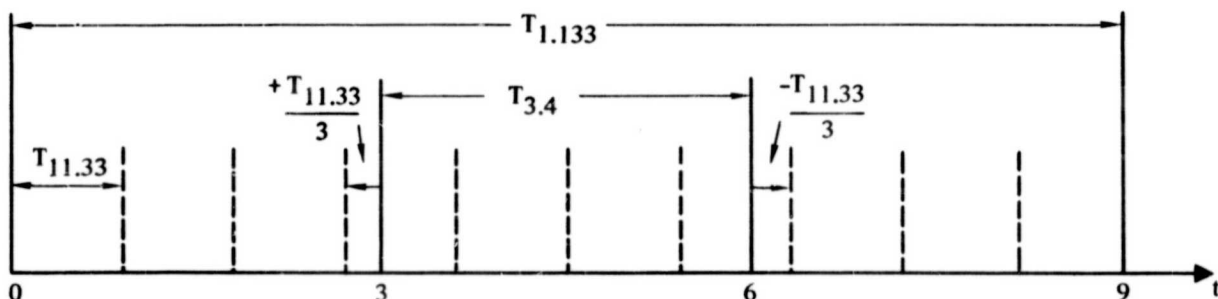
1. Using the procedures of *SIMPLIFIED TIME DETERMINATION TECHNIQUES, Epoch Determination, Phase Techniques*, compute the indicated *phase error* of the local clock with respect to a 10.2-kHz Omega signal.
2. Adjust the local epoch until the indicated 10.2-kHz epoch is reduced to zero. The clock is now set approximately to either of the times t_0 through t_9 .
3. As in (1), compute the indicated phase error on 13.6 kHz. Depending upon the magnitude of this error, proceed with one of the following:
 - (a) For an error of approximately zero, the clock is set at time 0,3,6, or 9 and need not be readjusted as yet.
 - (b) For an error of approximately +33 cec, the clock is set at time 1,4, or 7 and may be advanced by one period of 10.2 kHz to reset the time to 0,3, or 6.
 - (c) For an error of approximately -33 cec, the clock is set at time 2,5, or 8 and may be retarded by one period of 10.2 kHz to reset the time to 3,6, or 9.
4. As a result of the preceding steps, the clock is set to time 0,3,6, or 9 and is correct to within some multiple of the 3.4-kHz period.

B. 1.133-kHz EPOCH RESOLUTION

1. Perform the indicated procedure for 3.4-kHz epoch resolution.
2. As in (A1), compute the indicated phase error on 11.33 kHz. Depending upon the magnitude of this error, proceed with one of the following:
 - (a) For an error of approximately zero, the clock is set at time 0 or 9 and need not be readjusted.
 - (b) For an error of approximately +33 cec, the clock is set at time 3 and may be advanced by one period of 3.4 kHz to reset the time to 0.
 - (c) For an error of approximately -33 cec, the clock is set at time 6 and may be advanced by two periods of 3.4 kHz to reset the time to zero.
3. As a result of the preceding steps, the clock is now set to time 0 or 9 and is correct to within some multiple of the 1.133 period.



A. 3.4-kHz EPOCH RESOLUTION	PRESET CONDITION	$E_{\phi_{10.2}}$	0 (CLOCK SET AT TIMES 0 + 9)									
	OBSERVED CONDITION	$E_{\phi_{13.6}}$	0 cec				$+\frac{T_{13.6}}{3} = +33-1/3$ cec			$-\frac{T_{13.6}}{3} = -33-1/3$ cec		
	CLOCK SET AT TIME	t	0	3	6	9	1	4	7	2	5	8
	CLOCK DELAYED FROM t_0	τ	0	294	588	882	98	392	686	196	490	784



B. 1.133-kHz EPOCH RESOLUTION	PRESET CONDITION	$E_{\phi_{3.4}}$	$E_{\phi_{10.2}} = E_{\phi_{13.6}} = 0$					
	OBSERVED CONDITION	$E_{\phi_{11.33}}$	0		$+\frac{T_{11.33}}{3} = 33-1/3$ cec		$-\frac{T_{11.33}}{3} = -33-1/3$ cec	
	CLOCK SET AT TIME	t	0	9	3	6		
	CLOCK DELAYED FROM t_0	τ	0	882	294	588		

Sample procedure 5. Two-frequency ambiguity resolution (refer to text on facing page).

ACCURACY OF TIME DETERMINATION TECHNIQUES

PULSE TECHNIQUES

Pulse timing techniques have been used for many years. They have significant advantages over phase techniques employing multiple frequencies, since there is no ambiguity problem except that associated with the repetition rate, which may be controlled by the system designer. Pulse techniques lack precision compared with phase comparison accuracies. Further, pulse techniques require relatively good signal-to-noise ratios.

Slow rise time

Because Omega transmitting antennas systems have high Q and narrow bandwidth on the order of 10 Hz, the envelope of the transmitted wave form will approximate a rising exponential of the form $e(t) = E_{\max}(1 - \exp. kt)$. The exact shape will be different owing to other time constants in the transmitter.* A typical rise is shown in figure 2.

The rise is exceptionally slow compared to most pulse transmissions.

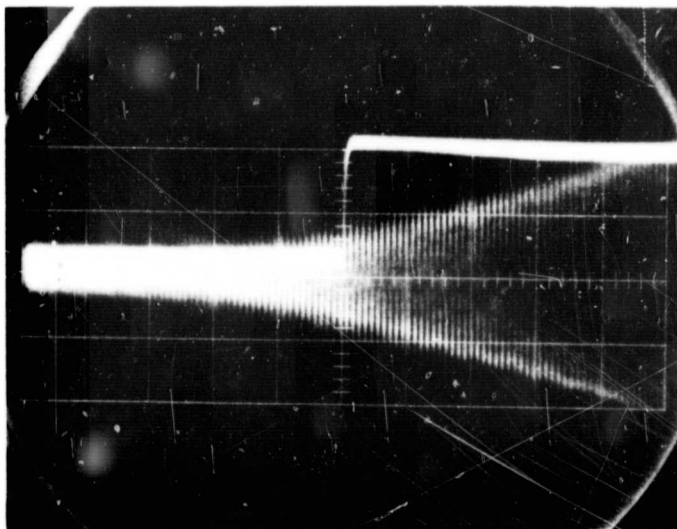


Figure 2. Haiku leading edge as received at NELC.

*Palmer uses a more general form stating that the rise is along an exponential curve 'more or less' of the form $e(t) = E_{\max}(1 - kt)^N$ (reference 5).

Shape distorted by medium

A pulse inherently will be distorted by dispersive effects of the propagation medium through which it is transmitted. The resulting shape at a remote receiver is, in general, complex (a good discussion is given in Stratton, ref. 6). Usually, it is necessary to define the point on the lead edge at which measurements are to be performed and to specify how the measurements are to be interpreted before the propagation delay can be specified. Although little theoretical or experimental work has been done on the absolute predictability of the Omega lead edge, speculations are that the prediction problem will not be severe, owing to the limited frequency components present in the transmitted signal. Further, the timing capability is not intended as a precise method, and hence relatively crude predictions can be employed. If the portion of the lead edge actually measured can be considered to have an effective velocity between the group velocity and the velocity of light, then the total range in the prediction uncertainty would be only about 100 μ sec over typical paths.

Crude predictions useful

No unusual instrumentation problems should be encountered in making absolute time measurements with the lead edge. The most severe problem is the poor signal-to-noise ratio, which can be overcome by photographic integration. Delays may be expected in the antenna coupler and receiver but these can be determined from analysis of the circuits employed and should remain stable to the accuracy required. Alternatively, a simple circuit can be constructed to simulate the Omega pulse, and the receiving system can be calibrated directly.

Vlf pulse timing has been investigated most recently by DePrins⁷ who found a precision on the order of 100 μ sec for a 500-km path to GBR and a 200- μ sec precision on a 3000-km path to NBA. Similar experiments at NELC have corroborated this increase in precision when the lower portion of the exponential rise is observable. The experiment was restricted to measurements of the 10.2-kHz signal from Haiku as received at NELC. The experimental arrangement included a receiver to obtain an unlimited rf within a relatively broad bandwidth of approximately 100 Hz. This bandwidth was that of the available receiver and will have some effect on the observed rise times. Eight-minute photographic integration was used on a normal oscilloscope display in which triggering was accomplished from a precision clock driven by a cesium frequency standard. A reference pulse was superimposed. High gain was used so that only the start of the 10.2-kHz pulse was observed. It was then assumed that the voltage-time relationship was linear for the first 2 to 3 msec, and a linear regression analysis was conducted to estimate the starting time. (The analysis treated time as the dependent variable so that statistical expressions for the uncertainty of the ordinate intercept could be used.) Seven lead-edges were analyzed. The results are summarized in table 1.

**Experimental measurements:
lead edge 10.2 kHz; Hawaii
to San Diego**

Two columns are of special interest. The 'Intercept' column indicates the actual value of the time determination from each photograph as compared with a superimposed reference pulse from a General Radio clock (1 unit equals 98 μ sec). The second column of special interest is 'Uncertainty Coefficient q.' Each timing estimate, including its associated

TABLE 1. RESULTS OF LEAD-EDGE EXPERIMENTS.

Lead-Edge Date/Time Nov 1967	Intercept Cycles of 10.2 kHz With Respect to Reference Pulse	Uncertainty Coefficient q, Cycles	Signal Width, cm
031900Z	-12.87	2.57	0.43
062245	-15.70	0.65	0.12
unmarked	-16.03	0.80	0.12
032245	-16.75	0.47	0.20
022330	-16.94	0.58	0.21
131925	-17.97	1.43	0.22
211900	-15.59	0.72	0.20

confidence limits, is given by the intercept $\pm qt$ where t is the value of the t distribution for approximately 12 degrees of freedom and confidence limits desired. Approximately 70 percent of the intercept should be within $\pm q$ while 95 percent should be within $\pm 2q$. Thus, the median value of q (approximately 71 μsec) should approximate the standard deviation of the intercept values (approximately 157 μsec). The disagreement can be explained by the 'width' of the trace used in the first determination. The record apparently was overexposed so that the indicated value was shifted slightly. Disregarding the first determination yields a median value of q of about 67 μsec while the standard deviation of the intercept is reduced to 90 μsec . Although the agreement is sufficiently close considering the various uncertainties, it is interesting to speculate on the improvement which might be possible using better instrumentation. The uncertainty coefficient reflects primarily variations on the photographs and scaling errors and linearization in the analysis. 'q' is thus most sensitive to experimental technique, while the standard deviation of the various intercepts must include not only experimental errors but also daily variations in propagation. If this interpretation is correct, then the primary errors in the determinations must be experimental rather than propagational.

One trailing edge was also investigated. Trailing edge measurements nominally offer the advantage of better signal-to-noise ratio. However, scaling difficulties were a substantial source of error, and the very low slope possible on the scope display led to an intercept uncertainty of 130 μsec . More elaborate instrumental techniques should lead to substantial improvement in accuracy.

The Omega pulses thus offer a means of timing to a precision of about 100 μsec , using only crude instrumental techniques. It seems likely that improved instrumentation and analysis will yield higher precision.

**Experimental precision:
90 μsec**

Trail-edge

Greater accuracy possible

PHASE TECHNIQUES

Rms timing uncertainty: bias and standard deviation

The accuracy of epoch estimates determined from carrier phase measurements depends upon the accuracy of the predictions for the nominal long-term average phase expected as well as the temporal stability of the medium. The errors may be described as a bias and a standard deviation which combine to yield a typical rms timing uncertainty. However, the rms timing uncertainty is recognized to have two separate components. The bias error will not contribute to errors in determining frequency, and hence only the standard deviation is of importance. Epoch errors, however, will directly reflect biases in prediction; epoch confidence cannot be improved beyond limitations imposed by prediction bias.

Over 1 000 000 hours of data

Since modern Omega operation began in 1966, over 1 million hours of phase measurements directly applicable to estimating the timing accuracy of Omega have been obtained. The data have been acquired primarily at monitoring sites associated with each transmitter. The monitors continuously record the phase difference between signals received from various remote Omega transmitters and the local transmitter. Since the propagation from the local transmitter to the associated monitoring site is predictable,⁸ the local transmitter signal can be viewed as stable synchronized injection to the monitor receiver. Hence, Omega transmitting station monitors may be viewed as timing receivers. Additional data have been acquired from propagation experiments at Wales, Alaska, where a receiver using specially designed injection calibration from a cesium standard was operated for over 1 year. The true epoch of the local reference was related to the Omega system epoch by repeated 'flying clock' calibration.

Similar data occasionally have been recorded at NELC in San Diego when the flying clock data have been available to relate the local epoch to that of the Omega system. Other direct comparisons are available as a result of flying clocks between the U.S. Naval Observatory and various Omega stations.⁹

(Measurements 1 to 8) Flag: 'S' = SID; 'P' = PCA; 3.8 μ sec over 24 hours

Various typical long-path phase measurements are given and compared with prediction in measurement listings 1 through 8. Observed phase differences normally are made hourly with time constants appropriate for navigation. The data are flagged to indicate measurements possibly affected by SID's (S) and PCA's (P). The last eight rows (under GMT, SWC, and RMS) are, respectively, Greenwich mean time (1 = 0100Z, etc.); flags indicating day or night periods (i.e., when the propagation path is completely sunlit or dark); number of observations (less SID's and PCA's); averages (less SID's and PCA's); standard deviation (including SID's but excluding PCA's); two semimonthly sky wave corrections; and the rms value of the observed phase error with respect to prediction. Statistics are summarized in table 2.

Short paths: useful if calibrated

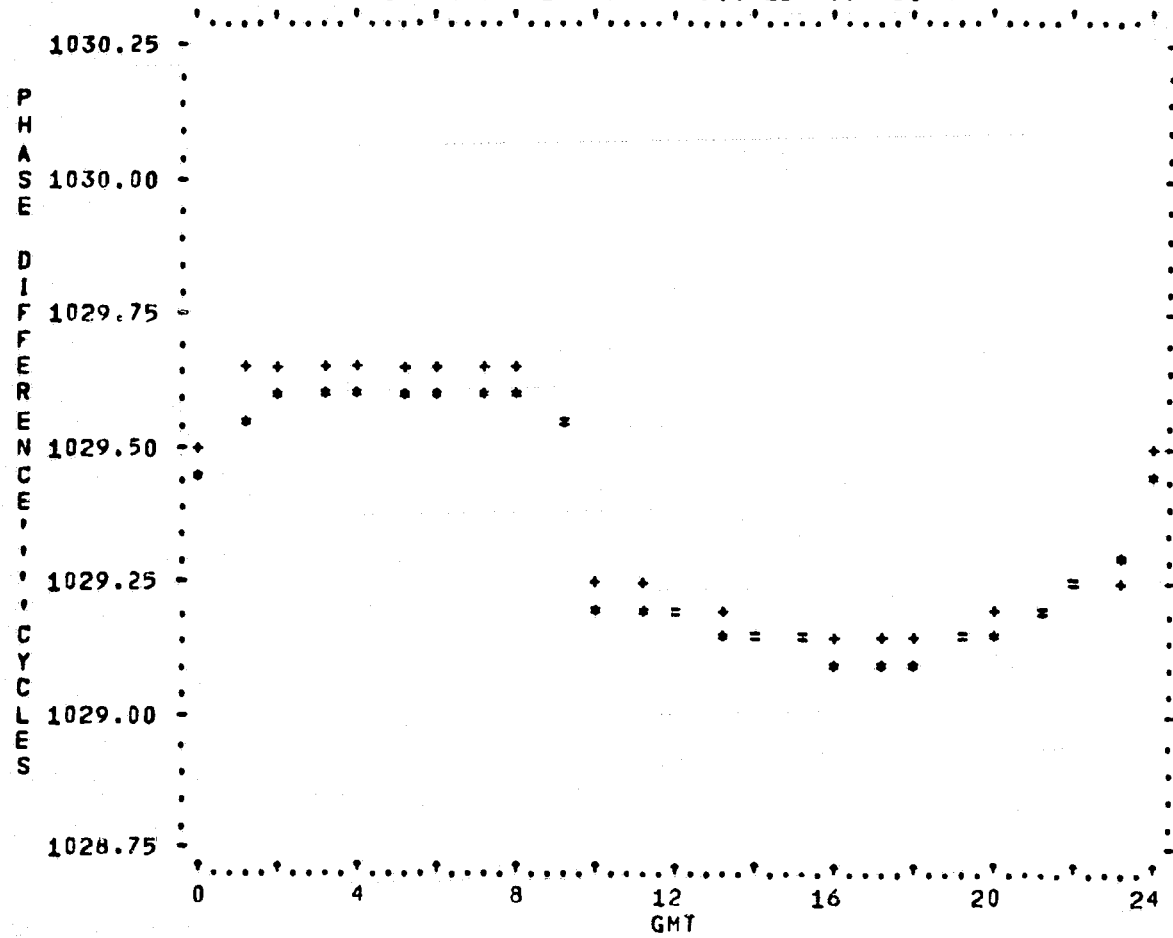
Short paths also may be used for timing under certain conditions. Prediction is extraordinarily difficult at short ranges where various propagation modes may be interfering. At certain distances, however, the resultant phase may be stable. If the nominal phase value can be determined

ROME, N.Y.

B-D JUN 69

10.2 KHZ

KEY: AVERAGE(+), PREDICTED(+), BOTH(=)

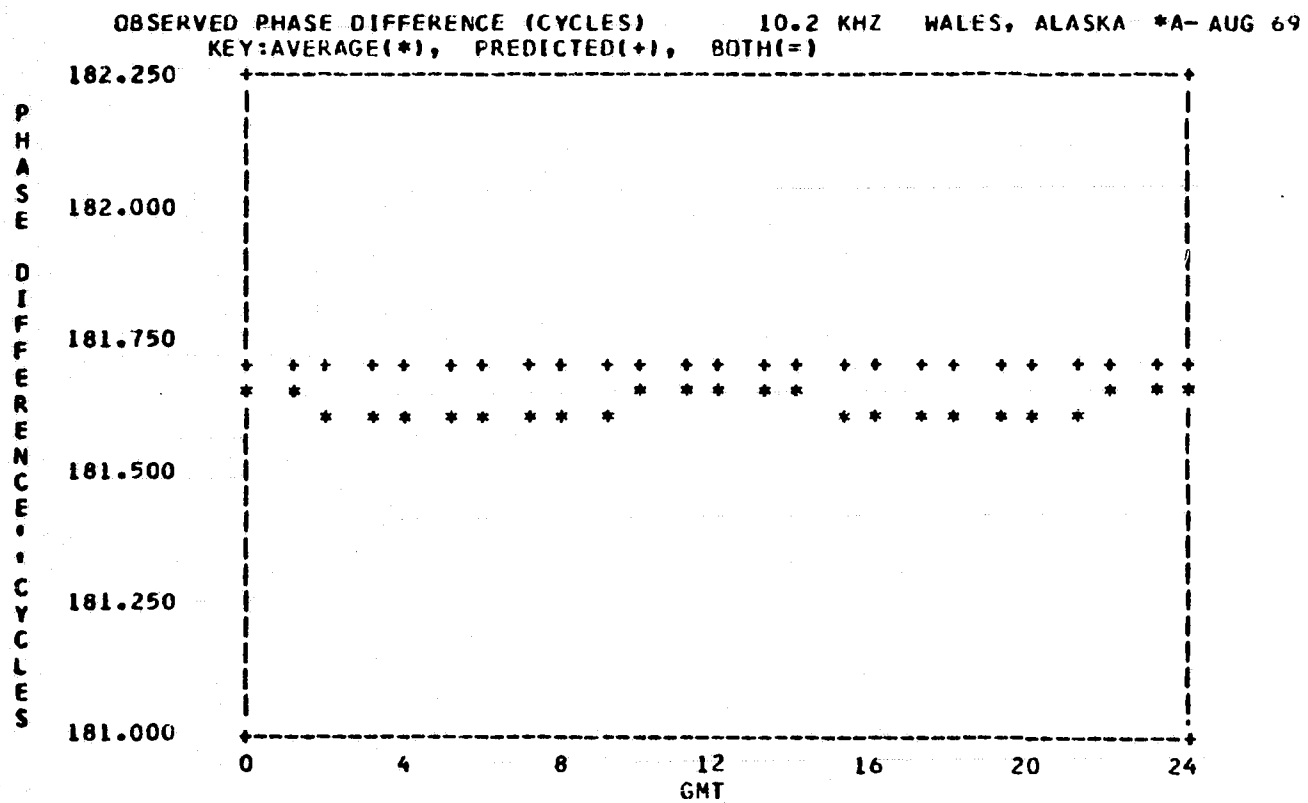


OBSERVED PHASE DIFFERENCE (CENTICYCLES) 10.2 KHZ																								ROME, N.Y.				B-D		JUN 69		NITE	
DATE	1	2	3	4	5	6	7	8	9	10	11	12	13	14	15	16	17	18	19	20	21	22	23	24			AV	SD					
	GMT																																
	N	N	N	N	N	N	N	N	N	N	N	D	D	D	D	D	D	D	D	D	D	D	D	D	D								
01 JUN 59	54	56	55	61	59	61	61	58	55	19	22	19	16	14	13	12	12	12	14	17	19	23	32	43	9	57.8	2.7						
02 JUN 59	53	59	58	60	62	61	61	61	55	17	22	19	17	15	13	11	12	13	14		20	23	32	45	9	58.9	2.9						
03 JUN 59	58	61	62	64	64	65	66	64	57	18	22	18	16	13	12	12	12	12	S14	S14	24	31	45	9	62.3	2.9							
04 JUN 59	56	60	60	61	60	62	63	63	56	19	22	19	14	13	11	S07	S97	S10	13	15	19	24	32	45	9	60.1	2.5						
05 JUN 59	54	61	S61	61	63	60	62	61	54	S18	S10	S11	13	S12	S95	S95	S03	08	12	15	S18		S31	S41	9	59.5	3.1						
06 JUN 59	S55	59	62	62	S62	S63	63	64	54	S17	S14	17	13	12	12	S11	S99	11	12	S11	18	24	32	S44	9	60.7	3.4						
07 JUN 59	S53	59	61	60	60	63	61	62	53	S18	S18	18	S11	13	12	12	12	13	S14	15	20	23	30	41	9	59.9	3.4						
08 JUN 59	52	55	62	63	61	61	63	62	53	17	21	19	15	13	S11	10	11	12	14	15	17	24	31	44	9	59.1	4.2						
09 JUN 59	54	58	58	58	59	57	56	58	54	18	21	19	14	12	11	11	11	12	13	16	17	21	32	46	9	56.9	1.7						
10 JUN 59	56	58	57	57	58	59	60	60	51	19	21	20	17	14	13	13	13	13	S13	15	19	24	31	47	9	57.3	2.6						
11 JUN 59	56	S59	59	60	59	62	64	65	56	20	23									14	17	20	24	33	46	9	60.1	3.0					
12 JUN 59	50	58	60	63	61	60	60	62	54	18	24	21	16	15	13	13	11	13	15	16	20	28	35	47	9	58.7	3.9						
13 JUN 59	55	61	60	61	60	59	60		54	21	23	20	17	14	12	S10	S02	S05	S09	16	20	25	34	45	8	58.8	2.5						
14 JUN 59	54	62	64	65	64	S62	62	62	54	19	21	19	16	13	13	12	12	13	14	17	S07	S08	S23	S44	9	60.9	3.9						
15 JUN 59	53	59	59	59	60	62	60	59	54	18	21	20	17	14	13	12	13	S10	15	16	20	25	33	43	9	58.3	2.7						
16 JUN 59	55	60	61	63	64	65	66	64	56	19	22	20	S11	13	13	13	12	12	S14	S16	S07	S15	S29	S46	9	61.6	3.7						
17 JUN 59	57	59	63	63	65	65	63	61	54	20	23	19	17	14	13	12	12	12	13	16	19	24	32	46	9	61.1	3.5						
18 JUN 59	57	63	61	62	62	62	61	60	58	18	22	19	16	13	11	12	12	S11	13	16	19	23	31	44	9	60.7	1.9						
19 JUN 59	53	61	63	64	63	59	56	56	51	18	22	19	16	14	12	12	12	S11	13	16	19	23	31	44	9	58.4	4.4						
20 JUN 59	56	59	58	60	60	63	65	62	53	19	23	19								16	20	23	31	43	9	59.6	3.4						
21 JUN 59	53	56	62	63	62	62	62	62	56	18	23	19	18	15	13	12	13	13	14	15	18	23	27	43	9	59.8	3.5						
22 JUN 59	55	58	57	58	58	59	57	58	53	20	22	20	17	13	13	12	12	13	14	16	19	25	31	44	9	57.0	1.8						
23 JUN 59	51	55	S57	57	55	56	58	57	51	21	21	20	16	14	13	13	12	13	14	16	20	24	30	44	9	55.0	2.4						
24 JUN 59	53	58	56	56	61	59	58	57	54	20	24	20	17	14	12	12	12	13	15	17	20	26	34	44	9	56.9	2.3						
25 JUN 59	52	55	56	56	59	60	62	58	52	21	23	19	17	15	15	12	12	13	15	17	19	24	33	42	9	56.7	3.2						
26 JUN 59	51	54	54	57	60	60	60	59	52	20	22	20	17	14	13	13	12	13	15	19	20	26	33	46	9	56.3	3.4						
27 JUN 59	53	55	58	59	59	60	65	65	59	20	23	20	17	15	13	12	13	13	15	16	20	25	34	42	9	59.2	3.7						
28 JUN 59	50	53	58	61	64	63	64	65	60	20	22	20	17	14	13	12	13	13	14	17	20	24	33	44	9	59.8	4.9						
29 JUN 59	57	57	61	62	59	61	62	61	58	19	22	20	17	14	13	12	12	13	14	17	19	26	32	45	9	59.8	1.9						
30 JUN 59	55	55	60	60	62	62		61	57	19	23	21	16	14	13	13	12	13	15	17	20	23	31	41	8	59.0	2.7						

GMT																								
	1	2	3	4	5	6	7	8	9	10	11	12	13	14	15	16	17	18	19	20	21	22	23	24
	N	N	N	N	N	N	N	N	N	N	D	D	D	D	D	D	D	D	D	D	D	D	D	D
54.0	58.1	59.5	60.5	60.8	61.0	61.4	60.9	54.6	19.1	22.2	19.4	16.1	13.7	12.6	12.1	12.0	12.3	13.8	16.2	19.3	24.1	31.9	44.2	
2.1	2.5	2.5	2.4	2.2	2.1	2.7	2.5	2.3	1.2	2.8	1.7	1.8	.9	3.4	3.3	4.3	1.8	1.4	1.4	3.2	3.6	2.2	1.6	

SWC																								
	1	2	3	4	5	6	7	8	9	10	11	12	13	14	15	16	17	18	19	20	21	22	23	24
- 46	- 46	- 46	- 46	- 46	- 46	- 46	- 46	- 46	- 40	- 10	- 7	- 4	- 2		2	3	3	2		- 2	- 4	- 7	- 10	- 35
- 46	- 46	- 46	- 46	- 46	- 46	- 46	- 46	- 46	- 41	- 10	- 7	- 4	- 2		2	3	3	2		- 2	- 4	- 7	- 10	- 33

RMS																								
	1	2	3	4	5	6	7	8	9	10	11	12	13	14	15	16	17	18	19	20	21	22	23	24
8.7	5.1	4.0	3.1	2.8	2.6	2.9	3.0	3.3	7.7	3.5	2.2	3.3	3.0	4.2	4.1	5.3	3.2	3.2	2.9	3.9	3.6	5.4	6.6	



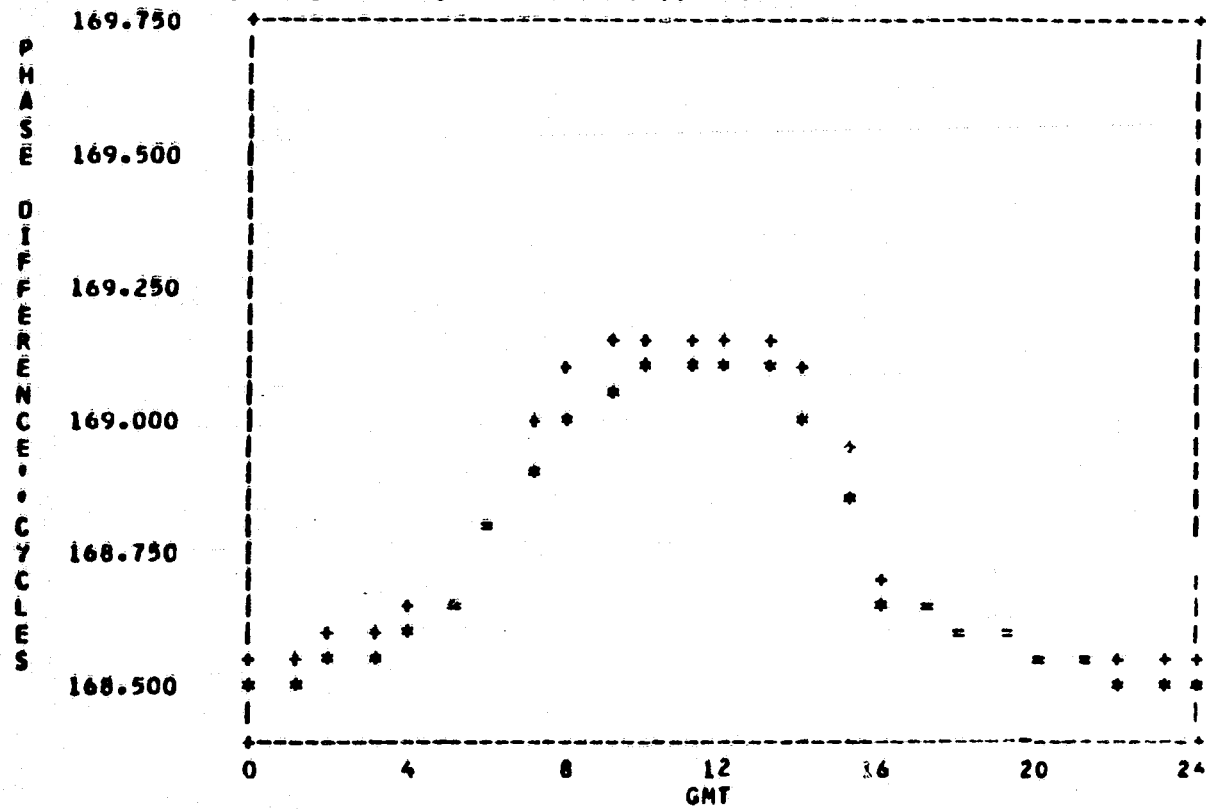
DATE	OBSERVED PHASE DIFFERENCE (CENTICYCLES)												10.2 KHZ								WALES, ALASKA								*A-	AUG 69		
	1	2	3	4	5	6	7	8	9	10	11	12	13	14	15	16	17	18	19	20	21	22	23	24	N	AV	SD					
1 AUG 69	65	S64	S60	S63	65	65	65	65	64	67	66	65	S63	S63	S63	S64	64	65	66	66	S66	S64	S66	S66	0	0.0	0.0					
2 AUG 69	65	64	64	64	65	65	64	64	63	64	65	66	S65	S62	S62	62	63	62	S63	S60	S58	60	60	61	0	0.0	0.0					
3 AUG 69	61	59	62	62	59	60	60	62	63	61	62	61	60	60	60	62	62	62	58	S58	S57	56	57	57	0	0.0	0.0					
4 AUG 69	59	S56	S57	58	59	59	59	61	62	62	61	59	60	61	62	62	60	60	S58	58	59	60	62	62	0	0.0	0.0					
5 AUG 69	61	62	61	59	58	58	56	58	61	62	64	60	S62	S60	61	61	61	61	S60	61	61	63	64	64	0	0.0	0.0					
6 AUG 69	64	61	59	55	58	57	56	57	59	62	64	65	63	61	61	62	62	63	63						0	0.0	0.0					
7 AUG 69																									0	0.0	0.0					
8 AUG 69																									0	0.0	0.0					
9 AUG 69																									0	0.0	0.0					
10 AUG 69																				S63	S64	65	65	66	0	0.0	0.0					
11 AUG 69	63	62	61	61	S59	61	61	61	61	58	64	S65	S63	62	S62	62	62	61	57	59	62	63	S63	64	0	0.0	0.0					
12 AUG 69	64	60	59	54	58	57	57	61	59	59	61	56	59	S61	S61	S62	S58	S51	S58	S58	59	59	S60	61	0	0.0	0.0					
13 AUG 69	59	58	59	59	59	59	58	59	60	59	59	60	62	62	61	61	62	62	61	61	61	58	60	61	0	0.0	0.0					
14 AUG 69	62	60	58	58	58	60	61	55	58	60	61	60	59	59	59	60	61	60	60	58	62	62	64	63	0	0.0	0.0					
15 AUG 69		62	61	61	62	62													63	S64	S65	63	63	64	0	0.0	0.0					
16 AUG 69	64	64	62	62	62	63	63	63	63	65	65	64	63	63	62	61	58	59	61	61	62	62	61	62	0	0.0	0.0					
17 AUG 69	62	60	54	54	55	58	59	58	61	62	63	63		63	62	62	63	62	60	60	60	60	62	62	0	0.0	0.0					
18 AUG 69	62	61	56	52	54	57	59	59	62	64	65	65	64	61	57	57	58	60	61	61	62	63	66	65	0	0.0	0.0					
19 AUG 69	62	60	56	53	55	58	57	59	59	62	63	62	59	60	60	59	54	53	57	60	60	64	62	62	0	0.0	0.0					
20 AUG 69	58	60	59	58	57	55	55	55	57	57	61	63	62	61	60	59	61	61	61	62	62	61	63	62	0	0.0	0.0					
21 AUG 69	63	62	59	59	56	56	56	59	62	66	67	66	65	S60	S58	58	56	59	59	58	62	61	63	63	0	0.0	0.0					
22 AUG 69	62	62	58	58	60	60	60	61	61	66	S66	S65	61	61	60	60	61	57	58	S59	S62	63	65	S65	0	0.0	0.0					
23 AUG 69	S61	57	55	58	57	54	58	60	63	63	66	63	64	61	S59	S58	S58	S59	S59	57	60	60	62	62	0	0.0	0.0					
24 AUG 69	62	58	56	59	52	52	53	56	59	63	65	65	62	S60	59	S58	59	S60	58	S59	S60	S62	64	64	0	0.0	0.0					
25 AUG 69	62	59	54	54	55	57	57	58	61	64	66	64	63	61	60	S60	S60	60	S59	S60	62	64	65	67	0	0.0	0.0					
26 AUG 69	66	62	59	59	58	57	S58		62	61	57	61	62	62	59	59	60	60	S61	S61	S61	65	67	67	0	0.0	0.0					
27 AUG 69	67	57	55	57	54	54	55	59	64	68	68	S66	S68	S64	S62	S57	S60	S60	S59	S61	S64	S64	S65	68	0	0.0	0.0					
28 AUG 69	68	63	61	59	58	58	58	60	65	69	65	69	71	67	64	62	61	62	59	63	65	67	70	72	0	0.0	0.0					
29 AUG 69	70	67	63	62	65	65	66	67	71	74	76	74	75	71	67	65	65	66	67	69	S72	76	76	75	0	0.0	0.0					
30 AUG 69	76	70	68	64	64	64	61	61	66	70	73	74	77	69	66	S63	64	65	67	69	67	71	75	76	0	0.0	0.0					
31 AUG 69	75	71		66	66	66	65	65	66	66	71	72	74	71	68	65	67	61	65	68	71	72	73	71	0	0.0	0.0					

	GMT																							
	1	2	3	4	5	6	7	8	9	10	11	12	13	14	15	16	17	18	19	20	21	22	23	24
	25	25	24	26	26	27	25	25	26	26	25	23	20	19	19	19	22	22	19	17	17	24	23	25
	64.1	61.6	59.1	58.7	58.8	59.1	59.2	60.1	62.0	63.6	64.7	64.2	64.2	62.9	61.5	61.0	61.3	61.0	60.9	61.6	62.2	63.1	64.8	64.8
	4.3	3.5	3.2	3.5	3.7	3.7	3.3	3.0	2.9	3.9	4.0	4.2	4.9	3.2	2.6	2.2	2.4	3.1	3.1	3.4	3.4	4.2	4.4	4.3

	SWC																							
	1	2	3	4	5	6	7	8	9	10	11	12	13	14	15	16	17	18	19	20	21	22	23	24
	2	2	2	2	2	2	2	2	2	2	2	2	2	2	2	2	2	2	2	2	2	2	2	2
	1	1	1	1	1	1	1	1	1	1	0	0	1	1	1	1	1	1	1	1	1	1	1	1

	RMS																							
	1	2	3	4	5	6	7	8	9	10	11	12	13	14	15	16	17	18	19	20	21	22	23	24
	6.0	7.6	9.8	10.1	10.2	9.9	9.8	8.7	6.9	5.9	5.6	6.0	6.2	6.5	7.4	7.8	7.7	8.4	8.4	7.9	6.7	6.6	5.6	5.4

OBSERVED PHASE DIFFERENCE (CYCLES) 10.2 KHZ MALES, ALASKA *C- MAY 69
KEY: AVERAGE (*), PREDICTED (+), BOTH (=)



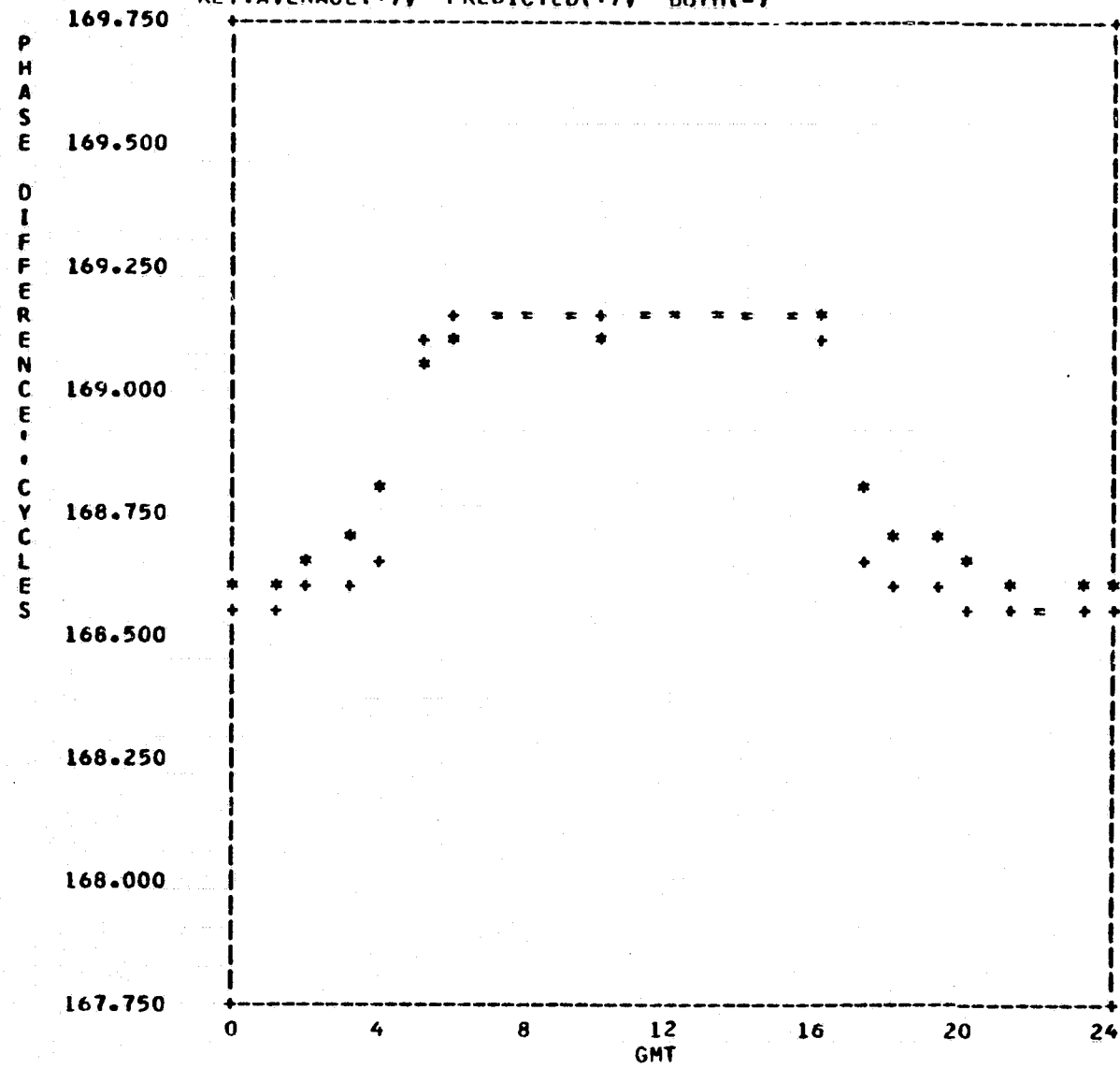
DATE	OBSERVED PHASE DIFFERENCE (CENTICYCLES)														10.2 KHZ						HALES, ALASKA						*C-		MAY 69	
	1	2	3	4	5	6	7	8	9	10	11	12	13	14	15	16	17	18	19	20	21	22	23	24	N	AV	SD			
8 MAY 69									N	N	N	N	N								D	D	D	D						
9 MAY 69	55	57	61	68	75	88	96	02	10	11	13	13	12							67	63	60	57	56	55	55	0	0.0	0.0	
10 MAY 69	54	57	61	67	74	89	01	04	09	09	10	15	11	08	94	68	67	63	60	58	55	54	54	53	5	11.8	1.2			
11 MAY 69	55	58	62	65	72	86	00	10	09	09	17	17	14	11	98	66	68	65	60	57	55	54	54	54	5	13.2	3.6			
12 MAY 69	55	54	59	64	70	86	96	07	10	12	13	11	09	03	87	65	66	63	60	57		54	53	52	5	11.0	1.4			
13 MAY 69	53	55	57	61	69	78	92	97	05	09	10	10	08	98	87	57	P60	P57	P55	P55	P54	P53	P52	P52	5	8.6	1.5			
14 MAY 69	P53	P54	P57	P61	P68	P80	P90	P96	P99	P04	P11	P11	P10	P04	P90	P68	P65	P62	P59	P56	P53	P52	P51	0	0.0	0.0				
15 MAY 69	P51	P55	P59	P63	P71	P86	P92	P92	P04	07	06	02	02	97	88	61	61	56	53	52	49	49	46	51	4	4.2	2.3			
16 MAY 69	52	54	57	61	S68	S82	88	97	02	03	05	06	05							58	52	53	50	51	53	5	4.2	1.5		
17 MAY 69	52	54	S45	55	64	79	88	94	03	07	11	08	04	94	S82	S62	S63	S53	S56	S1	S51	S50	S3	S3	5	10.4	3.0			
18 MAY 69	53	46	S45	55	64	79	88	94	03	07	11	08	04	94	S82	S62	S63	S53	S56	S1	S51	S50	S3	S3	5	6.6	2.9			
19 MAY 69	52	55	58	63	67	77	91	96	01	04	08	07	06	01	S82	60	59	58	55	51	47	47	50	S51	5	5.2	2.5			
20 MAY 69	S45	50	51	53	59	73	84	94	01	03	03	03	03	98	82	66	S65	60	59	S48	53	53	S49	50	5	2.6	0.8			
21 MAY 69	50	48	56	56	63	77	86	90	00	05	07	06	01	94	82	61	S62	59	55	52	49	47	46	47	5	3.8	2.8			
22 MAY 69	48	47	53	58	57	72	87	94	01	09	11	10	07	98	84	58	62	60	S58	S39	49	50	50	51	5	7.6	3.6			
23 MAY 69	53	54	57	61	66	76	92	01	06	13	15	13	09	99	79	63	63	59	56	54	53	53	52	51	5	11.2	3.2			
24 MAY 69	53	56	59	63	69	S81	89	97	03	07	S07	08	08	01	84	65	66	62	58	55	53	53	52	54	5	6.5	1.9			
25 MAY 69	52	52	55	58	63	76	87	93	01	03	09	12	09	03	84	62	S61	S57	54	52	S41	47	47	49	5	6.8	4.1			
26 MAY 69	50	49	54	58	64	74	87	91	01	06	11	11	09	00	83	64	66	63	57	56	54	53	51	52	5	7.6	3.8			
27 MAY 69	S44	53	57	62	67	77	89	98	05	07	08	15	14	04	88	62	64	62	60	58	56	55	54	55	5	9.8	4.0			
28 MAY 69	56	58	61	64	69	81	96	04	08	09	09	09	S09	99	S85	65	63	61	59	58	54	48	53	51	5	8.7	0.4			
29 MAY 69	47	55	58	63	61	77	89	02	09	12	15	11	09	03	S86	68	68	63	62	S36	52	51	53	53	5	11.2	2.2			
30 MAY 69	51	53	56	60	67	77	85	98	09	12	13	12	07	99	84	64	64	60	59	55	54	52	53	52	5	10.6	2.2			
31 MAY 69	54	56	58	62	70	78	93	01	06	09	11	14	13	05	86	64	66	62	59	S39	52	S34	46	53	5	10.6	2.9			

GMT																								
1	2	3	4	5	6	7	8	9	10	11	12	13	14	15	16	17	18	19	20	21	22	23	24	
								N	N	N	N	N	N								D	D	D	D
19	21	20	21	20	19	21	21	21	22	21	22	21	20	20	16	19	15	18	19	16	18	20	21	21
52.4	53.4	57.3	61.0	66.6	79.1	90.8	98.4	5.0	8.0	10.4	10.2	8.1	1.0	85.9	63.3	64.4	61.2	58.0	54.9	52.8	51.6	51.3	52.1	
3.2	3.4	3.7	3.7	4.5	4.6	4.6	5.1	3.4	3.0	3.4	3.7	3.5	4.3	4.2	2.9	2.4	3.1	2.6	6.7	3.6	4.5	2.7	1.8	

SWC																							
1	2	3	4	5	6	7	8	9	10	11	12	13	14	15	16	17	18	19	20	21	22	23	24
3	0	-2	-5	-8	-24	-45	-54	-54	-54	-54	-54	-54	-54	-48	-10	-7	-4	-1	1	3	4	4	3
3	1	-2	-4	-7	-18	-39	-51	-54	-54	-54	-54	-54	-47	-23	-8	-5	-2	0	2	4	5	5	4

RMS																							
1	2	3	4	5	6	7	8	9	10	11	12	13	14	15	16	17	18	19	20	21	22	23	24
5.2	5.6	5.4	4.0	4.3	3.6	8.9	12.7	8.4	5.6	4.2	4.5	5.7	7.2	7.7	4.8	2.2	2.8	2.6	8.4	4.4	5.4	3.7	3.3

OBSERVED PHASE DIFFERENCE (CYCLES) 10.2 KHZ WALES, ALASKA *C- OCT 69
KEY: AVERAGE(*), PREDICTED(+), BOTH(=)

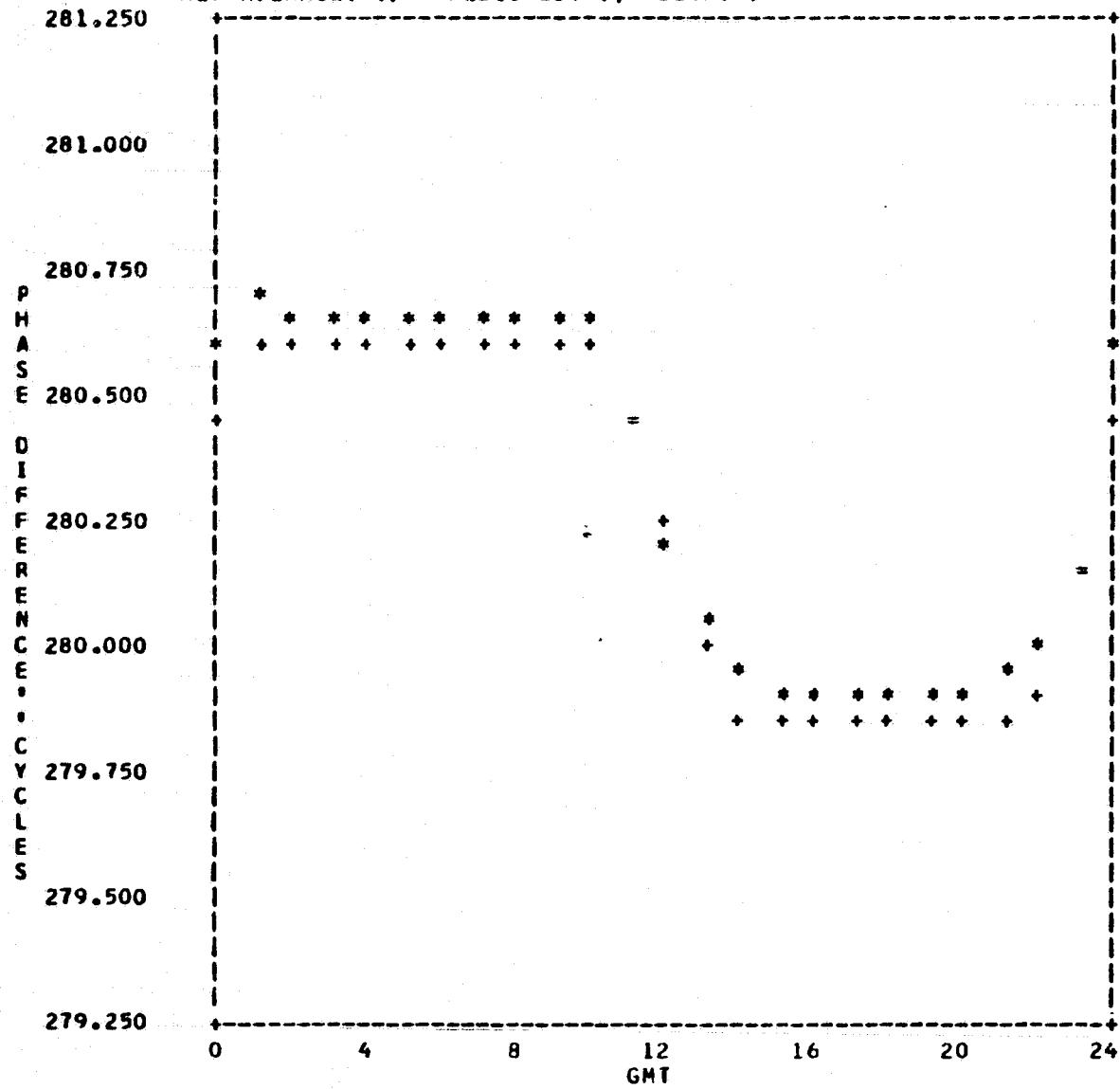


OBSERVED PHASE DIFFERENCE (CENTICYCLES) 10.2 KHZ																								WALES, ALASKA				*C-	OCT 69		
DATE	1	2	3	4	5	6	7	8	9	10	11	12	13	14	15	16	17	18	19	20	21	22	23	24	N	AV	SD				
	D	D				N	N	N	N	N	N	N	N	N	N	N	D	D	D	D	D	D	D	D							
1 OCT 69	S55	S55	58	62	97	06	14	12	12	11	13	11	11	12	11	11	54	55	58	57	54	50	51	S51	11	11.3	1.9				
2 OCT 69	S54	S53	56	61	96	08	06	09	11	07	S11	S09	S12	11	S11	S07	54	53	55	52	51	49	46	48	11	8.7	2.0				
3 OCT 69	S50	S51	56	58	94	05	08	05	07	C8	08	09	08	08	10	06	58	55	55	53	52	52	53	50	11	7.5	1.5				
4 OCT 69	51	53	57	63	96	07	08	09	08	08	10	13	13	14	11	13	S65	S61	57	56	51	51	51	52	11	10.4	2.4				
5 OCT 69	51	53	57	67	97	05	09	06	11	12	11	12	10	11	10	09	63	59	58	52	51	50	51	52	11	9.6	2.2				
6 OCT 69	51	55	63	67	95	02	08	12	11	13	14	S15	13	S12	S12	S09	S65	S59	59	S59	56	54	55	54	11	10.4	3.4				
7 OCT 69	51	57	S68	S70	S97	07	10	13	12	10	11	12	13	13	12	12	69	63	64	61	57	54	53	52	11	11.4	1.7				
8 OCT 69	54	56	61	68	S98	07	12	15	15	15	17	S19	16	12	08	S1C	S70	S61	S60	58	56	55	53	55	11	13.0	3.6				
9 OCT 69	53	56	61	68	01	09	10	11	09	09	11	14	15	16	S15	S14	69								11	11.6	2.6				
10 OCT 69	59	S61	S67	S68	00	07	07	07	14	08	09	13	S13	S12	12	12	S72	S67	S67	S57	S52	S52	S52	S56	11	9.9	2.6				
11 OCT 69	58	61	65	74	05	12	13	14	11	12	10	11	15	14	S14	S15	S77	67	65	64	60	55	S54	S43	11	12.4	1.6				
12 OCT 69	S58	S65	S64	71	03	07	12	15	15	15	18	19	18	16	14	14	82	70	67	64	61	57	57	58	11	14.7	3.0				
13 OCT 69	60	63	73	86	07	16	18	19	17	16	18	17	18	18	14	16	81	65	66	60	59	57	56	57	11	17.0	1.3				
14 OCT 69	60	64	73	86	10	15	16	17	14	15	15	20	18	16	16	14	81	S63	64		58	55	55	55	11	16.0	1.7				
15 OCT 69	56	S59	65	79	11	16	19	17	14	15	17	S16	S16	S17	S18	S18	S85	S78	74	68	65	61	62	63	11	16.3	1.4				
16 OCT 69	66	69	77	91	13	18	20	20	17	19	19	19	19	17	17	16	82	71	73	70	66	64	63	62	11	18.2	1.3				
17 OCT 69	63	65	74	89	10	15	17	17	18	17	18	15	15	14	18	20	90	77	75	S67	S61	S61	S59	S59	11	16.7	1.7				
18 OCT 69	57	64	71	86	07	13	17	14	13	13	14	17	16	15	17	18	89	71	S70	S66	S56	59	59	61	11	15.2	1.8				
19 OCT 69	S62	S65	73	88	11	15	17	18	18	14	S14	S19	S19	19	S18	S20	S88	S69	S70	S67	S61	61	61	62	11	16.8	2.0				
20 OCT 69	63	59	71	83	15	16	15	14	13	11	S12	S17	14	18	S19	S19	S87	70	74	67	60	53	S51	S47	11	14.4	2.6				
21 OCT 69	S58	65	73	89	08	10	13	15	16	14	14	14	14	17	18	S17	S87	S75	S72	S70	66	63	60	60	11	14.5	2.1				
22 OCT 69	64	67	81	92	09	16	16	13	10	12	11	S13	S14	12	14	S18	S94	S74	S72	S68	65	S62	S57	61	11	13.0	2.3				
23 OCT 69	63	71	81	94	13	15	14	12	11	12	12	12	S13	S16	S14	13	95	S77	S71	S67	68	57	S58	S59	11	12.6	1.4				
24 OCT 69	S62	S67	81	97	09	12	13	13	S14	S14	13	15	S14	S13	S11	S11	S93	81	76	68	S64	S64	65	66	11	13.2	1.2				
25 OCT 69	69	75	85	99	12	13	15	10	09	10	14	12	11	14	16	16	95	78	76	71	62	57	58	57	11	12.7	2.4				
26 OCT 69	S59	S62	S72	81	10	11	13	13	13	S09	11	13	S09	S12	S12	S14	S94	S74	73	68	65	64	64	67	11	12.3	1.6				
27 OCT 69	70	S76	S83	00	13	15	14	13	14	11	10	15	15	S16	S14	16	98	80	78	73	S68	S57	S64	66	11	13.7	1.8				
28 OCT 69	69	74	83	98	10	10	12	12	13	12	12	13	11	12	11	S13	S98	78	76	S73	S69	65	63	65	11	11.8	0.9				
29 OCT 69	67	72	S79	S93	11	13	14	13	14	13	14	12	11	11	12	97	S70	S67	62	61	61	61	62	11	12.7	1.1					
30 OCT 69	64	67	77	94	11	13	15	16	15	15	15	16	16	15	11	13	97	78	73	71	68	66	65	S66	11	14.5	1.5				
31 OCT 69	S68	73	84	01	13	14	16	17	17	15	15	14	11	09	13	13	99	79	76	72	68	66	62	64	11	14.0	2.3				

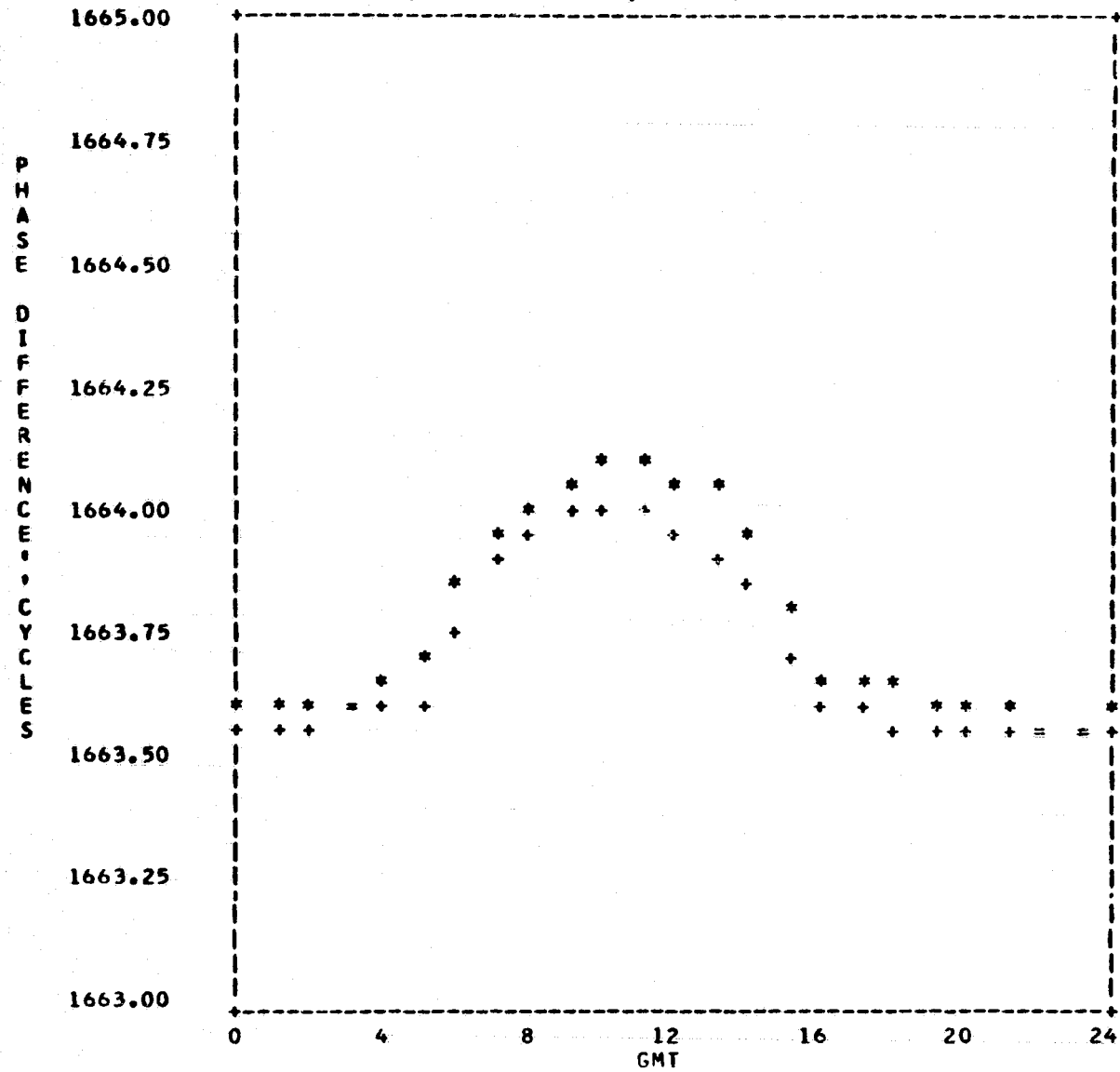
																								GMT			
1	2	3	4	5	6	7	8	9	10	11	12	13	14	15	16	17	18	19	20	21	22	23	24	N	AV	SD	
D	D				N	N	N	N	N	N	N	N	N	N	N	D	D	D	D	D	D	D	D				
60.0	63.8	70.2	81.9	6.4	11.2	13.3	13.3	13.1	12.5	13.3	14.1	14.0	13.9	13.2	13.6	80.7	69.4	67.8	63.3	60.0	57.4	57.6	58.7				
5.9	7.0	9.0	13.2	6.6	4.1	3.6	3.6	2.8	2.9	2.9	2.8	2.7	2.7	2.9	3.5	13.8	8.1	7.0	6.3	5.7	5.1	5.0	6.2				

																								SWC			
2	0	-1	-3	-50	-54	-54	-54	-54	-54	-54	-54	-54	-54	-54	-54	-4	-2	0	2	3	3	3	3	N	AV	SD	
1	-1	-2	-7	-54	-54	-54	-54	-54	-54	-54	-54	-54	-54	-54	-54	-13	-2	-1	1	2	2	2	2				
6.1	7.7	13.6	21.1	7.1	4.4	3.7	3.7	2.9	2.9	3.0	3.4	3.1	3.1	3.1	3.7	17.4	11.9	11.1	9.2	6.8	5.0	4.8	6.1				

OBSERVED PHASE DIFFERENCE (CYCLES) 13.6 KHZ NEL, SAN DIEGO, CAL 8- DEC 69
 KEY: AVERAGE(*), PREDICTED(+), BOTH(=)



OBSERVED PHASE DIFFERENCE (CYCLES) 13.6 KHZ PYRAMID ROCK HAWAII A-C MAY 69
 KEY: AVERAGE (*), PREDICTED (+), BOTH (=)



OBSERVED PHASE DIFFERENCE (CENTICYCLES) 13.6 KHZ														PYRAMID ROCK HAWAII A-C MAY 69															
DATE	1	2	3	4	5	6	7	8	9	10	11	12	13	14	15	16	17	18	19	20	21	22	23	24	N	AV	SD		
1 MAY 69	54	53	56	61	67	83	96	02	04	07	09	10	05	99	81	57	D	D	D	D	54	54	53	52	54	57	0	0.0	0.0
2 MAY 69	56	57	61	66	69		92	02	10	09	07	08	03	88	60	62	63	S38	S53	S47	49	49	48	52		0	0.0	0.0	
3 MAY 69	54	57	60	64	72	87	94										63	57	58	S51	55	53	55	56		0	0.0	0.0	
4 MAY 69	58	61	66	70	73		95	01	07	10	11	11	08	02	83	67	68	62								0	0.0	0.0	
5 MAY 69	56	55	61	68	76	91	00	08	14	11	10	S08	S98	94	81	S66	64	61	56	55	S50	51	53	49		0	0.0	0.0	
6 MAY 69	50	54		S61	68	88	95	00	05	06	08	07	07	96	81	S66	68	63	56	56	57	58		56		0	0.0	0.0	
7 MAY 69	57	56	58	65	67	82	98	05	08	11	11	11	09	02	84	69	73	70	68	65	63	63	64	66		0	0.0	0.0	
8 MAY 69	64	64	66	70	72	89	02	05	10	12	12	12	07	00	85	65	67	66	62	63	62	62	63	60		0	0.0	0.0	
9 MAY 69	59	59	63	69	72	89	97	04	07	08	07	09	09	02	86	68	71	69	65	64	62	63	58	58		0	0.0	0.0	
10 MAY 69	58	60	64	68	72	88			09	13	14	14	11	04	87	70	71	67	63	63						0	0.0	0.0	
11 MAY 69																								63		0	0.0	0.0	
12 MAY 69	63	63	68	71	78	94	04	11	13	16	13	11	09	00	85	70	73	70	64		63	60	60	60		0	0.0	0.0	
13 MAY 69	61	62	64	69	73	90	02	06	09	10	11	07	05	96	P76	P57	P50	P44	P42	P40	P40	P41	P41			0	0.0	0.0	
14 MAY 69	P42	P40	P40	P45	P52	P65	P74	P81	P86	P91	P90	P89	P88	P80	P63	P48	P50	P48	P45	P39	P38	P38	P39	P37		0	0.0	0.0	
15 MAY 69	P42	P47	P54	61	72	90	96	01	06	05	04	02	00	91	81	63	59	60	59	58	53	57	53	58		0	0.0	0.0	
16 MAY 69	58	59	66	71	S71	S86	94	99	02	03	02	03	01	97	86	70	72	66	65	61	59	58	59	63		0	0.0	0.0	
17 MAY 69	61	62	61	63	70	87	94	02	08	10	11	09	10	02	86	70	69	66	64	S46	S63	65	63	63		0	0.0	0.0	
18 MAY 69	53	53		60	68	80	92	97	03	09	06	02	02	96	S79	S67	S69	S54	S60	54	S55	S57	64	61		0	0.0	0.0	
19 MAY 69	62	64	66	71	74	82	95	02	03	07	12	06	04	93	S75	59	60	64	62	60	59	59	62	S60		0	0.0	0.0	
20 MAY 69	S55	59	58	60	67	82	91	00	02	03	06	07	03	S96	85	71	S69	68	64	S57	61	63	S60	S57		0	0.0	0.0	
21 MAY 69	57	50	62	60	66	81	92	96	01	08	07	05	03	91	75	62	S64	64	58	57	59	55	54	52		0	0.0	0.0	
22 MAY 69	54	58	61	65	62	80	95	01	07	11	11	07	02	93	77	62	66	63	S61	S40	56	58	59	60		0	0.0	0.0	
23 MAY 69	61	60	66	69	70	84	01	04	07	09	08	06	01	95	90	65	64	62	61	60	60	60	59	59		0	0.0	0.0	
24 MAY 69	62	64	67	71	74	S80	93	99	03	06	S05	07	06	93	77	65	68	64	63	61	59	58	56	61		0	0.0	0.0	
25 MAY 69	58	56	61	63	68	84	96	00	05	08	08	S07	S04	97	83	66	S59	S63	60	58	S44	54	51	54		0	0.0	0.0	
26 MAY 69	57	58	63	65	70	82	95	02	06	08	07	04	02	96	82	66	70	67	60	58	S56	57	59	60		0	0.0	0.0	
27 MAY 69	S45	S60	65	69	74	88	98	04	08	13	14	10	03	93	80	65	68	69	67	64	62	62	62	63		0	0.0	0.0	
28 MAY 69	63	66	68	72	75	82	97	08	09	09	07	03	S02	90	S71	61	59	60	60	60	57	S53	59	58		0	0.0	0.0	
29 MAY 69	S53	57	58	64	60	72	86	96	01	07	06	02	01	S93	S72	S65	66	63	61	S33	S46	44	45	47		0	0.0	0.0	
30 MAY 69	46	50	53	59	64	76	92	96	00	02	05	04	00	92	78	63	61	62	61	57	58	57	58	57		0	0.0	0.0	
31 MAY 69	59	61	63	66	70	82	93	01	05	08	11	10	06	98	80	63	69	67	63	S42	S53	S31	47	57		0	0.0	0.0	

GMT																									
1	2	3	4	5	6	7	8	9	10	11	12	13	14	15	16	17	18	19	20	21	22	23	24		
25	27	26	28	28	25	28	27	28	28	27	26	25	26	23	23	24	25	24	25	24	19	19	23	24	25
57.6	58.4	62.5	66.0	70.1	84.5	95.5	1.9	6.1	8.5	8.8	7.2	4.6	96.1	81.8	65.2	66.5	64.4	61.4	59.4	58.2	57.3	56.9	58.0		
4.7	4.1	3.7	4.0	4.0	4.8	3.8	3.7	3.5	3.1	3.1	3.2	3.3	4.1	4.2	3.5	4.2	6.1	3.6	7.9	5.1	6.9	5.2	4.3		

SWC																							
-117	-119	-120	-122	-124	-140	-154	-160	-163	-163	-163	-160	-156	-148	-132	-122	-120	-119	-117	-116	-116	-115	-116	-116
-116	-118	-119	-121	-123	-133	-149	-155	-158	-159	-159	-156	-151	-143	-127	-121	-119	-118	-116	-115	-115	-115	-115	-115

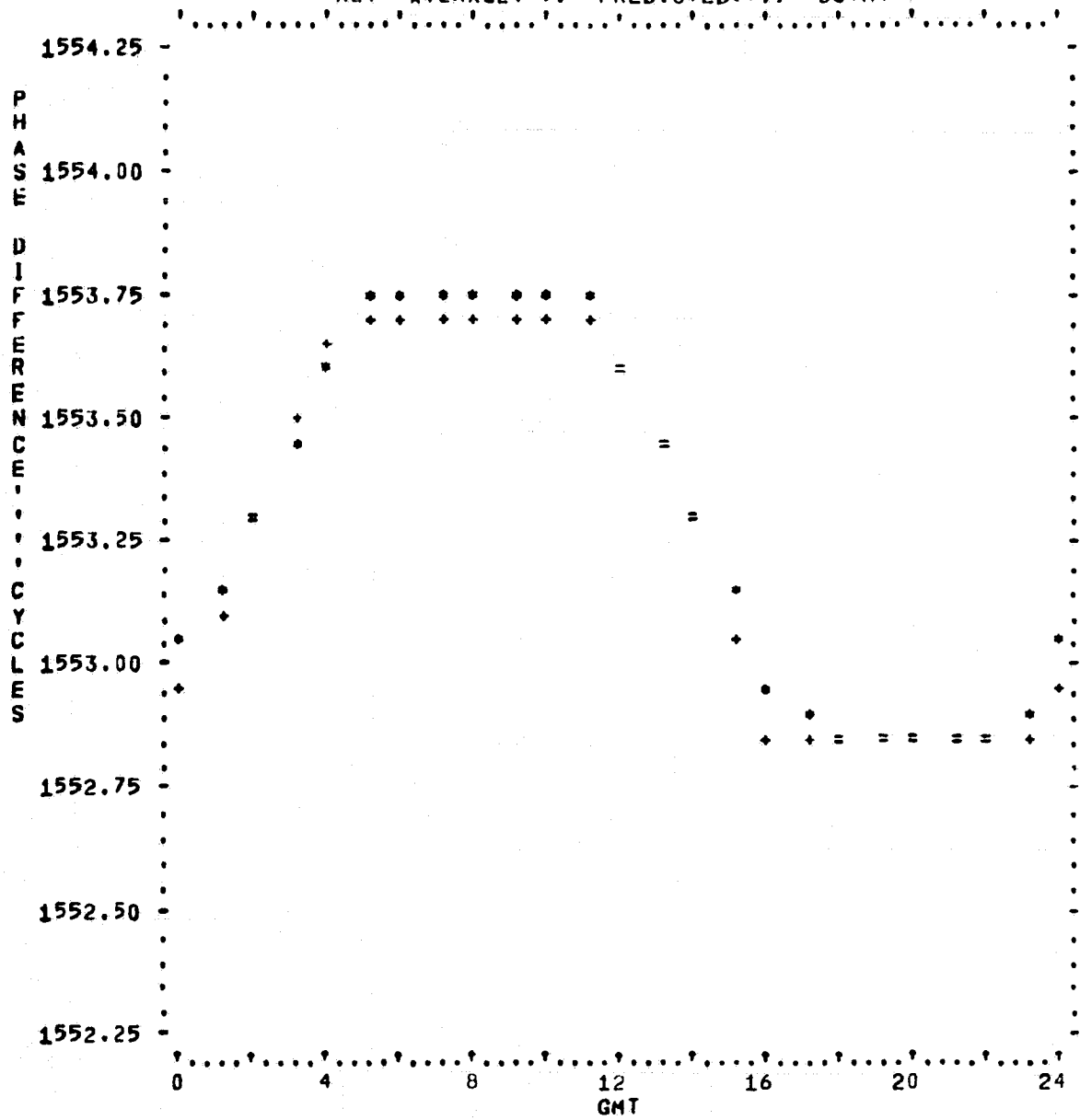
RMS																							
5.1	4.5	6.0	7.2	9.2	11.1	7.0	7.4	8.2	9.9	10.1	11.5	13.2	13.2	14.0	6.5	9.5	8.8	7.3	8.0	5.9	7.4	6.2	6.1

ROME, N.Y.

C-D OCT 69

13.6 KHZ

KEY: AVERAGE(*), PREDICTED(+), BOTH(=)



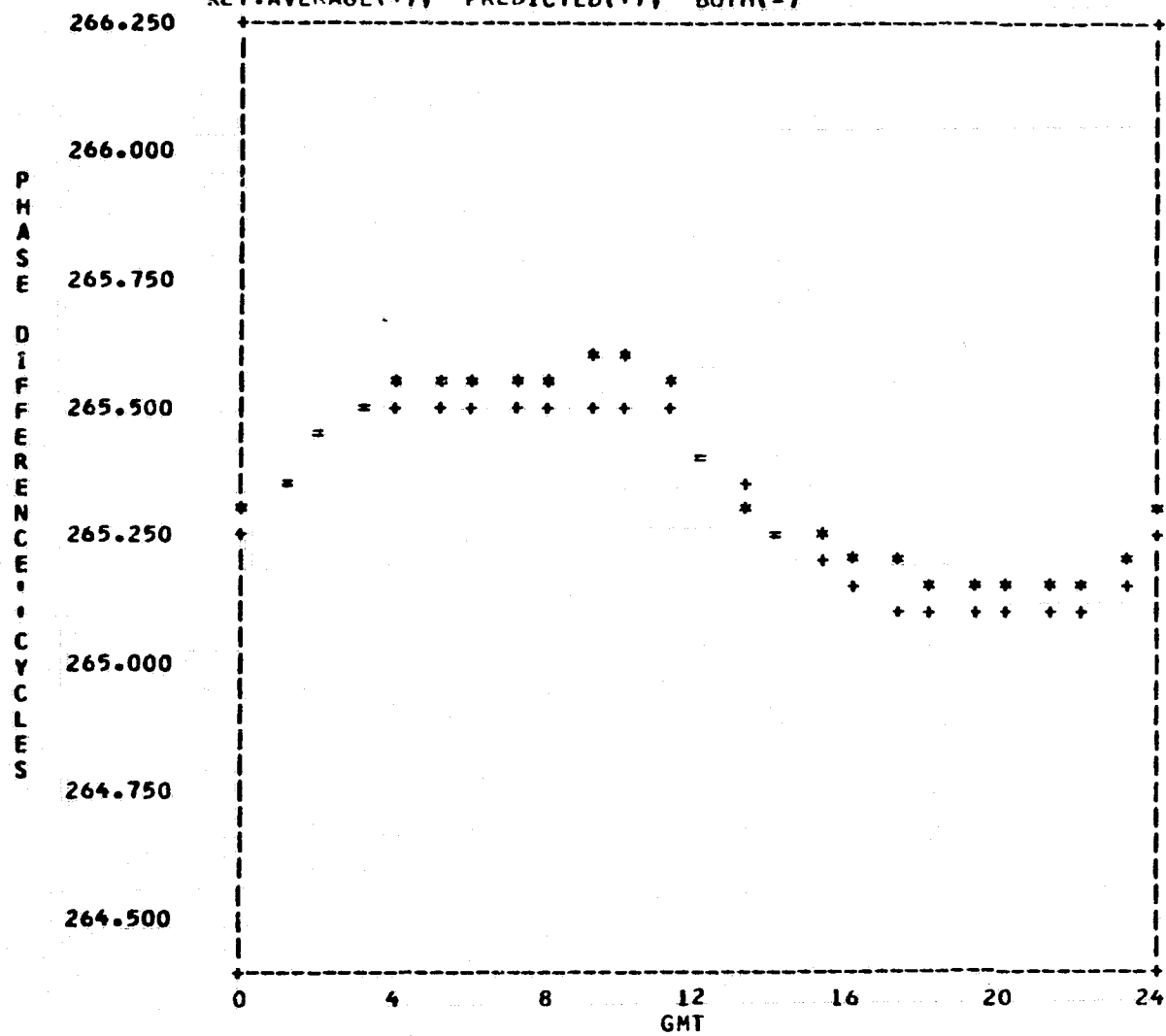
		OBSERVED PHASE DIFFERENCE (CENTICYCLES) 13.6 KHZ													ROME, N.Y.				C-D OCT 69				NITE						
DATE		1	2	3	4	5	6	7	8	9	10	11	12	13	14	15	16	17	18	19	20	21	22	23	24				
		GMT																											
		N													D				N			AV			SD				
01	OCT 69	S02	S19	33	54	57	70	72	69	69	67	57	49	38	27	11	83	83	83	83	81	80	78	78	S86	7	67.3	4.5	
02	OCT 69	S01	S15	32	49	59	71	73	66	64	59	S58	S40	S37	29	S10	S84	83	83	79	78	79	80	79	88	7	65.3	5.6	
03	OCT 69	S02	S19	40	53	61	71	73	71	69	69	61	53	40	26	07	81	80	81	79	77	78	78	83	90	7	67.9	4.5	
04	OCT 69	06	21	36	52	53	71	70	74	74	71	65	55	41	27	04	81	S79	S78	75	75	73	74	80	90	7	69.7	3.9	
05	OCT 69	98	09	27	46	50	66	71	67	71	71	66	55	41	24	07	87	81	82	83	78	78	78	79	88	7	67.4	3.7	
06	OCT 69	01	23	45	59	66	67	67	69	68	68	64	S58	44	S28	S10	S81	S80	S75	73	S74	76	75	79	88	7	67.0	1.5	
07	OCT 69	01	24	S45	S55	S61	69	71	75	73	75	71	57	41	29	12	87	84	83	83	81	82	84	86	93	7	72.3	4.5	
08	OCT 69	06	23	43	58	69	70	74	79	79	78	78	S61	47	32	11	S88	S83	S85	S83	80	79	81	85	01	7	75.3	4.0	
09	OCT 69	11	29	43	58	70	71	70	73	76	77	74	60	48	33	S14	S87	85									7	73.0	2.6
10	OCT 69	09	S25	S47	S55	57	72	74	73	76	79	73	57	S43	S28	12	89	S86	S84	S84	S78	S70	S72	S75	S91	7	73.4	3.4	
11	OCT 69	05	23	40	55	72	77	77	76	73	75	74	59	47	33	S14	S86	S85	86	83	84	85	85	S85	S86	7	74.9	1.8	
12	OCT 69	S08	S33	S46	56	69	73	76	74	79	80	75	60	49	36	16	92	87	85	83	82	82	82	85	98	7	75.1	3.4	
13	OCT 69	14	31	51	67	79	81	82	82	79	81	76	58	46	30	15	93	89	89	88	85	84	85	91	05	7	80.0	2.0	
14	OCT 69	19	35	52	69	79	81	81	83	81	79	79	59	47	32	17	94	89		86	84	83	83	87	02	7	80.4	1.4	
15	OCT 69	17	S34	52	68	92	83	82	83	81	81	80	S61	S47	S33	S17	S95	S90	S89	86	85	85	86	90	05	7	81.7	1.0	
16	OCT 69	20	38	54	70	81	82	83	83	83	82	85	65	49	34	17	94	88	87	87	85	86	84	87	03	7	82.7	1.2	
17	OCT 69	17	31	47	61	73	77	79	81	82	81	80	63							86	S78	S82	S86	S90	S04	7	79.0	2.9	
18	OCT 69	11	30	48	64	75	80	82	82	82	82	78	63	50	35	19	96	90	88	S87	S85	S80	87	94	11	7	80.1	2.5	
19	OCT 69	S28	S43	55	68	74	80	82	82	80	78	S80	S61	S49	36	S21	S97	S87	S85	S82	S84	S83	87	97	08	7	79.3	2.6	
20	OCT 69	21	33	48	64	77	79	78	75	75	77	S80	S63	51	35	S18	S94	S87	87	86	85	85	85	S86	S99	7	76.8	1.7	
21	OCT 69	S19	36	50	64	74	77	77	73	71	77	79	61	47	31	15	S93	S85	S80	S80	S82	83	85	91	03	7	75.4	2.6	
22	OCT 69	19	34	50	65	77	79	79	77	76	77	76	S60	S44	29	10	S91	S83	S84	S83	S81	83	S82	S86	03	7	77.3	1.2	
23	OCT 69	17	34	50	65	75	77	77	77	76	73	73	59	S45	S29	S10	92	86	S86	S82	S85	85	86	S90	S05	7	75.4	1.7	
24	OCT 69	S23	S39	55	70	79	81	80	80	S79	S77	77	59	S44	S29	S11	S92	S87	87	86	85	S85	S84	93	08	7	79.4	1.4	
25	OCT 69	22	37	52	68	80	82	83	80	79	80	77	59	45	30	16	96	88	88	86	86	86	86	95	11	7	80.1	1.8	
26	OCT 69	S26	S40	S53	66	74	76	78	80	80	S76	74	54	S44	S33	S20	S02	S83	S90	89	88	87	88	01	15	7	77.0	2.4	
27	OCT 69	29	S43	S54	65	75	76	76	76	75	74	73	58	44	S31	S14	03	92	91	90	90	S70	S86	S02	16	7	75.0	1.1	
28	OCT 69	29	43	55	65	70	73	73	78	78	79	77	61	47	35	19	S03	S93	93	90	S88	S88	87	99	17	7	75.4	3.2	
29	OCT 69	29	41	S56	S69	80	82	81	82	82	80	79	65	53	41	23	06	98	S94	S96	96	99	03	13	23	7	80.9	1.1	
30	OCT 69	33	44	56	70	81	85	82	84	83	80	78	65	58	44	27	08	97	96	94	93	95	98	08	S21	7	81.9	2.2	
31	OCT 69	S31	44	55	65	71	72	76	80	78	79	75	60	45	30	20	06	95	91	89	88	88	89	03	15	7	75.9	3.2	

		GMT																										
		1	2	3	4	5	6	7	8	9	10	11	12	13	14	15	16	17	18	19	20	21	22	23	24			
		N													D				N									
22	21	25	28	30	31	31	31	30	29	28	28	24	22	23	19	17	17	D	D	D	D	D	D	25	23	23		
15.2	31.6	46.8	51.9	72.6	75.8	76.7	76.9	76.4	76.2	74.1	58.9	46.3	32.1	14.6	93.4	87.9	87.1	84.7	84.7	84.7	84.7	84.7	84.1	83.5	84.6	90.6	3.5	
10.3	9.1	7.5	6.7	6.7	5.1	4.4	5.0	4.8	5.1	6.7	4.9	4.3	4.2	5.0	7.5	4.7	4.7	4.8	4.8	4.9	6.0	6.1	9.1	10.7				

		SWC																							
-119	-137	-155	-176	-179	-179	-179	-179	-179	-179	-179	-179	-169	-153	-136	-115	-97	-95	-94	-93	-93	-93	-94	-95	-103	
-126	-143	-161	-179	-179	-179	-179	-179	-179	-179	-179	-179	-173	-158	-141	-120	-97	-96	-94	-94	-93	-94	-95	-96	-110	

		RMS																								
8.4	7.3	5.9	7.9	7.6	9.0	9.4	9.8	9.3	9.2	8.6	4.7	3.9	5.3	8.7	9.8	4.8	5.3	4.9	5.0	5.8	5.8	10.0	10.4			

OBSERVED PHASE DIFFERENCE (CYCLES) 13.6 KHZ WALES, ALASKA *D- OCT 69
KEY: AVERAGE (*), PREDICTED (+), BOTH (=)



OBSERVED PHASE DIFFERENCE (CENTICYCLES) 13.6 KHZ													WALES, ALASKA								*D-		OCT 69					
DATE	GMT																											
	1	2	3	4	5	6	7	8	9	10	11	12	13	14	15	16	17	18	19	20	21	22	23	24	N	AV	SD	
1 OCT 69	S29	S34	36	N	N	N	N	N	N	N	N	N	17	16	14	10	05	02	05	06	10	06	07	S15	8	42.1	5.0	
2 OCT 69	S25	S27	34	43	47	42	44	42	44	34	S35	S27	S15	13	S13	S10	07	00	05	99	10	10	11	19	8	42.3	4.2	
3 OCT 69	S28	S30	35	39	45	51	49	57	54	57	43	27	11	10	11	04	05	05	06	06	05	10	11	20	8	49.3	6.2	
4 OCT 69	31	35	39	43	46	51	57	59	55	46	46	31	24	20	17	13	S10	S09	98	03	03	07	10	18	8	50.3	5.6	
5 OCT 69	27	32	36	49	54	57	59	60	53	49	45	31	28	27	18	17	11	09	10	05	03	04	03	18	8	53.2	5.0	
6 OCT 69	26	40	39	46	50	52	54	50	57	60	44	S30	26	S16	S15	S11	S96	S94	96	S04	08	08	10	48	8	51.6	5.0	
7 OCT 69	31	45	S46	S48	S53	58	53	52	55	55	50	34	23	24	25	23	10	06	10	11	17	19	16	19	8	53.8	2.9	
8 OCT 69	24	28	36	39	S49	47	49	51	52	51	S40	31	22	08	S06	S02	S08	S06	00	04	06	10	21	8	48.5	3.9		
9 OCT 69	24	31	40	49	56	56	48	50	56	56	50	37	19	19	S21	S15	10	S05	11	09	S10	00	00	11	8	52.6	3.4	
10 OCT 69	27	S41	S49	S43	54	50	60	64	66	65	46	39	S28	S23	16	10	S08	S16	S12	S08	07	S06	S12	S26	8	57.8	8.4	
11 OCT 69	36	47	50	52	61	58	53	52	56	59	46	31	26	16	S12	S21	S09	08	11	16	21	19	S11	S21	8	54.6	4.5	
12 OCT 69	S33	S47	S44	50	53	57	57	43	50	45	41	31	20	18	23	11	17	06	15	15	18	16	18	31	8	49.5	5.7	
13 OCT 69	40	45	57	60	64	62	58	59	65	68	42	26	28	26					11	16	11	14	11	20	29	8	59.7	7.4
14 OCT 69	32	50	54	58	58	59	55	57	58	60	44	31	19	21	11	12	08		11	04	05	99	09	14	8	56.1	4.8	
15 OCT 69	19	S27	38	43	48	48	47	50	47	54	45	S26	S20	S22	S20	S16	S10	S16	14	16	18	17	23	31	8	47.7	3.1	
16 OCT 69	38	44	52	52	56	56	54	53	59	64	58	41	39	43	32	22	19	10	14	18	12	14	12	30	8	56.5	3.6	
17 OCT 69	40	44	51	54	60	60	56	62	59	62	55	38							26	S27	S22	S20	S22	S30	8	58.5	2.9	
18 OCT 69	33	43	58	61	61	66	58	58	60	63	49	37	35	30	29	31	27	25	S27	S25	S18	32	46	54	8	59.5	4.7	
19 OCT 69	S59	S60	63	62	60	64	67	58	57	S56	S38	S27	18	S25	S24	S18	S18	S12	S12	S11	14	29	42	8	60.7	3.7		
20 OCT 69	47	46	50	57	60	65	57	60	62	70	S67	S44	37	37	S38	S27	S16	32	25	30	22	16	S14	S29	8	61.5	4.4	
21 OCT 69	S41	45	55	56	56	62	65	53	53	54	58	35	39	38	33	S20	S04	S05	07	S04	05	11	25	34	8	57.1	4.1	
22 OCT 69	39	50	57	61	62	59	59	63	67	49	S39	S27	19	20	S19	S12	07	S02	S03	11	S14	S26	40	8	59.9	4.8		
23 OCT 69	54	57	64	59	63	57	61	59	57	66	65	37	S31	S33	S39	30	28	S20	S23	S19	24	19	S16	S28	8	62.1	3.4	
24 OCT 69	S39	S44	53	60	49	54	58	57	S58	S59	59	39	S22	S21	S18	S19	S20	19	28	23	S22	S27	48	44	8	56.2	3.4	
25 OCT 69	43	51	69	67	65	64	63	62	64	65	61	51	40	41	41	39	32	27	26	26	29	21	29	29	8	63.8	1.8	
26 OCT 69	S34	S41	S48	57	60	59	61	53	61	S69	67	54	S42	S48	S43	S34	S30	S26	22	20	24	31	50	62	8	59.7	4.8	
27 OCT 69	70	S73	S70	73	74	70	73	75	66	62	57	54	37	S27	S25	19	26	31	34	30	S18	S11	S21	29	8	68.7	6.1	
28 OCT 69	39	48	58	62	62	60	60	67	64	68	69	52	46	46	40	S29	S26	16	24	S28	S29	18	30	35	8	64.0	3.4	
29 OCT 69	45	54	S61	S67	67	67	64	65	68	67	69	51	44	44	41	33	30	S33	S27	17	19	29			8	66.7	1.5	
30 OCT 69		48	58	58	66		63	63		68	69	52	43	45	47	34	31	30	18	21	24	25	36	S44	6	64.5	3.7	
31 OCT 69	S55	55	63	65	61	61	64	55	58	63	62	37	30	22	23	20	20	15	21	20	22	23	37	38	8	61.1	3.1	

GMT																							
1	2	3	4	5	6	7	8	9	10	11	12	13	14	15	16	17	18	19	20	21	22	23	24
			N	N	N	N	N	N	N	N	N	N	N	N	N	N	N	N	N	N	N	N	N
21	21	25	28	29	30	31	29	29	28	24	22	23	18	16	16	18	18	24	22	24	26	23	23
36.4	44.7	49.8	54.0	57.3	57.3	57.0	56.6	57.9	57.8	52.9	38.2	30.1	26.7	24.9	20.5	17.8	14.4	14.7	13.9	13.9	14.8	21.2	31.1
11.3	10.2	10.4	9.1	7.2	6.4	6.7	7.0	6.3	8.7	10.2	8.9	9.2	10.8	11.1	9.1	9.8	10.3	9.4	9.3	7.8	8.5	12.9	12.0

SWC																							
-110	-117	-123	-127	-128	-128	-128	-128	-128	-128	-128	-127	-116	-107	-100	-94	-89	-88	-88	-88	-88	-88	-88	-88
-116	-123	-127	-128	-128	-128	-128	-128	-128	-128	-128	-128	-121	-112	-105	-99	-93	-89	-88	-88	-83	-88	-89	-108

RMS																							
9.8	9.0	9.4	9.3	9.1	8.8	8.8	8.8	9.1	11.2	10.0	8.9	8.7	9.4	10.5	9.4	10.1	10.7	10.1	9.7	8.6	8.7	12.5	10.3

TABLE 2. SUMMARY OF PHASE MEASUREMENTS 1-8.

f	Monitor Site	Time Period	XMTR	LOP	Night			Transition			Day			24 Hours		
					N*	RMS	σ	N	RMS	σ	N	RMS	σ	N	RMS	σ
10.2 kHz	Rome, New York	Jun 69	Trinidad	129.165	268	4.34	2.38	149	5.60	2.42	285	3.63	2.55	702	4.37	2.46
	Wales, Alaska	Aug 69	Norway	181.696	—	—	—	502	7.66	3.77	130	7.56	2.73	632	7.64	3.58
		May 69	Hawaii	168.586	109	5.81	3.45	309	6.42	4.10	87	4.28	3.32	505	5.99	3.84
		Oct 69			341	3.35	3.17	154	15.06	10.54	241	7.37	6.07	736	8.39	6.32

10.2 kHz Median	cec	5.83	3.03	6.81	3.71
	μ sec	5.7	3.0	6.7	3.6

13.6 kHz	NELC, San Diego, California	Dec 69	Trinidad	279.089	80	6.03	3.98	101	8.99	4.08	24	7.41	1.21	205	7.80	3.82
	Pyramid Rock, Hawaii	May 69	Norway	362.385	—	—	—	574	8.75	4.43	83	8.48	4.76	657	8.72	4.47
	Rome, New York	Oct 69	Hawaii	351.895	217	9.01	5.47	365	7.62	7.46	148	5.18	5.07	730	7.64	6.48
	Wales, Alaska	Oct 69	New York	264.234	246	9.36	7.84	301	9.71	10.65	182	9.64	9.19	729	9.58	9.42

13.6 kHz Median	cec	7.95	4.92	8.26	5.48
	μ sec	5.8	3.6	6.1	4.0
Average	μ sec	5.8	3.3	6.4	3.8

*Number of samples

either by direct calibration or by deduction using other propagation paths, the path can then be used for epoch measurement. An example is the observation of Omega New York at the U.S. Naval Observatory. Although the recorded value is about 40 μ sec from anticipated, the measurement is stable.¹⁰ Calibration techniques are described in appendix D.

FREQUENCY ESTIMATION TECHNIQUES

Frequency estimates: regression of phase on time

As described previously, frequency estimates are best obtained by making a regression of phase on time using periodic measurements of estimated epoch error. Usually, long-term estimates are desired, in which case the time interval over which the regression is conducted is long with respect to the inherent autocorrelation period of the medium. In any case, the frequency is obtained from

$$f = \frac{12 \sum_{i=1}^n i \phi_i - 6(n+1) \sum_{i=1}^n \phi_i}{Tn(n^2 - 1)} \quad (3)$$

where ϕ_i = phase estimate at the i^{th} interval in cycles

T = period between measurements in seconds

n = number of phase measurements

as previously given and derived in appendix A. If the epoch estimates are made sufficiently far apart that they are uncorrelated, then the accuracy of the frequency estimate obtained from equation (3) is derived in appendix A as

$$\frac{\sigma_f}{f} = \frac{\sqrt{12}}{T \sqrt{n(n^2 - 1)}} \sigma_t \quad (4)$$

when σ_t is the standard deviation of epoch measurements in seconds.

If the phase measurements are accurate to 1 μ sec, an accuracy of one part in 10^{11} can be obtained after 2 days while a precision of 10^{-12} is obtained after about 10 days and 10^{-13} after 2 months. A plot of the anticipated precision in frequency as a function of the observation period is given in appendix A (fig. A2).

Seasonal effects

Equation (4) applies only when the variations in the epoch estimates are not autocorrelated. For example, seasonal changes in propagation at 10.2 kHz, if not corrected with appropriate propagation predictions, can yield an apparent frequency error of 2×10^{-12} . Obviously, any seasonal phase changes not removed properly by predictions will be

10⁻¹² expected in 1 month

correlated over long periods and will introduce frequency error. Similarly, if the observations times were chosen improperly and significant diurnal changes were occurring, large frequency errors could be introduced. Seasonal or periodic variations are discussed in appendix E.

Phase stability quoted in the previous section, 3.8 μ sec, may be used with equation (4) to calculate the accuracy of frequency estimates derived from a single daily Omega epoch measurement where the observation time has been selected at random. Table 3 gives results for relevant frequency stabilities.

TABLE 3. ACCURACY OF FREQUENCY ESTIMATED FROM REPEATED OMEGA EPOCH MEASUREMENTS (RANDOM OBSERVATION TIME).

Frequency Stability	Observation Duration, Days Spanned
10 ⁻¹¹	6
10 ⁻¹²	26
10 ⁻¹³	133

Were the observation time favorably chosen, techniques employed to eliminate anomalous data or to introduce redundancy would improve the anticipated frequency stability. Note that fixed prediction or instrumentation errors do not introduce errors in frequency.

Figure 3 shows a regression of phase on time that can be used to deduce frequency. The data illustrate long-path measurements which could be obtained using 12.0 kHz with the U.S. Master Clock exciting the transmitter. In practice, the data were gathered by a reverse arrangement and are derived from daily measurements at the Naval Observatory¹¹ of the 12.0-kHz transmissions from Omega Trinidad, as published in reference 10. The radio path length is 3468 km, and the time reference at the receiving site is the U.S. Master Clock. Epoch errors were derived as previously indicated using sky wave corrections interpolated from those for 10.2 and 13.6 kHz. Since Trinidad is controlled to follow the Naval Observatory, a direct comparison of the indicated epoch error would be illustrative of success in controlling the Omega system as well as propagation and frequency estimation. To eliminate complexity, the measurements have been adjusted by the known phase shift introduced between one of the cesium standards at Trinidad and the transmitter. The adjustment renders the plot equivalent to transmitter excitation directly from the chosen cesium; hence, the plot is a comparison of a particular cesium standard to the U.S. Master Clock using an Omega vlf link. The standard used, cesium serial 112, was chosen for its exceptional stability. Although propagation fluctuations cannot be completely distinguished from cesium fluctuations, the shorter-term fluctuations and probably most of the fluctuations over periods of a month or two are believed to be due to propagation. The cesium appears to have been not only amazingly constant in frequency but also nearly on the precise frequency. Over the 1-1/2 years covered in the plot, the total phase shift was less than 30 μ sec,

**Experimental measurements:
12.0 kHz; Trinidad to Naval
Observatory**

indicating a typical frequency offset of 6×10^{-13} . During part of the period, one of the other cesium standards at Trinidad was also exceptionally stable and in excellent agreement with cesium serial 112. Throughout the entire period, three cesiums were intercompared at Trinidad, thus enhancing confidence in the performance of the chosen cesium.

Four 60-day periods were selected from figure 3 for frequency estimation (table 4).

TABLE 4. FREQUENCY ESTIMATION OVER SELECTED PERIODS.

Period	Frequency Est.	Remarks
May-Jun 70	$(15 \pm 12) \times 10^{-14}$	numerous propagational disturbances, particularly magnetic storms
Jul-Aug 69	$(-2 \pm 4) \times 10^{-14}$	stable propagation during summer
Mar-Apr 69	$(104 \pm 7) \times 10^{-14}$	apparent uncorrected seasonal change
Mar-Apr 70	$(139 \pm 5) \times 10^{-14}$	apparent uncorrected seasonal change

During the most disturbed period, the confidence in the frequency estimate was 12 parts in 10^{14} , while under more favorable conditions, confidence on the order of five parts in 10^{14} was obtained. Significantly, the frequency estimates do not agree as well as might be expected from the confidence calculations. Presumably, the differences are due to slow long-term variations in the frequency of the standard itself, uncompensated seasonal propagation change, or both. The first two estimates are statistically comparable but are not compatible with the last pair of measurements. However, the latter two measurements are both believed contaminated by uncorrected seasonal variation and are approximately equal to each other. Apparently, uncompensated seasonal propagation change has limited accuracy to perhaps one part in 10^{12} during the March - April period. Since the seasonal errors introduced in 1969 appear to have been repeated in 1970, a self-calibration of the path would be practicable. The frequency estimates for the March - April period in 1969 are not, however, in perfect agreement with those made in 1970. The data indicate to 99-percent confidence that the standard changed frequency between 1969 and 1970.

Direct comparisons between frequency measurements by flying clock and frequency estimates obtained from long vlf paths have also been made by Kugel using the specialized case of the Omega interstation paths.⁹ Since measurements are made at both ends of these 'reciprocal' paths, calibration of reciprocal propagation phenomena is possible. Thus,

Confidence: 10^{-13} in 2 months

Seasonal limitation: 10^{-12}

TRINIDAD CESIUM 112 PHASE SHIFTER POSITION, μ SEC

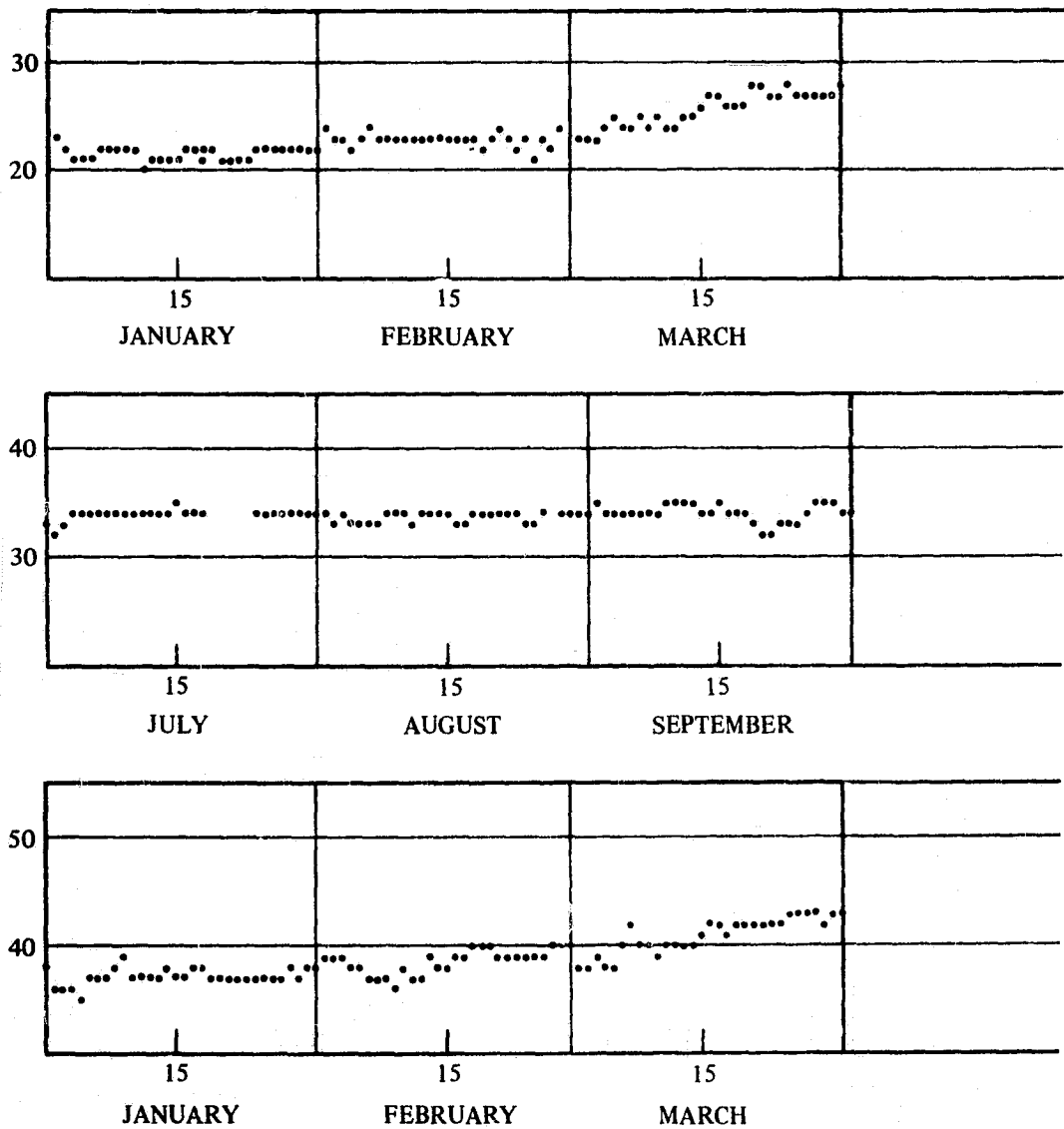
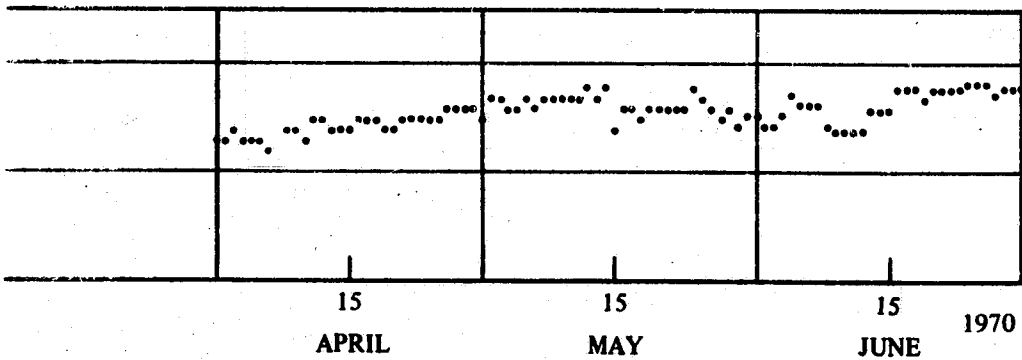
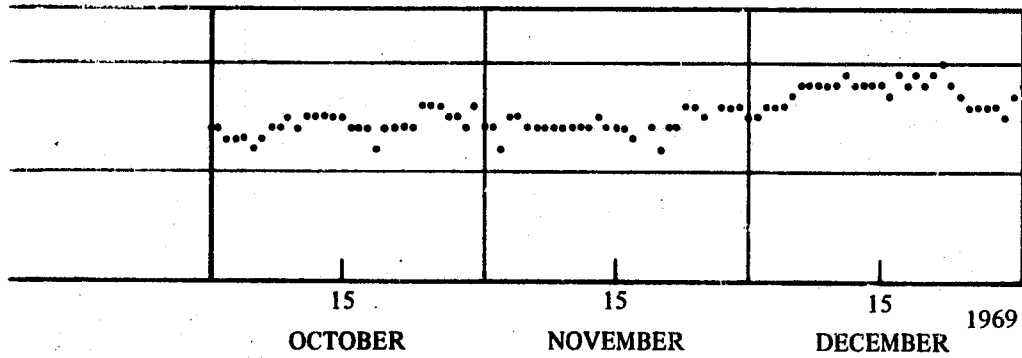
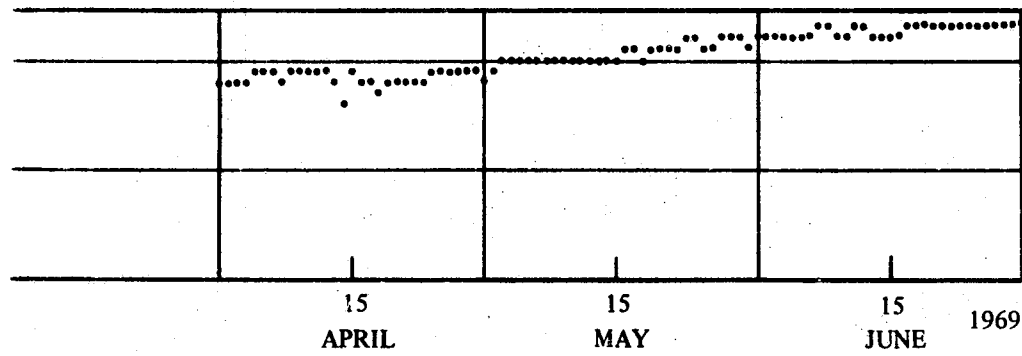


Figure 3. Frequency offset of cesium 112 from Naval Observatory master clock.

Direct flying clock comparisons: better than 10^{-12}

the epoch errors are of higher quality than normally would be expected. Discrepancies between frequency estimates using a 60-day regression and short-term (2-3 day) measurements by flying clock were less than one part in 10^{12} . The discrepancies are believed due primarily to uncertainties in the short-term measurements and experimental complications rather than the radio determination.

Although of little interest at a timing site in continuous operation, techniques also are available to make short-term frequency estimates such as might be needed in an emergency resulting from gross malfunctions. In this case, measurements are made over a duration short with respect to the autocorrelation period of the propagation medium. As shown in appendix A, we might expect to be able to obtain frequency estimates



accurate to about one part in 10^9 in 15 to 20 minutes using a propagation path stable to $1 \mu\text{sec}$. Wright made direct measurements using Omega signals received in Austin, Texas, to deduce the accuracy of short-term velocity estimates.¹² Although Wright's interest was in deducing the velocity and he made no mention of the accuracy in frequency estimation, the two are equivalent, since

$$V = \frac{(\Delta\phi) \lambda}{t}$$

where $\Delta\phi$ = phase change in cycles

λ = wavelength

t = time separation between observations

Since Wright obtained 0.2 knot during the day and 0.5 knot at night for a 15-minute observation span, the observed phase changes must have been 0.35 and 0.9 cec; i.e., 0.3 and 0.7 μsec , respectively. The corresponding frequency estimates are thus accurate to about 5×10^{-10} . Direct measurements thus show a better capability for short-term frequency measurement than indicated in appendix A.

**Fast estimation: 5×10^{-10} in
15 minutes**

AMBIGUITY RESOLUTION PROBABILITIES

Ambiguity or epoch resolution does not have intrinsic accuracy characteristics but instead must be considered on a probability basis. The relevant quantity is the probability that a certain epoch (3.4, 1.133 kHz, etc.) can be correctly identified within another larger but possibly ambiguous epoch interval. For example, a user with only the three simple carrier signals would need some additional information in order to resolve the ambiguity of the 1.133 epoch. Because such information from other Omega frequencies, pulse techniques, satellite updates, etc., most likely will be available, this section will concentrate on the resolution probability for the 3.4 kHz.

**Ambiguity resolution: proba-
bility of success—not accuracy**

Such resolution, of course, will depend directly on the ability to predict the carrier phase delays at the various monitor sites. Assuming that prediction capability is constantly improving and that results from past operation will be applicable to the future, we may consider some statistical studies undertaken to investigate lane resolution probabilities. These studies are summarized in references 13, 14, and 15, which present results based on thousands of hours of phase data taken at Omega frequencies at several sites around the globe. Although the reader may consult the references to assess the significance of the statistics to the data under consideration, the overall impression is that lane resolution is possible under all but a few types of serious propagation conditions; notably, PCA and SID onsets and large diurnal transitions. The ability to maintain the difference frequency epoch under disturbed conditions depends not only upon the behavior of the ionosphere, but also upon the ability of different receiver channels to respond similarly and of recorded tracks to indicate the same time on all frequencies. Some of the lane resolution failures found in the aforementioned studies possibly resulted from data being taken on different receivers and recorders, which may cause serious problems during rapid phase changes or high noise conditions. Experience has shown that Omega receivers exhibit a wide range of dynamic response depending upon integration time constants and sensitivity.^{16,17} Such variations may produce significantly different behavior

High probability of success

during large PCA onsets which have been known to exceed 1 cycle of carrier phase in a few minutes. The user likely will be aware of disturbances as they occur and will not worry about apparent lane loss at those times. However, without some additional warning service to corroborate the existence of a disturbance, the sight of all carrier phase tracks moving downscale simultaneously might lead the user to suspect his equipment, and some additional checks could be made. (If the monitor is on the sunlit side of the earth, all paths are partially sunlit and would react to a disturbance. The difference in the reactions distinguishes clock failure from an SID, as some paths will be affected more than others.

If possible epoch loss during disturbances can be avoided, or at least recognized, there still remains the problem of prediction errors during undisturbed times. Evidently, if the 10.2-kHz carrier phase cannot be predicted to within 50 cec, the correct 10.2 lane cannot be established. However, such data would not be of use for fine epoch estimation but could still be used to resolve the 3.4 epoch provided the 13.6-kHz phase has a similarly gross prediction error (also of the same sign). Long path measurements between the Omega stations indicate that the direction, if not the magnitude, of prediction error bias tends to be similar on all frequencies.

Possible exceptions to this are polar paths, which only recently have received the attention they warrant,^{18,19} and equatorial propagation in general.^{20,21} *OPERATIONAL CONSIDERATIONS, Path Selection*, discusses prediction problems more completely and considers the types of paths which are most likely to cause trouble.

Note that there are two separate and distinct needs for epoch resolution at a timing site—initialization and verification. When first established, the timing site must determine crude epoch. For example, the initial epoch determination of the 3.4-kHz (294- μ sec) period from 10.2- and 13.6-kHz measurements must rely on propagation predictions. However, the initial measurements can be made over several propagation paths during stable periods so as to minimize the effects of prediction errors. Since the probability of an epoch error in a daytime measurement over a single path is less than 10^{-3} , the probability of obtaining the same epoch error over several paths under stable conditions should be vanishingly small. Once the epoch has been set initially, continuous measurements can be made and any residual prediction differences noted. Therefore, subsequent epoch verifications need not be degraded by differential prediction errors between the various frequencies. In essence, a 24-hour capability for epoch verification or reestablishment is obtained.

The probability of an epoch resolution error can be reduced almost to an arbitrarily small value. The technique of 'selective resolution' demands that a 'good' epoch match be obtained from the two measurements being employed to resolve epoch. For example, if a 10.2-kHz carrier phase of 0 cec is indicated, we should like the 3.4-kHz beat to measure 0, 33, or 67 cec exactly. If the actual measurement is 16 cec, then the best estimate would be that the epoch was in the first period of

Initialization: prediction required

Verification: calibration possible

Timing requirements difficult to specify

the 10.2 kHz, but the estimate would be nearly a guess, since a difference measurement of 17 cec would have yielded the second 10.2-kHz period as the best estimate. By demanding close epoch agreement, we reduce the probability of epoch resolution, since no choice will be forced under marginal conditions. However, the probability of *incorrect* epoch resolution is vastly reduced. During the day, it is possible to reduce the probability of correct 10.2-to-13.6-kHz resolution from 0.999 to 0.998 while reducing the probability of incorrect identification from 10^{-3} to 10^{-5} . If even closer agreement is required, the probability of error can be further reduced.

Since the epoch resolution capability is due primarily to the high correlation of phase fluctuations at different frequencies over the same propagation paths, attempting an epoch resolution using measurements on different frequencies over different paths will generally result in an excessive number of failures. However, if the phase measurements normally made to adjust fine epoch are taken during favorable periods and if residual prediction errors are removed, the accuracy and correlation of the measurements over two separate paths might be adequate for continuing epoch verification. If the coarse epoch is indicated as questionable, then epoch resolution measurements over common paths can be made. Otherwise, the epoch would be verified by the usual adjustment measurements. This procedure reduces the number of measurements required while still yielding a significant number of relatively independent observations. Of course, personnel making the calculations must recognize the possible implications of large disagreements in epoch estimate.

PROBLEM ANALYSIS

Timing requirements typically are among the hardest to specify. In practice, timing specifications often result which are not appropriate for the timing uses which must be provided. For example, if a clock to be provided for a given operation must operate reliably to a typical accuracy of 10 μ sec for 1 year, the resulting specification might require a frequency standard with a stability of 3×10^{-13} and an MTBF of 10 years. Not only is such a standard unavailable, it is unnecessary. If the standard were available, it might not be an acceptable solution, since even though the probability of a failure would be small, any failure would be catastrophic, in that the clock could not be reset. The original requirement had been for a method of determining *epoch*, which could have been satisfied by radio methods using a moderate-quality quartz oscillator.

Timing requirements difficult to specify

In specifying any timing requirement, the following topics should be considered:

- Frequency or epoch
- Accuracy
- Coarse epoch requirements
- Duty cycle
- Duration
- Reliability

Example: specific timing requirements for Omega navigation receiver

Often there are several timing requirements rather than one. Consider the Omega navigation receiver as an example. For Omega, phase comparisons (epoch measurements) are desired to an accuracy of 1 μ sec.

The equipment should operate reliably and continuously with 0.1 duty cycle on each receiving channel. Since intercomparisons always are made between signals at the same frequency, there is no epoch ambiguity problem in the measurements. However, there are other timing requirements. In order to select the proper stations, the commutator must be set to within about 0.1 second of the system time. Further, since the signals to be compared are not transmitted simultaneously, the received phase (epoch) must be stored for as much as 4 seconds before it can be compared. This storage requirement thus yields an additional requirement wherein the *frequency* of the internal oscillator is controlled to within 3×10^{-7} . Aside from frequency stability, there is also a requirement on the maximum *absolute* frequency error of the internal standard; i.e., if the absolute error exceeds the tracking bandwidth within the receiver, the signals never can be acquired. Thus, within one receiver designed for microsecond comparisons, the actual timing requirements are for frequency to be maintained or controlled to within 3×10^{-7} and gross time maintained to within 0.1 second while the largest epoch of any interest is the 10-second repetition rate of the commutation pattern. Note that there is no requirement for any fixed relation between carrier period and commutation pattern ambiguities. Further, the frequency requirement must apply over only about 4-second periods. (In practice, consideration must also be given to the interrelationships between tracking bandwidth and oscillator stability in poor signal-to-noise ratios.)

Since time is so fundamental to physical measurements of various types and is also used to synchronize various events, there is a justifiable tendency to develop central 'clocks' which then provide time for various separate functions. For example, we use a wrist watch to synchronize our arrivals at work, meetings, and other affairs; we also use a watch to measure duration of events. The basic timing requirements thus become blurred. Nonetheless, the fundamental problems and requirements occasionally manifest themselves, as, for example, when we arrive for a meeting 'on time' 1 hour or 1 day early (epoch ambiguity).

Relative timing

Absolute timing

'Preferred' epoch ambiguities

In more sophisticated applications, such as the timing of NASA tracking stations, the diverse applications of 'precise' time render an analysis of the actual requirements extremely complex. For example, if measurements from two separate tracking stations are to be combined to deduce precise orbital parameters of a satellite, then the *relative* timing at the two sites must be accurate. Indeed, in synthesizing timed measurements from various tracking stations, the *relative* (rather than absolute) epoch between sites must be maintained. Conversely, relations between orbital velocity and height necessarily require absolute frequency. Since the periods of the phenomena being observed differ substantially, coarse epoch requirements or the necessary reliability of epoch resolution are also difficult to specify. Certain epoch ambiguities, however, can be recognized as more permissible than others. The most obvious and trivial example is gross epoch error on an Apollo recovery mission. Since Apollo normally is brought into near-Earth orbit prior to recovery, a coarse epoch error of one period (about 90 minutes) would be highly embarrassing but not disastrous; i.e., recovery could occur in the same area but later. If, however, an error of one-half period were made, the consequences indeed could be disastrous. This example was trivial only in that the resolution of epoch to such a gross scale is trivial. Other 'preferred' epoch ambiguities also may be identified from an appropriate analysis. Although such an analysis is beyond the scope of this report, we must expect natural periods to arise as result of preferred spins for satellite stabilization, telemetry commutation, etc. Such considerations underscore the importance and interrelation between timing and almost all aspects of satellite operation. It is almost arbitrary whether the possible epoch ambiguities in the timing system (blunder modes) are matched to telemetry commutations or whether the telemetry commutations are matched to the inherent periods in the timing system. Compatible choices, however, will simplify initialization problems and eliminate many failure modes.

Interrelation between timing ambiguities, commutation periods, reliability, and initialization

Diverse applications yield 'general' timing requirements

Because of the diverse applications made of timing at NASA tracking sites, there is a strong case for designing the timing system independently of any specific application. This is true particularly when improvements in technology occur and new and unanticipated experiments are suggested. Using this approach, nominal timing requirements are set and met without special attention to present engineering details. Failure modes and accuracy characteristics of the timing system are then determined and explicitly stated. Future engineering efforts then may obtain practical advantages by matching telemetry commutation, etc., to inherent periods in the timing system.

Requirements: epoch; frequency; continuous availability

Although today's uses of time at NASA tracking sites are explicit, the timing problem will be treated independently of application. Although the requirements may be stringent, the problem is reduced to that of timing any fixed site at which a general-purpose clock is to be maintained. Therefore, there are nominal requirements for epoch and frequency and a strong requirement for continuous availability.

The requirement that the time be continuously available suggests the presence of a clock; e.g., an atomic or electronic oscillator and appropriate dividers. The requirement that the epoch be maintained correctly implies a need for a method of comparison and adjustment. Since the sites are remote, either a comparison standard must be transferred periodically between sites (flying clock) or provision must be made for common observation of various sites of common or synchronized phenomena (e.g., radio observation of the same or synchronized transmissions). Additionally, an adjustment procedure is required so that epoch and frequency can be steered to continuously provide the best practical time estimates from the available facilities. Since there is some probability that the complete system or dividers will operate improperly, provision must also be made for initialization and periodic verification of coarse epoch.

Reset interval vs. clock quality

Temporarily disregarding any intrinsic requirements for accurate frequency, the interrelationship between reset interval and quality of the frequency standard can be readily estimated by using Omega signals for deducing fine epoch. Table 5 shows the results of calculations intended to maintain typical epoch errors of 1 and 10 μ sec based on an assumed stability of the Omega signals in the range of 1 to 10 μ sec.

TABLE 5. INTERRELATIONSHIP BETWEEN OSCILLATOR STABILITY AND RESET INTERVAL.

Oscillator Stability	Observation and Adjustment Interval for Epoch Maintenance	
	to 1 μ sec	to 10 μ sec
10 ⁻⁶	none (impossible)	none (almost impossible)
10 ⁻⁷	none (impossible)	10-sec interval (i.e., continuously)
10 ⁻⁸	none (impossible)	1-minute interval
10 ⁻⁹	none (impossible)	1-hour interval
10 ⁻¹⁰	none (impossible)	1-day interval
10 ⁻¹¹	none (impossible)	several-day to 1-week interval
10 ⁻¹²	1-day interval	1-week interval
10 ⁻¹³	1-day interval	1-month interval

Table 5 shows that epoch can be maintained to an accuracy of 10 μ sec with an oscillator stability of better than one part in 10⁶ but that an oscillator of stability on the order of one part in 10¹² is required to maintain epoch to a nominal tolerance of 1 μ sec. In effect, this means that a cesium frequency standard is required if the epoch is to be maintained on the order of 1 μ sec. If an accuracy of 10 μ sec is to be

maintained, use of a computer-receiver and a state-of-the-art temperature-compensated oscillator to provide almost immediate fine epoch is theoretically possible. However, the fast acquisition is not likely to be of importance in a fixed timing application. Even with a computer-receiver, use of an oven-stabilized oscillator of greater stability would be appropriate. Aside from being automatic, a computer-receiver for fixed timing thus has relatively little advantage over a good oscillator with periodic manual adjustments. Periodic manual adjustments should not be required often, if the chore is not to become burdensome.

Normal procedures should not require attention to timing measurements and adjustments more frequently than daily, although hourly adjustments can be considered as an emergency backup procedure. An oscillator capable of holding $10 \mu\text{sec}$ for 1 day requires a stability of one part in 10^{10} , which may be obtained with a high-quality quartz oscillator selling for about \$3000. Since the autocorrelation of vlf phase fluctuations is on the order of 10 hours and little is gained unless measurements are averaged over several days, such an oscillator is incapable of providing useful time averaging of the incident Omega signals. Averaging over several days can allow refinement of epoch of the order of $1 \mu\text{sec}$, provided the error introduced by the frequency standard is small. Thus, accuracies significantly better than $10 \mu\text{sec}$ are best obtained by use of cesium frequency standards.

Apollo tracking stations are adequately equipped with oscillators to maintain fine epoch of the order of 1 to $10 \mu\text{sec}$ using adjustments derived from Omega. Sites presently have one cesium, one rubidium, and one quality quartz oscillator. The cesium permits an attempt to maintain a nominal accuracy of about $1 \mu\text{sec}$ by assiduous attention using long-term averages. Should the cesium fail, the rubidium, with a presumed stability on the order of 10^{-11} , will enable the epoch to be maintained to an accuracy of several microseconds. Should both fail, the quality quartz can be employed to meet a $10\text{-}\mu\text{sec}$ requirement with tractable procedures and daily attention.

The existence of good frequency standards considerably simplifies the requirements for time dissemination. We need not continuously make epoch comparisons; only one or two good observations per day are necessary. Hence, periods of greatest transmission stability may be selected. Unusual ionospheric disturbances can be avoided if recognized. The time dissemination problem requires not a 24-hour technique but rather a daily procedure for selecting appropriate periods for observation, observation techniques, and adjustment techniques. Backup emergency procedures should, of course, consider any eventuality.

Atomic standard simplifies timing: infrequent measurement of optimum signals

OPERATIONAL CONSIDERATIONS

EQUIPMENT

The quality and types of equipment to be used for Omega timing applications depend upon the tolerances to which time is specified to be maintained. *PROBLEM ANALYSIS* has discussed the requirements for local oscillator stability and frequency accuracy. The following sections consider similar requirements for the other components of the general phase or time comparison circuitry; specifically, antennas, receivers, clocks, phase shifters, recorders, logs, and records.

ANTENNAS

Antennas: loop; whip; probe

Omega phase difference measurements have been made with loops, vertical whip antennas, and probe antennas. Since any reasonable antenna is electrically short at vlf, a wide selection of possible antenna configurations has been employed. In measurements by Baltzer,²² vlf signals were received via a parallel-plate antenna of 2 square-inch area, 1/32 inch from the ground plane. More practically, 10- to 30-foot whips or 2 m² loops are employed. In special instances, a cardioid can be used to obtain improved directionality. The various possibilities for modes of reception present both advantages and dangers to the user. The main advantage is the ability to select the type of antenna most appropriate to the location, environment, etc., while the danger lies in the very real possibility of a deteriorating installation providing apparently acceptable but actually faulty operation. Such an instance is described in reference 23 wherein deterioration of the coupler and lead-in altered the configuration from electric to magnetic reception with the resulting catastrophic effects on the observations. Other experiences have shown that the high sensitivity of Omega receivers may nearly compensate for loose antenna connections and again lead to *almost* satisfactory operation. In most cases, increasing experience with the equipment will lead the user to be suspicious of anomalous behavior and thus reduce the severity of possible malfunctions.

When selecting an antenna, relevant considerations include rejection of environmental noise, directionality, unwanted coupling to surrounding structures, and maintainability. Depending upon the predominant types of ambient conditions, noise, precipitation static, 60-Hz motors, power lines, etc., whips may have significant advantages over loops and vice versa. The whip is omnidirectional but a loop may be sufficient if a monitor is observing stations in the same general direction. The whip is more convenient to the measurement as the phase predictions are made for the electric field vector. Use of a loop antenna requires

Location not critical

a quadrature correction to the predicted phase to account for the 90° lag of the E-field from the H-field. Reference 24 describes some undesirable effects of placing whip antennas too near to trees, power lines, etc. However, normal care in siting the antenna ordinarily will preclude any difficulty.

Calibration by injection

To date, all precise epoch measurements via Omega have employed injection calibration of whip antennas, and, accordingly, such an arrangement can be confidently recommended. The NELC monitor at Wales, Alaska, has operated for over a year with injection calibration and little instrumental difficulty. Injection has several advantages. Most Omega receivers are designed for phase difference measurements and thus have no specification on the absolute long-term phase stability of the receiving system. Further, parameters of the antenna system can change owing to dirty insulators or component degradation. Injection is the only way to guarantee the absolute measurement without assiduous extensive engineering review and test of the actual antenna systems and receivers employed. However, injection has certain disadvantages. Not only is injection circuitry costly, it also necessitates local generation of coherent signals at the carrier frequencies. Depending on construction details, there may be considerable danger of leakage affecting the radio measurements. The speculation is that an antenna-coupler-receiver arrangement which is inherently stable can be designed, thus eliminating the need for injection. Alternatively, circuitry suggested by Palmer⁵ calibrates the antenna system in the process of making the measurements.

RECEIVER

'Microsecond' readout undesirable

Many considerations enter into the choice of a receiver for time applications. Because Omega is basically a phase system, a receiver which measures and reads out phase differences is required. With the several frequencies available, a receiver operating in cycles has a distinct advantage over one designed to convert phase to time and read out in microseconds. The 100-kHz reference frequency used by most timing receivers is satisfactory for checking the frequency of the local clock, but the methods of generation render reestablishment of the epoch impossible if the dividers should jump. In effect, most vlf 'timing' receivers are actually frequency comparison aids and cannot be used to determine time; i.e., frequency *and* epoch.

The receiver must be able to operate over a wide range of amplitudes and must have as little internal phase shift with amplitude as possible. Because Omega receivers are designed to operate in a relative rather than an absolute mode, absolute phase stability with temperature, etc., ordinarily is not required. For timing applications, a stable receiver using a cesium standard as the local oscillator would provide satisfactory performance; i.e., the recorded phase difference would be between the received signal and the phase of the reference signal. In normal Omega

navigation reception, this value would be stored until a similar measurement of a signal from another station was made, and after subtraction the local oscillator phase would cancel out. In the timing application, there is no cancellation of local phase so that stability considerations for the receiver become critical.

Modified navigation receiver and injection

One procedure designed to permit the use of a less-stable receiver is local signal injection into the antenna circuit. This method is discussed under *Antennas*, and has the advantage of being able to use commercial, off-the-shelf Omega receivers such as those at the Wales and NELC sites.

High reliability

The stringency of timing requirements also implies a high degree of reliability and maintainability for the receiver, as well as the other equipment. Modern receivers are rugged, solid-state instruments, some of which are designed to meet rigid specifications for airborne, ship-board, or submarine use and have been shown to meet the reliability and maintainability requirements. One report on a certain receiver noted that the maintainability could not be evaluated as the receiver never failed during 20 000 hours of operation.

Long adjustable time constants

An important characteristic of a receiver is the time constant for the integration period of the received pulses. A long time constant, commensurate with the stability of the local oscillator and predictable diurnal phase changes, is appropriate, but not if such long integration precludes the ability to detect ionospheric disturbances. If only one time constant can be used, it must be long enough to smooth out random fluctuations in propagation but short enough to respond to rapid onsets of SID's or large PCA's. A more suitable approach for the timekeeping would be to use different time constants for different types of signals. Some signals could then be used to monitor solar and ionospheric activity while other signals could be used primarily for timing. Evidently, the choice for time constants can be made more easily when the quality of signals to be observed is known for the particular monitor sites considered.

Receiver and recorder errors

If a user has available a high-quality oscillator-clock signal source and follows some approximation to an optimum synchronization control procedure, another feature of the receiver which becomes significant is accuracy. All receivers will have nonlinearities, biases, etc., and satisfactory performance may require that these defects be calibrated and accounted for when observations are made. Rather than permit the existence of errors due to failure to constantly check the linearity of the receiver, the user should consider acquiring equipment which possesses an accuracy much better than that for the recording devices, which ultimately limit the accuracy of the measurement. Present instruments range from about 5 to 0.1 percent of a lane, or as good as 0.1 μ sec on the 10.2-kHz carrier. Because recorders usually are not accurate to more than 1 or 2 percent (see below), the need for better than present receiver accuracies is not pressing.

The user must also consider the various configurations possible for monitoring and recording; i.e., do we monitor many stations on one frequency or a few stations on many frequencies, and how should the

outputs be displayed? Assuming we will not have enough equipment to observe all possible signals, some choices in addition to signal quality are required.

One such choice involves the probability for detection of a failure in one or more receiver channels. If only 10.2-kHz information were available from several stations, a failure in the reference channel would manifest itself as an apparent clock drift (or step) of equal magnitude on all signals. When other frequencies were available, such failures would most likely be equivalent in μsec but vary in percent of a cycle at different frequencies if the clock drifted, but would be inconsistent in all units for a single receiver channel failure.

The possibility for monitoring difference frequencies directly also exists, as does circuitry for permitting tunable receivers to operate on more than one frequency 'simultaneously.'

Depending upon specific user requirements, specially designed receivers may be more appropriate than commercial equipment or the military navigation receiver versions. If design of such a receiver is undertaken, consideration should be given to the concepts detailed by Palmer in reference 5, which represents a realistic approach to the proposal of using the Omega format for time dissemination purposes. An additional refinement might be to consider the use of a local oscillator frequency halfway between the 10.2 and 13.6 carriers to produce an intermediate frequency of 1.7 kHz and two sidebands which could be separated and used to monitor both frequencies simultaneously.

OSCILLATOR

A discussion of the requirements for the local oscillator has been presented in *PROBLEM ANALYSIS*. The conclusion to be drawn from the discussion is that the most acceptable operation will be produced by a cesium-beam frequency standard. In view of the successful operation of the Omega stations over the past 4 years, we can recommend the cesium standard as a most reliable piece of equipment. Although the specified frequency accuracy of the models used at the stations is $\pm 1 \times 10^{-11}$, experience has shown that typical values are usually between five and ten times better than the specification. The day-to-day stabilities for the better standards do approach the quoted value of a few parts in 10^{13} , while long-term drift is usually within a few parts in 10^{12} . If cesiums with frequency offsets similar to that of the Trinidad standard analyzed in *ACCURACY OF TIME DETERMINATION TECHNIQUES* become common, timed sites could expect epoch drifts of only 20 μsec or so over a year's time and could be more flexible in the choice of a control procedure using radio signals. Present instruments already seem to be significantly more stable than the uncertainties in making long-path phase measurements, and any improvement in the state of the art could relegate all radio timing systems to the position of updating the time every few months.

Cesium-beam frequency standards recommended

CLOCK (FREQUENCY SYNTHESIZERS, PHASE SHIFTER)

If a standard Omega receiver is used as a time receiver, appropriate signals from the local clock must be inserted into one or more channels. Because the receiver normally makes comparisons between two signals of the same frequency, the local signal must be equal to the Omega frequency which is to be observed. Therefore, some means of generating the Omega frequencies from the cesium standard output is required. At the Omega stations, this problem is overcome by the format generators and synthesizers which provide all the relevant frequencies. This equipment necessarily must be reliable and designed to minimize the probability of divider jumps. It should operate from one of the standard cesium output frequencies such as the 1 MHz and include a phase shifter (Western Electric or Nilsen Company) operating on this frequency also. It is this phase shifter which may be adjusted to control the indicated clock epoch as represented by the outputs of the synthesizer.

RECORDERS

The apparatus most likely to limit the accuracy of time determination procedures is the device used to record the relevant phase differences. The data need to be recorded in analog form so that the operator will have some idea of what normal and abnormal operation are supposed to look like and also of what is happening at the time of a particular measurement. The various types of recorders available use pen and ink, pressure-sensitive paper, slide-wire (multipoints), and heated pen. Each type of recorder has its advantages and disadvantages, and no one type is considered to be the ultimate at present. All types are subject to calibration changes and require periodic checks and adjustments of zero and full-scale readings. Time indication may also be a problem, even with the ac motors geared down to drive the paper feed. Because the propagation phenomena of interest to both the navigation and time-keeping functions must be averaged over relatively long periods of time, recorders must be run at very slow speeds, such as 1 inch per hour. Although high accuracy can be obtained from instruments designed to operate at much greater speeds, typical accuracy for Omega type recorders is about 1-2 percent of full scale. When cost is a major consideration, the Rustrack recorder with the 1-percent accuracy option can be selected.

The selection of recorders also depends upon the convenience and application of the tracks to be observed. If multipoint recorders are used to observe more than four or five signals, care must be taken to ensure that the tracks are not easily confused or misidentifiable. If signals from only one station appear on a single recording, the limited number of similarly shaped tracks are readily separable (different colors). This method of recording is also more convenient for setting and especially for maintaining the correct difference frequency epochs. The

Recorders: expensive; troublesome; and/or inaccurate

operator soon becomes accustomed to seeing the tracks in a certain area of the paper, can easily note the differences between frequencies, and will be suspicious of irregular behavior. Such an arrangement also is most convenient for observing modal interference effects, as variations of diurnal shape with frequency are readily apparent. If the monitor can maintain its epoch to within the specified tolerances, multifrequency tracks have the historic scientific value of demonstrating the apparent correlation of simultaneous ionospheric effects at various frequencies.

Multipoint recorders are also used to display single-frequency observations from many stations. If four or five stations are observable, the appearance of such recordings is not confusing. Increasing the number of tracks (by adding one other frequency) is possible but not satisfactory, if operator recognition of irregularities is given high priority. The user must consider the relative merits of possible combinations, and trial and error operation may be required until an acceptable format is found. Use of many single-channel recorders would provide many sources of random—it is hoped—errors in linearity, calibration, etc., but have the advantage of not losing a large number of tracks when one instrument fails. Economics and reliability necessarily need to be considered.

LOGS AND RECORDS

In addition to the recorded observations, pertinent remarks concerning the operation of equipment, ionospheric disturbances, epoch adjustments, or calibration procedures are an integral part of the time or phase measuring process. The user may find it most convenient to note appropriate comments directly on recordings so that historical reviews have all the relevant information in one place. Alternatively, separate logs may be kept denoting the time of occurrence for the events enumerated above. Such records are an invaluable aid in reviewing overall operation and for detecting errors which were not recognized as such at the time of occurrence. Logs can be conveniently combined with epoch reduction work sheets to provide an orderly calculation procedure as well as a permanent record of observations.

Working forms and logs desirable

PATH SELECTION

Some general properties of vlf propagation in general and Omega propagation in particular are given in appendix B. Propagation considerations for timing a fixed site are somewhat different from those for navigation. Generally, a navigator must obtain a fix whenever required and must employ signals from at least three stations. Further, the navigator generally will have no prior experience with specific signal characteristics in his precise location at the observation time. In contrast, signals from only one station are required for timing at a fixed site. Further, good

Navigation and timing requirements differ

frequency standards ordinarily will be available, thus permitting selection of the most favorable observation times. In addition, since normal observations will be made according to a standard routine, considerable past history will be available for the measurements. Propagation knowledge is thus most useful in recognizing and avoiding disturbed observations and in selecting the paths, frequencies, and times of observation.

Initial path selection critical

Path selection is most critical in establishing initial crude epoch, as no prior history is available and an assessment of possible prediction errors must rest entirely on propagation theory. It is also important to choose paths and observation times which minimize the contamination of the resultant epoch errors by improperly predicted seasonal or diurnal changes. An inappropriate choice of observations which results in poor stability due to low received signal strength, for example, will not be a serious hazard, since the problem is easily detected and an alternative selection can be made. Appendices D, E, and F discuss spatial and temporal aspects of path selection.

PHASE PREDICTABILITY

Diurnal phase variation

The most obvious feature of phase measurements at a fixed site is diurnal variation. Typical diurnal variations of phase are shown in appendix B. At 10.2 kHz, the diurnal variation is typically constant, or 'flat,' during the night and then ramps during sunrise to a slow variation, or 'curvature,' during the day. Measurements during the day are most repeatable and those at night least repeatable.

Spatial prediction: modal interference at night

Spatial prediction of phase is best during the day and worst during transitions. Prediction at night is complicated by modal interference and also sensitivity of many of the propagation parameters to slight changes in magnetic dip angle or direction of propagation,

Preferred observation time: midpath noon

Selection of an appropriate observation time depends on a number of factors including: normal manning hours of the site, subsequent use of the observations, diurnal variation of stability, variation of predictability, and variation of amplitude or signal-to-noise ratio. In the vast majority of cases, the best observation time will be near midpath noon. An optimum choice normally is insensitive to a variation of 1 or 2 hours. Stability and predictability are usually best near midpath noon. Further, midpath noon ordinarily will fall during normal working hours. Exceptions can arise because of local conditions such as high noise near noon or low received amplitude owing to the generally high attenuation rates during the day. Usually, however, noise can best be overcome by increasing the time constants within the receiver rather than changing the observation time. An exception might be made if primary emphasis were placed on determining the correct frequency. The resultant effect of uncompensated seasonal propagation changes might be more severe than would uncertainties introduced by lesser stability at night.

Practical seasonal changes are of two types which may be described as 'apparent' and 'fundamental.' Since the diurnal shape is controlled primarily by the solar zenith angle, the phase expected at any

Seasonal variation

portion of a propagation path which is sunlit must reflect daily ephemeral changes. Thus, measurements during transitions on a north-south path may exhibit large daily changes. Indeed, measurements at any time of 'day' will change slightly owing to changes in zenith angle. Fundamental seasonal changes with ionospheric temperature (scale height) also occur. These will also introduce seasonal phase shift. At 10.2 kHz, seasonal changes near noon can be 10 to 20 μ sec over temperature latitude paths.

NOISE AND STABILITY

Ionospheric variation limits accuracy

Variations limiting epoch measurement ordinarily will be due to various relatively long-term (10 hour) changes in ionospheric conditions or even longer-term variations in ground conductivity. Such changes affect the propagation path from transmitter to receiver and hence the received phase. Ionospheric variation will affect the 'transfer' or 'mapping' function by which epoch information is carried from transmitter to receiver. No improvement in the quality of epoch measurements can be obtained by increasing the transmitted power. In contrast, normal electromagnetic environmental noise is due to interfering signals, primarily from lightning strokes in thunderstorms throughout the world. In the case of interfering noise, measurement quality can be improved by traditional methods such as increasing transmitter power, increasing integration time constants, directional antennas, etc. Since attenuation is less at night, signals ordinarily will appear 'better' at night than during the day. However, epoch measurements will be worse at night than during the day owing to differences in the inherent stability of the 'mapping' function.

MODAL INTERFERENCE

Important at night on short paths

The usual theoretical model for vlf propagation is that of a concentric spherical waveguide between the earth and the ionosphere within which various modes propagate. At sufficient distances, the mode with the lowest attenuation rate will dominate and the resultant phase will vary linearly with path length. At shorter distances, several modes may contribute to the total mode sum, and the observed phase will vary with path length in a relatively complex manner. Modal complexity renders prediction difficult and, in the event the modes tend to cancel, may result in low field strength and poor phase stability. In the case of two nearly equal but nearly oppositely phased modes, the phase can assume a value anywhere between 0 and 1 cycle depending upon which mode dominates. Since the modal dominance can change owing to very minor ionospheric variations, a path with these particular features would be useless for timing. Modal complexity is most severe under

Theoretical path assessment

night propagation conditions near the equator on the higher very low frequencies. Under certain conditions, significant modal complexity may be expected at all ranges. ^{25,26}

Theoretical phase and field strength plots as a function of distance from Hawaii to the NASA tracking station in Santiago, Chile, are shown in figures 4A and 4B. Full-wave computations of the Omega field to several tracking stations are given in reference 27. Modal interference effects are less severe during the day but may be important for dual frequency timing applications with narrowly spaced frequencies, as shown in figure 5. Additional computations have recently been made by Hamilton and

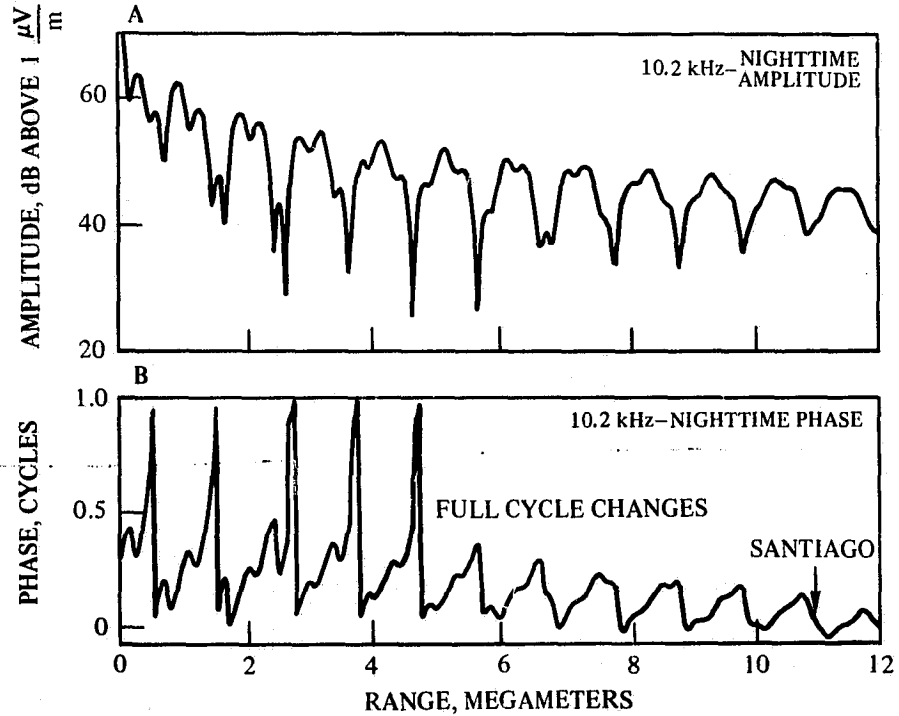


Figure 4. Omega transmissions from Hawaii to Santiago, Chile (Wait's $\beta = 0.5 \text{ km}^{-1}$, $H' = 87 \text{ km}$ profile).

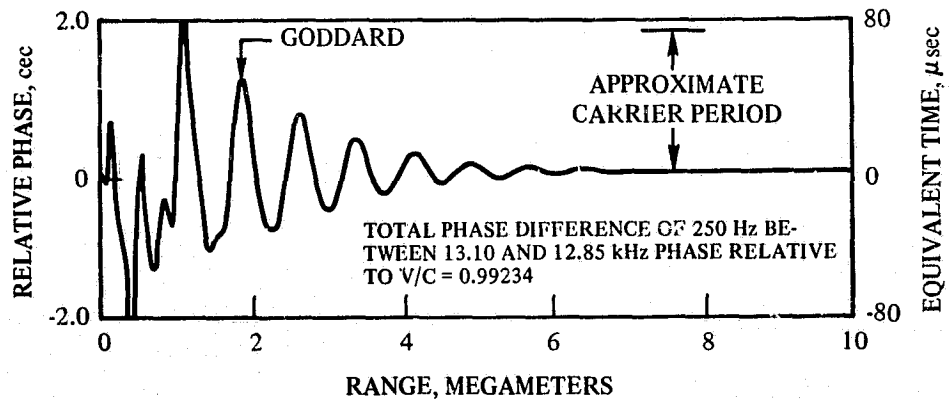


Figure 5. Relative phase of daytime Omega difference frequency, North Dakota to Goddard (Wait's $\beta = 0.5 \text{ km}^{-1}$, $H' = 70 \text{ km}$ profile).

Jespersen.²⁸ Thus, a preliminary estimate of propagation to any site can be made prior to installing timing equipment. Note that the Omega field usually is sufficiently simple during the day that elaborate calculations need not be made for the most desirable observation periods if only carrier measurements or widely spaced multiple frequencies are being considered.

CALIBRATION

Spatial prediction error can be removed by calibrating the propagation paths. Calibration may be achieved by flying a clock^{29,30} from an Omega station to the receiving site and then comparing the clock epoch with the epoch obtained from Omega. Repeated clock flights would be required to remove seasonal prediction errors. Special calculations would be required to estimate slow changes due to variation in the solar cycle.

**Calibration: flying clock;
cross path**

Cross path calibration is less expensive although not as desirable as flying clock calibration. The most predictable signals may well be obtained over long propagation paths and at frequencies which normally are not used for epoch determination owing to poor signal-to-noise ratio. By repeated measurement, the epoch estimate from poor signals can be refined. Hence, more data may be employed in evaluating possible prediction error at the timing site than ordinarily are used in deducing epoch. For example, if the prediction error on all paths to a typical timing site were 5 μ sec and the prediction errors were uncorrelated, then epoch based on four signals could never be established to better than $2\frac{1}{2}$ μ sec. Appendix D shows existing prediction errors to be such that measurements over several paths may be synthesized to calibrate epoch to 1 μ sec. Subsequent observations on only the four best signals would be needed to maintain epoch near 1 μ sec, as shown in appendix F.

ADDITIONAL REFINEMENTS

REDUNDANCY – OPTIMUM WEIGHTING

One of the biggest advantages to be gained from the use of Omega for timekeeping purposes is the large number of signals available. For an ideal monitor capable of receiving transmissions from all stations, the fully implemented system would provide at least 32 and possibly 40 different signals along eight different propagation paths. In reality, any specific monitor might be expected to receive four to five stations, which still provides for 16 to 25 possible signal inputs. Apparently, some procedure is required for managing this amount of information and for combining the numerous epoch estimates in an optimum manner. Some form of optimization is required to compensate for the expected variation in the quality of both the received signals and the predictions at a given site; i.e., the user would attach more weight to his most reliable information.

**Multiple paths: redundancy;
improved reliability and
accuracy**

Given that the monitor site has computed several estimates for the indicated epoch error, an ensemble of errors E_i now exists. A relation for the weighted ensemble error E_c can be written as:

$$\hat{E}_c = w_1 E_1 + w_2 E_2 + w_3 E_3 + \dots + w_n E_n = \sum_{i=1}^n w_i E_i (\mu\text{sec}) \quad (5)$$

where:

$$\sum_{i=1}^n w_i = 1 \quad (6)$$

We assume that all E_i will have an associated uncertainty N_i with a variance of $\text{var } N_i$. The ensemble error in terms of the true error E_c and the various uncertainties can now be written as:

$$\hat{E}_c = \sum_{i=1}^n w_i E_i = \sum_{i=1}^n w_i (E_c + N_i) = \sum_{i=1}^n w_i E_c + \sum_{i=1}^n w_i N_i \quad (7)$$

$$\hat{E}_c - E_c \equiv N_c = \sum_{i=1}^n w_i N_i$$

We wish to minimize the variance of the difference between the estimated error and the true error (or the ensemble noise), so the variance of equation (7) can be taken as:

$$\text{var } N_c = \sum_{i=1}^n w_i^2 \text{var } N_i \quad (8)$$

where zero correlation has been assumed between the various noise components. Differentiating (8) partially with respect to the w_i yields the results that the w_i are related inversely as the $\text{var } N_i$ and that any particular w_j is given by:

$$w_j = \frac{1}{1 + \text{var } N_j \sum_{i \neq j} \frac{1}{\text{var } N_i}} \quad (9)$$

The minimum variance for the ensemble noise is now:

$$\text{var } N_c = \frac{1}{\sum_{i=1}^n \frac{1}{\text{var } N_i}} \quad (10)$$

In the special case in which n paths of similar stability are synthesized, the noise variance of the synthesized estimate is seen to be $(1/n)$ of that of the typical path. Thus, if information from four independent but similar paths is available, the synthesized variance will be only one quarter that over the typical path; i.e., the standard deviation will be halved. If the path variations are not independent, then the possible gain from information synthesis will be reduced. However, little is presently known about the correlation of fluctuations on different propagation paths.

The problem facing the monitor site then is the determination of the var N_j . For long path estimates, much is already known about the expected stabilities of Omega signals and will be used as an initial estimate for the probable paths to be used. This knowledge is based upon past operation of the present four-station system and would have to be refined to account for the proposed new stations and the increased power levels. After some experience, the user will be able to make his own judgment concerning the relative observed quality of signals in his area and to assign the weights accordingly. Short-path signals which are 'calibrated' to remove modal interference effects will have var N_j based upon the uncertainty of the calibration as well as any indicated deviations observed during ongoing operations. Difference frequency or 'composite' estimates will have var N_j based upon the stability of the composite data and any calibration required if a short path is being used.

Additional protection against noise contamination is provided if we compute the E_j as *medians* of several observed errors taken over a day or week instead of relying upon data from only the end of such an interval. Additionally, further considerations must be made with regard to the reliability of the computed E_j . These are discussed in the following sections.

Medians discriminate against anomalous measurements

SID, PCA MINIMIZATION, ETC.

The predictions for the expected received phase are based upon the normal undisturbed ionosphere as the prevailing condition for propagation. Unfortunately, for our purposes, the sun, which is responsible for the stability of the daytime ionosphere, periodically produces solar flares which directly influence the stability of the prevailing propagation. The two most common phenomena are X-ray absorption (SID) and Polar Cap Absorption (PCA) events. Both types of events result in lowering of the effective reflecting height of the ionospheric D-region and are consequently manifested as apparent phase advances of the remote signal.

X-ray events are usually directly correlated with the optical detection of a solar flare and are characterized by rapid onsets and slower exponential recoveries, usually within an hour or so. During extremely active solar cycles, experience has shown that periods of up to 10 hours may be affected by several consecutive SID's or one very large and slow-to-recover event. Fortunately, the day-to-day stability of undisturbed

Ionospheric disturbances

SID's: sunlit paths; abrupt run-off; 1/2-hr recovery

vlf propagation is so high for at least some signals in a given area that the identification of SID events over sunlit propagation paths presents no significant difficulties to even an inexperienced user.

Figure 6 shows the typical effect of SID's on a long-path phase track.

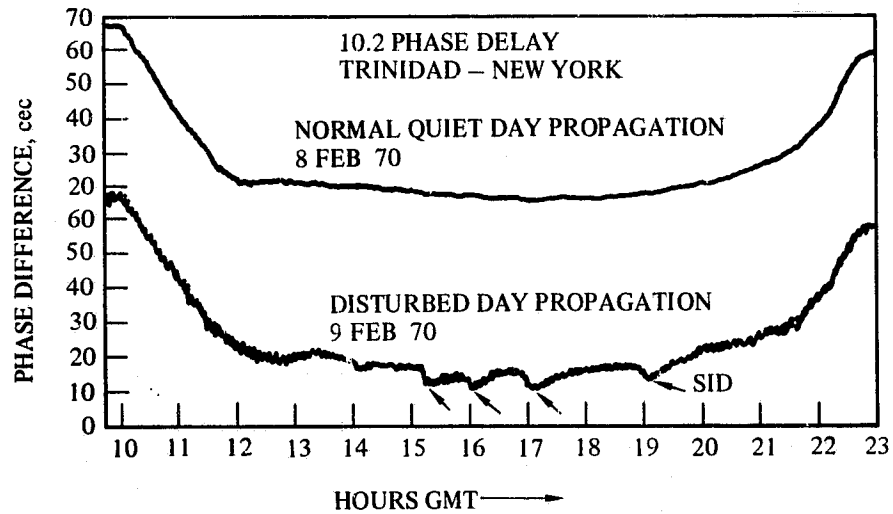


Figure 6. Effect of X-ray absorption on a long-path phase track.

PCA events are produced by streams of solar protons rather than X-rays, and their effects on received phase are usually more severe and prolonged than those of a typical X-ray event. Onset times range from a few minutes to a few days, and recovery times require days to weeks depending upon the severity (fig. 7). Again, fortunately, such events are confined to the polar ionosphere and are becoming better correlated with disturbance warning systems³¹ which utilize data from satellite-borne proton-sensing devices. The user will know beforehand which signals are subject to PCA disturbances and likely will not rely on these signals in ongoing operations. For a monitor which gets its strongest signal over such a path, the change from normal propagation should be evident and lead to the temporary deletion of precise epoch estimates from this path. Only 'precise' estimates need be discarded, as the coarse estimates available from difference frequency computations are not as severely affected, as discussed below.

PCA's: arctic paths; prolonged

Figure 7 shows a plot of the average error as observed on the reciprocal path of Norway-Haiku at 0900Z and 1100Z on 10.2 kHz during the period 31 August to 8 September.³²

Before describing the various procedures which have been suggested for minimizing the effects of ionospheric disturbances, we must be acquainted with their expected magnitude in relation to normal propagation. At Omega frequencies, diurnal phase variations seem to be limited to approximately 1 to 1½ cycles of the carrier signal, or about

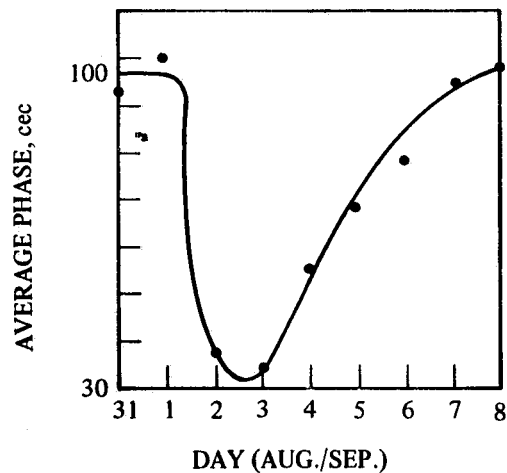


Figure 7. Recovery of Haiku-Norway path from PCA of 2 September 1966.

100-150 μ sec. SID's may range up to 100 μ sec, a typical disturbance being about 10-20 μ sec. PCA's may also range up to 100 μ sec or more, the average event being about 50 μ sec. SID effects increase with both length of propagation path and percentage of the path which is sunlit. PCA effects may occur continuously day and night over some paths and increase with percentage of the path which is in a polar region. Evidently, if epoch estimates are to be made during disturbed propagation conditions, some means of reducing the significant effects of anomalous solar activity must be employed.

Composite Omega: protection during disturbed conditions

The most useful type of disturbance minimization scheme involves epoch estimates made from difference frequency, or 'composite', observations. Because disturbances have similar effects on all Omega signals from a given transmitter, there should exist some preferred weighted combination of data at these frequencies which remains constant even under disturbed conditions. Historically, the simple 3.4-kHz difference frequency has proved useful in this regard, and the composite concept of Professor J. A. Pierce³³ may also be useful during large arctic path disturbances. Reference 13 contains numerous computer printout tabulations of typical raw Omega phase data and also the derived data for the 3.4 difference and composite frequencies, and can serve as a guide as to what results can be expected from such methods.

As stated previously, accurate epoch estimates are difficult if not impossible to make under disturbed propagation conditions. If continuous recordings are available, the existence of a disturbance should be clear, and we should wait until the propagation normalizes before attempting an epoch determination. If a spot check is being made, constancy of the 3.4 or composite (or other combination) would indicate no significant discrepancy in the local clock. The term 'significant' is stressed because the clock could drift a small amount which presently available equipment for observing the 3.4 could not detect. For example,

if the 3.4 difference phase were predicted perfectly at a given site, and the clock were to drift 1 μ sec, the 10.2-kHz track would drift about 1 cec while the 13.6-kHz track would move about 1-1/3 cec, with a resulting 3.4 drift of only 1/3 cec. The local clock would have to drift 3 μ sec before the 3.4 would show a change of 1 cec and 6 μ sec before it would show a change of 2 cec. (*Adjustment Procedures* considers the possibility of using such data for maintaining epoch continuity.)

TRANSITIONS, DOWNTIME, WEAK SIGNALS, ETC.

Transitions less predictable

In addition to disturbed propagation times, there are instances when the probability of making accurate epoch estimates is reduced. One type of error occurs during the transition time when the sun is either rising or setting on part of the path and is caused by the greater likelihood of prediction error during those times. Preferred times for observing signals are during the undisturbed daytime when the normal solar radiation dominates all other ionizing influences and accounts for the noted stability of vlf propagation. Nighttime propagation may be used but acceptable stability may be possible only on paths short enough to be unaffected by magnetic storms but long enough to be free of modal interference. Very short paths are usable if they are 'calibrated' as discussed in *ACCURACY OF TIME DETERMINATION TECHNIQUES*. The user must also be able to note when a station is not transmitting or when signals are so weak as to be seriously degraded by noise. Receivers are designed to exhibit various forms of behavior when signals are off, and the user must be aware of the characteristics of his particular equipment. When continuous tracks are maintained, station downtimes and weak signals are as self-evident as disturbances and should pose no problems to the user. Weak or noisy signal estimates can be made but only if a long integration time, on the order of 30 minutes or so, is used on a track which appears to have random noise impressed upon it.

EQUIPMENT CALIBRATION

Receiver checks: operational; channel interchange

Except for careful engineering checkout, comparison, and calibration when the equipment is assembled, little calibration of the antenna, coupler, or rf receiver section is possible in the field (unless injection equipment is used). However, receiver tracking channels and recorders can be calibrated by intercomparison or internal test facilities. Since the tracking and recording functions are performed after the intermediate frequency is generated, interchanging the receiver channels will allow comparison. Alternatively, receivers can be operated simultaneously to measure the same signal.

ADJUSTMENT PROCEDURES

Continuous adjustment to maintain time

Maintenance of proper time requires procedures by which the epoch of the local clock can be adjusted to synchronism with external reference information. As previously described, the receiving equipment from which the epoch estimate is derived will include an antenna, coupler (if required), phase tracking receiver, and suitable calibration injection or reference generation equipment. Inputs to the receiving complex thus include a time reference from the local clock and the radio signals. The output will be phase comparisons which are processed to obtain estimates of the error in the local epoch. The clock is independent of the receiving complex and may be illustrated schematically as in figure 8. An adjustment procedure is thus a sequence of operations from which periodic changes in the phase shifter position are derived such that the clock output is nearly correct as often as practicable.

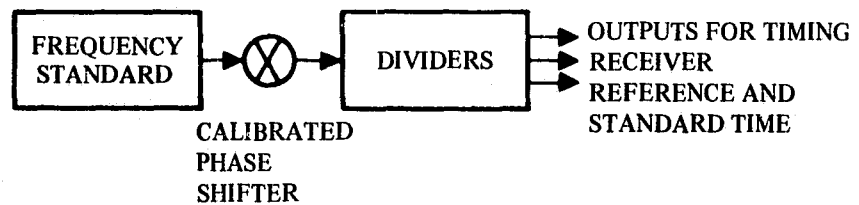


Figure 8. Schematic diagram of clock.

A specific procedure: 60-day frequency estimation; weekly epoch adjustment

Timing synchronization has been and still is being studied extensively in its application to the Omega system,³⁴⁻³⁷ which represents an attempt to maintain several remote clocks in agreement with each other and also with an external reference in the most convenient and optimum manner. The formulations presented here are some of the results of these studies which are applicable to the general remote clock synchronization problem. This section contains only a brief outline of the suggested procedures while appendix C contains the complete algebraic formulations. The procedure is a specific one which presently is being used to synchronize the Omega system and includes four hourly adjustments for frequency offsets and weekly phase corrections for indicated epoch errors. The frequency estimates are based on a 60-day least-squares regression of nine data points 1 week apart. The procedure is convertible to other regression schedules and waiting periods between epoch adjustments.

The starting point for this discussion is an equation relating the epoch* of a clock at the present time t to some past time $t-1$:

Fundamental equation

$$\phi_t = \phi_{t-1} + E_t + F_t T \quad (11)$$

*The epoch terms used here may refer to phase or time as long as all quantities have the same units in the equations.

where: ϕ_t = phase epoch at the end of the t^{th} interval

ϕ_{t-1} = phase epoch at the end of the $(t-1)^{\text{th}}$ interval

E_t = phase correction applied during t^{th} interval

F_t = frequency radiated over t^{th} interval

T = interval length

Equation (11) states that the epoch that existed at time $t-1$ has been altered by a discrete adjustment inserted by the timekeeper and also by the accumulated phase offset produced by the frequency difference between the local clock-plus-phase shifter combination and the 'perfect' reference. This frequency difference is given by:

$$F_t = f_t + \delta f_t \quad (12)$$

where: f_t = cesium standard frequency offset from perfect reference over t^{th} interval

δf_t = negative of the estimated cesium frequency offset, or 'accumulation,' over t^{th} interval

The 'accumulation' is the least-squares estimate based upon the nine previous positions of the phase shifter P_i :

$$\delta f_t = A \sum_{i=t-9}^{t-1} jP_i - B \sum_{i=t-9}^{t-1} P_i \quad (13)$$

where A and B are the constants determined from the specific case of nine data points in a 60-day analysis as given by equation (3) ($A=1/60$, $B=1/12$). 'j' is the index multiplier ranging from 1 to 9. The successive P_i are related by the directed changes E_i and δf_i :

$$P_t = P_{t-1} + E_t + \delta f_t \quad (14)$$

where: P_t = the phase shifter position at the end of the t^{th} interval

P_{t-1} = the phase shifter position at the end of the $(t-1)^{\text{th}}$ interval

If no adjustment were being made for the inherent frequency offset of the cesium standard, the term f_t would cause the epoch to advance or retard depending on whether this offset were positive or negative. Because the estimate term δf_t is computed from phase shifter adjustments intended to remove the apparent cesium offset, the regression line will

have a slope opposite in sign to the offset, and the addition of the two terms in (12) should cancel one another and result in no change to the epoch. In reality, the estimates are imperfect and will result in some indicated epoch discrepancy at the end of every interval. The correction term E_i is designed to remove this error and is given by:

Correction term

$$E_t = \theta \hat{\phi}_{t-1} = \theta(\phi_{t-1} + N_{t-1}) \quad (15)$$

where: $\hat{\phi}_{t-1}$ = the estimated epoch at the end of the (t-1)th interval

ϕ_{t-1} = the true phase epoch at the end of the (t-1)th interval

N_{t-1} = the noise on the estimate $\hat{\phi}_{t-1}$

θ = parameter to be found

The parameter θ is considered to be a 'believability' or weighting factor which permits the flexibility of using the known stability of the standards as a guide for interpreting the real epoch error as something different from 100 percent of the indicated estimate $\hat{\phi}$. Because minimization of the variance of the epoch errors is desired, a result of θ as a negative fraction is expected from this exercise.

The initial steps in the analysis are to use equations (13) and (14) to recurse the least-squares estimate δf_t back to the initial conditions for the operation of the standard as a clock. The result of this exercise is:

Frequency estimate after recursion

$$\delta f_t = \sum_{p=-1}^{\bar{c}} \sum_{q=t-1}^{t-n} c_p E_q + \bar{E} \quad (16)$$

where the c_p are constants given in appendix C, and E is some initial noise-free estimate (possibly zero) made for the initial operation of the cesium. Using the above result, the starting equation for ϕ_t also can be recursed back in time to yield the dynamic behavior of the true epoch in terms of noise, cesium stability, and various constants. In its simplest form, this relation is:

Epoch: a function of frequency changes and measurement noise

$$\phi_t = \sum_t^{t-n+1} (Kf)_j + \theta \sum_{t-1}^{t-n} (AN)_j \quad (17)$$

where the K_j and A_j are constants dependent upon θ and the previously shown c_p .

Taking the variance of (17) yields:

Epoch stability

$$\text{var } \phi_t = \sum_t^{t-n+1} K_j^2 \text{var } f_j + \theta^2 \sum_{t-1}^{t-n} A_j^2 \text{var } N_j \quad (18)$$

where zero correlation between the f_j and also the N_j has been assumed; i.e., cesium fluctuations are uncorrelated and noise is random. The results to be obtained are critically sensitive to any autocorrelation which may be present. The noise in the weekly phase measurements probably is not significantly autocorrelated except for the influence of seasonal or solar cycle variations. Information originally supplied by the manufacturer³⁸ of the standards indicated no autocorrelation for observation intervals from about 1 minute to 1 day. More recent information from the manufacturer indicates appreciable correlation for measurements from 1 to 10 days.³⁹ Experience with cesium standards at the Omega stations also apparently indicates some significant long-term autocorrelation.

Optimization

Although the correct procedure for determining θ would be to minimize the derivative of (18) with respect to θ , the complicated nature of the constant terms makes the procedure laborious. Instead, probable values for $\text{var } f_j$ and $\text{var } N_j$ are inserted until a θ giving the minimum variance for ϕ_t is determined. The results of this procedure given in appendix C, and summarized in figure 9, show that for an oscillator stability of about 1×10^{-12} and noise variance of up to $1 \mu\text{sec}^2/\text{week}^2$, an optimum θ does exist so that $\text{var } \phi$ may be minimized to better than $1 \mu\text{sec}^2/\text{week}^2$.

Short-term frequency errors

Although minimization of $\text{var } \phi_t$ will also maintain the correct long-term frequency for the adjusted clock output, the required phase shifter adjustments may have significant effects upon the short-term frequency. If we desired to determine an optimum θ for minimizing the variance of short-term frequency estimates, the parameter T representing the 'waiting period' between epoch adjustments in the starting equation must be considered a variable which will depend on the stability of the standards, propagation noise, and θ . If only a fixed T is considered, as in this analysis, we must consider the effect of θ on the variance of successive ϕ_t where the time τ between the relevant θ_t is allowed to vary over any range shorter than the long-term frequency observation period. This is one of the numerous areas of time and frequency control theory that need further study which has not been attempted in this report.

The plots shown in figure 9 were obtained from a graphical analysis of several $\text{var } \phi_t$ versus θ plots as shown in appendix C. θ_{optimum} is the apparent minimum of those curves while $\sigma_{\phi_{\text{min}}}$ is related to the value of $\text{var } \phi_t$ resulting at those minimums. The figure indicates that θ_{optimum} varies inversely with noise and directly with oscillator stability, as expected. The plot of $\sigma_{\phi_{\text{min}}}/\sigma_f$ is intended to indicate the linear variation of epoch with noise for any standard variability when the

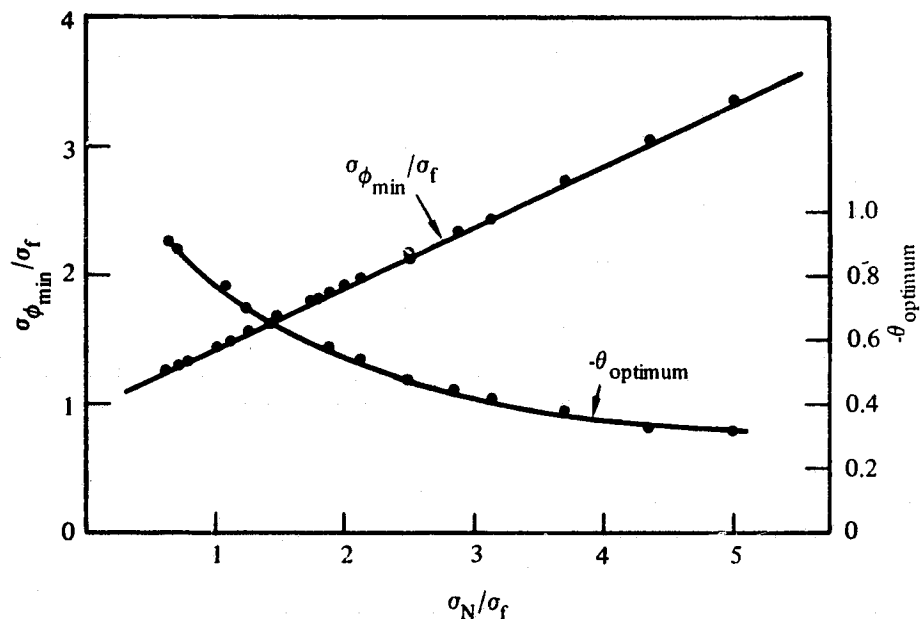


Figure 9. Control procedure analysis results.

optimum θ is being applied; e.g., when the noise is five times the standard variability, the application of a θ of -0.3 results in an epoch variability of only about 3.5 times worse than the standard. The apparent extrapolation to 0,1 indicates that under conditions of zero noise, the epoch variability can be no smaller than that of the standard.

SUMMARY OF PROCEDURES

A timing site may be established by installing suitable equipment and selecting suitable signals for observation. At the present time, a convenient choice of equipment would be a conventional navigation receiver with a whip antenna modified for signal injection calibration using a special injector and keyer. Path selection studies can be made for the specific receiving site; however, daytime measurements near noon on the Omega transmissions between 10.2 and 13.6 kHz probably will prove most satisfactory. Gross epoch can be established by lead-edge techniques. Epoch resolution then can be employed to identify particular rf carrier periods. Once initially set, epoch can be maintained by reliable dividers and periodic fine epoch measurements at various carrier frequencies. If the signal stabilities are adequate, epoch verification may be possible via signals from different stations at different frequencies. If significant differences are indicated, direct measurements for epoch verification should be initiated. Clock frequency is derived from a combination of a quality

Equipment: navigation receiver; whip antenna; injection

Noon measurements

Gross epoch: lead-edge

Fine epoch: carrier phase measurements; maintained by dividers

Daily epoch measurements

Adjustment procedure applied

frequency standard and a periodically adjusted phase shifter. The frequency error of the standard is estimated by a regression of indicated epoch on time and is compensated by periodic phase shift. Adjustments are obtained from daily epoch errors derived over perhaps four propagation paths and are applied in accordance with an adopted adjustment procedure. Through the use of a cesium frequency standard and a 60-day regression to deduce frequency, maintenance of change of epoch to better than $3 \mu\text{sec}$ and frequency to about one part in 10^{12} is possible. If special techniques are used, theoretical computations indicate the possibility of maintaining epoch continuously to better than $1 \mu\text{sec}$.

**Accuracy: epoch: better than
 $3 \mu\text{sec}$; frequency: 10^{-12}**

With special techniques: $1 \mu\text{sec}$

**Additional work needed:
adjustment procedures; pulse
timing; correlation effects**

CONCLUSIONS AND RECOMMENDATIONS

By means of the techniques described, epoch at timing sites may be deduced and maintained to better than $3 \mu\text{sec}$ and frequency can be maintained to about one part in 10^{12} via Omega transmissions. Theoretically, employing special techniques should make possible the maintenance of epoch to better than $1 \mu\text{sec}$. Prior to implementation of a complete global Omega system in the early 1970's, a useful timing capability presently is available from the existing four stations although at reduced accuracy in remote areas. The procedures described are essentially those which have been employed in synchronizing Omega for the past 6 years⁴⁰ and hence may be recommended as practicable for immediate implementation.

However, much additional work remains to be done. The areas requiring special attention include pulse timing, receiver installation design, propagation prediction, interpath cross correlation and signal autocorrelation, adjustment procedure optimization, and autocorrelation of the frequency variations of quality standards. The correlation questions are potentially the most important and most difficult. Conflicting data are presently available, and even relatively low long-term correlation in frequency standards can drastically change the optimization of the adjustment procedure. Similarly, cross correlation of phase fluctuations on various paths may be significantly different for timing applications than for navigation owing to the elimination of recognized disturbances.

REFERENCES

1. National Bureau of Standards Technical Note 329, *Standard Time and Frequency: Its Generation, Control, and Dissemination From the National Bureau of Standards, Time and Frequency Division*, by J. B. Milton, August 1969
2. Swanson, E. R., "Time Dissemination Effects Caused by Instabilities of the Medium," p. 181-198 in North Atlantic Treaty Organization Advisory Group for Aerospace Research and Development, Electromagnetic Wave Propagation Committee, *Phase and Frequency Instabilities in Electromagnetic Wave Propagation*, K. Davies, ed., Technivision Services, 1970 (AGARD Conference Proceedings No. 33)
3. Shapiro, L. D., "Time Synchronization From LORAN-C," *IEEE Spectrum (Institute of Electrical and Electronics Engineers)*, v. 5, p. 46-55, August 1968
4. Chi, A. R., and Witt, S. N., "Time Synchronization of Remote Clocks Using Dual VLF Transmissions," p. 588-612 in U.S. Army Electronics Command, *Proceedings of the 20th Annual Symposium on Frequency Control*, 21 April 1966
5. Palmer, W., Contract N00024-67C-1416; OMEGA Technical Note 17, *Proposal For Standard Time and Frequency by OMEGA*, December 1969
6. Stratton, J. A., *Electromagnetic Theory*, Section 5-18, McGraw-Hill, 1941
7. Guisset, J. L. and others, "Réception de Signaux Horaires sur Ondes Myriametriques," *Bulletin de la Classe Des Sciences (Academie Royale de Belgique). 5th Series*, v. 52, p. 490-499, 5 March 1966
8. Watt, A. D., *VLF Radio Engineering*, Appendix C, Pergamon Press, 1967
9. Naval Electronics Laboratory Center Report 1529, *OMEGA System Synchronization*, by C. P. Kugel, 10 January 1968
10. U.S. Naval Observatory, *Daily Relative Phase Values* (Issued weekly)
11. U.S. Naval Observatory Time Service Letter, *Instructions to Interpret the 'Phase Values' Bulletins and Teletype Messages*, 30 September 1968
12. Wright, J., "Accuracy of Omega/VLF Range-Rate Measurements," *Navigation*, v. 16, p. 71-79, Spring 1969
13. Naval Electronics Laboratory Center Report 1657, *Composite OMEGA*, by E. R. Swanson and E. J. Hepperley, 23 October 1969

14. Navy Electronics Laboratory Report 1305, *OMEGA Lane Resolution*, by E. R. Swanson, 5 August 1965
15. Navy Electronics Laboratory Technical Memorandum 1085,* *OMEGA Lane Resolution—Further Measurements in the Absolute Mode*, by E. R. Swanson and E. J. Hepperley, 23 March 1967
16. Naval Electronics Laboratory Center TN 1472,* *Tests of OMEGA Receiver AN/SRN-12*, by J. E. Britt, 5 March 1969
17. Naval Electronics Laboratory Center TN 1529,* *Accuracy Tests on TRACOR 3-599R OMEGA Receivers*, by J. E. Britt, 21 August 1969
18. Naval Electronics Laboratory Center TN 1445,* *High Latitude D-Region*, by I. J. Rothmuller, 4 November 1968
19. Naval Electronics Laboratory Center TN 1505,* *Auroral Zone Effects on OMEGA*, by I. J. Rothmuller, 12 June 1969
20. Naval Electronics Laboratory Center TN 1429,* *Effect of Higher Order Modes on OMEGA Frequencies at Night*, by J. A. Ferguson, 10 September 1968
21. Goddard Space Flight Center Report X521-69-346, *Dual VLF Timing Capability Observed at Some Intermediate Ranges*, by J. H. Roeder and M. E. Shawe, June 1969
22. Baltzer, O. J., TRACOR, INC., private communication
23. Naval Electronics Laboratory Center TD41, *OMEGA Navigation System—Synchronization and Operation, 1966-1968*, by E. R. Swanson and C. P. Kugel, 27 August 1968
24. Naval Electronics Laboratory Center TN 1778,* *Calibrated VLF Phase Measurements*, by E. R. Swanson and R. H. Gimber, 4 December 1970
25. Burgess, B., "Experimental Observations on the Phase Variability of 200 Hz Difference Frequencies Derived From VLF Transmissions Obtained Over Large Distances," p. 71-75 in North Atlantic Treaty Organization Advisory Group for Aerospace Research and Development, Electromagnetic Wave Propagation Committee, *Phase and Frequency Instabilities in Electromagnetic Wave Propagation*, K. Davies, ed., Technivision Services, 1970 (AGARD Conference Proceedings No. 33)

*NEL technical memoranda and NELC technical notes are informal documents intended chiefly for use within the laboratory.

26. Naval Electronics Laboratory Center TN 1593,* *Phase and Amplitude Variations With Distance and Azimuth at 20 kHz: Theory and Experiment*, by W. D. Westfall and J. A. Ferguson, 3 December 1969
27. Naval Electronics Laboratory Center TN 1777,* *An Assessment of OMEGA Signals at NASA Tracking Stations*, by D. B. Sailors, 4 December 1970
28. National Bureau of Standards Technical Note 610, *Application of VLF Theory to Time Dissemination*, by W. F. Hamilton and J. L. Jespersen, November 1971
29. Bodily, L. N. and Hyatt, R. C., " 'Flying Clock' Comparisons extended to East Europe, Africa and Australia," *Hewlett-Packard Journal*, v. 19, p. 12-20, December 1967
30. Bodily, L. N. and others, "World-Wide Time Synchronization, 1966," *Hewlett-Packard Journal*, v. 17, p. 13-20, August 1966
31. Essa Space Disturbance Laboratory, *The National Operational Space Disturbances Forecasting System*, 1 April 1969
32. Navy Electronics Laboratory Preliminary Letter Report, *High Latitude Propagation Effects on Omega Norway Operation During 1966*, by C. P. Kugel and E. R. Swanson, 15 February 1967
33. Harvard University. Engineering and Applied Physics Division Technical Report 552, *The Use of Composite Signals at Very Low Radio Frequencies*, by J. A. Pierce, February 1968
34. Pickard and Burns Electronics Publication 886B, *OMEGA - A World-Wide Navigational System, System Specification and Implementation*, by J. A. Pierce, 1 May 1966
35. Palmer, W., Contract NObsr 95033; OMEGA Technical Note 9, *Intermittent Control of Synchronization, Part I. First Order Control Systems*, 24 August 1966
36. Naval Electronics Laboratory Center Report 1544, *Omega-System Synchronization in the Absolute Mode of Operation*, by C. R. Phipps, 13 March 1968
37. Navy Electronics Laboratory, *Omega Station Standard Operating Procedure For Synchronization in the Absolute Mode*, 18 February 1966
38. Bodily, L. N., "A Summary of Some Performance Characteristics of a Large Sample of Cesium-Beam Frequency Standards," *Hewlett-Packard Journal*, v. 18, p. 16-20, October 1966
39. Hewlett-Packard Specification, *Cesium Beam Frequency Standard, Model 5061A*, 1 September 1969
40. Naval Electronics Laboratory Center Technical Report 1757, *Omega Synchronization and Control*, by E. R. Swanson and C. P. Kugel, 19 March 1971

*NEL technical memoranda and NELC technical notes are informal documents intended chiefly for use within the laboratory.

APPENDIX A: RADIO TIMING*

SUMMARY

The effects of pertinent parameters of the medium on the dissemination of time are discussed. Time is defined generally to include both frequency and epoch.

A clear distinction is drawn between 'noise' in the usual electrical sense and 'noise' in the statistical sense. Statistical noise important to time dissemination arises primarily from random variations in the medium through which 'time' is propagated from the transmitting antenna to the remote receiver. The statistical properties of this transfer or 'mapping' cannot be changed by increasing transmitter power to improve the signal-to-noise ratio.

Time dissemination is affected by both the repeatability and the predictability of the medium. Repeatability affects both frequency and epoch; predictability primarily affects dissemination of epoch. The relationships between the statistical properties of the medium and the accuracy to which time can be disseminated are developed. Two schemes are considered: 'lead edge' pulse techniques and phase tracking techniques. Both schemes may be used to distribute epoch in addition to frequency, provided a means is available to resolve the inherent ambiguity in phase tracking to a usefully long period. Phase tracking ambiguities are usually resolved by combination with lead-edge techniques or by tracking several frequencies. In either case, the precision of the epoch is determined by the phase measurements after acquiring the correct time period. Factors affecting prediction are also discussed briefly.

Although the approach is sufficiently general to apply to any frequency range, primary emphasis is placed on the vlf bands.

INTRODUCTION

Time dissemination may be defined as the process of transferring time from one location to another. For the following discussion a simplified concept of 'time' will be employed. While 'time' is virtually impossible to define in any absolute sense, we may all use intuitive notions which will

*This appendix closely follows reference 2 in the report proper. The original paper has been slightly revised to reflect more recent developments and abridged to concentrate especially on very low frequencies. This appendix was included in the original issue of this report for completeness and also because the original paper was not then generally available owing to delay in publication of the symposium proceedings.

suffice in the present analysis. Atomic frequency standards may now be constructed so that the periodic time base derived from atomic oscillations is very nearly 'uniform.' Furthermore, if 'absolute' standards are considered, the time bases of any two standards will have the same periods to a very high accuracy. Such standards may now be carried to various points on the terrestrial sphere and, if properly synchronized initially, provide 'identical' time at any locations of interest. This theoretical ability to physically transfer timing standards is of great convenience, because we can envision one uniform worldwide time scale against which to measure our success in disseminating time by radio means. In practice, atomic clocks can now be flown around the world to provide nearly synchronous time scales at separated sites. Unfortunately, the accuracy of transferred time scales, using presently available standards, degrades rapidly compared with time available from radio signals. Nonetheless, physical transfer of standards provides a method of performing experiments and establishing initial conditions. Relativistic effects will vary the time of clocks which have been physically transferred; however, present standards are not sufficiently stable to show significant effects through displacement on the surface of the earth.

The concept of 'time' includes two major subdivisions: frequency and epoch. Frequency refers to the uniformity or periodicity of the time scale; epoch refers to the actual location or timing of the periodic events. If we say a wrist watch 'gains' or 'loses,' we mean the frequency is high or low, respectively. Even if a watch neither gains nor loses, it must be properly set initially and, indeed, changed on entering a new time zone. These concepts can be readily appreciated using a distance analog as shown in figure A1, where segment lengths represent periods and the dividing segment marks indicate epoch. A and B illustrate identical frequency and epoch; segments are the same length (period) and ticks are at the same points (epoch). C and D illustrate identical frequency but different epochs. E and F illustrate different frequencies. Note that although the first ticks on E and F are identical — i.e., the 'epoch' was initially the same — the ticks rapidly separate. This illustrates that epochs remain defined and constant between two separate clocks only if the frequencies are identical.

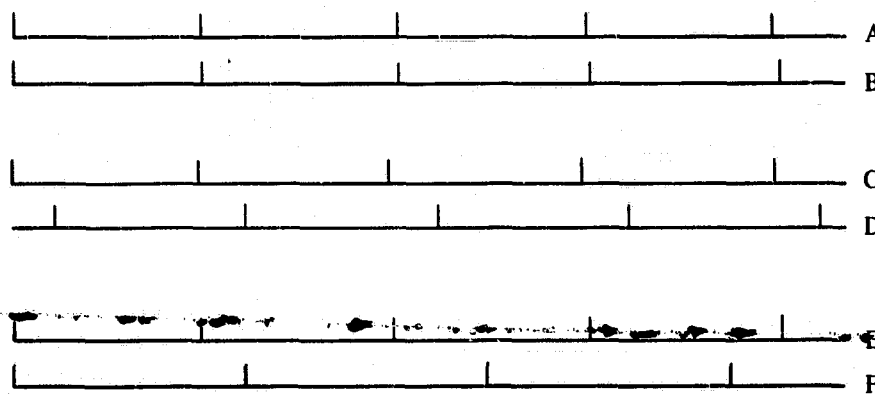


Figure A1. Distinction between frequency and epoch.

Depending on application, it may be necessary to know either frequency or epoch, or both. For example, if a cake requires 1 hour to bake, the time standard used must have the correct frequency, but the epoch is irrelevant. If an airplane is to depart at a given time, the epoch must be known, but the frequency is of little importance. The study of time dissemination must therefore include consideration of both frequency and epoch.

Frequency is usually determined by periodic epoch measurements. If some property of a radio wave, such as the electric vector, is represented by a sinusoid of unit amplitude, then measurements of this property yield the argument, or phase, of the sinusoid. Phase is thus equivalent to epoch. If such measurements are repeated, then the frequency may also be determined, because frequency is the derivative of phase. Hence, time dissemination can be completely deduced from a sufficiently general study of epoch or phase dissemination.

Ambiguities inherently arise in epoch determinations. This occurs as a result of choosing regular 'periodic' physical phenomena to derive time bases. The hour may be determined by the rotation of the earth; however, this is ambiguous with a period of 24 hours. The day may be determined by the revolution of the earth about the sun; however, this is ambiguous with a period of 1 year. If any aspect of a continuous radio wave is used to determine epoch, it will be ambiguous by an integral number of wave periods. The very regularity of the phenomenon chosen for a time measurement usually renders the physical characteristics used to determine epoch indistinguishable from one period to the next. Ambiguities may be 'avoided' by comparing clocks initially and counting periods; e.g., we habitually count years and collectively are careful not to forget any particular year. These ambiguities may also be 'resolved' by combining two or more epoch determinations using phenomena with different characteristic periods. We determine accurate or 'fine' time by using a sundial to measure the earth's rotation; however, we use the revolution of the earth about the sun to resolve the 24-hour ambiguity associated with the 'fine' measurement. Typically, multiple phase determinations allow greater accuracy than a single determination while retaining a long interval between ambiguities. In the example of the sundial, the accuracy of the time measurement would be determined entirely from the reading of the sundial, while a large error in determining the coarse measurement of the earth's rotation about the sun would result in choosing the wrong day. This illustrates the important distinction between the inherent accuracy of a timing device or mechanism and the associated methods of expanding the epoch ambiguity. Note that in continuous operation we do not ordinarily resolve epoch ambiguities through combination with other mechanisms of longer period; rather, we attempt to maintain an unerring count of fundamental oscillations. For example, we count days rather than resort to celestial observations to determine day of year. There is, however, some finite probability of failing to maintain proper count of fundamental clock periods. Similarly, if a method of resolving epoch is envisioned, there is some finite probability that the method will fail on any given application.

Most radio time dissemination schemes include some method for resolving the ambiguities in period associated with the fundamental

mechanism being employed to determine precise time. For example, time ticks transmitted every second can be used to determine epoch to within the accuracy permitted by the transmission medium and the equipment used. If ticks were transmitted exactly once per second every second, no method would be available to distinguish individual seconds. Individual seconds may be distinguished by also transmitting a second pattern which has a characteristic period of, say, 1 minute. The timing accuracy of the transmission of a 1-minute period must be better than about $\frac{1}{2}$ second or it will not be possible to identify the individual seconds ticks. Normally, such systems are designed so that the probability of erroneous choice of the seconds ticks would be negligible; however, the error probability is never zero. As an example, a 1-minute period may be created by deleting the seconds tick once per minute. Each individual tick provides epoch to an accuracy of a small fraction of a second while the absent tick allows identification of individual seconds ticks within the 1-minute period. This method is presently employed and is normally reliable. However, under very adverse signal-to-noise conditions it may still be possible to get accurate information from the individual seconds ticks and yet be extraordinarily difficult, and uncertain, to determine the location of the deleted 1-minute ticks. Even if the correct second can be identified within the 1-minute period, some other means or other periodic features of the transmission must be used to determine the correct minute within the hour, correct hour within the day, correct day within the year, and so on. Each of these steps involves the resolving of the epoch as determined from one fundamental period in terms of another phenomenon of longer period. Each step has an associated probability of error. Fortunately, many methods are available to determine the longer time periods such as hours, days, and years. Typically, high-precision radio dissemination schemes are not concerned with the longer periods but only provide methods to resolve time intervals shorter than a few seconds. Other methods, such as calendars, mechanical clocks, and even voice radio transmissions are assumed available to resolve the epoch ambiguity beyond a few seconds. Methods employed for coarse time determination are well known and need not be belabored here. A complete time determination must employ some such methods and, indeed, these methods may vary from one user to another depending on equipment available. Epoch resolution problems must be considered whenever the inherent ambiguities are short with respect to 1 second. Carrier phase measurements may be quite accurate for timing purposes in some systems such as Loran C and Omega. However, these carrier measurements are ambiguous by the period of the respective carriers, and some method must be provided to determine individual periods. For Loran C to work correctly, the 'coarse' timing measurements must be accurate to about 5 microseconds, a rather stringent requirement for 'coarse' timing. Such a coarse timing method is provided by the Loran C system. The coarse timing accuracy does not affect the resultant epoch determined from a Loran C clock unless the correct carrier period is not identified — in which case the system is considered to be functioning improperly. When accuracy is considered, it is the accuracy of the fine epoch measurement which is meant. Reliability may be used to

represent the probability of determining the correct fine period. The two aspects are conceptually separate and distinct.

The time dissemination problem can thus be solved by: (1) developing a theoretical expression relating epoch dissemination capability to frequency dissemination capability, (2) performing experiments to determine epoch dissemination capability, and (3) finding the probability of correctly determining the individual period of the phenomenon used for fine timing in terms of longer, readily identifiable, periods. In practice these require knowledge of the variance and autocorrelation function of epoch fluctuations determined over appropriate radio paths under various conditions.

RELATIONSHIP BETWEEN FREQUENCY AND EPOCH

An expression relating the frequency of a simple repetitive phenomenon to information contained in periodic epoch measurements is desired. Phase and epoch are simply related as phase is the dimensionless argument of the function representing the phenomenon while epoch is the time associated with this fractional period. Frequency is related to phase by

$$f = \dot{\phi} \quad (A1)$$

where f is frequency, ϕ is phase in cycles, and the dot operator is used to denote differentiation with respect to time. Assuming frequency is constant, then two phase measurements separated in time by t give the frequency

$$f = \frac{\phi_2 - \phi_1}{t} \quad (A2)$$

In practice the phase measurements will be noisy and have uncertainties indicated by the standard deviations σ_1 and σ_2 . Assuming phase stability is stationary,

$$\sigma_1 = \sigma_2 = \sigma_\phi$$

Now, provided an accurate time reference is available and if the observations were sufficiently separated so as to be uncorrelated, the uncertainty in the frequency measured from the two phase observations will be

$$\sigma_f = \frac{\sqrt{2} \sigma_\phi}{t} \quad (A3)$$

If the uncertainty of the phase measurements, σ_ϕ , is entirely due to limitations in the propagation medium, then equation (A3) gives the theoretical uncertainty of frequency as determined by ideal equipment and reference standards from only two epoch measurements. Repeated phase measurements

are desirable, since these allow determination of a regression line of phase as a function of time. The slope of the regression line is then the estimate of frequency. If discrete phase measurements are made periodically, every T seconds, then the frequency is given by

$$f = \frac{12 \sum_i i \phi_i - 6(n+1) \sum \phi_i}{Tn(n^2 - 1)} \quad (\text{A4})$$

where n is the number of phase measurements. The standard error for the estimate is given by

$$\sigma_f = \frac{\sqrt{12}}{T\sqrt{n(n^2 - 1)}} \sigma_\phi \quad (\text{A5})$$

Equations (A3), (A4), and (A5) lack generality, since the basic observable phase stability, σ_ϕ , is used. It is more convenient to assume that the phenomenon being measured has a known period, in which case time units can be assigned to the uncertainties of the phase measurements. Since one cycle of the phenomenon is equivalent to one period in time, $\sigma_t = \sigma_\phi/f$, whence (A5) becomes

$$\frac{\sigma_f}{f} = \frac{\sqrt{12}}{T\sqrt{n(n^2 - 1)}} \sigma_t \quad (\text{A6})$$

Equation (A6) may be used to estimate the fractional uncertainty in frequency determined by making noon phase measurements of radio signals using ideal standards. For this application $T = 24$ hours and the total time spanned by the observations is $t = T(n-1)$. Figure A2 shows σ_f/f as a function of t.

The previous equations have been restricted to measurements sufficiently separated in time so as to be considered uncorrelated. In the simple case of two measurements, the uncertainty including the effects of auto-correlation is given by

$$\sigma_f = \frac{\sqrt{2}}{t} \sigma_\phi \sqrt{1 - r(t)} \quad (\text{A7})$$

where $r(t)$ is the correlation between phase fluctuations at the first observation and those at an observation t later. To be generally applicable, the equation requires the correlogram giving $r(t)$ for the applicable time dissemination transfer function.

Derivation of more general expressions for frequency and its uncertainty are beyond the scope of this paper. The problem is that of estimating the slope of a regression line when the error terms are correlated. It is apparent that a general solution requires knowledge of the complete correlation, $r(t)$, for all time separations present in the sampling. In the nomenclature of

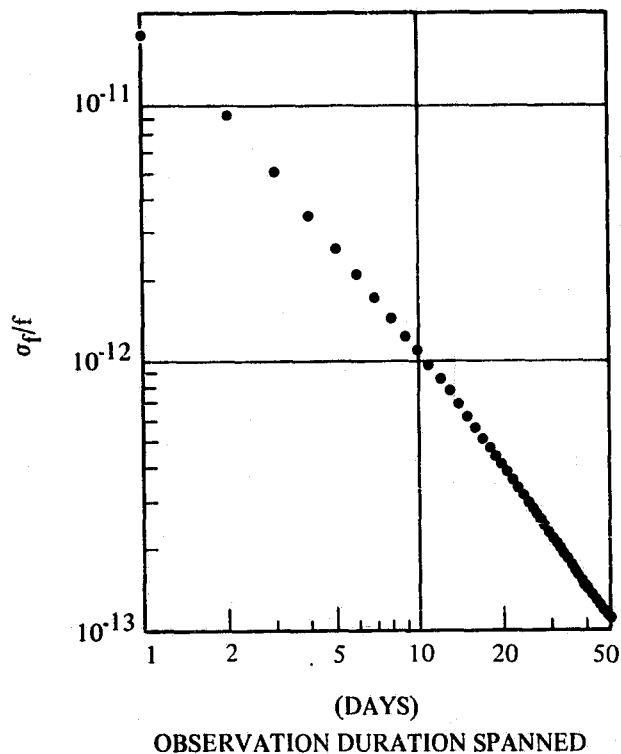


Figure A2. Frequency uncertainties from daily phase measurements of 1-microsecond accuracy.

discrete periodic sampling previously considered, this requires knowledge of $r(T), r(2T), r(3T), \dots, r(nT)$. The problem is statistically difficult, since least-squares estimation is not free from bias in this case. A brief review of the problem was recently given by Kendall and Stuart.¹ (The first detailed discussion was apparently given by Cochrane and Orcutt² and, although dealing with econometric examples, is a good general introduction.)

Some qualitative aspects of correlation require elaboration. Equation (A3) shows that the uncertainty in frequency increases inversely as the time between two phase measurements is reduced. As the time between measurements is reduced, eventually the measurements will become correlated and equation (A7) must be used. If the autocorrelation is such that $r(t)$ may be expressed as a sum of exponentials, then as $t \rightarrow 0$, $r(t) \rightarrow 1 - t/\alpha$ and

$$\lim_{t \rightarrow 0} \sigma_f = \sigma_\phi \sqrt{\frac{2}{\alpha t}} \quad (\text{A8})$$

where α is approximately equal to the autocorrelation period, τ , at which $r(\tau) = 1/e$. The interrelationship between correlated and uncorrelated conditions for a simple two measurement frequency determination is illustrated in figure A3. The illustration shows the fractional uncertainty in frequency for various separations of phase measurements assuming $\sigma t = 1$ microsecond and

¹See *REFERENCES*, p. 98.

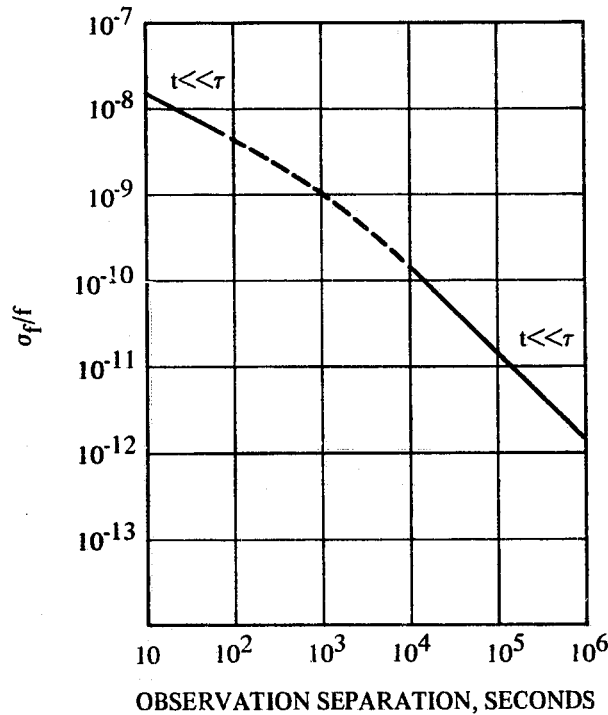


Figure A3. Frequency uncertainties from two phase measurements of 1-microsecond accuracy.

$\alpha = 1000$ seconds. Note that the accuracy of a frequency determination for short sampling times is greater than would be indicated if the phase stability function were not autocorrelated. A similar limit would occur if the frequency were determined by periodic phase measurements; however, exact uncertainties would be difficult to estimate. One approximation for continuous integration has been given by Watt and Plush³. They note that the uncertainty of a phase measurement integrated over time T is approximated by

$$\sigma_{\phi_{av}} \approx \frac{0.7}{\sqrt{T/\tau}} \quad T/\tau > 1 \quad (A9)$$

They then replace σ_{ϕ} in equation (A3) by $\sigma_{\phi_{av}}$ and obtain

$$\sigma_f \approx \frac{\sigma_{\phi} \tau^{1/2}}{T^{3/2}} \quad T/\tau \gg 1$$

where T is the sampling interval and two such intervals are required; i.e., the total duration of measurements is $t = 2T$ so that

$$\sigma_f \approx \frac{2.9 \sigma_{\phi} \tau^{1/2}}{t^{3/2}} \quad T/\tau \gg 1 \quad (A10)$$

Equation (A10) assumes that the frequency will be determined by averaging phase over two adjacent intervals of length T and then determining frequency from the average of the two intervals. This is a very special way of determining frequency and is not optimum. If phase measurements are processed in more detail, but still using interval averages over intervals longer than the autocorrelation period, the resultant standard error of the frequency may be obtained by substituting (A9) into (A5), which in the limiting case becomes

$$\sigma_f \approx \frac{2.4\tau^{1/2}}{t^{3/2}} \sigma_\phi \quad T/\tau \gg 1 \quad (A11)$$

More accurate estimates of frequency should be possible if the phase measurements are made continuously and processed in some optimum way based on knowledge of the autocorrelation function for the phase fluctuations.

A related problem is how well an observer can measure frequency using imperfect local timing standards. Timing standards exhibit both short-term timing uncertainties which tend to be statistically stationary and also longer variations which are regarded as frequency uncertainties or 'drift.' The variance of local time reference is thus conveniently divided into two parts. The first portion is a simple noise term, σ_{nt}^2 , representing the short-term timing uncertainties of the standard. It is related to short-term frequency instability. The second term represents accumulated timing uncertainty due to frequency uncertainty. Because the ratio of the uncertainty in elapsed time to the elapsed time associated with long-term frequency uncertainties can be represented by the fractional uncertainty in frequency, the total variance of elapsed time is

$$\sigma_{\text{elapsed time}}^2 = \frac{t^2 \sigma_{fr}^2}{f_r^2} + 2 \sigma_{nt}^2 \quad (A12)$$

where both the initial and final timing measurements are noisy and σ_{fr} is the standard long-term error of the reference frequency f_r . Assuming the frequency determination through the medium is made from two uncorrelated phase measurements separated by time t , we have as before (A2)

$$f = \frac{\phi_2 - \phi_1}{t}$$

Taking the total derivative yields

$$\Delta f = \frac{1}{t} \Delta \phi_2 - \frac{1}{t} \Delta \phi_1 - \frac{\phi_2 - \phi_1}{t^2} \Delta t$$

whence

$$\sigma_f^2 \approx 2 \left(\frac{\phi_2 - \phi_1}{\{t_2 - t_1\}^2} \right)^2 \sigma_{\text{elapsed time}}^2 + \frac{2\sigma_\phi^2}{t^2}$$

But $t_2 - t_1 \approx t$, $\phi_2 - \phi_1 \approx ft$; $\sigma_\phi \approx f\sigma_t$; and using equation (A12)

$$\frac{\sigma_f^2}{f^2} \approx \frac{\sigma_{fr}^2}{f_r^2} + \frac{2\sigma_t^2 + 2\sigma_{nt}^2}{t^2} \quad (\text{A13})$$

Previously the timing capability without experimental timing uncertainties on the local reference was $(\sigma_f/f)^2 = (2\sigma_t/t)^2$. Comparison with equation (A13) shows that the actual accuracy with experimental uncertainty in local standards may be computed from an expression similar to that for the theoretically attainable accuracy but with (1) the time dissemination capability of the medium degraded on an rms basis with short-term timing uncertainties of the standards, $\sqrt{\sigma_t^2 + \sigma_{nt}^2} \rightarrow \sigma_t^1$, and (2) the result further degraded on an rms basis with the frequency uncertainty of the local standard. Conversely, if drift and timing uncertainties of the local reference are known, their effects on experiments can be estimated. It is implicit in (A13) that frequency cannot be quantitatively determined with higher accuracy than the local standard.

EPOCH MEASUREMENT

Epoch 'measurements' are indirect in the sense that all determinations of physical characteristics are indirect. Fundamentally, we compare physical manifestations of the same type and magnitude. For example, the length of a given object is 'measured' by comparison with a scale marking on a ruler. The actual observation is of the correspondence between the end of the object and a scale marking. The quantitative determination depends inductively on various assumptions of uniformity of the scale markings. Comparison of similar measurements by two observers will also depend on the relative values of the two standards employed as initially determined by some direct or indirect comparison and usually assumptions of invariance of the standards through displacement in time and space. The fundamental nature of measurements is especially important in considering epoch determination, and considerable confusion has arisen. Time is never measured directly. Measurements are made of sundial shadow positions, pendulum locations, electric field values, etc. The quantities measured are assumed to have a known periodic behavior. A fictional association is then made between phase of the periodic phenomena and time; viz., $t = \phi T_p$, where ϕ is phase in cycles and T_p is the assumed period of the phenomenon. This is a convenient concept and, indeed, has already been used in this paper. It allows timing capabilities of various diverse phenomena to be directly compared, provided we know the respective periods. While it is easy to determine periods of various phenomena *approximately* with respect to an international timing standard, it is impossible to do this exactly. It is also unsound to assume that a given phenomenon will have the same period as determined by various observers using different time references. Since the differences

generally will be small, we can express a standard error of a phase measurement in equivalent time units with no loss in accuracy. However, the meaning must be clearly understood. Crombie⁴ has written an excellent paper urging the experimental community to publish the quantities actually measured rather than 'time' equivalents.

The concept of epoch 'measurement' is thus superficial but useful. Epoch measurement means the comparison of phase of measurable physical phenomena of 'known' period expressed in 'equivalent' time units.

EXPERIMENTAL METHODS

There are two fundamental approaches to epoch measurements. One method is to attempt to maintain accurate time and the second is to arrange for a differencing geometry wherein the test signal is somehow returned to the origin or sent by different paths to a common point.

Accurate time may be maintained in two ways. An accurate clock may be employed, in which case (1) the short-term timing uncertainties of the clock must not be much greater than those of the phenomenon being studied, and (2) the long-term timing uncertainty associated with uncertainties in the frequency of the clock must not be such that large timing uncertainties can develop within several correlation periods, τ , of the phenomenon being investigated. These are absolute minimum requirements. In practice experimental design would favor:

$$\sigma_t \gg \sigma_n$$

$$\sigma_t \gg \tau \left(\frac{\sigma_f}{f} \right)$$

although accurate experiments may be performed if $\sigma_t \gtrsim 3\sigma_n$ and

$$\sigma_t \gtrsim 3\tau \left(\frac{\sigma_f}{f} \right)$$

and the observed measurements are appropriately corrected. The second method of maintaining accurate time requires a second system or time source to maintain synchronism between the various standards in the experiment. In this case the accuracy of the time reference system should be much greater than the nominal repeatability of the phenomenon being studied, as otherwise the autocorrelation function could not be determined for short lags. Frequently, time reference systems are used to reset clocks. Clocks provide accurate short-term stability while the reference system provides long-term accuracy. Unless accurate time may be continuously maintained with negligible error, it is important that variations in the reference timing system not be correlated with instabilities in the phenomenon being studied.

The second class of experimental design requires a spatial arrangement in which the phenomenon being studied occurs over various paths and is measured at a common point. Frequently the observation point is also the origin of the original exciting source. In this case the only clock in the experiment is used to generate the original exciting function and no differential time errors occur. A common example of this type of arrangement is a hyperbolic navigation system employing a slave and a master. The master station has a timing reference which determines system time. The slave simply operates as a reflector. Measurements of the difference between slave and master signals are thus independent of differential timing uncertainties. However, the interpretation of the results depends on any spatial correlation of the fundamental processes involved.

NOISE

Time dissemination programs require studies of the capability of a transmission medium to support epoch dissemination. The phenomenon being studied may be regarded as having a transfer or 'mapping' function through the medium. This transfer function is a random variable or mapping function generating observable values at the receiver from input excitations at the transmitter. The transfer is thus statistically 'noisy,' since the disseminated epochs will have variance and an autocorrelation function. The epoch statistics are conceptually indicative of the transfer properties of the phenomenon being observed through a given medium. As there is a direct causal relationship between the excitation of the medium and the transfer through it, the transfer function produces no output without input. This distinguishes the transfer function itself from the actual statistics of any observable epoch measurements, as the latter may exhibit the effects of extraneous inputs. In particular, the characteristics of a medium to allow epoch determination through the propagation of electromagnetic waves are independent of prevailing signal-to-noise ratio. Signal-to-noise ratios depend on the amount of extraneous receiver input and are not solely related to the uncertainties caused by transmission through the medium. Experimental data should be carefully analyzed so that the resultant statistics are free from the effects of extraneous noise. The effects of carrier to noise are discussed in reference 3.

AMBIGUITY RESOLUTION

Some precise time distribution systems utilize high-precision measurements of some short-period phenomenon and also provide less-accurate measurements of a phenomenon of longer period to provide a means of identifying specific integral periods of the precise timing mechanism. That is, the short-period phenomenon provides a 'fine' time scale while the longer period provides a 'coarse' time scale for use in determining integral periods

of the fine scale. The resultant simultaneity of the two phenomena is illustrated in figure 4, where the coarse time scale is assumed periodic to an integral multiple of the period of the fine scale. Let the short period be p and the long period be q . The fine measurement yields an estimate of epoch

$$\hat{t}_f = \phi_f p + np$$

while the coarse measurement yields an estimate

$$\hat{t}_c = \phi_c q + mq$$

where n and m are integers. The correct integral period of the fine measurement can be determined, within the inherent ambiguity of the coarse measurement, if

$$|\phi_c q - \phi_f p| < [1/2] p$$

where ϕ_c and ϕ_f are the phase of the coarse and fine measurements in cycles. The probability of correct epoch resolution is then the probability of

$$\left| \phi_c \frac{q}{p} - \phi_f \right| < 1/2.$$

It follows that

$$\text{var} \left[\phi \frac{q}{p} - \phi_f \right] = \frac{q^2}{p^2} \text{var} \phi_c + \text{var} \phi_f - 2 \frac{q}{p} \text{cov}(\phi_c, \phi_f) = Q$$

whence, if variations are normally distributed, the probability of correct fine period determination is given by

$$P = \frac{1}{\sqrt{2\pi Q}} \int_{-1/2}^{1/2} e^{-\frac{x^2}{2Q}} dx$$

The solution to a comparable problem when the ratio of the period of the coarse phenomenon to that of the fine phenomenon is a proper fraction rather than an integer is given in reference 5.

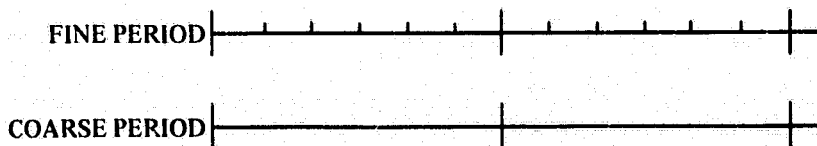


Figure A4.

AUTOCORRELATION CHARACTERISTICS

Correlograms from which epoch characteristics of radio signals over long paths can be determined are not generally available. However, the fade period or autocorrelation period, τ , has been determined for carrier measurements in the frequency range from 10 to 100 kHz. Watt and Plush³ have shown that fade period as a function of frequency is approximately log-log linear between 16 and 100 kHz. The relationship may be represented by

$$\log \tau_{\text{sec}} = 7 - 2.5 \log f_{\text{kHz}}$$

and extrapolates to approximately 10 hours for 10.2 kHz, a value subsequently obtained by the author. The relationship is based on limited data and applies only to long paths. Fluctuation periods observed over long paths are typically longer than those observed by vertical incidence sounding. Autocorrelograms from sounding measurements at vlf by Paulson, Gossard, and Moler show markedly shorter periods and less frequency dependence.⁶ However, the sounding measurements included filtering to remove longer periods.

PREDICTION

Characteristics of epoch dissemination are given by the transfer or mapping function of the propagation mechanism used. Most important for epoch determination is the mean or average value expected. In the general case of disseminating time to some arbitrary remote point, the mean will be unknown and must be estimated by some empirical or theoretical modeling of the propagation mechanism. The measured epoch can be no more accurate than the accuracy of the theoretical prediction.

A meaningful discussion of prediction for a wide range of propagation mechanisms, frequencies, and geographic areas is virtually impossible. It is common to make special 'calibration' measurements to reduce prediction errors for areas of particular interest. Hence, prediction uncertainties for given propagation paths should be estimated individually. Prediction errors for epoch measurements from the 10.2-kHz Omega carrier signals were reduced to a few microseconds over an extensive area⁷ while 100-kHz groundwave carrier signals on Loran C can be predicted to a few tenths of a microsecond in well calibrated areas.

Since predictions frequently include diurnal or seasonal variations, some interaction between prediction theories and experimental statistical characteristics invariably occurs. Normally, transmission capabilities of a medium are quoted after allowances have been made for all predictable variations. If the correlation periods are short and diurnal changes slow, allowances can be made by passing the data through a filter of long time constant after, perhaps, separating data into groups according to diurnal period. These conditions are not satisfied at vlf, and data are frequently

sampled every 24 hours and then filtered to remove seasonal variations. The technique works well to determine the variance but may lose most of the autocorrelation characteristics of interest.

Prediction errors do not affect frequency determinations if the errors are not time-dependent. That is, frequency is determined from epoch measurements through an equation of the form

$$f = \frac{[\phi'(t_2) - \epsilon(t_2)] - [\phi'(t_1) - \epsilon(t_1)]}{t_2 - t_1}$$

where $\phi'(t)$ is the observed phase at time t corrected by the predicted value and $\epsilon(t)$ is the error in the prediction at the time t . If

$$\epsilon(t_1) = \epsilon(t_2),$$

then the indicated frequency depends simply on the differences of the observed epochs as in equation (A2). Excluding seasonal changes, estimated values of epoch determined from most propagation mechanisms are very nearly independent of time, provided that day and night periods are considered separately and day-night transitions are disregarded. A conspicuous exception to this generality is vlf carrier propagation during daytime conditions for frequencies near 10 kHz. In this range, predictable changes occur throughout the day which correspond to fractional frequency changes on the order of one part in 10^9 ; seasonal changes corresponding to fractional frequency errors of 2×10^{-12} also occur.

EPOCH REPEATABILITY

Epoch repeatability deduced from carrier measurements of single reflection sky wave radio propagation during the day has been shown to vary approximately in a log-log linear relationship with frequency for frequencies from about 10 to 100 kHz.⁸ The relationship may be written

$$\log \sigma_{t_1 \mu\text{sec}} = 1.1 - 0.8 \log f_{\text{kHz}}$$

and indicates uncertainties of about 1 μsec for 20 kHz and 2 μsec for 10.2 kHz.

CONCLUSION

The capability of a medium for time dissemination can be completely determined if the mean, variance, and autocorrelation of the phase transfer function for the particular propagation mechanism are known. Much work

remains to be done to refine phase transfer statistics. However, various mechanisms are available by which time may be disseminated over great distances with accuracy on the order of a few microseconds.

REFERENCES

1. Kendall, M. G. and Stuart, A., *The Advanced Theory of Statistics, Vol. 3: Design and Analysis of Time-Series*, p.497-498, Hafner Publishing Company, 1966
2. Cochrane, D. and Orcutt, G. H., "Appreciation of Least Squares Regression to Relationships Containing Auto-Correlated Error Terms," *American Statistical Association. Journal*, v.44, p.32-61, March 1949
3. Watt, A. D. and Plush, R. W., "Power Requirements and Choice of an Optimum Frequency For a Worldwide Standard-Frequency Broadcasting Station," *Journal of Research of the National Bureau of Standards. Section D: Radio Propagation*, v.63D, p.35-44, July-August 1959
4. Crombie, D. D., "Phase and Time Variations in VLF Propagation Over Long Distances," *Journal of Research of the National Bureau of Standards. Section D: Radio Propagation*, v.68D, p.1223-1224, November 1964
5. Navy Electronics Laboratory Report 1305, *OMEGA Lane Resolution*, by E. R. Swanson, 5 August 1965
6. Paulson, M. R., Gossard, E. E. and Moler, W. F., "The Nature and Scale Size of Irregularities in the D-Region of the Ionosphere as Observed on a Near Vertical Incidence VLF Sounder," Chapter 6 in North Atlantic Treaty Organization. Advisory Group For Aeronautical Research and Development. Avionics Panel. Ionospheric Research Committee Meeting, 7th, Munich, 1962, *Propagation of Radio Waves at Frequencies Below 300 Kc/s*, Macmillan, 1964
7. Navy Electronics Laboratory Technical Memorandum 781, *Present Predictability of Omega 10.2 Kc/s Nighttime Signals*, by E. R. Swanson, 18 March 1965 (NEL technical memoranda are informal documents intended chiefly for use within the laboratory)
8. Watt, A. D. and others, "Worldwide VLF Standard Frequency and Time Signal Broadcasting," *Journal of Research of the National Bureau of Standards. Section D: Radio Propagation*, v.65D, p.617-627, November-December 1961

APPENDIX B: OMEGA*

SUMMARY OF APPENDIX B

Omega is a very-long-range, very-low-frequency (vlf) radio navigation system which will provide global coverage for ships and aircraft. Present Omega coverage provides signals which are already the most widely distributed radio navigation aids in the world. A worldwide network of eight stations is planned for completion within the next few years and will provide redundant global coverage. Omega concepts are presented together with the transmission format and station placement. Omega derives not only its accuracy and reliability but also its limitations from the characteristics of vlf radio propagation. A section describes features of vlf propagation which are related to Omega navigation or timing.

INTRODUCTION

Omega is a very-low-frequency (vlf) navigation system operating in the internationally allocated navigation band in the electromagnetic spectrum between 10 and 14 kHz. Global coverage will be obtained in the mid 1970's with eight transmitting stations; four stations are presently operational although not in final configuration nor at design power. In marine navigation, Omega normally is used as a single-frequency hyperbolic system, although several frequencies are available and the system can be used in the range-range mode.

The present stations have been in essentially continuous 24-hour operation for over 6 years. Over 1000 receivers have been constructed, of which about half have been sold commercially. The Navy is installing Omega on most ships capable of independent operation. Plans also have been made to install Omega on several Navy aircraft. Some fishing boats and merchantmen are now Omega equipped. As Mr. Jones observed at a recent meeting of the British Institution of Navigation: "... (Omega) is already the most widely deployed ground-based navigation aid in the world by a very substantial margin."¹

*This appendix was written in conjunction with preparation of 'Omega,' a paper presented to the National Marine Meeting of the Institute of Navigation at the U.S. Coast Guard Academy, New London, Conn., 13-14 October 1970, which emphasizes navigational aspects and applications of Omega. (Swanson, E. R., 'Omega,' *NAVIGATION*, v. 18, no. 2, p. 168-175, summer 1971.)

¹See *REFERENCES*, p. 123.

HISTORICAL

Omega itself may be considered the oldest vlf navigation system. However, the system has evolved considerably from its earlier form. In 1947 J. A. Pierce first proposed a hyperbolic navigation system based on phase-difference techniques rather than time differences.² In particular, a system operating in the vicinity of 50 kHz with a sine-wave modulation of 200 Hz was suggested. An experimental system of this type was constructed by the Naval Electronics Laboratory and called Radux. Subsequently, in 1955, it was suggested that the Radux information from the lf signal be combined with a separate vlf transmission near 10 kHz. This system was called Radux-Omega and initial 10.2-kHz transmissions were made in 1955. Later the lf transmissions were discontinued and ranges were expanded to lead to a single-frequency Omega system and, later, a multifrequency Omega system. Omega can thus trace a 20-year evolutionary history and has included transmissions at the system base frequency for 17 years.

Modern transmissions using the stations shown in figure B1 began in 1966. Previously, stations were used in a conventional slave-master configuration. Modern transmissions are derived from a bank of cesium frequency standards at each station, and each station is controlled as a source of standard signals. The modern arrangement is especially practical for a global system in that the navigator can pair stations in any convenient way to obtain useful hyperbolic geometry and signals. The modern configuration has also proved more reliable than older arrangements.

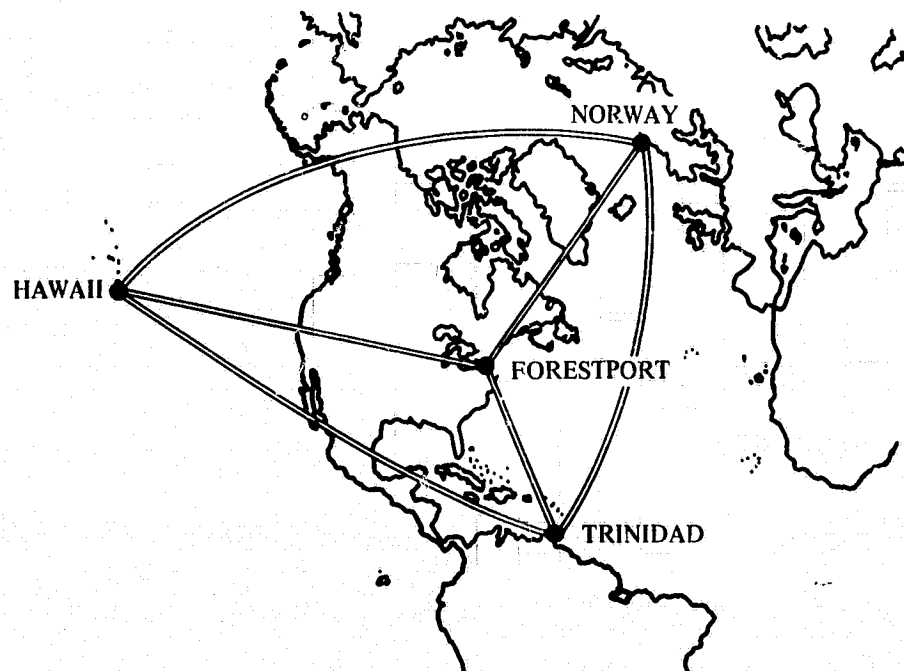


Figure B1. Geographic location of present Omega stations (North Dakota not shown).

IMPLEMENTATION

Global implementation is planned for the mid 1970's. Electronics at the existing four stations will be replaced by operational electronics common to all eight stations. Contracts have been awarded for construction of two transmitters (on-line and backup), timing, control, and tuning equipment for all stations. Generally, existing stations will be modified to radiate the system design power of 10 kW at 10.2 kHz and refitted with new electronics. However, because of geometric and antenna limitations, Forestport, New York, will not be improved. Rather, a new station has been constructed in North Dakota to replace the Forestport station. It is planned that the additional transmitting stations will be constructed in cooperation with the respective host nations. Possible locations are shown in figure B2, although the positions deliberately have been left vague, since negotiations are in progress. The government of Japan has, however, started construction of an Omega station on Tsushima.

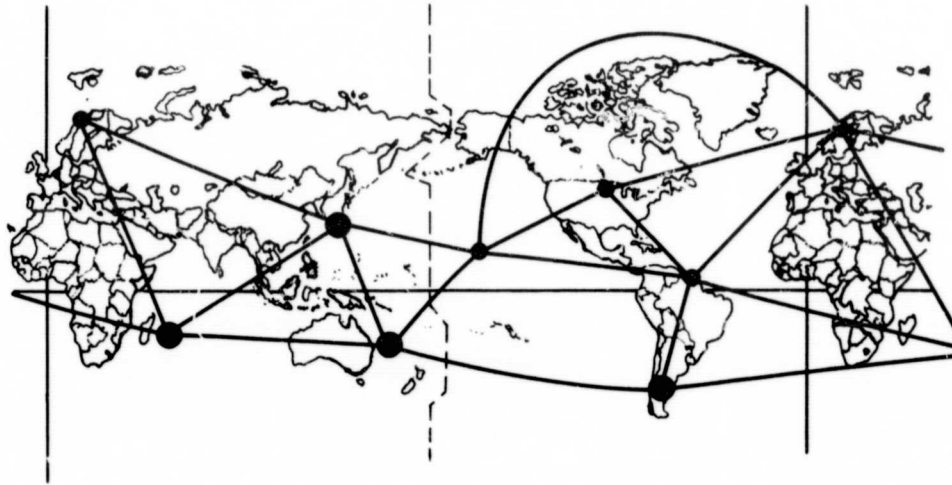


Figure B2. Possible locations for eight stations in the implemented global Omega system (cylindrical projection).

SYSTEM FORMAT

Basic Omega signals consist of very-low-frequency, 10.2-kHz, continuous-wave pulses transmitted sequentially from each station. Since the transmissions are time-shared, a commutator is required to separate each station within the 10-second commutation pattern shown in figure B3. The commutation scheme is unambiguous and synchronized to international time, with the 10-second period beginning at 0000 hours 1 January 1972 and repeating at 10-second intervals except that 1-second jumps, when taken internationally, will not be followed by Omega.

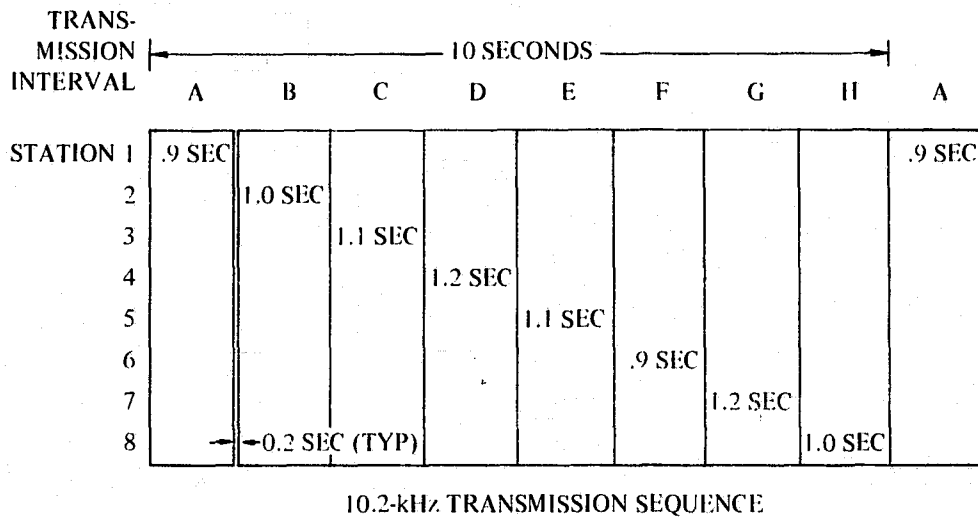


Figure B3. Simplified 10.2-kHz transmission format.

A hyperbolic Omega receiver measures the phase of two or more Omega stations against a reference generated from an internal oscillator. The internal oscillator permits storage of the phase information so that the relative phases of the different stations can be intercompared. Readout is the phase difference in centicycles (ccc) between selected stations and ordinarily is recorded continuously on strip-chart recorders. Since the comparisons are all between signals of the same frequency, no internal ambiguity can arise within the receiver due to divider jumps. Further, a hyperbolic Omega receiver has no intrinsic specification for absolute radio-frequency phase shift, since shifts common to all stations will be removed in the hyperbolic differencing. The system does, however, have an inherent physical ambiguity. Since adjacent carrier cycles cannot be distinguished, the measured phase of each carrier is inherently ambiguous by one cycle. Hyperbolic phase differences on a baseline between two stations are ambiguous by the hyperbolic spacing of one-half wavelength.

Because of continuous operation, the navigational lane ambiguity problem inherent in a single-frequency system generally is not troublesome to the navigator. However, additional frequencies are included in the full Omega format to permit reestablishment of lane should difficulties occur (fig. B4). Additional frequencies included for lane identification are 13.6 and 11-1/3 kHz; they may be used independently in exactly the same manner as the 10.2-kHz transmissions. However, ambiguities in the 13.6-kHz lines-of-position will be coincident with those at 10.2 kHz only every 24 miles. Similarly, LOP's at 11-1/3 will be coincident only every 72 miles. Comparison of the coincidence of LOP's obtained at the various frequencies can thus serve to establish the proper lane of the 10.2-kHz carrier within the 72-mile ambiguity of the lowest beat frequency.^{3,4,5}

Figure B4 also shows proposed additional transmissions on unique frequencies indicated by f_1, f_2, \dots, f_8 . The additional frequencies would be used primarily for system control but could also be convenient for other

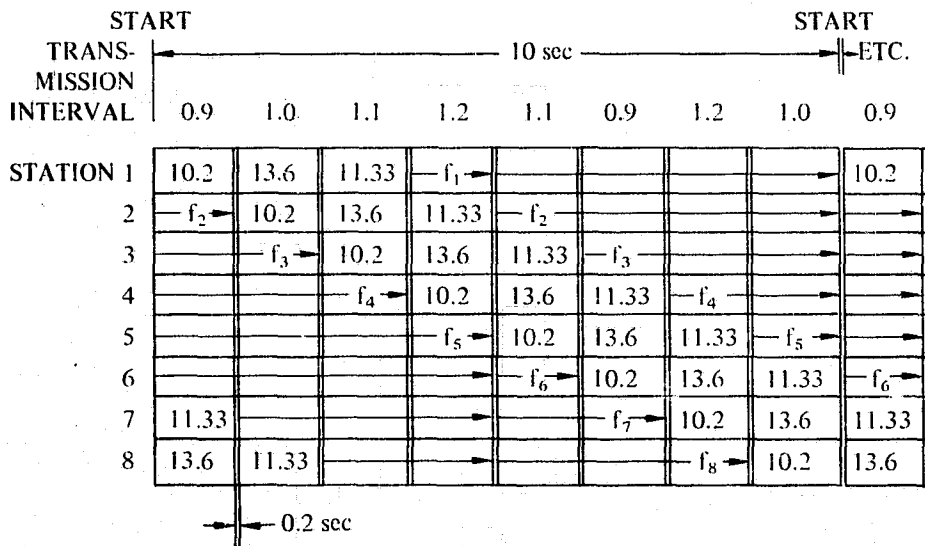


Figure B4. Omega signal format.

purposes such as time dissemination, since no commutator would be required for reception. It also has been proposed that each station transmit two unique frequencies separated by 250 Hz instead of the one shown. This would permit intrasystem control transmissions by FSK and also enable development of 250-Hz beat signals for timing. A five-frequency capability is being implemented.

Table B1 gives periods available from Omega transmissions if two unique frequencies between 12 and 13 kHz separated by 250 Hz are implemented at each station. The table is illustrative rather than exhaustive. A large selection of frequencies is available or may be derived to produce desirable periods for timing.

TABLE B1. FREQUENCIES AVAILABLE FROM OMEGA TRANSMISSIONS.

Frequency	Period	Type	Source
13.6 kHz	74 μ sec	Carrier (time-shared)	Carrier
12 - 13	77-83 μ sec	Carriers (unique)	Carrier
11-1/3	88 μ sec	Carrier (time-shared)	Carrier
10.2	98 μ sec	Carrier (time-shared)	Carrier
3.4	294 μ sec	Beat	13.6 - 10.2
2266-2/3 Hz	441 μ sec	Beat	13.6 - 11-1/3
1133-1/3	882 μ sec	Beat	11-1/3 - 10.2
800	1.25 msec	Beat	Unique carriers and 11.33 or 13.6
250	4 msec	Beat	Unique carriers
10	100 msec	Pulse	0.1-sec component of commutation pattern
0.8	1.25 sec	Pulse	Average segment repetition
0.1	10 sec	Pulse	Commutation repetition
0.033-1/3	30 sec	Multiple beat	Multiple: 1/3 Hz of 11-1/3 kHz with commutation pattern

PROPAGATION

Omega is a propagation-limited system. Accordingly, familiarity with propagation phenomena is useful not only for a basic understanding of the system but also to assist in obtaining better than nominal timing.

EARTH-IONOSPHERE WAVEGUIDE

One convenient analytical model for vlf radio propagation is that of a spherical waveguide formed between the earth and the ionosphere. In this approach, 'rays' and 'hops' are not explicitly considered; rather, the natural resonance 'modes' of the guide are used. Figure B5 illustrates earth-ionosphere mode resonances. Note that two modes are shown. In general, all resonant modes will propagate although with different characteristic velocity and attenuation.

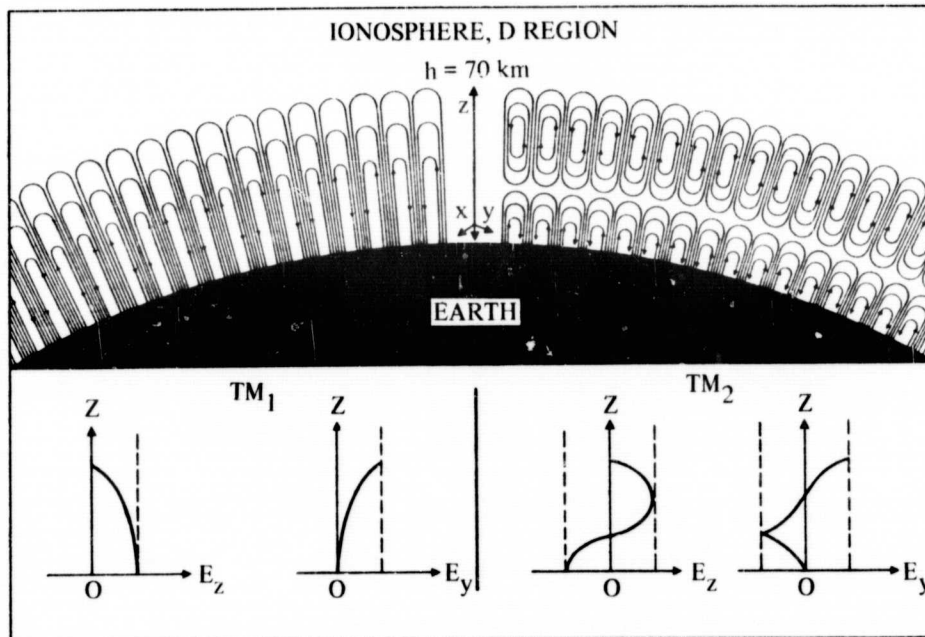


Figure B5. Electrical field structure for waveguide modes (from Watt and Croghan, ref. 6).

The concept of a spherical waveguide leads immediately to several valid conclusions. For example, energy will propagate around the world in all directions and may reinforce at the antipodal point from the transmitter. This phenomena has been observed and illustrates the extreme range obtained at vlf. (In fact, a unit of length frequently used is the megameter, $1 \text{ Mm} = 1000 \text{ km}$.) Also, since the lower ionosphere, or D-region, is controlling at vlf, we should expect severe attenuation when the wavelength becomes comparable with the height of the guide at about 70 to 90 km; i.e., a frequency of about 4 kHz. A severe increase in attenuation is observed as expected. Another generality, very important to timing systems, is that if one mode is dominant, then phase and amplitude should vary regularly as a function of distance from the transmitter without fluctuations due to interference between various modes. This condition may occur at any distance but in practice is especially true for frequencies near 10 kHz at distances greater than about 1000 km. Note that the regularity is occurring at *large* distances. This is just the opposite from the usual experience, in which the groundwave propagation at short distances is regular and multihop sky wave can cause irregularities at longer distances.

Vlf propagation has been studied for many years. This is due not only to its practical use as the mainstay of fleet communications for a half century but also because of the extreme repeatability of measurements. Although diurnal variations occur, measurements over paths from 5000 km to 10 000 km long typically show repeatability of about 1 dB in field strength while phase variations are measured in microseconds. The obvious challenge of predicting the absolute values of such repeatable phenomena has been

accepted by many workers in the past. Presently, the field is both theoretically and experimentally active. Accurate theoretical predictions depend on detailed knowledge of the ionosphere; conversely, vlf measurements may be used to develop ionospheric models. Both ionospheric models and theories are presently being refined. The already voluminous literature is expanding at an exponential rate. Even at the present, enough is known to design systems to within a few dB.

The most accurate theoretical work is now being done with digital computers used to solve the waveguide problem. However, expressions developed by J. R. Wait and others may provide some insight. For long paths in which only one mode is dominant, the waveguide theory of the sharply bounded ionosphere yields

$$E = \frac{3 \times 10^5}{h} \left[\frac{P\lambda}{a \sin d/a} \right]^{1/2} e^{-\alpha' d} \Lambda \quad (\text{B1})$$

where E = Received field strength in $\mu\text{V/m}$
 h = Height of the ionosphere
 P = Radiated power in kilowatts
 λ = Wavelength
 a = Radius of the earth
 d = Path length (great-circle distance)
 α' = Attenuation coefficient (Napiers/Mm); $\alpha_{\text{dB/Mm}} = 8.68 \alpha'$
 Λ = Excitation factor

Note that the field strength decreases exponentially with distance modified by a 'focusing' term, $\sin d/a$, to take into account the convergence of the spherical field in the far half of the world. The excitation factor, Λ , accounts for the transfer of energy into the propagating mode. Expressions similar to equation (B1), or similar equations employing a superposition of contributions from various modes, result from a number of ionospheric models.

THEORETICAL CHARACTERISTICS

Wait and Spies have made extensive computations to determine the theoretical characteristics of vlf propagation under a variety of conditions.⁷ From equation (B1) and the associated discussion, it is apparent that the important parameters are the propagating mode, characteristic attenuation, characteristic velocity, and characteristic excitation. Theoretical assumptions include mode, n; effective ionospheric height, h; effective ionospheric gradient, β ; ground conductivity, σ_g ; and, in the case of anisotropic models, path orientation with respect to magnetic field. Other assumptions, which include an ionospheric conductivity parameter related to the effective electron collision frequency, and the specific definitions of various terms are beyond the scope of this paper (cf. ref. 6). For present purposes it is sufficient to note that the assumptions may be adequately realistic to yield

meaningful computations, although detailed calculations for specific propagation paths may differ significantly because of the sensitivity of many of the modal parameters to precise path characteristics.

Figure B6 shows computed attenuation rates such as might apply over a seawater propagation path for various frequencies. The curve for $h = 70$ is approximately applicable during day while the curve for $h = 90$ km applies at night. Note that the minimum attenuation occurs around 16 kHz, increasing slowly for higher frequencies but increasing more rapidly at lower frequencies because of the aforementioned cut-off when the waveguide height approaches one wavelength. While figure B6 was for the first mode, figure B7 shows the attenuation rate for the second mode. Note that at night at 10 kHz the attenuation rate of the second mode is 9 dB/Mm compared with 1½ dB/Mm for the first mode, but at 20 kHz it is only 3 dB/Mm compared with 1.7 dB/Mm. Figures B8 and B9 show the excitation factors for the two modes which indicate the relative ease with which propagation may be established. Excitation factors for night conditions at 10 and 20 kHz for the two modes are shown in the following table:

Excitation Factors

Mode	Frequency	
	10 kHz	20 kHz
1	-1.0	-10
2	+1.3	+ 2.5

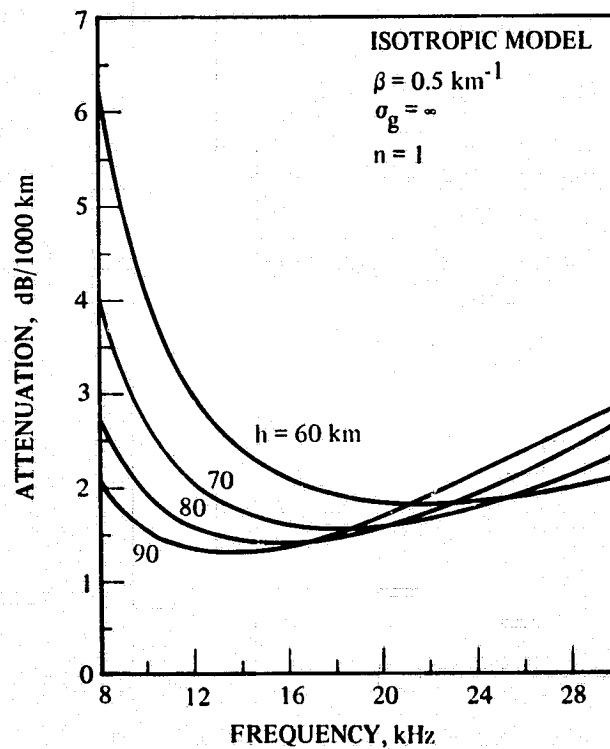


Figure B6. Theoretical attenuation rates for first mode (from Wait and Spies).

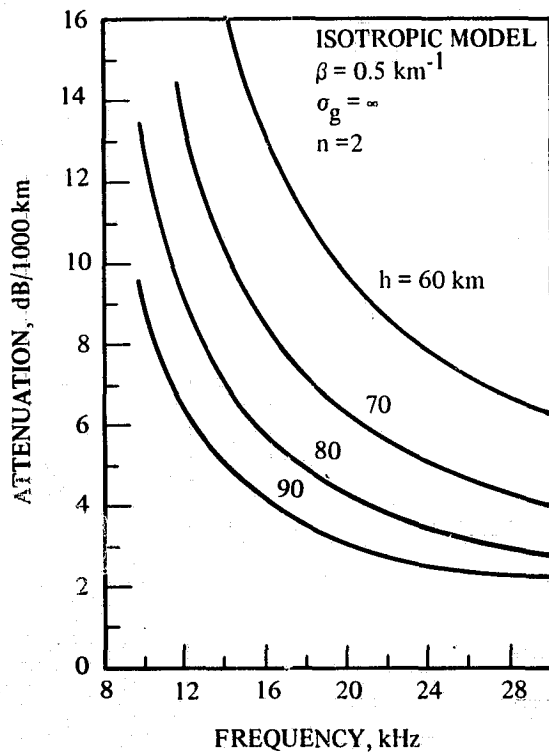


Figure B7. Theoretical attenuation rates for second mode (from Wait and Spies).

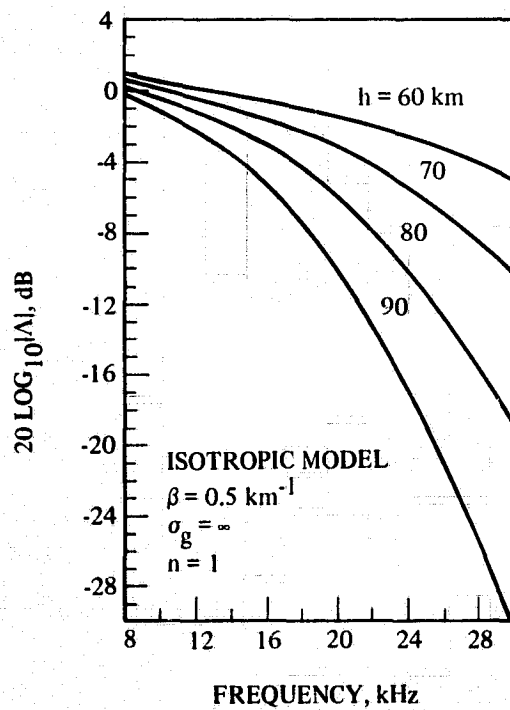


Figure B8. Theoretical excitation factors for first mode (from Wait and Spies).

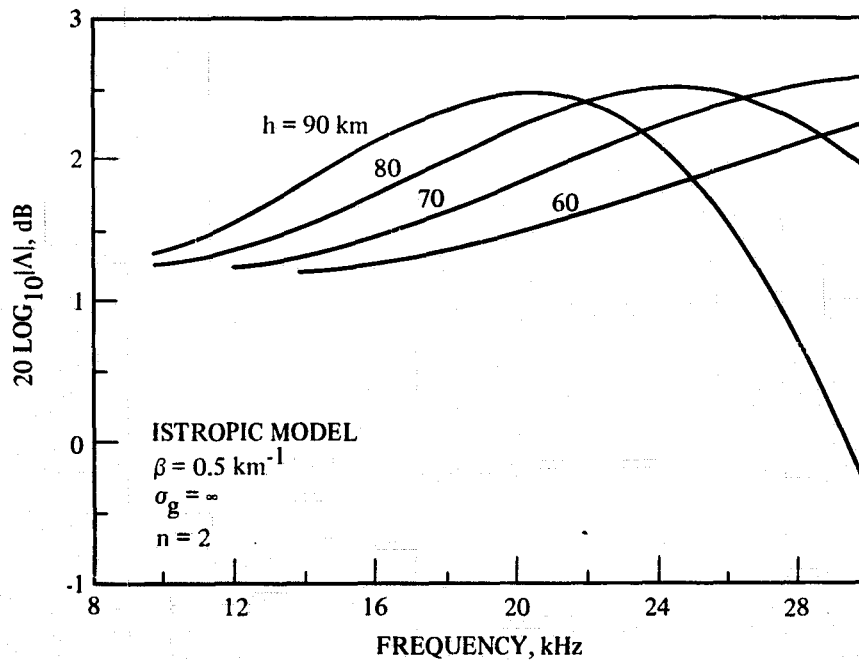


Figure B9. Theoretical excitation factors for second mode (from Wait and Spies).

In both examples shown it is easier to excite the second mode than the first. However, at 10 kHz the difference is only 2.3 dB while at 20 kHz it is 12.5 dB. These differences should be compared with differences in attenuation rates between modes for the respective frequencies. At 10 kHz the first mode will equal the second mode after 0.3 Mm while at 20 kHz equality will not occur for nearly 10 Mm. As a consequence, the interference pattern formed between the first and second modes is much less consequential at the lower vlf frequencies than in the upper portion of the frequency range. The spatial irregularities in isophase lines are thus generally negligible at large distances at frequencies near 10 kHz but must be considered at almost any range for frequencies near 20 kHz propagating at night.

The previous conclusions have been based on the isotropic model of Wait and Spies. Their results provide a useful starting point as an introduction to vlf propagation, but it is worthwhile to make specific comparisons with more general theory and with observation. Pappert has developed a computer solution to the problem of propagation in the earth-ionosphere waveguide.⁸ The formulation provides for general ionospheric electron density profiles, exponential variation of gyro frequency with height, magnetic dip angle, magnetic field strength, magnetic path orientation, and ground conductivity. Snyder and Pappert have performed numeric calculations for the specific propagation paths between San Diego and Hawaii.⁹ Results for both the isotropic case and the anisotropic case were obtained (figures B10-B13). Since their formulation is different from that of Wait, they have a somewhat different definition of height – i.e., h' instead of h – but the distinction is not significant here. It is important to note that they are computing for a different height but one which is also considered to be representative

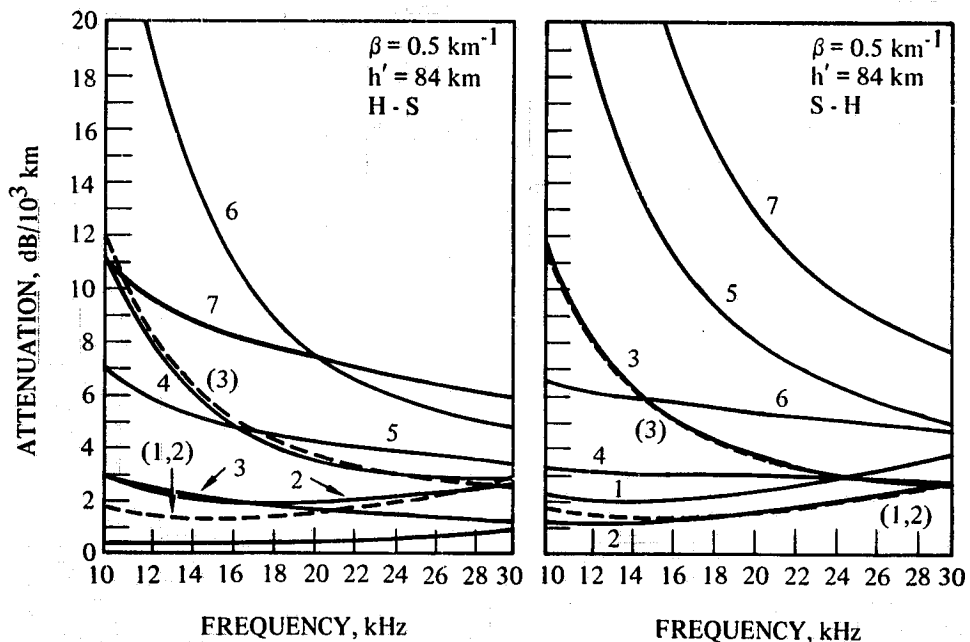


Figure B10. Attenuation versus frequency. Hawaii-to-San Diego path, solid curves. Isotropic ionosphere, dashed curves.

Figure B11. Attenuation versus frequency. San Diego-to-Hawaii path, solid curves. Isotropic ionosphere, dashed curves.

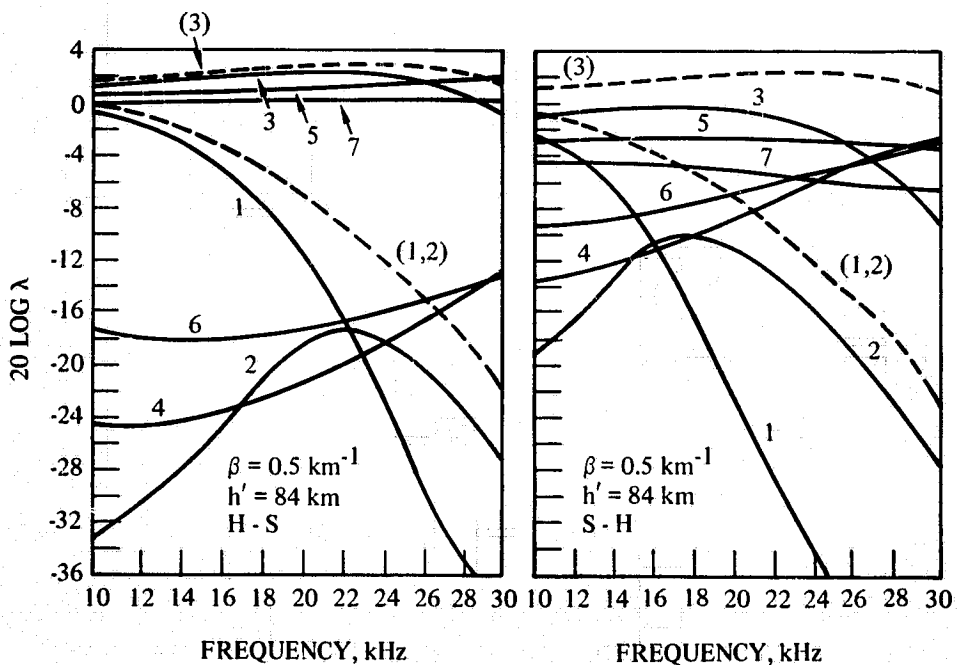


Figure B12. Magnitude of the excitation factor in dB versus frequency. Hawaii-to-San Diego path, solid curves. Isotropic ionosphere, dashed curves.

Figure B13. Magnitude of the excitation factor in dB versus frequency. San Diego-to-Hawaii, solid curves. Isotropic ionosphere, dashed curves.

of propagation conditions at night. Further, their mode numbering system is necessarily arbitrary. Attenuation rates and excitation factors for seven modes are shown in figures B6 through B9 for the isotropic case and also for both propagation from Hawaii to San Diego and from San Diego to Hawaii. Note in table B2 that the attenuation rates are generally less for propagation to the east. Table B2 gives the contributions to the mode sum from the first few modes for three separate cases: the isotropic model of Wait and Spies with $h = 90$ km, full-wave calculations from Snyder and Pappert for isotropic propagation between San Diego and Hawaii with $h' = 84$ km, and anisotropic calculations for propagation from San Diego to Hawaii. As mentioned previously, the isotropic nighttime results from Wait and Spies show equality between contributions from the first and second modes at $1/3$ km for 10.2 kHz but at 10 Mm for 20 kHz. Modal constants for the isotropic model with slightly lower effective ionospheric reflection height as calculated by Snyder and Pappert are generally similar to those of Wait and Spies except that the second mode is attenuated somewhat more rapidly. The anisotropic modal constants are quite different. Mode 2 shows the lowest attenuation rate but is so weakly excited as to be suppressed even at 10 Mm at 10.2 kHz. At 10.2 kHz, mode 3 is nearly equal to mode 1 at $1/3$ Mm but is rapidly dominated by the first mode at greater distances. At 20 kHz, mode 1 is suppressed at all distances, but there is a change in dominance between modes 2 and 3. Indeed, propagation near 20 kHz is even more complex than indicated by table B2, since more than the first three modes are important. Figure B14, from Snyder and Pappert, shows the phasor mode sum as a function of distance as obtained by summing a partial set of modes and summing the first seven modes. Propagation near the upper end of the vlf band is thus quite complex. Since the variations in amplitude with distance shown in figure B14 also imply irregular variation of phase with distance, propagation prediction for navigation using a frequency near 20 kHz would be considerably more difficult than prediction for a frequency near 10 kHz. However, prediction is not necessarily impossible. Figure B15 compares predicted and observed amplitude variation over the path from Seattle to Hawaii. Both measurements and calculations are from Bickel, Ferguson, and Stanley.¹⁰

Phase velocities for the first mode are shown in figure B16. Note that the velocity is lower at night. In practice, timing systems using phase measurements may place stringent demands on knowledge and predictability of phase velocity. For example, an error of one part in 10^4 in phase velocity would cause a timing error of 3 μ sec at 5000 miles. At this precision, curves such as those in figure B16 are not especially useful, as many secondary factors can contribute to change the velocity significantly. For example, figure B17 shows the theoretical variation of phase velocity with ground conductivity.* Note both the minor differences occurring between sea water and normal ground with a conductivity near 10 mmho/m and the significant dependence of the velocity when the conductivity is exceptionally poor. Theoretical variation of velocity with ground conductivity for 10.2 and 13.6 kHz is shown in figures B18 and B19 for both day and night conditions.

*This example is given in reference 11 and was computed from the anisotropic model.

TABLE B2. COMPARISON OF RELATIVE AMPLITUDES OF VARIOUS MODES.

Model	Frequency, kHz	Propagation Constants			Relative Field Strength (dB) at		
		n	α , dB/Mm	Re Λ , dB	1/3 Mm	1 Mm	10 Mm
Wait & Spies h = 90 km	10	1	1.5	-1	-1.5	-2.5	-16
		2	8.8	1.3	-1.6	-7.5	-86.7
	20	1	1.7	-10	-10.6	-11.7	-27
		2	3.0	2.5	1.5	-0.5	-27.5
Snyder & Pappert SD-Hawaii isotropic h' = 84 km	10	1,2	1.7	0	-0.6	-1.7	-17
		3	12.0	1.8	-2.2	-10.2	-118.2
	20	1,2	1.5	-6.5	-7.0	-8.0	-21.5
		3	3.7	2.5	1.3	-1.2	-34.5
Snyder & Pappert SD- Hawaii h' = 84 km	10	2	1.2	-18.5	-18.9	-19.7	-30.5
		1	2.2	-2.0	-2.7	-4.2	-24.2
		3	11.5	1.8	-2.0	-9.7	-113.7
	20	2	1.7	-11.0	-11.6	-12.7	-28.0
1		2.3	-21.8	-22.6	-24.1	-44.8	
3		3.7	3.0	1.8	-0.7	-34.0	

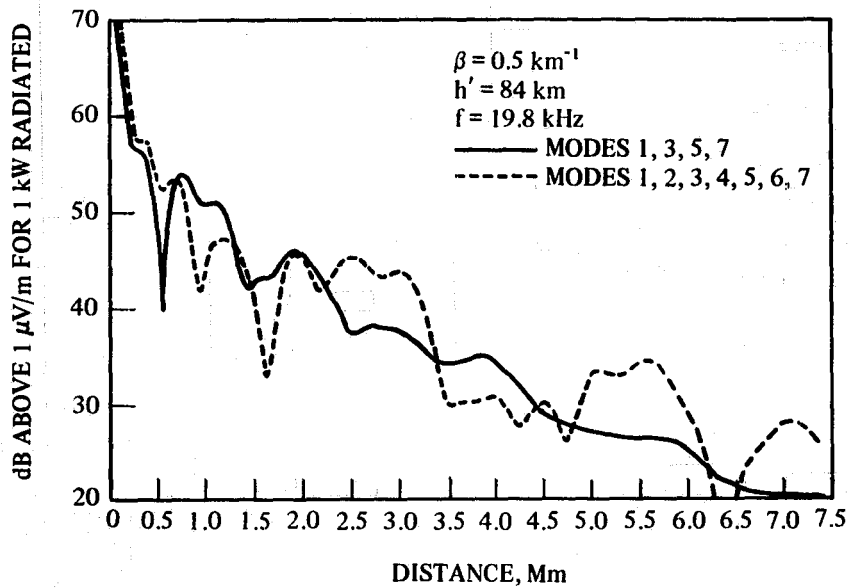


Figure B14. Amplitude of the vertical component of the electric field at the ground in dB above $1 \mu\text{V/m}$ for 1 kilowatt of radiated power versus distance for the SH path.

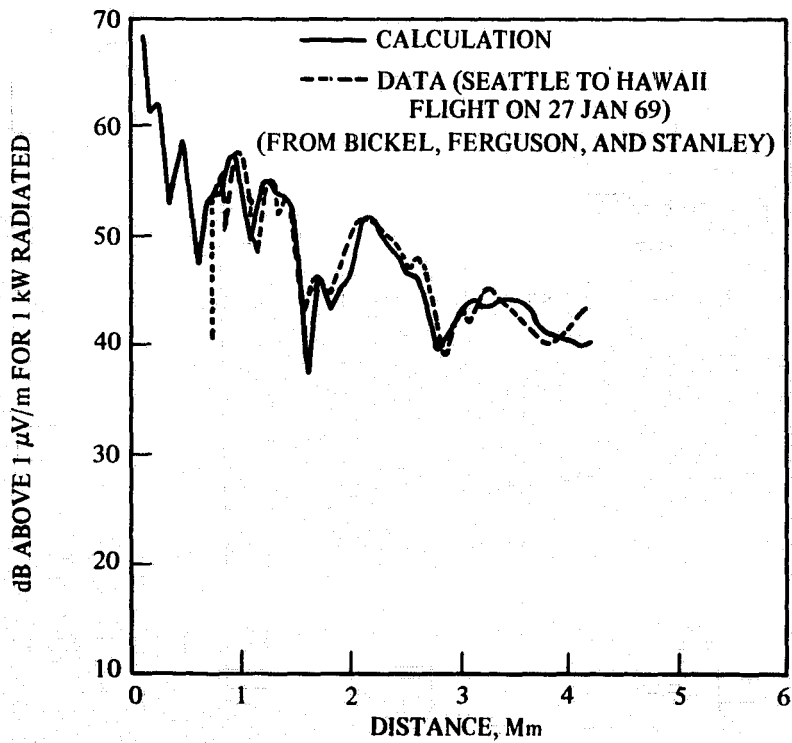


Figure B15. Measured and calculated amplitude at 23.4 kHz.

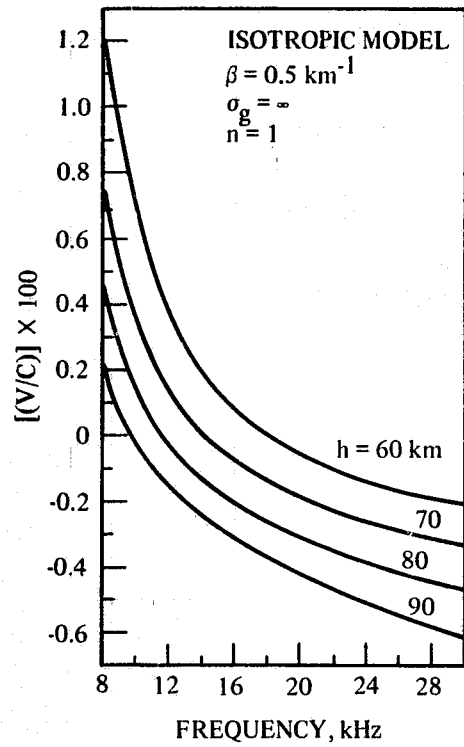


Figure B16. Theoretical phase velocities (from Wait and Spies).

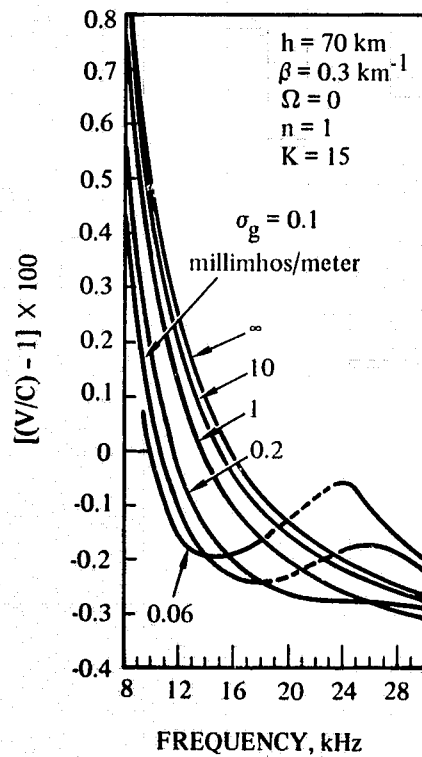


Figure B17. Phase velocity for a wide range of ground conductivities.

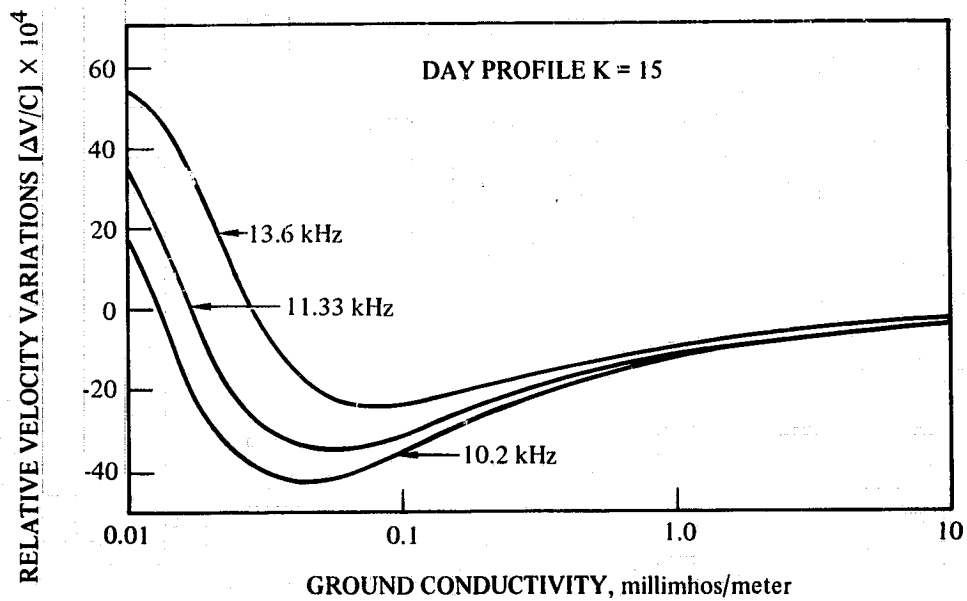


Figure B18. Variation of velocity with ground conductivity (from Gallenberger, ref. 12).

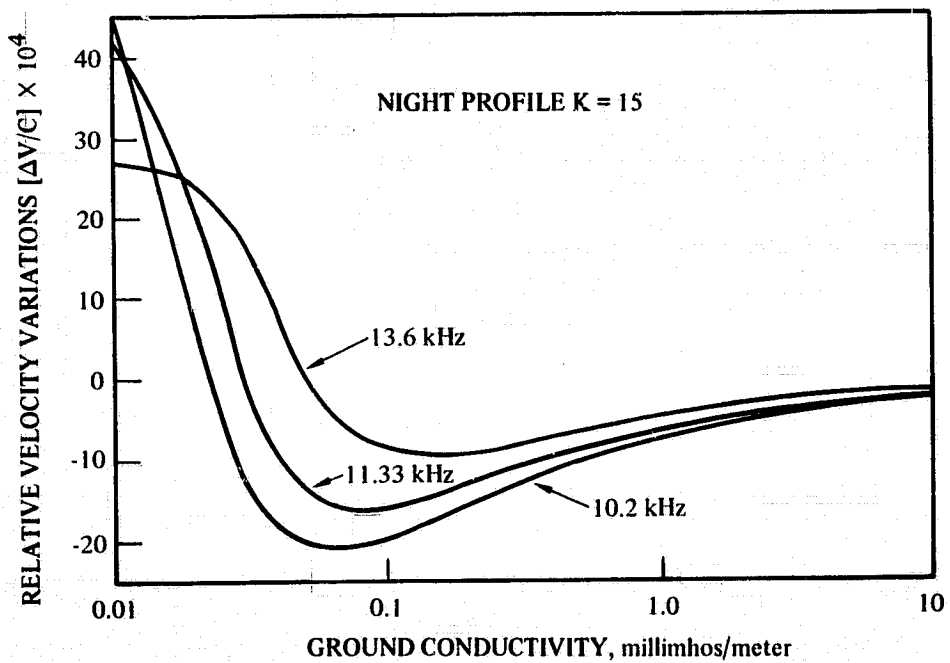


Figure B19. Variation of velocity with ground conductivity (from Gallenberger, ref. 12).

A marked variation on attenuation rate by variations in ground conductivity also occurs. For example, while a ground conductivity of 10 mmho/m might increase the attenuation rate 1/2 dB/Mm over that for sea water, a further decrease to 1 mmho/m may increase the attenuation rate by over 2 dB/Mm. Figures B20 and B21 show theoretical variation of attenuation rate with ground conductivity.

Previous theoretical characteristics of the various propagation modes have been from the work of various authors. The interested reader can find many other results in the references. Perusal of the hundreds of functions shown will provide a good qualitative and quantitative introduction to vlf propagation. Despite the sophistication and success of modern vlf theory, some variations do occur, while other aspects are well known experimentally, although some discussions still occur as to the details of the physical causation.

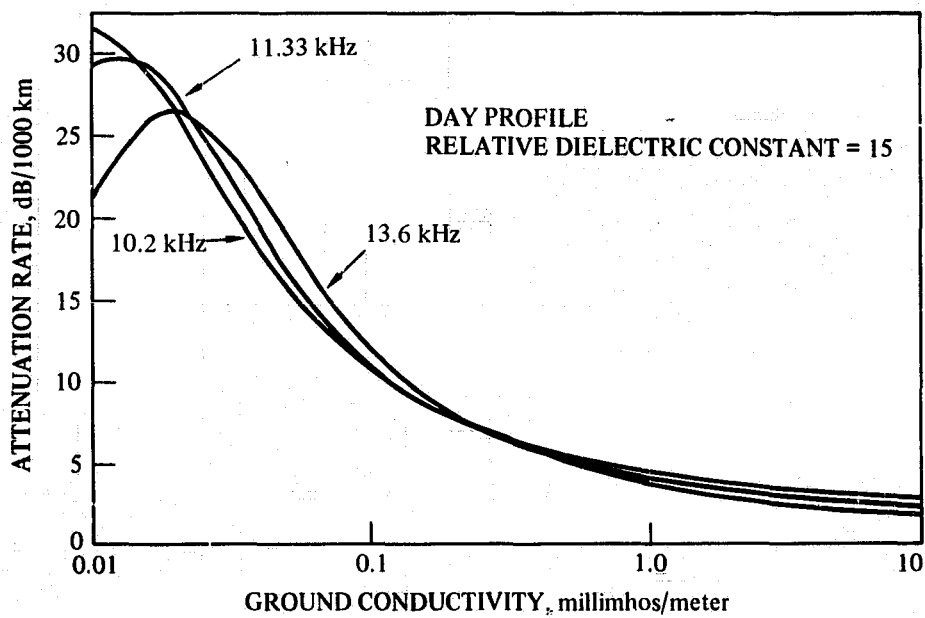


Figure B20. Attenuation as a function of ground conductivity (from Gallenberger, ref. 12).

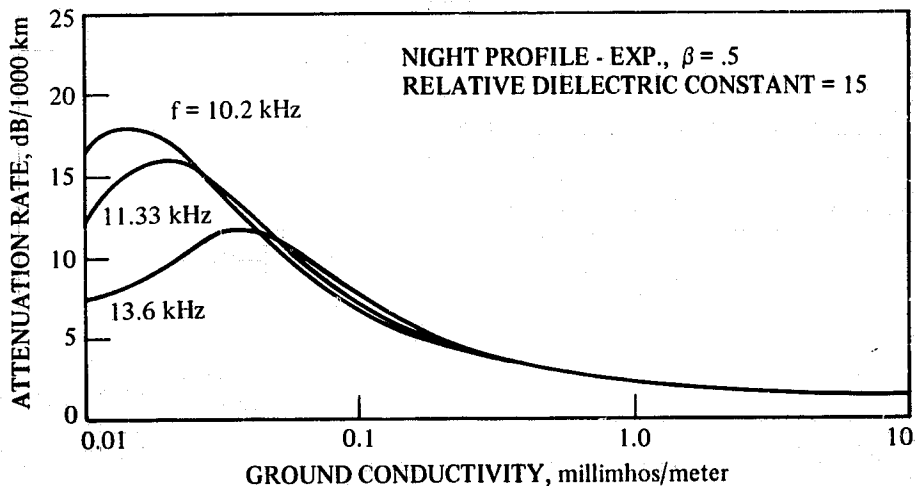


Figure B21. Attenuation as a function of ground conductivity (from Gallenberger, ref. 12).

EXPERIMENTAL OBSERVATIONS

The most important changes are the diurnal variations of phase and amplitude. They are typically associated with ionospheric change related to variation of the solar zenith angle over the propagation path being studied. Two typical examples of diurnal variation of amplitude are shown in figures B22 and B23. Note that the field strength tends to be constant at night and decreases following the transit of the sunrise line over the propagation path to a lower value just after the entire path becomes sunlit and finally reaches a nominal value during the day.* Typical diurnal variations of phase are shown in figures B24 and B25. Figure B24 shows variation at 10.2 kHz, where a constant for 'flat' night is observed shifting into a slow variation or 'curvature' during the day. At higher frequencies within the vlf range, phase tends to be somewhat less stable during the night but more stable at midday. Figure B25 shows that the diurnal variation can be considerably more complex than is usually observed at 10.2 kHz.

*The decrease just after sunrise is very common for frequencies near 10 kHz and is typically about 4 dB and lasts for about an hour. Although the details of this particular sunrise decrease are not well understood, they presumably are related to both the dynamics of ionospheric dissociation and recombination rates leading to daytime equilibrium and another phenomenon especially important in the 20- to 30-kHz frequency range; viz., mode conversion caused by the sunrise line.

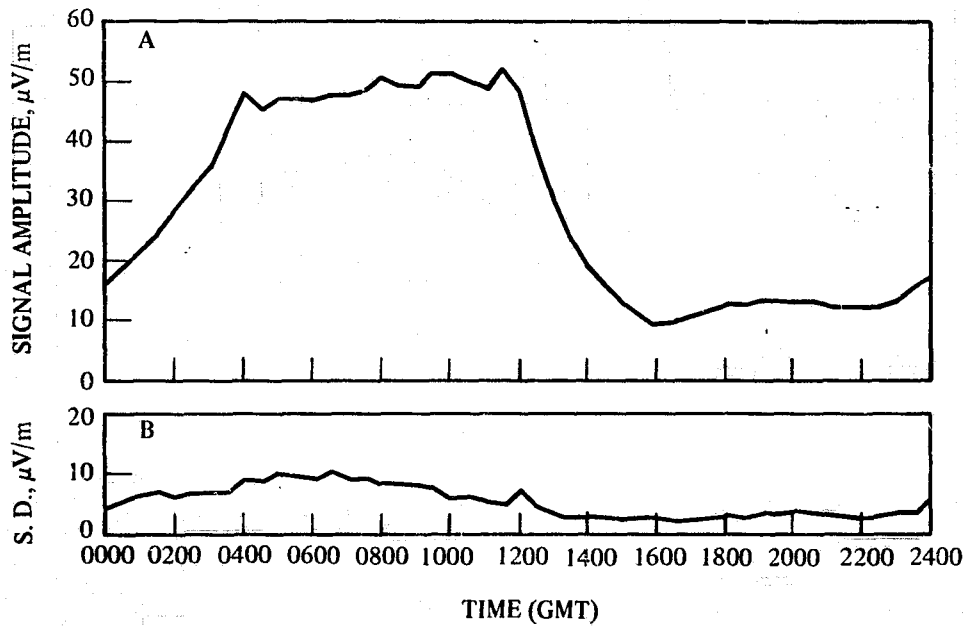


Figure B22. Plot of average field strength (A) and corresponding standard deviation (B) for 10.2-kHz signal received at Rome, N. Y., from Haiku, Hawaii, 24 October-10 November 1962.

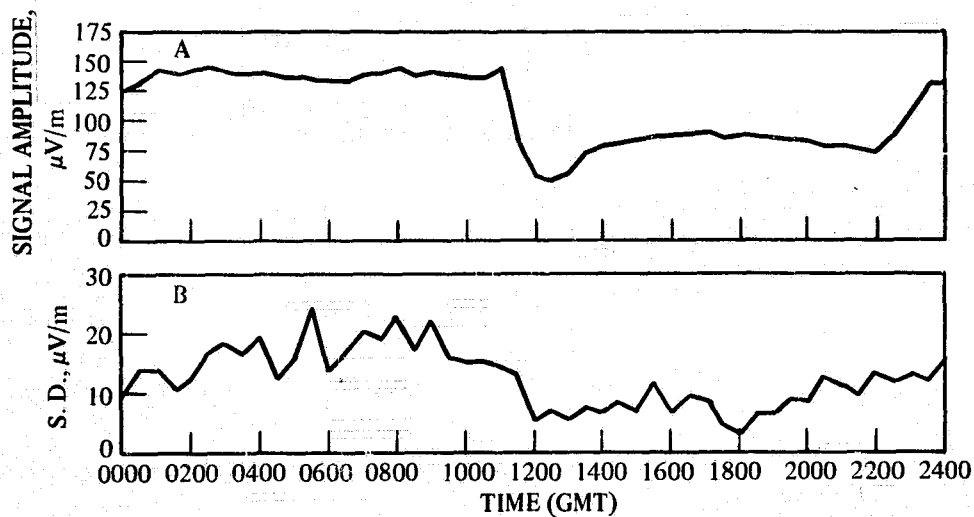


Figure B23. Plot of average field strength (A) and corresponding standard deviation (B) for 10.2-kHz signal received at Farfan, C. Z., from Forestport, N. Y., 27 November - 21 December 1962.

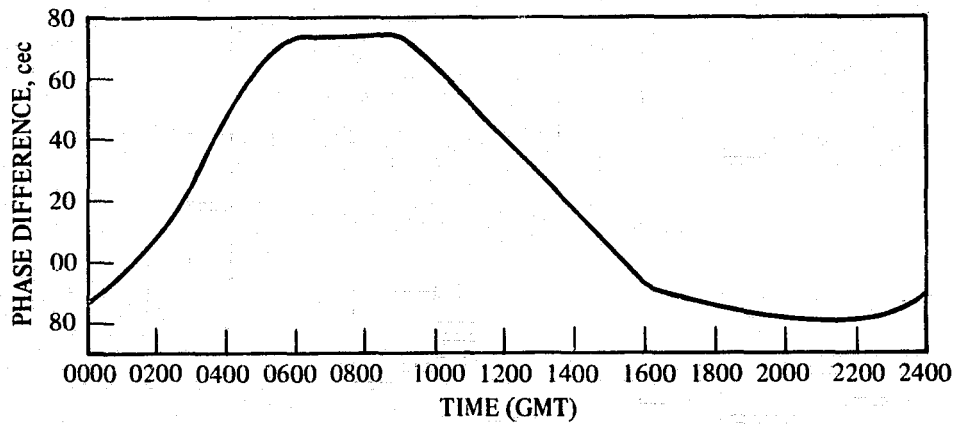


Figure B24. Average 10.2-kHz phase of Haiku, Hawaii, received at Forestport, New York, 17-24 May 1966. Standard deviation approximately 2 cec.

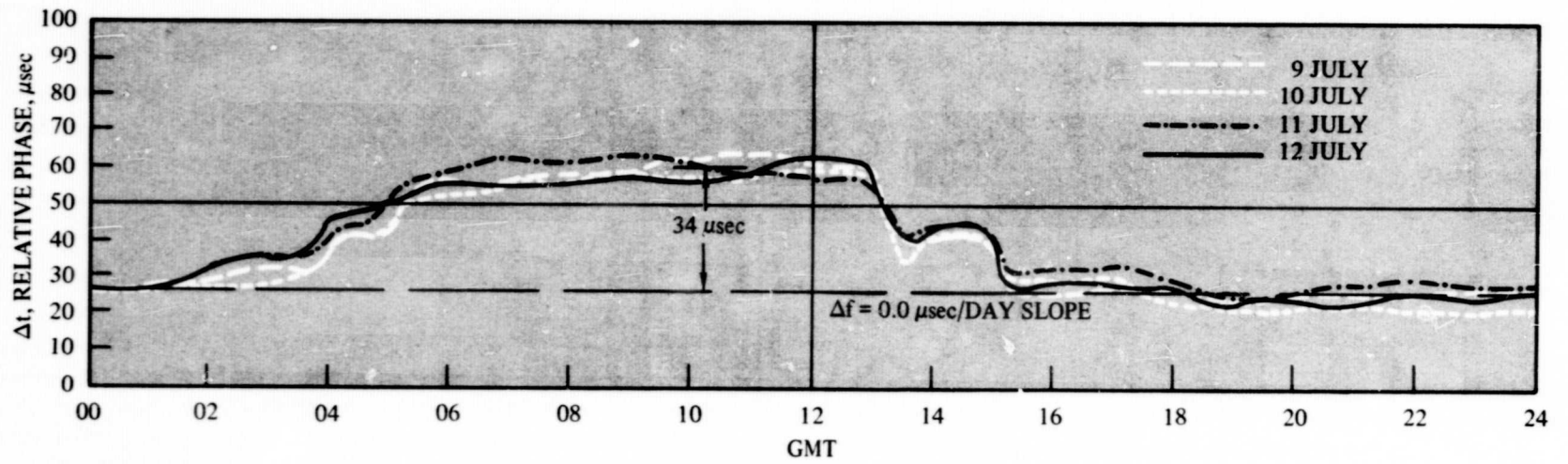


Figure B25. 19.8-kHz NPM (Hawaii) phase recorded in San Diego, 9-12 July 65 (from Bickel, reference 13).

As previously mentioned and shown in figures B22 and B23, field strength is typically repeatable to a standard deviation of about 1 dB from day to day at 10.2 kHz. Repeatability of phase is, however, one of the most useful properties of vlf. Phase variations occur because of ordinary random variations in the ionosphere or, usually to a much lesser extent, to variations in ground conductivity. Occasional larger variations occur. Sudden phase anomalies (SPA's) usually appear as a sharp advance in phase followed by a recovery typically taking about 1/2 hour. These are related to X-ray radiation from the sun and affect only sunlight paths. Their frequency of occurrence is related to the sunspot cycle. During disturbed periods, several SPA's may occur on a given day. Conversely, during quiet periods, years may pass with little of consequence noted. Polar cap absorptions (PCA's) also affect vlf propagation near the geomagnetic poles. Their effect is severe and may persist up to a week. Phase stability has been extensively studied at the Omega frequencies of 10.2 and 13.6 kHz. Stabilities appropriate for single propagation paths of various lengths from about 4 Mm to 10 Mm are given in table B3.

TABLE B3. STANDARD DEVIATIONS OF VLF SIGNALS (μ sec).

Period	Frequency	
	10.2 kHz	13.6 kHz
Day	3	2
Night	5	4
Transition	4	4

The higher very-low frequencies tend to be more stable during the center portion of the day but less stable at night.

In all discussions of the repeatability of phase measurements it is very important to draw a distinction between day-to-day statistical scatter, or 'noise,' and electromagnetic noise. Repeatability is limited by the stability of the transfer or 'mapping' function affecting the signal after it leaves the transmitting antenna and until it is received at the receiver. This type of repeatability is affected by random variations in the ionosphere or ground and will not improve by increasing the electromagnetic signal-to-noise ratio. Normally, the signal-to-noise ratio does not significantly affect repeatability except over exceptionally long paths and/or with unusually weak transmitters.

Natural noise at vlf is primarily due to electromagnetic signals radiated from thunderstorm lightning. The total thunderstorm noise must be computed on a global basis from all 'storm centers.' In addition, the noise is highly impulsive, and proper receiver techniques may yield improvements in excess of 10 dB over what could be obtained if the noise were Gaussian. While the ambient noise usually is high, arctic areas typically are quiet, and reception of weak signals is common. These characteristics, as well as the

wide variation in signal strength which may occur depending on propagation path length, combine to give stringent specifications for vlf receivers.

Propagation blackouts, of the type sometimes experienced at higher frequencies, are rare to the point of being virtually unknown at vlf. Although significant fades have sometimes been associated with PCA's, normal blackouts may well produce signal enhancements at vlf.

PREDICTIONS

The anticipated phase of a signal at any time of day or season may be obtained from a 'skywave correction' for the location. Skywave corrections are designed for navigation and incorporate diurnal, seasonal, and undesirable spatial variations so that, when a skywave correction is added to an observed phase delay, the corrected measurement may be referred directly to specially prepared line-of-position charts. The procedure allows the skywave corrections to be relatively insensitive to position while the corrected measurements are extremely sensitive to position as is desirable for navigation. Skywave correction tables are published by the Naval Oceanographic Office.¹⁴ All previously published skywave correction tables have been based on a global theory of Omega propagation incorporating theoretical and empirical physical principles. The relative contributions of the various effects are determined by regression analysis on millions of hours of data. The physical model has undergone continual refinement at the Naval Electronics Laboratory Center for 10 years. Beginning with the fall 1970 skywave corrections, limited areas are also receiving the benefit of a 'force fit' wherein local prediction errors are determined by monitoring and then removed over whatever spatial extent may be justified by the statistics.¹⁵ Regardless of the method of derivation, the purpose of the skywave correction is to remove undesirable variations so that the observations can be corrected to charted LOP's with the best practical accuracy. A sample skywave correction table is shown in exhibit B1.

DATE	LOCATION: 16.0 N 40.0 W STATION A: NORWAY																
	GMT																
	00	01	02	03	04	05	06	07	08	...	18	19	20	21	22	23	24
1-15 JAN	-71	-71	-71	-71	-71	-71	-71	-71	-71		-24	-40	-61	-71	-71	-71	-71
16-31 JAN	-71	-71	-71	-71	-71	-71	-71	-71	-68		-20	-36	-57	-71	-71	-71	-71
1-14 FEB	-71	-71	-71	-71	-71	-71	-71	-71	-59		-16	-31	-52	-71	-71	-71	-71
15-28 FEB	-71	-71	-71	-71	-71	-71	-71	-67	-44		-9	-24	-45	-71	-71	-71	-71
1-15 MAR	-71	-71	-71	-71	-71	-71	-70	-59	-32		-5	-17	-39	-70	-71	-71	-71
...																	
16-31 DEC	-71	-71	-71	-71	-71	-71	-71	-71	-71		-26	-43	-65	-71	-71	-71	-71

Exhibit B1. Sample skywave correction table.

Application of skywave corrections to timing is straightforward. Except for sign reversal, a skywave correction is an estimate of the expected phase at the location from which a first order variation with distance has been removed:

$$-SWC = P - L$$

where SWC denotes the skywave correction, P the predicted phase, and L the navigational LOP in circular coordinates for the frequency:

$$L = 0.9974 \frac{df}{c}$$

where d is the geodetic distance in kilometers, f the frequency, and c the velocity of light. Clearly

$$P = L - SWC$$

Hence, expected phase may be computed from skywave corrections and distances.*

REFERENCES

1. Jones, S. S. D., "VLF Techniques for Navigation," *Journal of the (British) Institute of Navigation*, v. 23, p. 23-26, January 1970
2. Harvard University. Cruft Laboratory Technical Report 17, *Radux*, by J. A. Pierce, 11 July 1947
3. Pickard and Burns Electronics Publication 886B, *OMEGA - A World-Wide Navigational System, System Specification and Implementation*, by J. A. Pierce, 1 May 1966
4. Navy Electronics Laboratory Report 1305, *OMEGA Lane Resolution*, by E. R. Swanson, 5 August 1965
5. Naval Electronics Laboratory Center Report 1657, *Composite OMEGA*, by E. R. Swanson and E. J. Hepperley, 23 October 1969
6. Watt, A. D. and Croghan, R. D., "Comparison of Observed VLF Attenuation Rates and Excitation Factors With Theory," *Journal of Research of the National Bureau of Standards. Section D: Radio Science*, v. 68D, p. 1-9, January 1964

*If the skywave correction is not applied at precisely the location for which it was computed, the above equations may be used as approximations. Precise relationships are given in appendix A of reference 4.

7. National Bureau of Standards Technical Note 300, *Characteristics of the Earth-Ionosphere Waveguide For VLF Radio Waves*, by J. R. Wait and K. P. Spies, 30 December 1964
8. Pappert, R. A., Gossard, E. E. and Rothmuller, I. J., "A Numerical Investigation of Classical Approximations Used in VLF Propagation," *Radio Science. New Series*, v. 2, p. 387-400, April 1967
9. Snyder, F. P. and Pappert, R. A., "A Parametric Study of VLF Modes Below Anisotropic Ionospheres," *Radio Science. New Series*, v. 4, p. 213-226, March 1969
10. Bickel, J. E., Ferguson, J. A. and Stanley, G. V., "Experimental Observation of Magnetic Field Effects on VLF Propagation at Night," *Radio Science. New Series*, v. 5, p. 19-25, January 1970
11. Wait, J. R. and Spies, K. P., "Influence of Finite Ground Conductivity on the Propagation of VLF Radio Waves," *Journal of Research of the National Bureau of Standards. Section D: Radio Science*, v. 69D, p. 1359-1373, October 1965
12. Naval Electronics Laboratory Center TN 1428,* *Effects of Ground Conductivity on Phase Velocity of Electromagnetic Waves at OMEGA Frequencies*, by R. J. Gallenberger, 11 September 1968
13. Navy Electronics Laboratory Technical Memorandum 909,* *Amplitude and Phase of NPM Recorded at San Diego From 9 May to 11 July on Five Very Low Frequencies*, by J. E. Bickel, 10 February 1966
14. U. S. Naval Oceanographic Office H.O. Publication 224, *Omega Skywave Correction Tables*, (Various dates)
15. Kasper, J. F., *A Skywave Correction Adjustment Procedure For Improved Omega Accuracy*, paper presented at Institute of Navigation National Marine Meeting U. S. Coast Guard Academy, New London, Connecticut, 12-14 October 1970

BIBLIOGRAPHY

The following reference, not specifically cited in the text, is particularly extensive and valuable:

Watt, A. D., *VLF Radio Engineering*, Pergamon Press, 1967

*NEL technical memoranda and NELC technical notes are informal documents intended chiefly for use within the laboratory.

APPENDIX C: ADJUSTMENT PROCEDURE

This appendix describes the algebraic manipulations required to analyze the control procedure which has been recommended as a usable time synchronization method. The analysis is done for the specific case of a 60-day regression estimate for the oscillator frequency offset and epoch adjustments applied once per week. Even such an apparently simple procedure is not readily analyzed, owing to the interaction of all the relevant variables and the truncation of the frequency estimates. The analysis begins with definitions of the pertinent quantities and then proceeds to perform the laborious recursion routines to derive (1) the frequency estimates as a function of the phase errors, and (2) the final phase as a function of propagation noise and oscillator variability. During the analysis, certain recurring groups of numbers or symbols are redefined as new symbols, and the reader must observe the various notation schemes. Interesting 'constants' are plotted where knowledge of their behavior seems relevant to the understanding of the dynamics of the problem. The analysis concludes with a substitution process for determining the optimum value of the weighting factor θ which will minimize the variance of the maintained epoch. The results are plotted for certain ranges of noise and oscillator variability which approximate the expected operational conditions.

I. CONTROL EQUATIONS AND DEFINITIONS

$$\text{Starting Error Control Equation: } \phi_t = \phi_{t-1} + E_t + F_t T \quad (C1)$$

where: ϕ_t = phase epoch at the end of the t^{th} interval
 ϕ_{t-1} = phase epoch at the end of the $(t-1)^{\text{th}}$ interval
 E_t = phase correction applied during the t^{th} interval
 F_t = frequency radiated over the t^{th} interval
 T = interval length

$$\text{Phase Correction Definition: } E_t = \theta \hat{\phi}_{t-1} = \theta (\phi_{t-1} + N_{t-1}) \quad (C2)$$

where: $\hat{\phi}_{t-1}$ = the estimated epoch at the end of the $(t-1)^{\text{th}}$ interval
 ϕ_{t-1} = the true phase epoch at the end of the $(t-1)^{\text{th}}$ interval
 N_{t-1} = the noise on the estimate $\hat{\phi}_{t-1}$
 θ = parameter to be found

$$\text{Frequency Definition: } F_t = (f_t + \delta f_t) \quad (C3)$$

where: f_t = oscillator offset from perfect frequency over t^{th} interval

δf_t = negative of the estimated oscillator offset, or 'accumulation,' over t^{th} interval

$$\text{Accumulation Definition: } \delta f_t = A \sum_{i=t-9}^{t-1} (jP)_i - B \sum_{i=t-9}^{t-1} P_i \quad (C4)$$

where: P_i = oscillator phase shifter position

A, B = constants determined for least-squares analysis of successive P_i 's ($A = 1/60$, $B = 1/12$ for nine points in 60 days)

j = index multiplier (ranging from 1 to 9 in this analysis)

$$\text{Phase Shifter Control Equation: } P_t = P_{t-1} + E_t + \delta f_t \quad (C5)$$

where: P_t = phase shifter at the end of the t^{th} interval

P_{t-1} = phase shifter at the end of the $(t-1)^{\text{th}}$ interval

II. RECURSION OF FREQUENCY ESTIMATE EQUATION

A. Let $t=0$ to simplify notation and rewrite (C4) and (C5) as:

$$\delta f_0 = \sum_{i=-9}^{-1} (jP)_i - B \sum_{i=-9}^{-1} P_i, \quad P_0 = P_{-1} + E_0 + \delta f_0$$

B. Eliminate B and expand δf_0 : ($B/A = 1/12 = 1/60$, $1/60 = \frac{1+9}{2} = 5$)

$$\delta f_0 = A \left[\sum_{i=-9}^{-1} (jP)_i - \frac{B}{A} \sum_{i=-9}^{-1} P_i \right] = A \left[\sum_{i=-9}^{-1} (jP)_i - 5 \sum_{i=-9}^{-1} P_i \right]$$

$$\begin{aligned} \delta f_0 = A & (P_{-9} + 2P_{-8} + 3P_{-7} + 4P_{-6} + 5P_{-5} + 6P_{-4} \\ & + 7P_{-3} + 8P_{-2} + 9P_{-1} - 5P_{-9} - 5P_{-8} - 5P_{-7} \\ & - 5P_{-6} - 5P_{-5} - 5P_{-4} - 5P_{-3} - 5P_{-2} - 5P_{-1}) \end{aligned}$$

$$\delta f_0 = A(4P_{-1} + 3P_{-2} + 2P_{-3} + P_{-4} - P_{-6} - 2P_{-7} - 3P_{-8} - 4P_{-9}) \quad (C6a)$$

C. Define new symbols $[H_i]$ and P to facilitate algebra:

$$[H_9] = [4, 3, 2, 1, 0, -1, -2, -3, -4]$$

$$\begin{matrix} -9 \\ P \\ -1 \end{matrix} = [P_{-1}, P_{-2}, P_{-3}, P_{-4}, P_{-5}, P_{-6}, P_{-7}, P_{-8}, P_{-9}]$$

$$\delta f_0 = A \begin{matrix} -9 \\ [H_9] \\ -1 \end{matrix} P, \delta f_{-1} = A \begin{matrix} -10 \\ [H_9] \\ -2 \end{matrix} P, \text{ etc.} \quad (C6b)$$

D. Substitute for δf_{-1} in expression for P_{-1} :

$$P_{-1} = P_{-2} + E_{-1} + \delta f_{-1} = P_{-2} + E_{-1} + A \begin{matrix} -10 \\ [H_9] \\ -2 \end{matrix} P$$

E. Eliminate P_{-1} from (C6a):

$$\delta f_0 = A(4P_{-2} + 4E_{-1} + 4A \begin{matrix} -10 \\ [H_9] \\ -2 \end{matrix} P + 3P_{-2} + 2P_{-3} + P_{-4} - P_{-6} - 2P_{-7} - 3P_{-8} - 4P_{-9})$$

$$\delta f_0 = 4AE_{-1} + 4A^2 \begin{matrix} -10 \\ [H_9] \\ -2 \end{matrix} P + A(7P_{-2} + 2P_{-3} + P_{-4} - P_{-6} - 2P_{-7} - 3P_{-8} - 4P_{-9}) \quad (C7a)$$

F. Define new symbols c_{-1} and $[H_8]$:

$$c_{-1} = 4A, [H_8] = [7, 2, 1, 0, -1, -2, -3, -4]$$

$$\delta f_0 = c_{-1}E_{-1} + c_{-1}A \begin{matrix} -10 \\ [H_9] \\ -2 \end{matrix} P + A \begin{matrix} -9 \\ [H_8] \\ -2 \end{matrix} P \quad (C7b)$$

G. Similarly eliminate P_{-2} from (C7a):

$$\begin{aligned}
 P_{-2} &= P_{-3} + E_{-2} + \delta f_{-2} = P_{-3} + E_{-2} + A[H_9] \begin{matrix} -11 \\ P \\ -3 \end{matrix} \\
 \delta f_0 &= (cE)_{-1} + c_{-1} A \left(4P_{-3} + 4E_{-2} + 4A[H_9] \begin{matrix} -11 \\ P \\ -3 \end{matrix} + 3P_{-3} + 2P_{-4} \right. \\
 &\quad \left. + P_{-5} - P_{-7} - 2P_{-8} - 3P_{-9} - 4P_{-10} \right) + A \left(7P_{-3} + 7E_{-2} \right. \\
 &\quad \left. + 7A[H_9] \begin{matrix} -11 \\ P \\ -3 \end{matrix} + 2P_{-3} + P_{-4} - P_{-6} - 2P_{-7} - 3P_{-8} - 4P_{-9} \right) \\
 \delta f_0 &= (cE)_{-1} + A(4c_{-1} + 7)E_{-2} + A^2(4c_{-1} + 7) [H_9] \begin{matrix} -11 \\ P \\ -3 \end{matrix} + c_1 A [H_8] \begin{matrix} -10 \\ P \\ -3 \end{matrix} \\
 &\quad + A(9P_{-3} + P_{-4} - P_{-6} - 2P_{-7} - 3P_{-8} - 4P_{-9}) \tag{C8a}
 \end{aligned}$$

H. Define new symbols c_{-2} and $[H_7]$:

$$\begin{aligned}
 c_{-2} &= (4c_{-1} + 7) A [H_7] = [9, 1, 0, -1, -2, -3, -4] \\
 \delta t_0 &= (cE)_{-1} + (cE)_{-2} + c_{-2} A [H_9] \begin{matrix} -11 \\ P \\ -3 \end{matrix} + c_{-1} A [H_8] \begin{matrix} -10 \\ P \\ -3 \end{matrix} \\
 &\quad + A [H_7] \begin{matrix} -9 \\ P \\ -3 \end{matrix} \tag{C8b}
 \end{aligned}$$

I. Note the emerging form for the $[H_i]$

$$[H_9] = [4 \ 3 \ 2 \ 1 \ 0 \ -1 \ -2 \ -3 \ -4]$$

$$[H_8] = [7 \ 2 \ 1 \ 0 \ -1 \ -2 \ -3 \ -4]$$

$$[H_7] = [9 \ 1 \ 0 \ -1 \ -2 \ -3 \ -4]$$

$$[H_6] = [10 \ 0 \ -1 \ -2 \ -3 \ -4]$$

$$[H_5] = [10 \ -1 \ -2 \ -3 \ -4]$$

$$[H_4] = [9 \ -2 \ -3 \ -4]$$

$$[H_3] = [7 \ -3 \ -4]$$

$$[H_2] = [4 \ -4]$$

$$[H_1] = [0]$$

Since $[H_1] = 0$, no additional $[H_i]$'s are possible. Therefore, the last term in δl_0 approaches zero and leaves only eight contributions from the $\sum_i \sum_j$ summations.

J. Note the emerging form for the c_i :

$$\begin{aligned} c_0 &= (1) \\ c_{-1} &= (4c_0)A \\ c_{-2} &= (4c_{-1} + 7c_0)A \\ c_{-3} &= (4c_{-2} + 7c_{-1} + 9c_0)A \\ c_{-4} &= (4c_{-3} + 7c_{-2} + 9c_{-1} + 10c_0)A \\ c_{-5} &= (4c_{-4} + 7c_{-3} + 9c_{-2} + 10c_{-1} + 10c_0)A \\ c_{-6} &= (4c_{-5} + 7c_{-4} + 9c_{-3} + 10c_{-2} + 10c_{-1} + 9c_0)A \\ c_{-7} &= (4c_{-6} + 7c_{-5} + 9c_{-4} + 10c_{-3} + 10c_{-2} + 9c_{-1} + 7c_0)A \\ c_{-8} &= (4c_{-7} + 7c_{-6} + 9c_{-5} + 10c_{-4} + 10c_{-3} + 9c_{-2} + 7c_{-1} + 4c_0)A \\ c_{-9} &= (4c_{-8} + 7c_{-7} + 9c_{-6} + 10c_{-5} + 10c_{-4} + 9c_{-3} + 7c_{-2} + 4c_{-1})A \\ c_{-10} &= (4c_{-9} + 7c_{-8} + 9c_{-7} + 10c_{-6} + 10c_{-5} + 9c_{-4} + 7c_{-3} + 4c_{-2})A \\ &\vdots \\ &\vdots \\ c_n^* &= (4c_{n-1} + 7c_{n-2} + 9c_{n-3} + 10c_{n-4} + 10c_{n-5} + 9c_{n-6} \\ &\quad + 7c_{n-7} - 4c_{n-8})A \end{aligned} \tag{C9a}$$

Beginning with c_{-8} , all c_i 's have only eight terms.

*n = negative number.

K. Define new symbols $[R_i]$ and c_i :

$$[R_8] = [14, 7, 9, 10, 10, 9, 7, 4]$$

$$c_{n-1} = [c_{n-1}, c_{n-2}, \dots, c_{n-8}]$$

$$c_n = A [R_8] c_{n-1} \quad (C9b)$$

Computer analysis gives the following plot for c_n and indicates that the value approaches a constant $\bar{c} = 2/9 = 0.22222$.

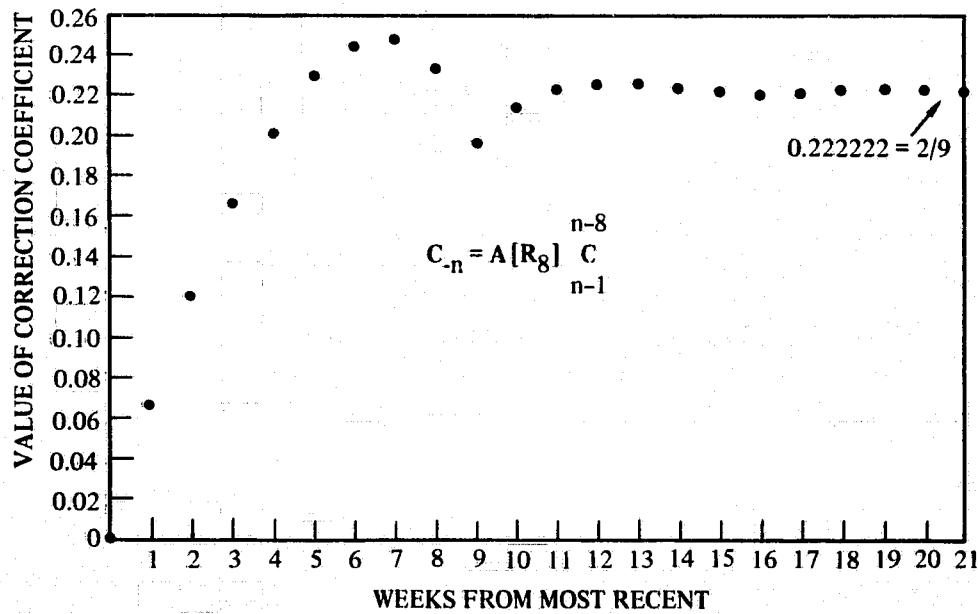


Figure C1. Frequency recursion coefficients.

L. Note the emerging form for δf_0 :

$$\delta f_0 = c_0 A [H_9] P_{-1}^{-9}$$

$$\delta f_0 = (cE)_{-1} + A \left(c_{-1} [H_9] P_{-2}^{-10} + c_0 [H_8] P_{-2}^{-9} \right)$$

$$\delta f_0 = (cE)_{-1} + (cE)_{-2} + A \left(c_{-2} [H_9] \frac{P}{-3} + c_{-1} [H_8] \frac{P}{-3} + c_0 [H_7] \frac{P}{-3} \right)$$

$$\delta f_0 = \sum_{-1}^{-8} (cE)_i + A \left(c_{-8} [H_9] \frac{P}{-9} + c_{-7} [H_8] \frac{P}{-9} + c_{-6} [H_7] \frac{P}{-9} \right. \\ \left. + c_{-5} [H_6] \frac{P}{-9} + c_{-4} [H_5] \frac{P}{-9} + c_{-3} [H_4] \frac{P}{-9} + c_{-2} [H_3] \frac{P}{-9} \right. \\ \left. + c_{-1} [H_2] \frac{P}{-9} + c_0 [H_1] \frac{P}{-9} \right) = 0$$

$$\delta f_0 = \sum_{-1}^{-9} (cE)_i + A \left(c_{-9} [H_9] \frac{P}{-10} + c_{-8} [H_8] \frac{P}{-10} + c_{-7} [H_7] \frac{P}{-10} \right. \\ \left. + c_{-6} [H_6] \frac{P}{-10} + c_{-5} [H_5] \frac{P}{-10} + c_{-4} [H_4] \frac{P}{-10} + c_{-3} [H_3] \frac{P}{-10} \right. \\ \left. + c_{-2} [H_2] \frac{P}{-10} + c_{-1} [H_1] \frac{P}{-10} \right) = 0$$

The coefficients of the $\frac{P}{i}$ change as one recurses, but after P_{-9} is eliminated, the contributions are confined to eight terms $\times A$ plus the summation of the $(cE)_i$.

M. Let the upper limit on the summations go back to 'n' such that all c_i 's have become equal to \bar{c} and can be factored out of the $A \left(c_i \frac{P}{i} \dots \right)$ term:

$$\delta f_0 = \sum_{-1}^n (cE)_i + A \bar{c} \left([H_9] \frac{P}{n-1} + [H_8] \frac{P}{n-1} + [H_7] \frac{P}{n-1} + [H_6] \frac{P}{n-1} \right. \\ \left. + [H_5] \frac{P}{n-1} + [H_4] \frac{P}{n-1} + [H_3] \frac{P}{n-1} + [H_2] \frac{P}{n-1} + [H_1] \frac{P}{n-1} \right)$$

N. Expand the H_i and regroup according to the subscripted P_i :

$$\begin{aligned} \delta f_o &= \sum_{-1}^n (cE)_i + A\bar{c} \left(\sum_1^9 [H_i] P_{n-1} + \sum_2^9 [H_i] P_{n-2} + \sum_3^9 [H_i] P_{n-3} \right. \\ &\quad + \sum_4^9 [H_i] P_{n-4} + \sum_5^9 [H_i] P_{n-5} + \sum_6^9 [H_i] P_{n-6} + \sum_7^9 [H_i] P_{n-7} \\ &\quad \left. + \sum_8^9 [H_i] P_{n-8} + \sum_9^9 [H_i] P_{n-9} \right) \\ \delta f_o &= \sum_{-1}^n (cE)_i + A\bar{c} (60P_{n-1} - 4P_{n-2} - 7P_{n-3} - 9P_{n-4} - 10P_{n-5} \\ &\quad - 10P_{n-6} - 9P_{n-7} - 7P_{n-8} - 4P_{n-9}) \\ \delta f_o &= \sum_{-1}^n (cE)_i + A\bar{c} \left(60P_{n-1} - [R_8] \begin{matrix} n-9 \\ P \\ n-2 \end{matrix} \right) \end{aligned} \quad (C10a)$$

O. Define new symbols: $\begin{matrix} \bar{c} \\ [c] \\ i \end{matrix}$ and $\begin{matrix} j \\ E \\ i \end{matrix}$ having the same significance as $[H_i]$ and P_i :

$$\begin{aligned} \begin{matrix} \bar{c} \\ [c] \\ -1 \end{matrix} &= [c_{-1}, c_{-2}, c_{-3}, \dots, \bar{c}, \bar{c}] \\ \begin{matrix} n \\ E \\ -1 \end{matrix} &= [E_{-1}, E_{-2}, E_{-3}, \dots, E_n] \\ \delta f_o &= \begin{matrix} \bar{c} \\ [c] \\ -1 \end{matrix} \begin{matrix} n \\ E \\ -1 \end{matrix} + A\bar{c} \left(60P_{n-1} - [R_8] \begin{matrix} n-9 \\ P \\ n-2 \end{matrix} \right) \end{aligned} \quad (C10b)$$

P. If P_n is considered to be the first phase-shifter position which results from the application of the full control procedure, then the positions P_{n-1} through P_{n-9} must refer to a time period when some *other* procedure was being followed. Although several possibilities exist, the most practical and algebraically convenient starting procedure is to use the first nine intervals for

obtaining an accurate and noise-free estimate of the oscillator frequency offset. This can be done by comparing the oscillator epoch to a known standard and adjusting the epoch to agree with the standard at the end of each of the nine successive intervals. The resulting phase-shifter positions are then related by (C5) except that the δf_i terms are all zero.

Using P_{n-10} as some unknown starting point, write the expression for P_{n-9} through P_{n-1} in terms of the correction term $E_{n-9} \rightarrow E_{n-1}$:

$$P_{n-10} = \text{starting point (could be zero)}$$

$$P_{n-9} = P_{n-10} + E_{n-9}$$

$$P_{n-8} = P_{n-9} + E_{n-8} = P_{n-10} + \sum_{n-8}^{n-9} E_i$$

$$P_{n-7} = P_{n-8} + E_{n-7} = P_{n-10} + \sum_{n-7}^{n-9} E_i$$

$$P_{n-6} = P_{n-7} + E_{n-6} = P_{n-10} + \sum_{n-6}^{n-9} E_i$$

$$P_{n-5} = P_{n-6} + E_{n-5} = P_{n-10} + \sum_{n-5}^{n-9} E_i$$

$$P_{n-4} = P_{n-5} + E_{n-4} = P_{n-10} + \sum_{n-4}^{n-9} E_i$$

$$P_{n-3} = P_{n-4} + E_{n-3} = P_{n-10} + \sum_{n-3}^{n-9} E_i$$

$$P_{n-2} = P_{n-3} + E_{n-2} = P_{n-10} + \sum_{n-2}^{n-9} E_i$$

$$P_{n-1} = P_{n-2} + E_{n-1} = P_{n-10} + \sum_{n-1}^{n-9} E_i$$

(C11)

Q. Substituting (C11) into (C10b):

	P_{n-10}	E_{n-9}	E_{n-8}	E_{n-7}	E_{n-6}	E_{n-5}	E_{n-4}	E_{n-3}	E_{n-2}
$[R_8] \begin{matrix} n-9 \\ P \\ n-2 \end{matrix} =$	4	4	4	4	4	4	4	4	4
	7	7	7	7	7	7	7	7	
	9	9	9	9	9	9	9		
	10	10	10	10	10	10			
	10	10	10	10	10				
	9	9	9	9					
	7	7	7						
	4	4							

$$[R_8] \begin{matrix} n-9 \\ P \\ n-2 \end{matrix} = 60P_{n-10} + 60E_{n-9} + 56E_{n-8} + 49E_{n-7} + 40E_{n-6} + 30E_{n-5} + 20E_{n-4} + 11E_{n-3} + 4E_{n-2}$$

$$\text{Let: } [Q_8] = [60, 56, 49, 40, 30, 20, 11, 4]$$

$$\delta f_o = \begin{bmatrix} \bar{c} \\ c \\ -1 \end{bmatrix} \begin{matrix} n \\ E \\ -1 \end{matrix} + A\bar{c} \left[60P_{n-10} + 60 \sum_{n-1}^{n-9} E_i - \left(60P_{n-10} + [Q_8] \begin{matrix} n-9 \\ E \\ n-2 \end{matrix} \right) \right]$$

$$\delta f_o = \begin{bmatrix} \bar{c} \\ c \\ -1 \end{bmatrix} \begin{matrix} n \\ E \\ -1 \end{matrix} + A\bar{c} \left(60 \sum_{n-1}^{n-9} E_i - [Q_8] \begin{matrix} n-9 \\ E \\ n-2 \end{matrix} \right)$$

R. If oscillator exhibited a constant frequency offset during initial 60 days, then all E_i in that period would be equal:

$$E_{n-2} = E_{n-9} = E_i \equiv \bar{E}, \quad \sum_{n-1}^{n-9} E_i = 9\bar{E}$$

$$[Q_8] \begin{matrix} n-9 \\ E \\ n-2 \end{matrix} = [Q_8] \sum \bar{E} = 270\bar{E}$$

$$\text{and } \delta f_o = \begin{bmatrix} \bar{c} \\ c \\ -1 \end{bmatrix} \begin{matrix} n \\ E \\ -1 \end{matrix} + A\bar{c}(60 \times 9\bar{E} - 270\bar{E}) = \begin{bmatrix} \bar{c} \\ c \\ -1 \end{bmatrix} \begin{matrix} n \\ E \\ -1 \end{matrix} + 270A\bar{c}\bar{E}$$

If: $A = 1/60$ and $\bar{c} = 2/9$:

$$\delta f_o = \begin{bmatrix} \bar{c} & n \\ c & E \\ -1 & -1 \end{bmatrix} + 270 \times 1/60 \times 2/9 \bar{E} = \begin{bmatrix} \bar{c} & n \\ c & E \\ -1 & -1 \end{bmatrix} + \bar{E} \quad (C12)$$

S. The frequency estimate is thus seen to be composed of two terms: one representing the initial estimate (\bar{E}); the other the ensuing alterations produced by the control procedure, noise, etc. If \bar{E} were a perfect estimate and no noise were to contaminate future estimates, no errors (E_i) would ever occur and δf_o always would be given by \bar{E} . In the more realistic case where the E_i will be random, the 'older' terms of $\sum \bar{c} E_i$ will cancel and δf_o will depend mainly on the more recent $\sum c_i E_i$, as would be expected.

For the accuracies and time intervals considered in this analysis, the assumption of equal E_i during the 'warm-up' period is satisfactory for a cesium standard.

III. RECURSION OF PHASE CONTROL EQUATION

A. If the interval length is taken as '1', then (C1), (C2), (C3), and (C12) can be combined as:

$$\begin{aligned} \phi_o &= \phi_{-1} + E_o + F_o T = \phi_{-1} + E_o + (f_o + \delta f_o)(1) \\ &= \phi_{-1} + E_o + \left(f_o + \begin{bmatrix} \bar{c} & n \\ c & E \\ -1 & -1 \end{bmatrix} + \bar{E} \right) \\ \phi_o &= \phi_{-1} + \left(E_o + \begin{bmatrix} \bar{c} & n \\ c & E \\ -1 & -1 \end{bmatrix} \right) + (f_o + \bar{E}) \\ \phi_o &= \phi_{-1} + \theta (\phi_{-1} + N_{-1}) + \theta \begin{bmatrix} \bar{c} & n \\ c & E \\ -1 & -2 \end{bmatrix} (\phi + N) + (f_o + \bar{E}) \end{aligned}$$

B. Recalling that $c_o = 1$, create one summation term as:

$$\phi_o = \phi_{-1} + \theta \begin{bmatrix} \bar{c} & n \\ c_o & E \\ -1 & -1 \end{bmatrix} (\phi + N) + (f_o + \bar{E})$$

C. Regrouping and manipulating:

$$\phi_o = \left(\phi_{-1} + \theta \begin{bmatrix} \bar{c}_o \\ c_o \end{bmatrix} \phi_{-1}^n \right) + \theta \begin{bmatrix} \bar{c}_o \\ c_o \end{bmatrix} N_{-1}^n + (f_o + \bar{E})$$

$$\phi_o = (\phi_{-1} + c_o \theta \phi_{-1}) + \theta [c_{-1}] \phi_{-2}^n + \theta [c_o] N_{-1}^n + (f_o + \bar{E})$$

$$\phi_o = (1 + c_o \theta) \phi_{-1} + \theta [c_{-1}] \phi_{-2}^n + \theta S_{-1}^n + \Delta F_o$$

where: $S_{-1}^n = [c_o] N_{-1}^n, \Delta F_o = f_o + \bar{E}$

Let: $(1 + c_o \theta) = K_{-1}$ and $\theta S_{-1}^n + \Delta F_o = \hat{S}_{-1}$

Therefore: $\phi_o = K_{-1} \phi_{-1} + \theta [c_{-1}] \phi_{-2}^n + \hat{S}_{-1}$

$$\phi_{-1} = K_{-1} \phi_{-2} + \theta [c_{-1}] \phi_{-3}^n + \hat{S}_{-2}$$

$$\phi_{-2} = K_{-1} \phi_{-3} + \theta [c_{-1}] \phi_{-4}^n + \hat{S}_{-3}$$

D. Eliminating ϕ_{-1} :

$$\phi_o = K_{-1}^2 \phi_{-2} + K_{-1} \theta [c_{-1}] \phi_{-3}^n + \theta [c_{-1}] \phi_{-2}^n + K_{-1} \hat{S}_{-2} + \hat{S}_{-1}$$

$$\phi_o = (K_{-1}^2 + c_{-1} \theta) \phi_{-2} + \left(\theta [c_{-2}] \phi_{-3}^n + K_{-1} \theta [c_{-1}] \phi_{-3}^n \right) + (K_{-1} \hat{S}_{-2} + \hat{S}_{-1})$$

Let: $(K_{-1}^2 + c_{-1} \theta) = K_{-2} = (1 + c_o \theta) K_{-1} + c_{-1} \theta$

*As all $[c_i]$ will hereafter go to \bar{c} , drop the \bar{c} superscript.

$$\phi_0 = K_{-2}\phi_{-2} + \left(\theta [c_{-2}] \phi_{-3}^n + K_{-1} \theta [c_{-1}] \phi_{-3}^n + (K_{-1} \hat{S}_{-2} + \hat{S}_{-1}) \right)$$

E. Eliminating ϕ_{-2} :

$$\phi_0 = K_{-2}K_{-1}\phi_{-3} + \left(K_{-2}\theta [c_{-1}] \phi_{-4}^n + \theta [c_{-2}] \phi_{-3}^n + K_{-1}\theta [c_{-1}] \phi_{-3}^n \right) + (K_{-2}\hat{S}_{-3} + K_{-1}\hat{S}_{-2} + \hat{S}_{-1})$$

$$\phi_0 = (K_{-2}K_{-1} + K_{-1}\theta c_{-1} + \theta c_{-2})\phi_{-3} + \left(K_{-2}\theta c_{-1} \phi_{-4}^n + K_{-1}\theta c_{-2} \phi_{-4}^n + \theta [c_{-3}] \phi_{-4}^n \right) + (K_{-2}\hat{S}_{-3} + K_{-1}\hat{S}_{-2} + \hat{S}_{-1})$$

$$\text{Let: } K_{-3} = (K_{-2}K_{-1} + K_{-1}\theta c_{-1} + \theta c_{-2}) = (1 + c_0\theta)K_{-2} + \theta(K_{-1}c_{-1} + c_{-2})$$

$$\phi_0 = K_{-3}\phi_{-3} + \theta \left([c_{-3}] + K_{-1}[c_{-2}] + K_{-2}[c_{-1}] \right) \phi_{-4}^n + (K_{-2}\hat{S}_{-3} + K_{-1}\hat{S}_{-2} + \hat{S}_{-1})$$

F. Note the emerging form for the K_i :

$$\begin{aligned} K_0 &= 1 & &= 1 \\ K_{-1} &= (1 + c_0\theta) K_0 & &= K_0 + (c_0 K_0)\theta \\ K_{-2} &= (1 + c_0\theta) K_{-1} + (c_{-1} K_0)\theta & &= K_{-1} + (c_0 K_{-1} + c_{-1} K_0)\theta \\ K_{-3} &= (1 + c_0\theta) K_{-2} + (c_{-1} K_{-1} + c_{-2} K_0)\theta & &= K_{-2} + (c_0 K_{-2} + c_{-1} K_{-1} + c_{-2} K_0)\theta \\ K_{-4} &= (1 + c_0\theta) K_{-3} + (c_{-1} K_{-2} + c_{-2} K_{-1} + c_{-3} K_0)\theta & &= K_{-3} + (c_0 K_{-3} + c_{-1} K_{-2} + c_{-2} K_{-1} + c_{-3} K_0)\theta \\ & \vdots & & \vdots \end{aligned}$$

$$K_n = (1 + c_0 \theta) K_{n+1} + (c_{-1} K_{n+2} + c_{-2} K_{n+3} + \dots + c_{n+1} K_0) \theta$$

$$\vdots$$

$$K_n = K_{n+1} + (c_0 K_{n+1} + c_{-1} K_{n+2} + c_{-2} K_{n+3} + \dots + c_{n+1} K_0) \theta$$

G. Note the emerging form for ϕ_0 :

$$\phi_0 = K_{-1} \phi_{-1} + \theta K_0 [c_{-1}] \phi_{-2}^n + (K_0 \hat{S}_{-1})$$

$$\phi_0 = K_{-2} \phi_{-2} + \theta (K_{-1} [c_{-1}] + K_0 [c_{-2}]) \phi_{-3}^n + (K_{-1} \hat{S}_{-2} + K_0 \hat{S}_{-1})$$

$$\phi_0 = K_{-3} \phi_{-3} + \theta (K_{-2} [c_{-1}] + K_{-1} [c_{-2}] + K_0 [c_{-3}]) \phi_{-4}^n + K_{-2} \hat{S}_{-3} + K_{-1} \hat{S}_{-2} + K_0 \hat{S}_{-1}$$

Before considering the general form for ϕ_0 , note the results of a computer solution for the emerging values of K_i and ΣK_i for various θ 's in the expected range of 0 to -1. The accompanying plot shows that both K_i and ΣK_i approach zero with the effective 'damping' increasing with θ . For ϕ_n as the initial epoch, the general form for ϕ_0 is given as:

$$\phi_0 = K_n \phi_n + \theta (K_{n+1} [c_{-1}] + K_{n+2} [c_{-2}] + \dots + K_{-1} \bar{c} + K_0 \bar{c}) \phi_{n-1} + (K_{n+1} \hat{S}_n + K_{n+2} \hat{S}_{n+1} + \dots + K_0 \hat{S}_{-1}) \quad (C15)$$

Since $K_n \cong 0$, the first term vanishes for large enough n ; i.e., the final epoch is *independent* of the initial epoch. Also, the second term is a coefficient for ϕ_{n-1} which occurs *before* the initial epoch and can be made nonexistent (zero) by definition. Therefore, ϕ_0 depends upon only the quantities in the last term which still contain θ , the N_i , f_i , and \bar{E} .

$$\phi_0 = K_{n+1} \hat{S}_n + K_{n+2} \hat{S}_{n+1} + \dots + K_0 \hat{S}_{-1} \quad (C16)$$

Again, since $K_n \rightarrow 0$, ϕ_0 will depend more heavily upon the more recent \hat{S}_i .

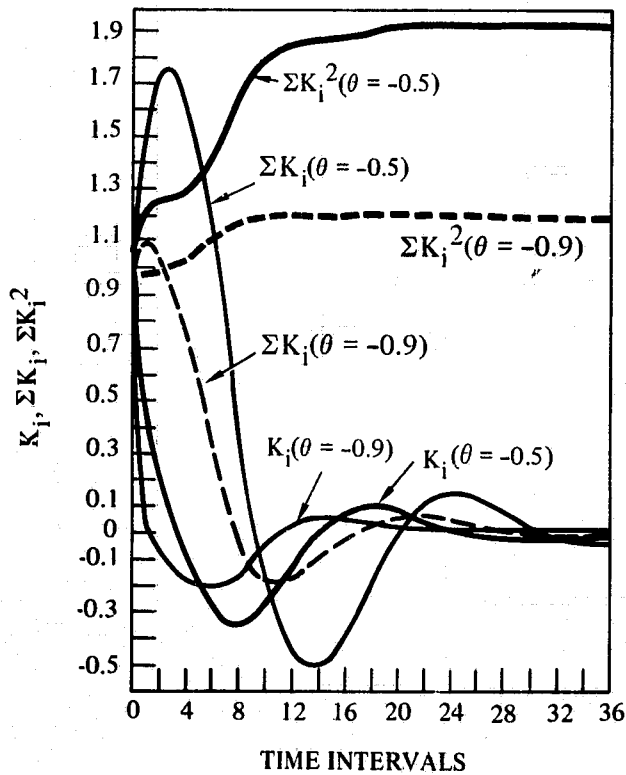


Figure C2. Successive K_i , ΣK_i , and ΣK_i^2 for $\theta = -0.5$ and -0.9 .

H. Substituting the definitions of \hat{S}_i and ΔF_i :

$$\phi_o = K_{n+1} \binom{n}{\theta S + \Delta F_{n+1}} + K_{n+2} \binom{n}{\theta S + \Delta F_{n+2}} + \dots + K_o \binom{n}{\theta S + \Delta F_o}$$

$$\phi_o = K_{n+1} \binom{n}{\theta S + f_{n+1} + \bar{E}} + K_{n+2} \binom{n}{\theta S + f_{n+2} + \bar{E}} + \dots + K_o \binom{n}{\theta S + f_o + \bar{E}}$$

Since $\Sigma K_i \rightarrow 0$, $\Sigma K_i \bar{E} \rightarrow 0$ and ϕ_o depends upon θ , the N_i , and f_i .

I. Substituting the definition of S :

$$\phi_o = K_{n+1} \binom{c_o^*}{\theta [c_o]} \binom{n}{N} + f_{n+1} + K_{n+2} \binom{c_{-1}^*}{\theta [c_o]} \binom{n}{N} + f_{n+2} + \dots$$

*Terms cannot go back to \bar{c} as there are only 1 and 2 c_i in $[c_o]$ and $[c_{-1}]$, etc.

$$\dots + K_{-1} \left(\theta \begin{bmatrix} \bar{c} \\ [c_0] \end{bmatrix} \begin{matrix} n \\ N \\ -2 \end{matrix} + f_{-1} \right) + K_0 \left(\theta \begin{bmatrix} \bar{c} \\ [c_0] \end{bmatrix} \begin{matrix} n \\ N \\ -1 \end{matrix} + f_0 \right)$$

J. Regroup the N_i and f_i terms:

$$\phi_0 = \sum_0^{n+1} (Kf)_i + \theta \left(K_{n+1} \begin{bmatrix} c_0 \\ [c_0] \end{bmatrix} \begin{matrix} n \\ N \\ n \end{matrix} + K_{n+2} \begin{bmatrix} c_{-1} \\ [c_0] \end{bmatrix} \begin{matrix} n \\ N \\ n+1 \end{matrix} + \dots + K_{-1} \begin{bmatrix} \bar{c} \\ [c_0] \end{bmatrix} \begin{matrix} n \\ N \\ -2 \end{matrix} \right. \\ \left. + K_0 \begin{bmatrix} \bar{c} \\ [c_0] \end{bmatrix} \begin{matrix} n \\ N \\ -1 \end{matrix} \right)$$

$$\text{or } \phi_0 = \sum_0^{n+1} (Kf)_i + \theta \left(K_0 \begin{bmatrix} \bar{c} \\ [c_0] \end{bmatrix} \begin{matrix} n \\ N \\ -1 \end{matrix} + K_{-1} \begin{bmatrix} \bar{c} \\ [c_0] \end{bmatrix} \begin{matrix} n \\ N \\ -2 \end{matrix} + \dots + K_{n+2} \begin{bmatrix} c_{-1} \\ [c_0] \end{bmatrix} \begin{matrix} n \\ N \\ n+1 \end{matrix} \right. \\ \left. + K_{n+1} \begin{bmatrix} c_0 \\ [c_0] \end{bmatrix} \begin{matrix} n \\ N \\ n \end{matrix} \right)$$

K. Again regroup the second term according to the subscripted N_i :

$$\phi_0 = \sum_0^{n+1} (Kf)_i + \theta \left[(K_0 c_0) N_{-1} + (K_0 c_{-1} + K_{-1} c_0) N_{-2} + (K_0 c_{-2} + \right. \\ \left. + K_{-1} c_{-1} + K_{-2} c_0) N_{-3} + \dots + (\sum K_p c_q + K_{n+2} c_0) N_{n+1} \right. \\ \left. + (\sum K_p c_q + K_{n+2} c_{-1} + K_{n+1} c_0) N_n \right]$$

L. Define new symbols A_i as:

$$A_{-1} = K_0 c_0, \quad A_{-2} = K_0 c_{-1} + K_{-1} c_0, \text{ etc.}$$

$$\phi_0 = \sum_0^{n+1} (Kf)_i + \theta \left[(AN)_{-1} + (AN)_{-2} + (AN)_{-3} + \dots + (AN)_{n+1} + (AN)_n \right]$$

For n very large, A_i becomes zero, as shown by the accompanying plot of A_i for various θ 's. Therefore, ϕ_0 still depends more on recent noise and frequency deviations.

$$\phi_0 = \sum_0^{n+1} (Kf)_i + \theta \sum_{-1}^n (AN)_i \quad (C17)$$

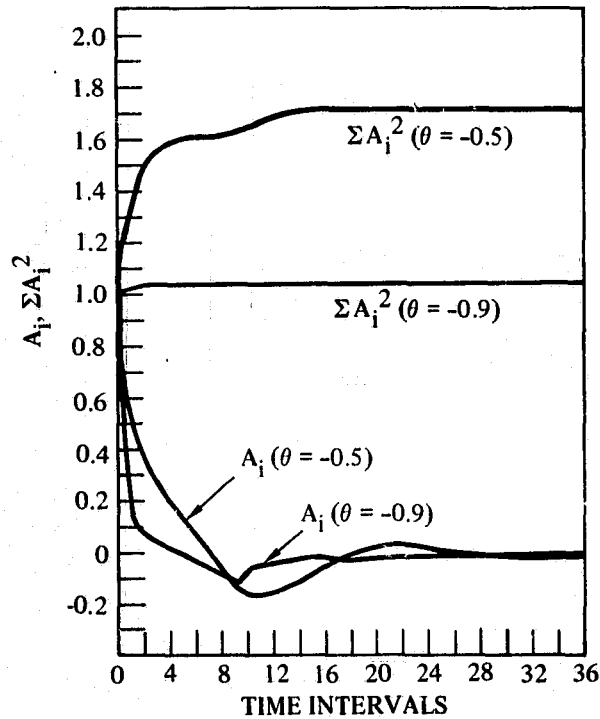


Figure C3. Successive A_i and ΣA_i^2 for $\theta = -0.5$ and -0.9 .

IV. OPTIMIZATION OF EPOCH VARIANCE EQUATION

A. Write the variance of (C17):

$$\text{var } \phi_0 = \sum_0^{n+1} K_i^2 (\text{var } f_i) + \theta^2 \sum_{-1}^n A_i^2 (\text{var } N_i) \quad (\text{C18})$$

where all covariance terms are assumed to be zero; i.e., noise is random and frequency fluctuations are uncorrelated. In practice, short-term correlations may exist in both noise and frequency and must be included for the analysis to be rigorous. For analysis purposes, frequency correlations can be at least partially accounted for by ascribing a larger value to the assumed variance of f_i .

B. To get the optimum θ for minimizing $\text{var } \phi_0$, differentiate $\text{var } \phi_0$ with respect to θ and equate to zero. Because all constants depend on θ , the differentials are complex, and satisfactory results will be found by a substitution procedure instead. Therefore, substitute expected values for θ , $\text{var } f_i$,

var N_j ; the limiting values for ΣK^2 and ΣA^2 (fig. C4) and look for a minimum in var ϕ_0 as a function of θ . If a minimum does exist, an optimum θ also exists, as shown by the plots of var ϕ_0 versus θ in figure C5.

The computer analysis indicates that for $\theta = -0.1$, more than 150 intervals are needed to reach the limiting value for ΣK_i^2 and ΣA_i^2 , so that the var ϕ_0 values plotted are not as accurate as for other θ 's. Also, the values for ΣA_i were found, and although not necessary to the analysis, they seem to behave similarly to the ΣK_i except that the final value is not zero but very close to ΣK_i^2 for the same θ 's. Knowledge of ΣA_i might be useful in equation (C17) if there were a large dc component to the propagation noise N_j .

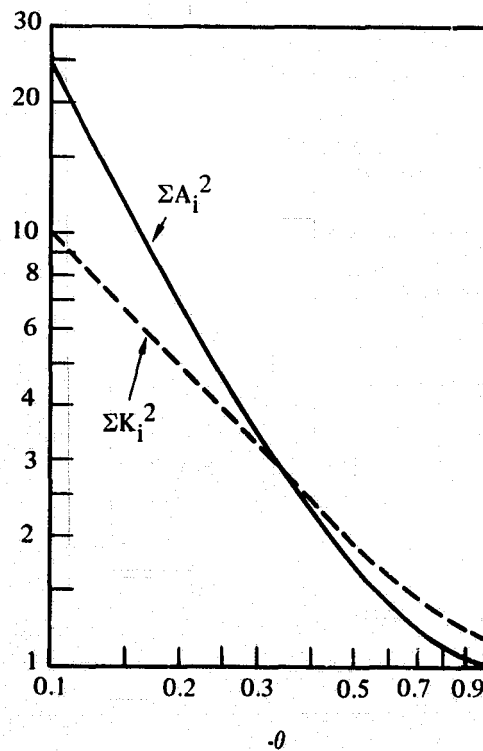


Figure C4. Limiting values for ΣK_i^2 and ΣA_i^2 vs. $-\theta$.

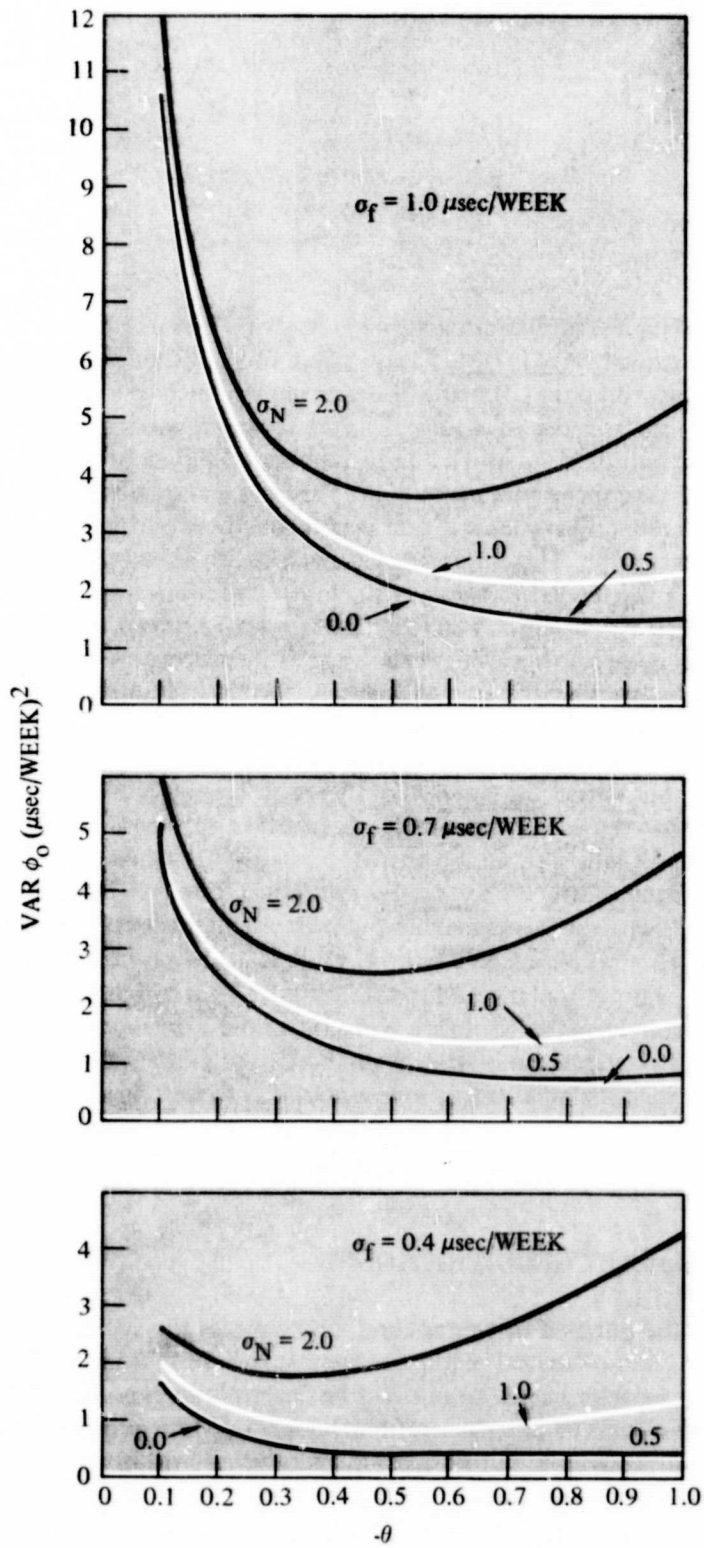


Figure C5. Variance ϕ_0 vs. θ for various σ_f and σ_N .

APPENDIX D: PATH CALIBRATION

INTRODUCTION

Three fundamental approaches may be followed to calibrate vlf paths for epoch dissemination: (1) direct application of published skywave corrections and geodetic information; (2) use of external means such as a single flying clock visit; (3) indirect use of skywave corrections and geodetic information in a "boot strap" approach in which a large number of signals are measured in order to reduce the mean prediction bias. This appendix addresses the third approach—the reduction of calibration bias through monitoring the large number of signals available. This approach offers three advantages over the direct application of published skywave corrections: (1) reduction of the site calibration bias below that which might be expected over only a few paths; (2) reduction of the relative biases between various measurements such that, in the event of various transmitting station failures, only minimum disturbances will be introduced in the timing site epoch; and (3) the possibility of calibrating short paths over which propagation characteristics may be too complex to predict precisely, but where the signal is observed to be highly repeatable.

Note that the prediction errors addressed in this appendix are those from the current global prediction theory.¹ Published skywave corrections are based not only on the global prediction theory, but, where sufficient data exist, are also "force-fit" using a statistical scheme described by Kasper.² Hence, actual published predictions may exhibit somewhat different features than indicated herein. Of particular potential importance to timing is the partitioning of errors from hyperbolic observations into their range-range components. Thus, the following analysis is strictly valid only for global predictions without statistical force-fit adjustments. However, it is to be hoped that the force-fit procedure may improve timing capability, and it is at least speculated that no serious degradation will have been introduced.

TEMPORAL CONSIDERATIONS

Since the purpose of this appendix is to assess the accuracy expected from the reduction of spatial prediction bias, it should first be asked whether such biases, or relative biases, can in fact be determined experimentally as distinct from the effects of normal temporal variations. The question leads to a number of considerations, but no serious operational problems.

¹ See *REFERENCES*, p. 156.

Analysis of Omega phase measurements at night has shown that they tend to be correlated for 8 to 10 hours. Long autocorrelation periods have also been observed during the day. Accordingly, we expect to have available measurements which exhibit reasonable temporal independence only about once per day or, perhaps, once during the day and once at night. The estimate of the signal bias of daily measurements will be contaminated by temporal scatter proportionally to the temporal standard deviation and inversely proportional to the square root of the number of measurements used to estimate the bias. Thus, in 4 days the bias estimate will be uncertain by about half the temporal scatter, while in 4 weeks it will be uncertain by about 20% of the temporal scatter. Taking as a conservative estimate of temporal scatter a standard deviation of 3.8 μsec , as indicated in table 2 of the report proper, for 24-hour monitoring including SID's, the contamination of the bias will be on the order of 0.8 to 2 μsec for monitoring from 4 days to 4 weeks. Typical prediction biases can be determined approximately from table 2, since the rms error may be expected to resemble an rss combination between inherent scatter σ and typical bias b :

$$\text{rms} = (\sigma^2 + b^2)^{1/2}$$

hence:

$$b = (\text{rms}^2 - \sigma^2)^{1/2} = (6.4^2 - 3.8^2)^{1/2} = 5.2 \mu\text{sec}$$

Thus, a few weeks' monitoring will allow bias estimates which are relatively insensitive to the effects of nominal temporal variation. It should be noted, however, that slower seasonal or periodic changes could become significant if not predicted correctly. Such changes could be considered as a slow change in the bias and, in time, could introduce first-order errors in epoch determinations. If relatively precise methods are used, as described in appendices E and F, then the contamination of the bias estimates would be still smaller than indicated above; but, to minimize the effects of poor modeling of lunar and semilunar periodicities, the monitoring should be conducted over a lunar period (29.53 days) or semilunar period (14.8 days). Thus, useful bias estimates can be obtained in only a few days, although there is some advantage to having measurements span 2 or 4 weeks. It may be noted that for monitoring up to 2 weeks, a cesium standard adjusted to 1×10^{-12} would drift less than $\pm 1 \mu\text{sec}$, so all measurements could be grouped without adjustment for drift. In practice, such a convenience is unnecessary, since it is the relative biases between various signals which are to be determined, and these will not be affected by drift of a common reference.

THEORETICAL CONSIDERATIONS

Having established that the relative biases can be determined experimentally, it is now necessary to determine the resulting epoch accuracy. Potentially, signals at five frequencies from eight stations each processed both

day and night can be considered. If all the prediction biases were about $5 \mu\text{sec}$ and uncorrelated, the 80 information inputs would theoretically allow the timing site epoch to be refined to about $5 \mu\text{sec}/\sqrt{80}$ measurements $\approx 1/2 \mu\text{sec}$. In practice, the information will be neither uncorrelated nor homogeneous, so a more thorough analysis is necessary.

Available signals include transmissions over various paths, frequencies, and diurnal periods. To some degree, all of the information may be expected to be correlated. All Omega predictions are based on structurally the same model. Hence, any structural errors are likely to be correlated. Predictions over separate paths to the same timing site may be correlated, particularly if signals arrive from similar azimuths such that the region of decoupling of the signal from the earth-ionosphere waveguide is partially in common. One would expect, however, that epoch estimates over different paths would be relatively independent. Predictions at different frequencies over the same path will all use the same, possibly erroneous, geophysical input such as estimated ground conductivity. Since timing errors resulting from ground conductivity errors tend to be similar for most ground conductivities, a correlation may be expected in the prediction biases from this error source. Errors due to modal interference, however, are not expected to be correlated and, under certain conditions, might even become negatively correlated. Some correlation may also exist between prediction biases observed at different diurnal periods. Although the propagation modal structure is considerably more complicated at night than during the day, the relative importance of errors in ground conductivity is usually in the same sense both day and night but greater during the day. These characteristics suggest possibly similar magnitudes between day and night prediction errors and some correlation.

EXPERIMENTAL DATA

To obtain quantitative estimates of the various correlations, use will be made of the prediction model developed in the fall of 1971 and described in reference 1, where results from 10.2-kHz measurements over the past 11 years at 300 site lines of position (equivalent statistically to 300 paths) are described. Results reflect propagation in the arctic and across the equator as well as in temperate latitudes but are restricted to identifiable diurnal periods—i.e., all propagation paths either completely dark or sunlit—and to paths greater than 840 km which are assumed to be of sufficient length that serious modal complexity over shorter paths is not included. Although only propagation at 10.2 kHz is described in reference 1, similar residual errors are available for 13.6 kHz and for the 3.4-kHz derived difference. While the residual error tabulations are sufficiently extensive to be assumed indicative of a true ensemble of global prediction errors, a few peculiarities should be noted:

1. Measurement durations range from 1 day to 1790 days (equivalent to 5 years of uninterrupted observation). Since the error observed on a particular day will be a combination of both the prediction bias and the temporal variation on the day of observation, the presence of residual errors from brief monitoring indicates that the resultant

rms residual error will be slightly higher than the true rms prediction bias and may exhibit slightly different correlations. However, as the median observation period is about 10 days, the rms residual errors should substantially reflect the prediction biases.

2. Three types of measurements are included: (1) absolute phase measurements over single paths with respect to a calibrated atomic frequency standard; (2) phase differences taken in the modern conventional way from transmissions developed by cesium frequency standards; and (3) older phase difference measurements taken in the slaved mode of system operation. In effect, various individual measurements may represent propagation over one, two, or three propagation paths.
3. The data sample is not uniform between diurnal periods and frequencies. For example, monitoring in the arctic during the summer will not produce "night" data. Some data are available from sites with only a single frequency capability.

Because of the above, use has been made, in the computations to follow, of statistics derived by selection from the general listings, where only measurements with common characteristics are used.

SPATIAL CORRELATION

Spatial correlation may be assessed by selecting only those observations which may be regarded as representing propagation over a single path. Two types of measurements may be regarded as absolute measurements of propagation over single paths. As noted earlier, measurements at monitors near transmitting stations may be taken as absolute measurements of the phases received from remote stations measured against an "injected" reference emitted by the local station and transmitted by stable propagation over a short path of less than 50 km. A few measurements also exist against references developed by flying clocks between the transmitting stations and observation sites. Table D1 summarizes measurements equivalent to propagation over single paths.

The correlation between prediction errors over separate paths at particular diurnal periods and frequencies may be obtained from table D1 by cyclically interchanging biases at a particular site so as to obtain all possible pairs of signal combinations. This procedure assumes that there is no *a priori* difference between the various transmitting stations, so all signals may be taken as from equivalent, although potentially correlated, statistical populations.* The results of the calculation are shown in table D2.

*Ordinarily, the correlation coefficient is defined so as to remove the effects of a nonunity scale ratio between pairs of variates; the interchange procedure forces unity scale ratio, as must be true for the parent populations if the transmitting station designations are irrelevant. Note that, for two measurements at a site, perfect positive correlation would be represented by pairs such as (0,0), (1,1), (2,2), etc., while perfect negative correlation would be (0,0), (1,-1), (2,-2), etc. For three measurements at a site, perfect positive correlation would be given by (0,0,0), (1,1,1), (2,2,2), etc., but a negative correlation coefficient less than -0.5 could not occur, since it is impossible to find three values all equal and opposite. Measurements such as (0,0), (1,2), (2,4), etc., would not result in perfect positive correlation after the cyclic interchange.

TABLE D1. SUMMARY OF RESIDUAL PREDICTION ERROR OVER SINGLE PATHS.

Monitor Site	Transmitter*	Residual Prediction Error, μsec						Average
		10.2 kHz			13.6 kHz			
		Day	Night	Average	Day	Night	Average	
Hestmona,	HA	1.3	2.1	1.7	2.4	0.2	1.3	1.5
Norway	TR	-7.5	-7.2	-7.3	-4.5	-6.8	-5.6	-6.5
NELC,	NY	0.7	1.4	1.0	3.2	-0.4	1.4	1.2
San Diego,	HA	7.8	4.6	6.2	5.7	7.1	6.9	6.6
California	TR	-0.1	3.9	1.9	2.8	2.6	2.7	2.3
Opana, Hawaii	NY	1.6	2.9	2.3	-2.9	0.2	-1.6	0.3
Pyramid Rock,	NO	0.1	-2.8	-1.4	-2.4	-5.9	-4.2	-2.8
Hawaii	NY	1.9	0.7	1.3	0.9	-1.1	-0.1	0.6
	NO	1.9	0.6	1.2	0.5	-1.4	-0.5	0.4
Rome, New	HA	-0.3	-3.5	-1.9	0.2	-3.2	-1.5	-1.7
York	TR	-2.2	0.5	-0.8	-2.7	-0.6	-1.6	-1.2
	NO	-5.8	-1.7	-3.7	-6.6	1.7	-2.5	-3.1
Trinidad	NY	-1.8	-2.8	-2.3	0.7	1.1	0.9	-0.7
	HA	-2.1	-0.8	-1.4	2.2	1.3	1.8	0.2
	NO	-7.3	-0.6	-3.9	-4.9	-5.7	-5.3	-4.6
Wales, Alaska	NY	5.0	3.7	4.4	-2.8	-1.3	-2.1	1.2
	HA	2.8	3.5	3.2	0.7	0.3	0.5	1.8
RMS		3.9	3.1	3.3	3.3	0.4	3.1	2.9

*HA - Hawaii
 TR - Trinidad
 NY - New York
 NO - Norway

TABLE D2. SPATIAL CORRELATION OF PREDICTION BIASES.

	10.2 kHz		13.6 kHz	
	Day	Night	Day	Night
Estimated Correlation	-0.12	0.20	0.12	0.24
95% Confidence Range	-0.5→0.3	-0.2→0.5	-0.3→0.5	-0.2→0.6

Since none of the correlations is statistically significant, we have the important result that *prediction biases over various paths may generally be considered uncorrelated*. The result is in accord with physical expectations which indicate slight if any significant correlation.

The foregoing conclusions indicate only that prediction biases are not necessarily correlated; hence, following normal statistical practice, correlation may generally be disregarded. It should now also be asked whether the slight median correlation of 0.16 is likely to be of practical importance or whether the maximum statistically plausible correlation is likely to be of practical importance. We seek an estimate for the reduction in the bias of an ensemble created from averaging various signals:

$$B = (b_1 + b_2 + \dots + b_n)/n$$

Considering only two signals of equal quality, $(\text{Var } b)^{1/2}$, we have:

$$\text{Var } B = \text{Var } b [(1 + \rho)/2]$$

Hence, the typical reduction in the ratio of the scatter of averaged biases over individual biases, $(\text{Var } B/\text{Var } b)^{1/2}$, is $[(1 + \rho)/2]^{1/2}$ for two stations and, by induction, is $(1 + \rho)/2$ for four stations and $[(1 + \rho)/2]^{3/2}$ for eight stations. Thus, disregarding a nominal correlation of 0.16 would only cause an 8% error in the improvement ratio expected using two stations, but, using eight stations, the error in the ratio could increase to 25%. The 95% upper bound for the lowest correlation obtained is less than the 0.24 estimate obtained for 13.6 kHz at night. Using a correlation of 0.24 as a pessimistic value, the maximum error in the improvement ratio using two signals is 12%, while the ratio might be in error by 39% using eight signals. Improvement factors for the expected error in average obtained over various numbers of paths are given in table D3.

A factor of two reduction in the site bias can thus be obtained by averaging over four to eight paths. In practice, greater reductions in site bias may be obtained if signals for which prediction errors are likely to be a minimum are processed favorably.

**TABLE D3. IMPROVEMENT FACTORS FOR
AVERAGING OVER MULTIPLE PATHS.**

	Number of Paths		
	2	4	8
Bias Correlation			
Uncorrelated ($\rho=0$)	1.4	2.0	2.8
Nominal ($\rho=0.16$)	1.3	1.7	2.3
Pessimistic ($\rho=0.24$)	1.3	1.6	2.0

**DISPERSIVE CORRELATION, DAY-NIGHT CORRELATION, AND
SIGNAL PREDICTION BIAS**

DATA SELECTION

Correlation between frequencies and diurnal periods is best obtained by first developing a "selected data list" wherein rms prediction errors at various frequencies and diurnal periods are tabulated only for sites for which all desirable entries are available. Such a list was prepared and contained data from 97 site lines of position for which 10.2- and 13.6-kHz data were available both day and night and at least partially for the same monitoring period, so 3.4-kHz difference frequency data were obtainable. Measurements were principally phase differences in the modern "absolute" mode of system synchronization and, hence, reflected differences in propagation predictions over two paths, although a few measurements were single path measurements against a calibrated reference. Since the measurements were selected for equivalent sampling and since biases over different paths were shown to be independent, the type of measurements contained is not of direct importance in determining relative correlations but is only significant in evaluating absolute scatter. Direct simple correlations between tabulated rms prediction errors for the frequencies and diurnal periods are shown in table D4. The rms prediction errors from the "selected list" are compared with equivalent rms prediction errors from the master lists in table D5.

**TABLE D4. SIMPLE CORRELATION BETWEEN
FREQUENCIES AND DIURNAL PERIODS.**

Frequency, kHz	Diurnal Period	Correlation	0.95% Range
10.2-13.6	Day	0.73	0.6→0.8
10.2-13.6	Night	0.33	0.1→0.5
10.2	Day-Night	0.31	0.1→0.5
13.6	Day-Night	0.49	0.3→0.6

TABLE D5. COMPARISON OF PREDICTION BIASES.

Frequency, kHz	Typical Bias Error, μsec			
	Day List		Night List	
	Master	Selected	Master	Selected
10.2	5.1	4.8	4.8	4.6
13.6	4.9	4.6	6.2	5.7

SIGNAL PREDICTION BIAS

Table D5 shows remarkable consistency between the various estimates of typical bias. In general, estimates from the master list are somewhat higher than corresponding estimates from the selected list, probably due to the presence of more older data reflecting propagation over three paths in the master statistics. Biases are also consistent between frequencies and diurnal periods, except that biases at 13.6 kHz at night are notably higher, presumably due to greater modal interference.*

*It may be asked whether the nominally poorer calibration of the 13.6 kHz night measurements is of practical significance. Consider the optimally weighted combination $C = \frac{p + Wq}{1 + W}$, where p and q are night biases of 10.2 and 13.6 kHz, respectively. Disregarding correlation between the two component biases, we have:

$$\text{Var } C = \frac{1}{(1 + W)^2} [\text{Var } p + W^2 \text{Var } q] \tag{D1}$$

which may be optimized by taking the partial derivative with respect to W and equating to zero to obtain the optimum weighting:

$$W_{\text{opt}} = \frac{\text{Var } p}{\text{Var } q}$$

Substituting in equation (D1) and simplifying yields the improvement ratio of the bias expected in the optimum combination to that expected from 13.6 kHz day alone:

$$\frac{\text{Var } C}{\text{Var } p} = \frac{1}{1 + W}$$

From table D5 we expect, for a single path, that $\text{Var } p = (4.6 \mu\text{sec})^2/2$ and $\text{Var } q = (5.7 \mu\text{sec})^2/2$, so $W_{\text{opt}} = 0.65$, which leads to an improvement ratio only 10% worse than would have been obtained if both 13.6 day and night were of the same quality as 13.6 day. Thus, considering information at the two frequencies and two diurnal periods as of equal quality corresponding to a single path prediction error of $3 \frac{1}{4} \mu\text{sec}$ will lead to no substantial inaccuracy in the predicted improvement even though optimum weighting differs by almost 2:1. Since the bias errors of table D5 from the selected data list are primarily due to prediction errors over two independent paths forming a phase difference, the median error of $4.6 \mu\text{sec}$ should be $(2)^{1/2}$ times that over a single path. A typical single path prediction error is thus on the order of $3 \frac{1}{4} \mu\text{sec}$, which may be compared with actual single path errors for the limited sample in table D1: 3.1 to $3.9 \mu\text{sec}$.

DISPERSIVE CORRELATION AND DAY-NIGHT CORRELATION

From foregoing discussions, it is clear that the various frequencies and diurnal periods yield roughly equivalent prediction biases equal to $3 \frac{1}{4} \mu\text{sec}$ over a single path and that this bias may be reduced by a factor of 2 through averaging biases over four to eight paths. We must now assess the further reduction of bias from the use of measurements at different frequencies and diurnal periods. Two approaches are available: (1) exact solution based on simultaneous consideration of all data in the selected list, and (2) inference based on simple correlations given in table D4. Because of the insight offered, the latter approach will be considered first.

Table D4 shows high correlation between prediction errors at 10.2 and 13.6 kHz during the day and moderate correlation at night. The correlation is expected physically and is desirable in that it reduces the probability of an epoch ambiguity resolution error. However, relatively high correlations indicate that comparatively little will be gained by averaging prediction bias errors.

If two sets of measurements have a correlation, ρ , and are of equal quality, the improvement ratio of the uncertainty in an optimum combination of measurements from both will be $[(1 + \rho)/2]^{1/2}$ as compared with $[1/2]^{1/2}$ if the measurements were uncorrelated. Thus, an additional measurement correlating with an existing one by 0.73 contributes no substantial new information; however, if the correlation is 0.33, the bias in the average of the means will be about 0.8 that of a typical mean bias instead of 0.7 if the observations were uncorrelated.

The foregoing considerations of prediction bias at 10.2 and 13.6 kHz and correlations given in table D4 yield the following statements and approximations:

1. Typical prediction biases are $3 \frac{1}{4} \mu\text{sec}$ independent of frequency or diurnal period.
2. Prediction biases over different paths are uncorrelated.
3. Biases day and night over the same path at the same frequency may be considered uncorrelated.
4. Biases between night measurements at the different frequencies may be considered uncorrelated.
5. Biases between day measurements at different frequencies are highly correlated.

Although not addressed specifically, it may be conjectured that the correlation between prediction errors at more closely spaced frequencies, such as 10.2 kHz and $11 \frac{1}{3}$ kHz, will be higher, so additional frequencies will contribute relatively little to bias refinement.

Since many of the prediction biases may be considered uncorrelated and are expected to be of similar magnitude, the expected error contribution from propagation prediction to epoch determination at a timing site is easily assessed. Considering 10.2 and 13.6 kHz, there will be three independent sources of calibration bias for each propagation path: 10.2 and 13.6 kHz at night and a common bias for daytime measurements. The nominally expected epoch bias is thus $3.25/(3N)^{1/2} = 1.88/(N)^{1/2} \mu\text{sec}$, where N is the number of paths.

If slight interpath correlation exists, improvement will be slower with the increasing number of paths considered, as indicated in table D3. Under the most pessimistic interpath correlation, 1- μ sec accuracy can be exceeded using all eight Omega stations. Nominally, one expects to achieve 1- μ sec accuracy using four or five stations. It should be noted, however, that at this precision a number of other error sources become significant. Some effect of temporal variations will be contained in bias estimates, so true relative biases will not be precisely known, although, the foregoing analytical approximation of bias errors by rms errors between observations and prediction entails, to some degree, an error of the same type; i.e., the typical path calibration error estimate of 3 1/4 μ sec is conservative as some error must have been introduced by finite averaging of temporal variations. Phase tracking and recording errors also tend to be on the order of 1 μ sec. Although typical instrumentation errors also must have contributed to the statistics used in the analysis, they may be more critical in particular applications as, for example, if serious "S" curve errors should be present on a phase tracking channel being used for a common reference.

Practical approximate methods for developing the site epoch and determining the relative prediction errors for the various measurements follow directly from the foregoing discussion. All information was approximated as of equal quality and, except for 10.2- and 13.6-kHz daytime determinations on the same path, as independent, from which the optimum epoch estimate closely approximated a grand average of all information, except that a single value should be assumed for daytime measurements over each path. At a particular site, however, some propagation paths will be more accurately predicted than others. Although factors affecting prediction accuracy are quite complex, a few generalizations may be noted:

1. Favorable path characteristics:
 - Moderate length: 2000 to 10,000 km
 - Favorable ground conductivity: sea water or normal land
 - Temperate latitude
2. Unfavorable path characteristics:
 - Short paths: especially important at night
 - Poor ground conductivity: especially important in arctic regions of very poor ground conductivity for predictions during the day
 - Arctic paths: greater predictive complexity due to polar cap and auroral zone; relatively more important at night, but ground conductivity uncertainties may also cause prediction difficulty during the day
 - Equatorial propagation: particularly important at night; predictions highly sensitive to azimuth

While the above do not provide quantitative guidance on the optimum weighting between biases over different paths, they do suggest that possible prediction biases may tend to be better than nominal over many paths,

though significantly worse than nominal in a few instances. Under these conditions, a median procedure may be recommended: it will be comparatively insensitive to a significant minority of relatively large biases. Conveniently, median procedures also tend to be insensitive to occasional computational errors and blunders and are easily followed without special computing equipment. In particular, a two-step procedure is recommended:

1. Average daytime results from 10.2 and 13.6 kHz over common paths.
2. Take the median between the single day result and both night results over all predictable paths.

Table D3 provides data for comparison of the above procedure with simple averaging. Although the data are limited so that comparisons are at most only suggestive, the median magnitude of the epoch error per site as deduced from simple averaging is 1.1 μ sec, while following the above procedure it is 0.7 μ sec. A refinement would be to flag data from paths which are especially difficult to predict and then compare the resulting medians, considering all data and only the supposedly more reliable data to obtain a qualitative estimate of calibration consistency.

The foregoing approximate assessment may now be compared with an exact solution for optimum weighting of 10.2- and 13.6-kHz measurements both day and night. Statistically, optimum weights between the two frequencies and diurnal periods over common paths may be obtained directly from the "selected list." Let x_j represent various biases for particular site lines of position such that $x_1 =$ bias for 10.2 kHz during the day; $x_2 =$ bias for 10.2 kHz night, $x_3 =$ 13.6 day, and $x_4 =$ 13.6 kHz night. We wish to optimally weigh the various bias estimates such that, for an ensemble formed from j site lines of position, $\text{Var}(\sum_j w_j x_{ij})$ is minimized subject to the condition $\sum w_j = 1$. Let $z_1 = x_1$, $z_2 = x_2 - x_1$, $z_3 = x_3 - x_1$, $z_4 = x_4 - x_1$, and we note the optimization will occur when $\text{Var}(z_1 + w_2 z_2 + w_3 z_3 + w_4 z_4)$ is minimized, which in turn corresponds to a regression problem of $-z_1$ on $z_2, z_3,$ and z_4 . Since a general-purpose regression program was used in computing the correlations in table D4, a minor modification produced the optimum weights shown in table D6.

TABLE D6. OPTIMUM WEIGHTS.

Index	Frequency and Diurnal Period	Weight
w_1	10.2 kHz { Day	0.21
w_2		Night
w_3	13.6 kHz { Day	0.26
w_4		Night

The optimum weights may be compared with the foregoing approximate procedure, but it is first worthwhile to note their implications for special syntheses such as composite Omega.

Pierce, reasoning from the observation that the product of the group and phase velocities is a constant for certain wave guides, has suggested that a 'composite' signal may be derived which is more stable than either carrier.³ Initial attention was directed toward temporal stability, but attention has also been given to reduction of diurnal variations and prediction bias. Since composite Omega is statistically equivalent to an optimum weighting scheme, table D6 may be directly compared with anticipated weights for composite Omega.^{4,5} Pierce has shown that a preferred relative weighting between 10.2- and 13.6-kHz signals should be $m = 9/4$ in the expression:

$$\hat{T} = mT_{13.6} - (m - 1)T_{10.2}$$

which indicates that $w_1 = -1.25$ and $w_2 = 2.25$. Since the actual optimum weights are not of the same order or sign, it is clear that the composite concept is not applicable in this case, except as it is statistically equivalent to an optimum combination of information from two frequencies. This observation should not, however, be interpreted as indicating that composite Omega concepts offer no advantage for timing application; it simply indicates that the nominal prediction biases based on the present global prediction model do not conform to a composite concept. The present model was derived to optimize predictions for 10.2 kHz, with additional optimization directed not only to 13.6 kHz but also to the 3.4-kHz beat. It is possible that a prediction model to optimize timing from both 10.2 and 13.6 kHz would be significantly different and might yield a significantly different relative weighting of bias errors. However, such a situation has not been investigated; hence, no conclusions other than for the predictions considered are presently warranted.

The weighting indicated by table D6 may now be compared with the previous approximate weighting. From the previous analysis, we expect the sum of the weights during the day to be about 0.33, while those at night should sum to about 0.67. In practice, the day weights total 0.47 and the night weights 0.53. Hence, the optimum day-night weighting is more nearly equal than previously indicated. Further, although the 10.2- and 13.6-kHz day information is weighted about equally, as indicated in the approximate analysis, the night weights significantly favor 10.2 kHz. The approximate analysis indicated that the 10.2-kHz night information should receive approximately twice the weight of the 13.6-kHz night information but that the use of equal weights would not significantly degrade the quality of the deduced epoch. Optimum weighting indicates that the 10.2 kHz night should be weighted about 3:1 over the 13.6 kHz night.

Optimum weights have been applied to the selected data list. The resultant median absolute error of 2.3 μsec indicates that a typical single path can be calibrated to an accuracy of about $2.3 \mu\text{sec}/\sqrt{2} = 1.6 \mu\text{sec}$. Hence, both optimum weighting and the approximate analysis indicate a capability for typically calibrating a site to better than 1 μsec through use of signals over multiple paths.

Optimum weights were also developed for information consisting of day and night carrier frequency biases and the 3.4-kHz bias. However, the explicit 3.4-kHz errors offered no additional information of significant value.

Thus, both the approximate and optimum weightings indicate the possibility of calibrating a remote site to about 1 μ sec, although the weights employed differ. Some adjustment of weights toward those indicated in table D6 may be desirable. However, the use of medians rather than averages may prove beneficial. As noted in the limited case of data from table D1, a more nearly optimum weighting may in practice produce worse results than a median procedure.

Following the foregoing, site epoch may be deduced based on a median procedure for various clock time estimates, each obtained by methods indicated in sample procedure 2, in the report proper. The differences between the median estimate of site epoch and the individual measurements thus indicate relative prediction errors. The effects of relative prediction errors can then be removed from further timing problems by replacement of the respective "REFERENCE PATH DELAYS, G_R " values of sample procedure 2 by values adjusted to yield the experimentally observed site epoch. In this way, each signal is individually calibrated to an accuracy of about 1 μ sec. Once propagation effects are calibrated, only those signals of especially good repeatability need be considered in continuing timing.

REFERENCES

1. Swanson, E. R., "VLF Phase Prediction," *VLF-Propagation: Proceedings From the VLF Symposium*, Sandefjord, Norway, 27-29 October 1971, G. Bjøntegaard, ed., p. 8-1 to 8-36 (Norwegian Institute of Cosmic Physics Report 7201, January 1972)
2. Kasper, J. F., Jr., "A Skywave Correction Adjustment Procedure for Improved Omega Accuracy," *Proceedings of the ION National Marine Meeting, U.S. Coast Guard Academy*, New London, Connecticut, 12-14 October 1970, v. II, p. 17-30
3. Harvard University. Engineering and Applied Physics Division Technical Report 552, *The Use of Composite Signals at Very Low Radio Frequencies*, by J. A. Pierce, February 1968
4. Navy Electronics Laboratory Report 1305, *Omega Lane Resolution*, by E. R. Swanson, 5 August 1965 (AD472854)
5. Naval Electronics Laboratory Center Report 1657, *Composite Omega*, by E. R. Swanson and E. J. Hepperley, 23 October 1969 (AD863791)

APPENDIX E: PERIODIC VARIATIONS

INTRODUCTION

Seasonal variations in vlf propagation have long been recognized. Of particular importance for timing is an annual variation related to the solar zenith angle, which causes the phase received during the day to vary slightly throughout the year. Although variation related to the solar zenith angle is included in published corrections, any errors will be particularly important for frequency comparisons, as they will introduce frequency biases. As an extreme example, the seasonal phase shift during the day between Hawaii and New York at 10.2 kHz is on the order of 15 μ sec. If this phase change were disregarded, an average bias on the order of 2 μ sec per month would occur, which would limit the accuracy of frequency dissemination to a value on the order of one part in 10^{12} . In practice, maximum rates of change are higher than average, so biases on the order of a few parts in 10^{12} might occur from using monthly determinations.

Other periodicities also have been recognized. Noonkester has shown that Omega phase data also contain semiannual and lunar tidal periodicities.¹ These periodicities presently are not included in the global prediction theory and, therefore, constitute sources of error in time dissemination.

Regardless of origin, unmodeled periodicities in vlf phase measurements will affect timing by introducing periodic fluctuations in deduced site epoch and frequency. As will be shown, the amplitudes of the various periodicities generally are smaller than typical scatter or prediction bias, so they may be neglected in many applications. However, in the most precise applications, periodicities should be considered, since, while timing errors due to normal random fluctuations can be averaged out through the use of data spanning several days or weeks, longer-term periodic components will not be corrected. In particular, processing techniques to deduce precise frequency should be designed to filter periodic components.

This appendix assesses the periodicities which may be expected in any Omega phase measurements, with specific attention to actually observed periodicities over paths between Hawaii and Rome, New York, and between Trinidad and Rome, New York. The data were analyzed in 5-year strings at several hours in the neighborhood of midpath noon and midnight. The path between Rome and Hawaii is a long, predominantly east-west path, while that between Rome and Trinidad is of moderate length and predominantly north-south. Attention to the two paths thus allows determination of periodicities over characteristically different paths by statistical means without development of a causal theory.

¹See *REFERENCES*, page 181.

This appendix is composed of four basic sections:

- Theoretical dependence of vlf phase variation on solar zenith angle and sunspot activity levels
- Periodic variations in phase to be expected from radiative and tidal phenomena
- Analytical methods for statistical detection of expected periodicities
- Discussion of results and conclusions

The first section discusses the effectiveness of the diurnal theory of Omega phase variation in predicting the periodic influence of the solar radiative flux on vlf daytime phase. Subsections consider the effects of variations in zenith angle, sunspot dependence, diurnal curvature, and time delays in limiting the validity of the simplified theory assumed to apply in the neighborhood of midpath noon. The conclusion is reached that the approximations used to represent the presently available prediction model, as, for example, implemented in published Skywave Correction Tables, are adequate for determination of direct solar flux-produced periodicities in Omega noontime phase measurements.

The second section discusses several aspects of celestial mechanics and geophysical phenomena pertaining to solar and lunar tidal influences on the ionosphere. Expected periodicities in vlf phase data are developed from knowledge of the relative motion of the earth/moon/sun system and some simplified algebraic expressions for variations in zenith angles.

The third section discusses the periodic analysis used to extract the expected discrete components from the 5-year data series. Specific topics covered include the utility of the 'round trip' phase, the regression analysis performed, and the statistical parameters being determined.

The final section summarizes the results and discusses the possible significance of the discovered periodicities in timekeeping operations.

PERIODIC INFLUENCES OF SOLAR FLUX

The diurnal theory of Omega phase variation represents phase as a function of time as the effective ionospheric response to a diurnal forcing function of the solar zenith angle.² The theory incorporates additional phenomena during sunrise and sunset but becomes relatively simple near noon, where the diurnal function becomes proportional to the cosine of the solar zenith angle. Lags are introduced between the observed diurnal phase variation and that expected directly from the diurnal function due to effective ionospheric time constants. Near noon, however, the forcing function is a close approximation to the expected phase variation.

The diurnal theory shows that the time-dependent variation of the phase of the forcing function near noon can be expressed by:

$$\Delta\phi'(t) = (\Delta\phi) M(t) (1 - \overline{\cos \chi}(t)) \quad (E1)$$

where M is an empirically deduced proportionality 'constant,' $\Delta\phi$ is the nominal diurnal phase change from night to what would be observed if the entire path

were normally illuminated, and $\overline{\cos \chi}$ is the average value of the cosine of the solar zenith angle over an effective path equal to the geometric path shortened by 6° at each end. M is time-dependent in that it may be related to the sunspot number by:

$$M(t) = 0.23 + 5 \times 10^{-4} (\text{sunspot number}) \quad (\text{E2})$$

where the sunspot number has typically an 11-year variation. The path average of $\cos \chi$ may be determined sufficiently by dividing the path length into 0.01-radian increments and averaging the individually determined $\cos \chi$ values:

$$\overline{\cos \chi} = \frac{1}{N} \sum_{i=1}^N \cos \chi_i \quad (\text{E3})$$

where the index i defines segments in the midpath between points 6° removed from the ends.

As a first step in attempting to isolate radiation and tidal periodicities in the data series analyzed here, the solar radiation effects represented by equation (E1) may be calculated and removed from the data. The residual variations then may be assumed to be related to either lunar or solar tidal phenomena, to additional unmodeled seasonal variations in ionospheric chemistry (stratospheric warming, winter anomaly, etc.), to random noise, or to galactic influences. In reality, any imperfections in the $M \cos \chi$ removal procedure may introduce additional undesired periodicities into the data string, and the possible adverse effects of this first step are presented in following sections.

Reference 2 discusses various methods of measuring the magnitude of M and $\cos \chi$ effects on Omega phase data. M is found to be sunspot-dependent according to equation (E2) and possibly seasonally dependent with a peak variation of 10%. Limits of effectiveness of $\cos \chi$ application are investigated and categorized as to whether the path average or end-point $\cos \chi$'s meet certain minimum acceptable criteria. Time delays between the solar forcing function and the observed phase changes also are investigated. To simplify the analysis of the data chosen for the present study, we wish to assume that the foregoing dependencies result in effects which are either (1) small enough to be considered insignificant, or (2) of the same period as the solar tidal phenomena. Although the separation of solar flux and tidal effects may be inherently impossible and probably unnecessary in this type of study, a detailed investigation of the possible residual periodicities after application of the approximate diurnal theory will show whether periodicities subsequently deduced are due to the approximations, to numerical uncertainties within an inherently correct diurnal theory, or to additional phenomena. The possible error contributions of the various dependencies are discussed below.

SOLAR ZENITH ANGLE DEPENDENCE

As mentioned above, equation (E1) represents a simplified daytime forcing function assumed to exist in the neighborhood of midpath noon. In addition to the near-noon restriction, the validity of the expression is also restricted by the range of the path average of $\cos \chi$. Empirical studies have

shown that the variation in observed phase begins to depart markedly from the path-average $\cos \chi$ when χ is large (or $\overline{\cos \chi}$ less than 0.3 or 0.5). For the Hawaii-New York path, $\cos \chi$ in the neighborhood of midpath noon is less than 0.5 for about 90 days during the winter season. This implies even lower (about 0.3) values of $\cos \chi$ at one of the end points, for which the theory is only marginally applicable. The prediction of the expected error between theory and observation in these regions is complex and will depend upon the number of path increments which do not meet the $\cos \chi > 0.5$ criterion and also upon their combined effects in $\overline{\cos \chi}$. Regardless of the magnitude of the effect, the error introduced will have an annual period and probably will be distorted so that additional harmonics of 1 year may appear. No similar error is expected on the Trinidad-New York path, as $\overline{\cos \chi}$ remains above the limiting level all year over this relatively short, north-south link.

DIURNAL CURVATURE DEPENDENCE

SUNSPOT VARIATION

Reference 2 gives equation (E2) for the sunspot number dependence of M . The sunspot number has its own periodic variation which, for the period 1966 through 1970, has been assumed to be of the quadratic form given by:

$$SSN_i = Ad_i^2 + Bd_i + C \quad (E4)$$

where d_i is the day number starting with 1 January 1966 = 1. The coefficients A, B, and C were obtained by a least-squares fit of the observed SSN to equation (E4) and yielded the relation:

$$SSN_i = -0.52 \times 10^{-4} d_i^2 + 0.1374 d_i + 18.9. \quad (E5)$$

Substituting (E5) into (E2) gives:

$$M = 0.240 - 2.6 \times 10^{-8} d_i^2 + 0.687 \times 10^{-4} d_i. \quad (E6)$$

Equation (E6) has been used to compute M for each day in the data string being analyzed and is intended to represent the variation in diurnal curvature produced by the mean variation in solar activity over the period being studied. The variation in sunspot number is assumed to be an adequate indicator of both the phase and amplitude of the general solar activity variation. Although large deviations from the mean activity did occur during some months of the highly active years of 1969 and 1970, the resulting deviations of the 'true' M from the 'smoothed' M should be random and contribute only to the noise in the data string.

If these predicted curvature effects were in error, the sunspot cycle variation period modulated by an annual period will be induced into the data series. A sunspot cycle variation can arise through diurnal relations from the change of M from 0.24 to 0.28 over the 5-year period being studied and the annual period from the variation in $\cos \chi$ over the seasons. For a path exhibiting a diurnal of 100 cec, the peak sunspot cycle variation would be about 0.4

cec in summer, when $\cos \chi$ is 0.9, and about 2 cec in winter, when $\cos \chi$ is only 0.5. The average summer and winter-peak variations are then 0.2 and 1 cec, respectively, leading to an overall average peak variation of 0.6 cec at the sunspot cycle period. The average annual variation is 0.32 cec. The peak periodic effects induced into the 5-year data string are then about 0.3 and 0.2 cec at the sunspot cycle and annual periods, respectively. The above results are indicative of the Hawaii-New York path; the Trinidad-New York path would show less than one half of these effects, or less than 0.1 cec at each period, due to the interrelationship between sunspot activity and diurnal theory.

SEASONAL VARIATION

Annual periodicities also can be introduced through incorrect modeling of the nominal zenith angle dependence. As noted earlier, M is believed accurate to about 10% with respect to possible variations between paths or seasonal variations. For a path of 100-cec diurnal phase change and for $\overline{\cos \chi} = 0.5$, a 10% uncertainty in M yields a 1.5-cec uncertainty in phase. Since $\overline{\cos \chi} > 0.5$ only during the winter, a potential error of 10% in M would appear as an annual period of amplitude about 0.75 cec. A variation of such magnitude is not easily distinguished from annual periodicities arising from other causes such as annual tidal effects or ionospheric variations due to galactic energy.

TIME DELAY DEPENDENCE

It has been shown (ref. 2) that the effective reflection height for Omega frequencies reaches a minimum about 1/8 hour after the calculated maximum in incident solar flux for paths which are nearly normally illuminated. Over paths for which $\overline{\cos \chi} > 0.5$, the maximum lag is assumed to be about 1/4 hour. Figure E1 depicts this effective difference between the observed phase response $\phi(t)$ and the forcing function $\phi'(t)$.

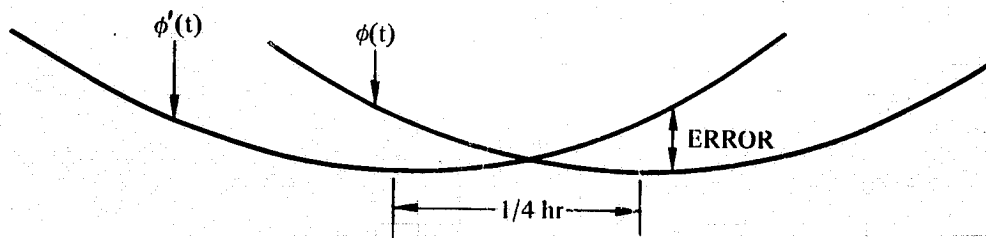


Figure E1. Time delay of $\phi(t)$ from $\phi'(t)$.

Comparison of the forcing function approximation computed for time t with data taken at time t will result in a discrepancy proportional to the change in $\cos \chi$ over a 1/4-hour interval and to the normal diurnal range observed. For the Hawaii-New York path, the maximum hourly change of

$\cos \chi$ in the neighborhood of noon is about 0.05. The maximum change over 1/4 hour is then about 0.012. For an M of about 0.3, the maximum range in $M \cos \chi$ will be about 0.004. As this path normally experiences a diurnal change of about 100 cec, the expected peak error in phase prediction is then about 0.4 cec. As this error at any particular hour near noon will always be of the same sign and appears to have an annual variation, the resultant residual periodicity, ± 0.2 cec, should be small and included in the annual period being searched. Hence, near noon, the elaborate recursive formulation normally used in diurnal theory is not required in the calculations to follow as the periodicities in observed phase due to zenith angle variations are nearly proportional to the variation of zenith angle itself.

REMOVAL OF SOLAR FLUX EFFECTS

Previous sections have indicated the possible contributions of various aspects of the simplified prediction model to annual and sunspot-cycle periodicities in the data series. If these contributions were to add in phase, the peak contamination in annual and sunspot variations over the Trinidad-New York path would be about 0.4 and 0.1 cec, respectively. The corresponding values for the Hawaii-New York path are about 1.2 and 0.3 cec, respectively, plus whatever allowance may be necessary because of possible departure from the region of phase proportionality to $\cos \chi$ in winter. The annual effect due to the $\cos \chi$ along path in the winter months would be least near noon and greater an hour or so removed from noon. If numeric results from various hours are similar, presumably significant departure from the region of phase proportionality has not occurred.

The nighttime data have not been adjusted for any solar or galactic effects, so that no additional periodic components are assumed to have been introduced into the 5-year series. Although galactic X rays are known to be partially responsible for the existence of the nighttime ionosphere, no periodic effects have been modeled in this study. In addition, the effects of specific X-ray sources have been neglected as being unimportant at Omega frequencies.³

The end result of the preceding analysis is that the periodicities introduced into the data by imperfections in the simplified model will be either (1) small or (2) of the same period or harmonic as the solar declination or sunspot cycle. In particular, periodicities greater than 0.4 cec on the Trinidad-New York path must be due to phenomena not presently modeled.

Removal of all solar flux-induced effects could be obtained by regressing a raw data string against all significant solar periods and their harmonics. The simplified prediction model, or $M \cos \chi$ removal approach, has been used to demonstrate the realizable reduction in variance possible from the present propagation prediction theory at Omega frequencies. The existence of significant residual amplitudes at the solar periods may indicate either the degree of lack of fit of the simplified diurnal theory or the presence of tidal effects. Following sections discuss possible approaches to developing a simplified theory for tidal periodicities to be expected in Omega data.

PERIODIC TIDAL INFLUENCES

To remove lunar variations from the data series being used to determine the ultimate timing capability of Omega, it is desirable to obtain suggested forms of periodic variations, including phase and amplitude changes, so as to be able to construct an appropriate filter. Noonkester has studied lunar tidal variations in Omega data using a traditional analysis of superimposing data from various years into 2-month blocks.¹ Periodic components investigated were those previously found in geophysical data and included variations at both the full and semilunar synodical periods. However, the phase and amplitude of the effects were found to vary between the various 2-month blocks studied; that is, phase and amplitude of the components varied throughout the year. The following analysis attempts to obtain possible morphologies for these effects. This approach differs from that of Noonkester, who placed primary reliance upon empirical observation. The purpose of the analysis is not the development of precise expressions but rather the investigation of possible linkages of phenomenology which could lead to simple expressions for the seasonal variations of lunar dependencies as determined by Noonkester. Proper modeling of these variations is required for a long-term periodic analysis if the results are to yield meaningful discrete components. If the response of the atmosphere to tide-raising potentials were assumed to be similar to that of the oceans, then standard tidal theory could be applied. If the significantly different compressibility of air from that of water is considered, however, a type of gravitational compression theory might be more applicable.

In practice neither of the foregoing simplistic notions is directly applicable. Ionospheric tidal theory is a specialized technical area of considerable sophistication. Magnetic field constraints on the motion of the ionosphere have been applied in the development of an electrodynamic theory of motion. Seasonal variations in ionospheric chemistry have been recognized. The effect of complexities was largely circumvented in Noonkester's approach. However, the present requirement for processing a long data series with significant discontinuities precludes both the approach used by Noonkester and spectral analysis. Hence, the present approach will be to identify a large discrete set of possible periodicities corresponding to different phenomenologies and then determine the components statistically. It is hoped that the observed periodicities will be completely specified by the periods of the phenomena responsible, even though the phasing may be arbitrarily related and the amplitude determined experimentally. The desired completeness will occur if the earth can be approximated as a first-order differential system. If significant second- or higher-order effects such as severe chemical changes occur, then modulations or harmonics of the driving periodicities may be induced and could appear, for example, as seasonal modifications. Noonkester's approach minimized the effects of complexities; the analysis to follow will necessarily smooth periodicities over the duration of the analysis and hence may underestimate peak effects if second-order effects are present.

Based on Noonkester's results, an appropriate approach seems to be to develop an oversimplified theory of the periodic forcing functions involved and then to perform a regression analysis on the data string to obtain the relevant parameters of the expected discrete frequencies. It will be assumed that these forcing functions are related to either the incident flux or

gravitational force of solar, lunar, or stellar sources and that periodicities of interest are proportional to the variation in zenith angle of the relevant source. Following sections consider the determination of astronomical zenith angle variations.

ASTRONOMICAL CONSIDERATIONS

If the earth were to rotate on an axis directly perpendicular to its plane of revolution around the sun (the ecliptic) and the moon were to revolve at constant radius about the earth in this same plane formed by the earth's equator and the ecliptic, the maximum tidal effects always would be expected near* the time of linear alignment of the three bodies; that is, the occurrence of a new or full moon. The lunar influence on the tidal amplitude would be identical in each synodical cycle (new moon to new moon) and be of sinusoidal form of period 29.53 days. If new- and full-moon effects are assumed comparable, however, the observed period is one half the above, or 14.76 days, with possible amplitude modulation at the 29.53-day period. This is essentially the case investigated by Noonkester. In reality, the earth's axis of rotation and the moon's plane of revolution are inclined to the ecliptic by approximately $23\frac{1}{2}^{\circ}$ and 5° , respectively, so the expected lunar tidal influences are no longer simple. There results a sinusoidally varying lunar declination of $\pm 28\frac{1}{2}^{\circ}$ relative to the earth's equator, which repeats at intervals of 27.32 days. The difference in period between the declination and synodical cycles results in a sinusoidally varying elevation for successive full or new moons in the sky over a year's time. For the time period 1966-70, full moons coincide with maximum declination (north) in winter and with minimum declination (south) in summer. New moons behave in exactly opposite manner. There is also the change in the orbital distance of the moon due to the ellipticity of its orbit. The time from perigee to perigee is 27.55 days, or the anomalistic month.

Since the relative ocean tidal effects of the lunar hour angle, declination, and orbital distance are known to vary with earth latitude, ionospheric data acquired over large latitude ranges may exhibit any or all of these effects. If, as a first approximation, the lunar orbital eccentricity is neglected, the resultant of the hour-angle and declination variations can be expected to exhibit the 'beating' phenomenon associated with two closely spaced frequencies. Due to purely geometrical considerations, the beat between the lunar hour angle and declinational periods is exactly 1 solar year, so the resulting tidal effect should demonstrate both an amplitude and a phase variation at this period. This is approximately what was found by Noonkester; that is, amplitude and phase variations with annual and semiannual periods, which are expected if both new- and full-moon effects are present.

Further understanding of expected tidal effects may be developed by reference to 'standard' tidal theory, which assumes the total tidal effect to be composed of a summation of periodic components — each due to a separate 'moon' or 'sun' exhibiting only one aspect of the respective body's motion. In that theory, emphasis is placed on the diurnal and semidiurnal variations of tides, and little is said about the longer-term variations which are of major interest in the present study. Since the Omega data being used are sampled

*Probably with some unavoidable time delay.

at 24-hour intervals, periodicities less than 2×24 , or 48 hours, cannot be found directly. However, the 'beat' frequency between the sampling rate and the short-term phenomena can be found. As the lunar and solar declinational and orbital eccentricity periods are much longer than 48 hours, these variations may be found directly and, therefore, need not be of any concern. The lunar hour angle, however, repeats at intervals of 24.8412 hours, so the beat with 24 hours is 29.53 days, or the synodical period, as previously discussed. Therefore, if one can show that the aforementioned periods should be found in the data, the 24-hour sampling rate will permit their determination successfully.

ZENITH ANGLE GEOMETRY

Irrespective of which tidal theory is found to apply to the D-region, the assumption is made that the observed effects will be some function of the zenith angle, χ , of the celestial body relative to a point on earth. The zenith angle may be defined as:

$$\cos \chi(t) = \cos \phi \cos \delta(t) \cos h(t) + \sin \phi \sin \delta(t) \quad (E7)$$

where: ϕ = geographic latitude of the observing point
 $\delta(t)$ = time-varying declination of the celestial body relative to the earth's equator
 $h(t)$ = time-varying hour angle of the celestial body relative to the meridian of the observing point

The form of (E7) is similar to that found in modulation processes wherein the multiplication of the various trigonometric functions gives rise to sum and difference frequencies corresponding to side bands and modulation envelopes. In the general case, both amplitude and phase modulation will be present. It is the existence of these apparent modulations, as found by Noonkester, which necessitates the application of a more elaborate theory than assumed by him. The basis of the elaboration will be the determination of the periodicities expected from the temporal and spatial variations of the $\cos \chi$ function.

As the effects exhibited by ionospheric data will be a function of path length, the path average of $\cos \chi$ normally is considered a better measure of these effects than $\cos \chi$ at any one point, such as the midpoint. However, for purposes of the analysis in this section we are interested primarily in the periods and not the amplitudes of the effects, so $\cos \chi$ at midpath (or any arbitrary point) should indicate all the possible periods of interest. The path average of $\cos \chi$ is expected to contain no more but possibly fewer periods than that at a point.

For any arbitrary point and time on path, equation (E7) can be written as:

$$\cos \chi = K_1 \cos \delta \cos h + K_2 \sin \delta \quad (E8)$$

where: $K_1 = \cos \phi$ and $K_2 = \sin \phi = \sqrt{1 - K_1^2}$.

Expansion yields:

$$\cos \chi = \frac{K_1}{2} [\cos(\delta + h) + \cos(\delta - h)] + K_2 \sin \delta, \quad (E9)$$

so the periodicities expected are those contained in the variation of $(\delta + h)$, $(\delta - h)$, and δ , where δ and h are generally sinusoidal functions of time.

Equation (E9) applies to lunar, stellar, or solar zenith angles. For data sampled at 24-hour intervals, the solar hour angle, h_s , is constant to within ± 20 minutes all year (equation of time variation), so the solar contribution is simply:

$$\cos \chi_s \approx A_m \cos(\delta_s \mp \theta_{O,S})$$

where:

$$A_m = \sqrt{\cos^2 h \cos^2 \phi + \sin^2 \phi}$$

$$\theta_{O,S} = \tan^{-1} (\tan \phi / \cos h)$$

$$\delta_s = \Delta_s \cos \left[\frac{2\pi t}{T_s} + \theta_s \right]$$

Δ_s = peak value of solar declination (23.5°)

T_s = period of earth's revolution

θ_s = arbitrary phase angle dependent on time reference

so

$$\cos \chi_s = A_m \cos \left[\Delta_s \cos \left(\frac{2\pi t}{T_s} + \theta_s \right) - \theta_{O,S} \right]$$

Thus, periodicities in $\cos \chi_s$ are given by a sinusoidal function and two phase terms where one, $\theta_{O,S}$, is dependent on location and the time of sampling as reflected in the latitude and hour angle and the second, θ_s , related to the arbitrary origin of the time scale. Disregarding the phase term related to the arbitrary origin of the time scale, θ_s , and expanding:

$$\begin{aligned} \cos \chi_s &= A_m \cos \left[\Delta_s \cos \frac{2\pi t}{T_s} - \theta_{O,S} \right] \\ &= A_m \cos \theta_{O,S} \cos \left[\Delta_s \cos \frac{2\pi t}{T_s} \right] + A_m \sin \theta_{O,S} \sin \left[\Delta_s \cos \frac{2\pi t}{T_s} \right] \\ &= A_m \cos \theta_{O,S} \left(1 - \frac{\Delta_s^2}{2!} \cos^2 \frac{2\pi t}{T_s} + \dots \right) \\ &\quad + A_m \sin \theta_{O,S} \left(\Delta_s \cos \frac{2\pi t}{T_s} - \frac{\Delta_s^3}{3!} \cos^3 \frac{2\pi t}{T_s} + \dots \right); \end{aligned}$$

$$\begin{aligned} \cos \chi_s = & A_m \cos \theta_{O,S} \left(\left(1 - \frac{\Delta_s^2}{4} \right) - \frac{\Delta_s^2}{4} \cos 2 \cdot \frac{2\pi t}{T_s} + \dots \right) \\ & + A_m \sin \theta_{O,S} \left(\left(\Delta_s - \frac{3\Delta_s^3}{4 \cdot 3!} \right) \cos \frac{2\pi t}{T_s} - \frac{\Delta_s^3}{4 \cdot 3!} \cos 3 \cdot \frac{2\pi t}{T_s} + \dots \right); \end{aligned}$$

for $\Delta_s = 23.5^\circ$,

$$\begin{aligned} \cos \chi_s = & A_m \cos \theta_{O,S} \left(0.96 - 0.04 \cos 2 \cdot \frac{2\pi t}{T} + \dots \right) \\ & + A_m \sin \theta_{O,S} \left(0.40 \cos \frac{2\pi t}{T_s} - 0.003 \cos 3 \cdot \frac{2\pi t}{T_s} + \dots \right). \end{aligned}$$

Thus, it is seen that the periodicities in $\cos \chi_s$ are those from the earth's revolutionary period T_s , the semiperiod, and higher harmonics of the revolutionary frequency. Variations at the revolutionary period and semiperiod are not simply related. At 45° latitude, the amplitude at the full revolutionary period will be at least 10 times that at the semiperiod. However, at the equator, the periodicity at the revolutionary period will vanish and terms in the semiperiod will dominate. With the data being analyzed at present, the semiperiod amplitude will be less than one fifth that associated with the full solar period.

The foregoing indicates that a process dependent on $\cos \chi_s$ will operate on a measurable so as to produce not only a periodicity at the period of the earth's revolution but also effects at the semiperiod and other harmonics of the revolutionary frequency. The induced periodicities will be in addition to any intrinsically arising from phenomenology directly associated with the second or higher harmonics of the revolutionary frequency. In practice, for the data to be investigated, the induced periodicities are expected to be much less than those from phenomena directly related to the semiperiod, as can be verified by comparing resultant amplitudes at semiperiods with those obtained at full periods. Harmonic contamination will be further reduced in the present analysis through removal of known zenith angle dependencies directly by computation based on exact zenith-angle expressions.

The lunar contribution is given by:

$$\cos \chi_m = \frac{K_1}{2} [\cos (\delta_M + h_M) + \cos (\delta_M - h_M)] + K_2 \sin \delta_M$$

where:

$$\delta_M = \Delta_M \cos \left(\frac{2\pi t}{T_M} + \theta_M \right)$$

$$h_M = \left(\frac{2\pi t}{T_H} + \theta_H \right)$$

Δ_M = peak value of lunar declination (28°)

T_M = period of lunar declination

T_H = period of lunar hour angle

θ_M, θ_H = arbitrary phase angles

The major periodicities of the lunar zenith angle are thus the period of lunar revolution, $T_M = 27.3216$ days, and the periods of upper and lower side bands formed by the sampling angle, h_M , which are the synodic period (upper) of 29.5306 days and a lower period of 25.4201 days.

Because of the sampling at constant solar time, it is self-evident that stellar zenith angles repeat with a period of 1 year.

EXPECTED PERIODICITIES

The foregoing indicates several periodicities to be expected in zenith angle dependencies which may affect the Omega measurements. Several mechanisms of interaction are possible. If direct radiation is important, such as might be true for galactic sources at night, then effects should be nominally proportional to the associated zenith angle. This proportionality might also be applicable if the vertical component of gravitational force is directly significant, as might be true if compressional effects are considered. In normal tidal theory, however, changes occur due to differences in the potential function at various points on the earth. In this case, we can show tidal effects to be proportional to $\cos^2 \chi$ after working out the equations for the force imbalances and noting a direct cancellation of first-order effects due to associated centripetal forces. From equation (E8), we have:

$$\cos^2 \chi = (K_1 \cos \delta \cos h + K_2 \sin \delta)^2.$$

Expansion yields:

$$\begin{aligned} \cos^2 \chi &= (K_1^2 \cos^2 \delta \cos^2 h) + (K_2^2 \sin^2 \delta) \\ &\quad + (2K_1 K_2 \cos \delta \cos h \sin \delta) \\ \cos^2 \chi &= \frac{K_1^2}{4} \left[1 + \cos 2\delta + \cos 2h + \frac{1}{2} \cos 2(\delta + h) + \frac{1}{2} \cos(\delta - h) \right] \\ &\quad + \frac{K_2^2}{4} [1 - \cos 2\delta] \\ &\quad + \frac{K_1 K_2}{2} [\sin(2\delta + h) + \sin(2\delta - h)] \end{aligned} \quad (E10)$$

Expansion of the sin and cos functions will yield results similar to those above for $\cos \chi$; that is, a series of fundamental and harmonic terms. The lunar contribution will result from variations in both δ_M and h_M so that all indicated periodicities will be present. The solar contribution is simplified by the near constancy of h_s , so that the only remaining source of periodic variation is $2\delta_s$ or the semiannual period $T_s/2$.

Table E1 presents the various components found in the foregoing analysis of zenith angle and classifies them as to whether they are 'true' periodicities or modulation products.

TABLE E1. EXPECTED TIDAL PERIODICITIES.

Function	True Periods, days		"Modulation Products," days	
cos χ	$\delta_s, (T_s)$	365.2422	$\delta_{M-h_M}, (T_s)$	365.2422
	$\delta_M, (T_M)$	27.3216	$\delta_{M+h_M}, (T_t)$	14.1916
cos ² χ	$2\delta_s, (T_s/2)$	182.6211	$2(\delta_{M-h_M}), (T_s/2)$	182.6211
	$2\delta_M, (T_M/2)$	13.6608		
	$2h_M, (T_H/2)$	14.7653	$2(\delta_{M+h_M}), (T_t/2)$	7.0958
			$2\delta_{M-h_M}$	25.4201
			$2\delta_{M+h_M}$	9.3401

Other periodicities of potential importance include the 11-year solar cycle and periods arising from orbital eccentricity.

The ocean tide-raising potentials of the sun and moon are known to vary with orbital distance. If atmospheric tides are correspondingly affected, an analysis of the expected periodic variations of these distances is required.

Assume that the orbits of the earth and moon are ellipses about the sun and earth respectively, with radius vectors given by

$$r(t) = \frac{a(1 - e)^2}{1 + e \cos \theta} = \frac{R}{1 + e \cos \theta}$$

where a is the semimajor axis, e the eccentricity, and θ the angle of revolution, which is related to the period of revolution by $\theta = 2\pi t/T_r$ (fig. E2).

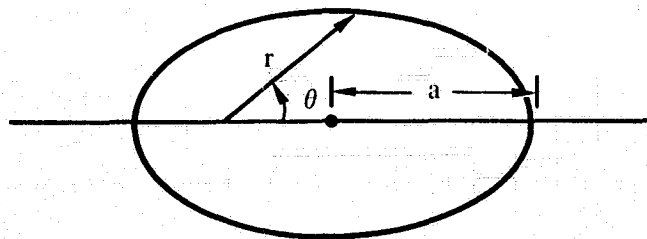


Figure E2. Elliptic Orbit.

Depending on the model assumed, we may consider gravitational forces or differences varying as $(1/r)^2$ or $(1/r)^3$. For an inverse square-law model:

$$F_T \propto \frac{1}{r^2(t)} = \frac{\left(1 + e \cos \frac{2\pi t}{T_r}\right)}{R^2} = \frac{1}{R^2} \left(1 + 2e \cos \frac{2\pi t}{T_r} + e^2 \cos^2 \frac{2\pi t}{T_r}\right)$$

As the eccentricities of the earth and lunar orbits are only 0.016 and 0.055, respectively, e may be considered small enough to neglect the second-order effect and leave:

$$F_T \propto \frac{1}{r^2(t)} \approx \frac{1}{R^2} \left(1 + 2e \cos \frac{2\pi t}{T_r}\right).$$

The earth's eccentricity then will contribute a peak variation of approximately 3% about the mean force. As the solar distance and declination have the same period and phasing ($T_r = T_s$), the earth's orbital variation will not contribute any additional periodicities to those already determined. The lunar eccentricity will contribute a peak variation of approximately 11% about the mean force but at a period which differs from that of the lunar declination by a significant amount. This difference results from the slow precession of the axis of the lunar orbit with respect to the fixed stars. The period of the precession is 8.85 years, which is also the beat period between the lunar declination and the time between lunar perigees, or the anomalistic month (27.55 days). This can be further visualized by noting that, since there are 13.4 lunar revolutions per solar year and approximately 0.23-day phase slippage of perigee from maximum declination per revolution, it will take 8.85 years for this slippage to add up to a full lunar revolution of 27.32 days. Ionospheric data exhibiting this long-term modulation can be assumed to be experiencing the effects of the lunar orbital variation.

Standard tidal theory states that the expected tidal effects should vary as $1/r^3$, or

$$\frac{1}{r^3(t)} = \frac{1}{R^3} \left(1 + 3e \cos \frac{2\pi t}{T_r}\right)$$

wherein the higher-order terms have been neglected due to e 's being small. The variable solar gravitational contribution is now about 5% of the steady value at the declination period, so it need not be considered further. The lunar contribution will be, approximately, 16% about the mean and at the period of the anomalistic month.

It is assumed that the percentage variation in the lunar orbit is significant enough to warrant inclusion in the periodicities to be searched for in the data series.

PERIODIC ANALYSIS

To determine the extent of solar and lunar periodicities in the Omega data, an analysis of several data strings versus expected periods was performed. To eliminate the effects of possible synchronization errors at the transmitting stations, the data used were one half of the round-trip propagation phase, as developed by adding the observed phase difference from each end of a reciprocal path

$$\frac{\phi_{RT}}{2} = \frac{1}{2} [(\phi_x - \phi_y + h_{xy})_y + (\phi_y - \phi_x + h_{yx})_x]$$

where the parenthetical terms represent the observed phase differences at the y and x ends of the path, respectively, and

- ϕ_x = phase of station x
- ϕ_y = phase of station y,
- h_{xy} = path phase delay from x to y
- h_{yx} = path phase delay from y to x

Simplifying, we have

$$\frac{\phi_{RT}}{2} = \frac{1}{2} (h_{xy} + h_{yx}).$$

It is the periodic variation of $\phi_{RT}/2$ which is of interest in this study.

Two distinctly different propagation paths were used in the analysis: Hawaii to New York (and return) and Trinidad to New York (and return). Both nighttime and daytime propagation were investigated. Groups of 3 hours centered about midpath noon and midnight were chosen to determine the confidence in the results and also to permit analysis of correlation between consecutive hours. The data strings were each of 5-year length, running from March 1966 to March 1971. Both 10.2- and 13.6-kHz data were analyzed. The total number of strings involved was 24. Periodicities to be investigated were developed in the previous section and are summarized in table E2.

TABLE E2. POSSIBLE PERIODICITIES IN OMEGA DATA.

Periods, days

365.2422
 182.6211
 29.5306
 27.5546
 27.3216
 25.4201
 14.7653
 14.1916
 13.7773
 13.6608
 4000.0000 (approx.)

The data strings were assumed to be of the form:

$$\phi(t) = \bar{\phi} + \sum R_i \cos\left(\frac{2\pi t}{T_i} + \theta_i\right) \quad (E11)$$

- where: $\bar{\phi}$ = average phase (round trip)
 T_i = period of observed propagation variation
 R_i = amplitude of observed propagation variation
 θ = arbitrary phase angle of propagation variation

Equation (E11) can be written as:

$$\phi(t) = \bar{\phi} + \sum \left[A_i \cos\left(\frac{2\pi t}{T_i}\right) + B_i \sin\left(\frac{2\pi t}{T_i}\right) \right] \quad (E12)$$

where the interrelationship of the variables is given by:

$$R_i = \sqrt{A_i^2 + B_i^2} \quad \theta_i = \tan^{-1}\left(\frac{B_i}{A_i}\right)$$

It is assumed that the data are expressible in the form of equation (E12) plus random variations. A method of solution is desired which will determine the amplitudes and other statistics for the periodicities given in table E2. It is apparent that the data string is too short for proper application of a normal series analysis, especially when the 4000-day period is considered. However, the periods are sufficiently different that they may be considered independently, except for the 27.32- and 27.55-day periods and their semiperiods, which have beats comparable with the sample duration. When a beat period is comparable with the

sample duration, it is possible to approximate either fundamental period by proper fit and phasing of the adjacent fundamental period. If the two periodicities are determined independently, both estimates will be separately the best approximation to the actual variations in the data if attributed to the respective periods. In this sense, the resultant solutions are each optimum but need not represent optimum partitioning of the periods. Indeed, it is incorrect to use both when computing a reduction in variance, since both tend to approximate the same fluctuations. The approach has thus been to treat the periodicities as independent but to note possible interrelationships in the results.

Periodicities can be determined even if the period in question is longer than the 5-year data sample if a simple regression analysis is used rather than the traditional solution. This is especially important in treating the 4000-day period taken to represent either the 11-year solar cycle or the lunar precessional period of 8.85 years. (The amplitudes would be indistinguishable between the two assumed periods for the 5-year sample being considered.)

From the foregoing, we assume the sampled phase on any given day to be given by

$$\left[\phi_j = \bar{\phi} + A \cos \frac{2\pi t_j}{T} + B \sin \frac{2\pi t_j}{T} + \epsilon_j \right]_i \quad (\text{E13})$$

where $\bar{\phi}$ is the average phase, A and B are amplitudes to be determined, T is the period, t_j is a time index, i is the component index, and ϵ_j is the discrepancy between the actual observation and the assumed periodic dependence due to random variations and the effects of other periodicities. The solution of equation (E13) for optimum A and B is:

$$\begin{pmatrix} A \\ B \end{pmatrix}_i = \begin{pmatrix} \sum_j \cos^2 \frac{2\pi t_j}{T} & - \sum_j \cos \frac{2\pi t_j}{T} \sin \frac{2\pi t_j}{T} \\ \sum_j \cos \frac{2\pi t_j}{T} \sin \frac{2\pi t_j}{T} & \sum_j \sin^2 \frac{2\pi t_j}{T} \end{pmatrix}^{-1} \begin{pmatrix} \sum_j (\phi_i - \bar{\phi}) \cos \frac{2\pi t_j}{T} \\ \sum_j (\phi_i - \bar{\phi}) \sin \frac{2\pi t_j}{T} \end{pmatrix}_i \quad (\text{E14})$$

Equation (E14) was employed sequentially to deduce the coefficients for all periodicities. It differs from the traditional solution only in the off-diagonal elements in the square matrix. Traditionally, a large number of periods are available; hence, the average value of $\cos 2\pi t_j/T \sin 2\pi t_j/T$ tends to zero and the square matrix becomes orthogonal, so the inverse is given simply by the reciprocals of the respective diagonal elements. The regression was performed on day and night data strings with all recognized disturbances removed and on daytime data with the expected $M \cos \chi$ variation removed. The analysis also determined the following: the variance of the initial data string, V; the reduction in variance produced by the periodic component R_i

$$RV_i = \frac{R_i^2}{2V};$$

the t statistic for linear regression coefficients used to determine confidence in the component R_i

$$t_i = \frac{R_i (N - 1)^{1/2}}{(2V - R_i^2)^{1/2}};$$

and the variance explained by the component R_i

$$EV_i = (RV_i)V.$$

RESULTS

The results of the analysis are summarized in tables E3 and E4, which give the amplitudes (R_i) of the components at specific periods (T_i). Figures E3 through E6 give the t values for confidence of these same components.

For the Trinidad-New York path, the observed amplitudes exceed the uncertainties produced by the solar flux removal technique, so that solar tidal effects are indicated during the daytime, and either solar tidal or galactic flux sources at night. The Hawaii-New York path also indicates solar tidal influences during daytime, and night effects similar to the Trinidad path.

As noted earlier, results for the 27.32- and 27.55-day periods and associated half periods may be coupled. The results indicate that significant components exist at the annual, semiannual, and solar cycle periods, with significant but still small components at some lunar periods at night.

TABLE E3. PERIODIC AMPLITUDES FROM REGRESSION ANALYSIS
(INCLUDING M COS χ REMOVAL FOR DAYTIME) FOR HAWAII-NEW YORK ROUND TRIP.

A. DAYTIME		R, cec					
T _p , days	1900		2000		2100		
	10.2 kHz	13.6 kHz	10.2 kHz	13.6 kHz	10.2 kHz	13.6 kHz	
365.2422	2.55	2.71	2.14	2.86	2.19	2.73	
182.6211	2.71	1.86	2.54	1.80	2.79	1.98	
29.5306	0.30	0.33	0.33	0.33	0.27	0.13	
27.5546	0.09	0.25	0.19	0.28	0.16	0.32	
27.3216	0.32	0.20	0.24	0.14	0.33	0.22	
25.4201	0.23	0.17	0.26	0.07	0.15	0.21	
14.7653	0.10	0.05	0.27	0.20	0.17	0.20	
14.1916	0.06	0.09	0.16	0.18	0.22	0.05	
13.7773	0.32	0.29	0.20	0.21	0.16	0.11	
13.6608	0.17	0.20	0.28	0.10	0.54	0.11	
4000.0000	0.37	0.45	0.37	0.35	0.56	0.53	

B. NIGHTTIME		R, cec					
T _p , days	0700		0800		0900		
	10.2 kHz	13.6 kHz	10.2 kHz	13.6 kHz	10.2 kHz	13.6 kHz	
365.2422	0.55	0.64	0.56	0.43	0.98	1.11	
182.6211	1.75	2.04	1.78	1.83	2.17	2.12	
29.5306	0.21	0.17	0.28	0.19	0.29	0.16	
27.5546	0.54	0.59	0.38	0.48	0.50	0.45	
27.3216	0.67	0.72	0.63	0.61	0.82	0.74	
25.4201	0.54	0.44	0.60	0.36	0.69	0.50	
14.7653	0.25	0.11	0.20	0.14	0.13	0.14	
14.1916	0.25	0.21	0.25	0.29	0.52	0.40	
13.7773	0.19	0.24	0.17	0.18	0.14	0.08	
13.6608	0.42	0.47	0.40	0.41	0.49	0.38	
4000.0000	1.59	1.06	1.84	1.29	1.96	1.37	

TABLE E4. PERIODIC AMPLITUDES FROM REGRESSION ANALYSIS
(INCLUDING M COS χ REMOVAL FOR DAYTIME) FOR TRINIDAD-NEW YORK ROUND TRIP.

A. DAYTIME		R, cec					
T _p , days	1600		1700		1800		
	10.2 kHz	13.6 kHz	10.2 kHz	13.6 kHz	10.2 kHz	13.6 kHz	
365.2422	0.68	1.28	0.79	1.40	0.81	1.38	
182.6211	0.06	0.14	0.14	0.13	0.23	0.06	
29.5306	0.10	0.09	0.15	0.12	0.09	0.03	
27.5546	0.24	0.21	0.25	0.19	0.23	0.14	
27.3216	0.22	0.07	0.19	0.05	0.22	0.08	
25.4201	0.05	0.10	0.04	0.13	0.07	0.05	
14.7653	0.16	0.13	0.11	0.08	0.07	0.07	
14.1916	0.13	0.12	0.18	0.14	0.25	0.08	
13.7773	0.07	0.11	0.09	0.09	0.04	0.08	
13.6608	0.13	0.09	0.17	0.07	0.16	0.08	
4000.0000	1.01	1.29	1.03	1.09	1.02	1.02	

B. NIGHTTIME		R, cec					
T _p , days	0400		0500		0600		
	10.2 kHz	13.6 kHz	10.2 kHz	13.6 kHz	10.2 kHz	13.6 kHz	
365.2422	1.02	2.13	0.73	1.92	0.71	1.79	
182.6211	1.34	1.79	1.40	1.93	1.46	1.87	
29.5306	0.34	0.14	0.32	0.22	0.37	0.24	
27.5546	0.09	0.23	0.04	0.16	0.11	0.23	
27.3216	0.37	0.40	0.29	0.33	0.30	0.37	
25.4201	0.19	0.31	0.30	0.39	0.25	0.32	
14.7653	0.10	0.06	0.21	0.09	0.21	0.06	
14.1916	0.10	0.04	0.02	0.06	0.03	0.11	
13.7773	0.04	0.09	0.02	0.09	0.14	0.11	
13.6608	0.26	0.34	0.32	0.38	0.28	0.36	
4000.0000	2.08	0.74	2.00	0.72	2.07	0.71	

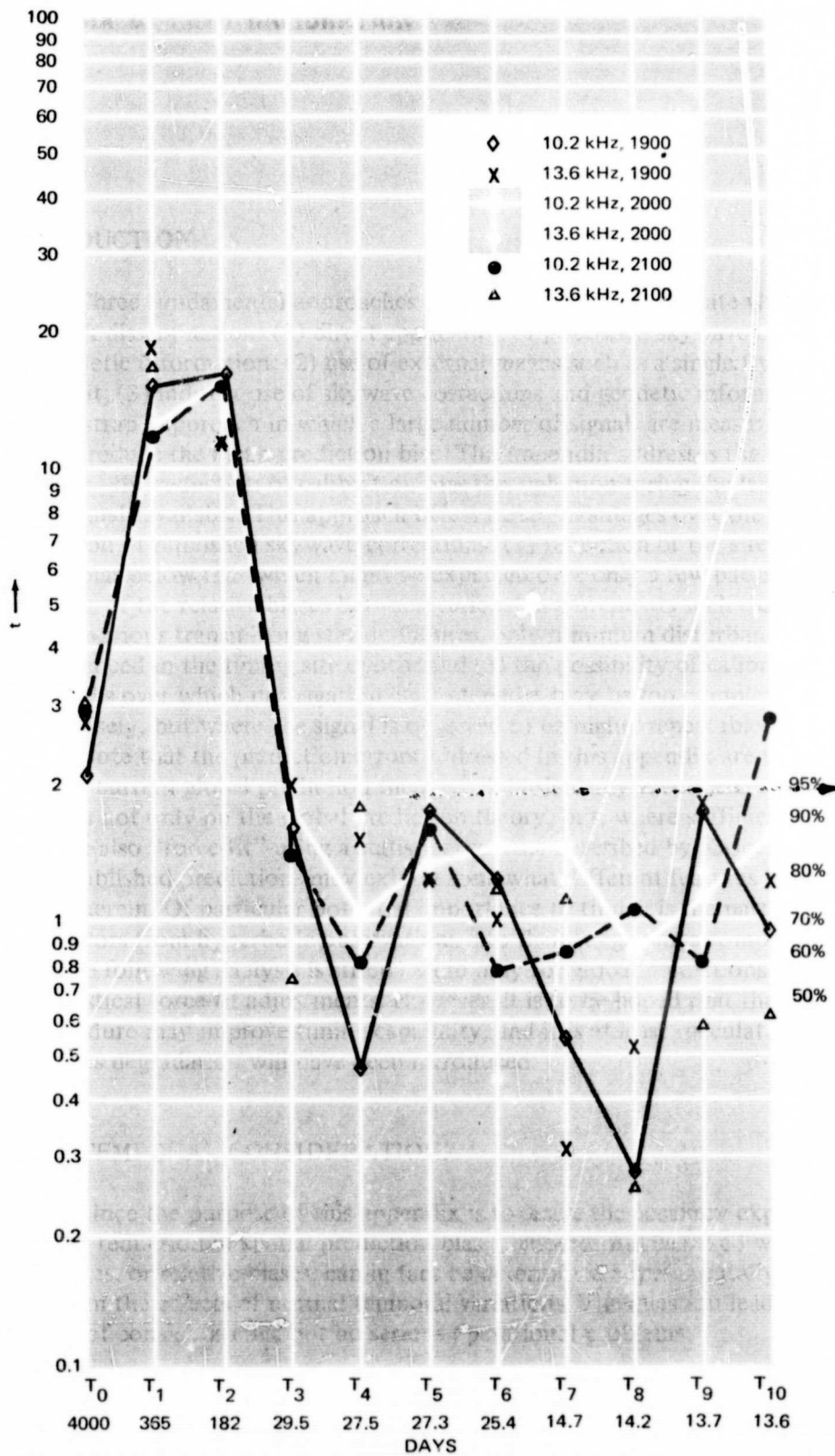


Figure E3. T statistics for periodic components in Hawaii-New York round trip under daytime conditions with $M \cos X$ effects removed.

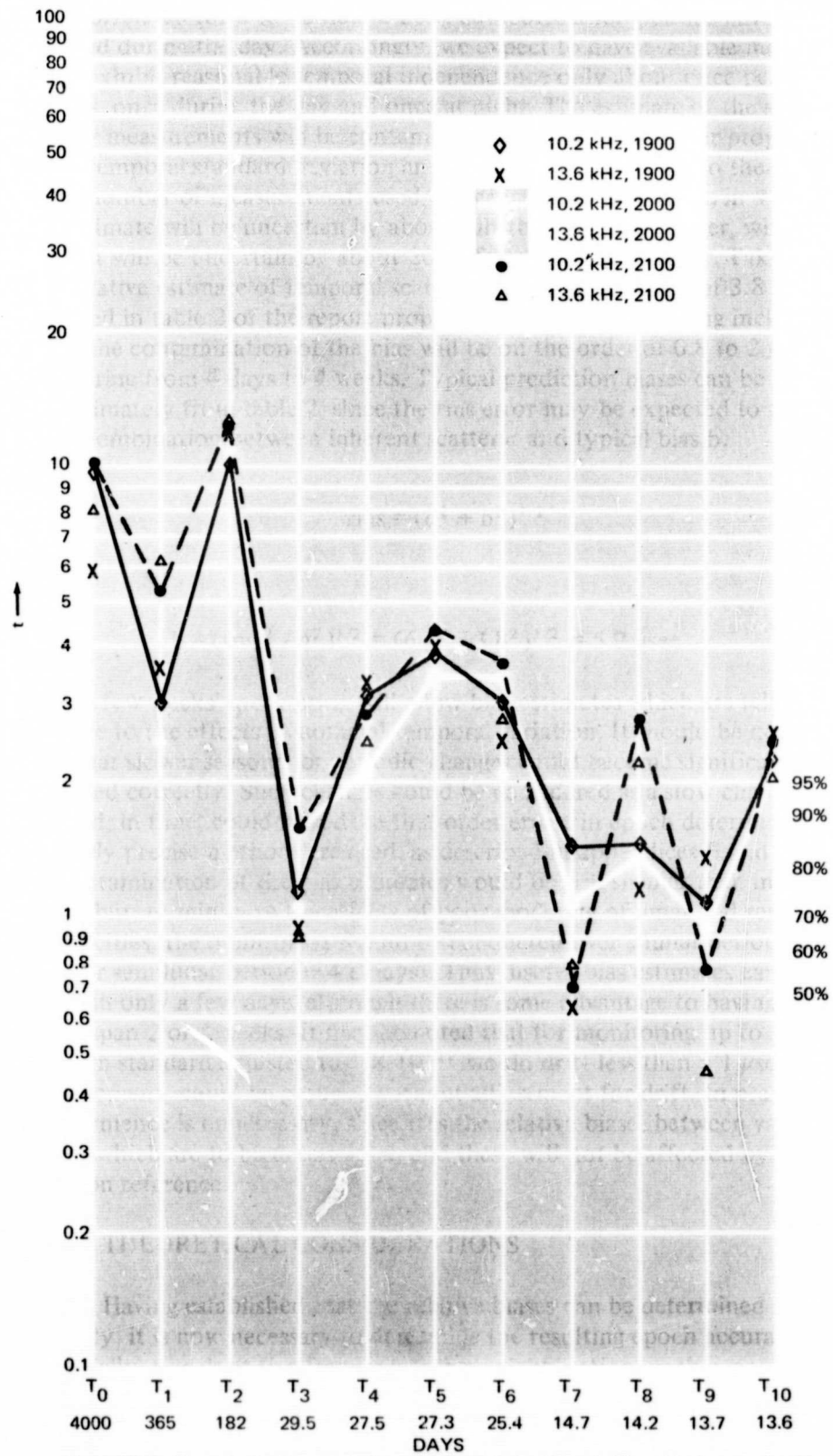


Figure E4. T statistics for periodic components in Hawaii-New York round trip under nighttime conditions.

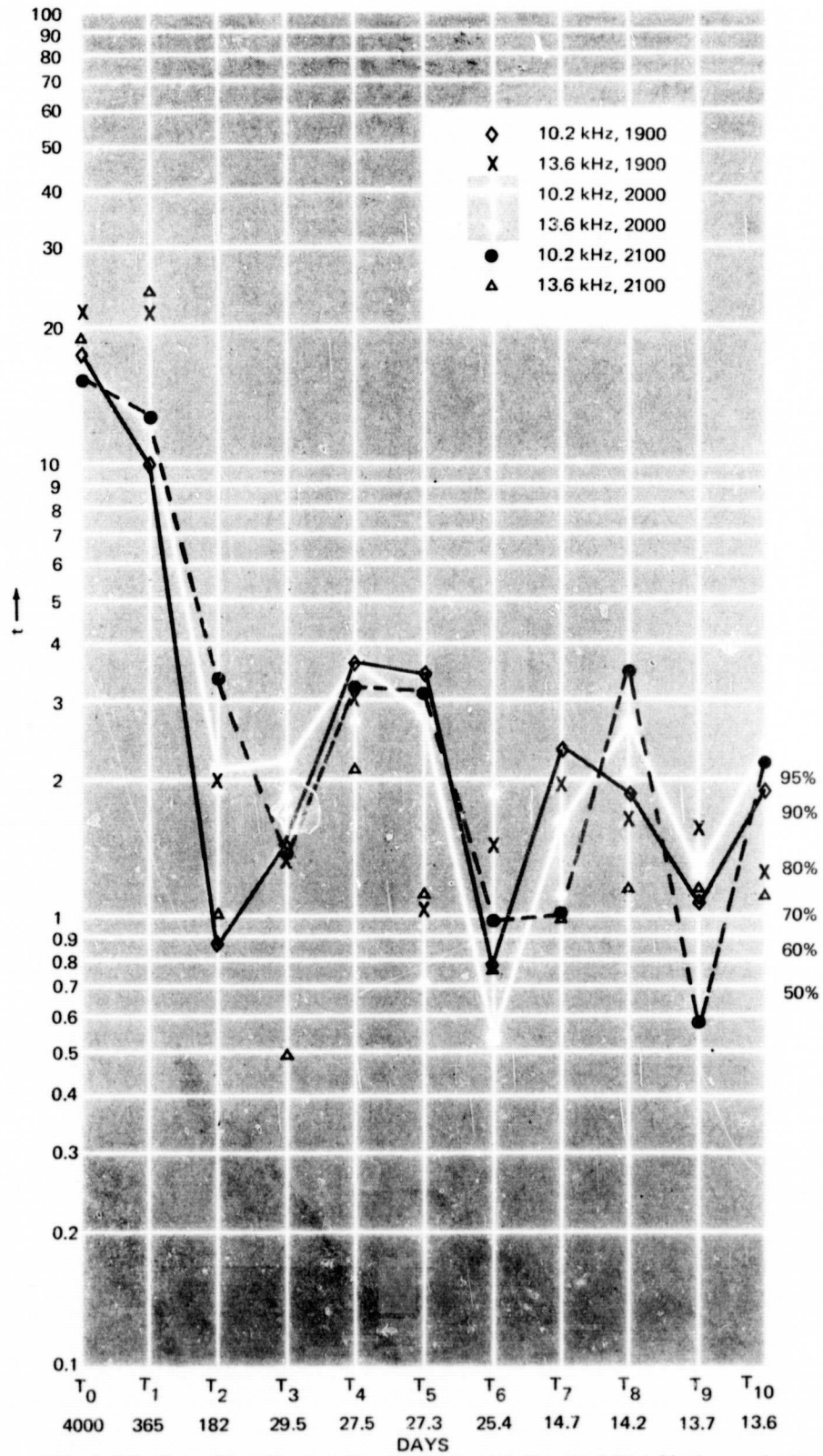


Figure E5. T statistics for periodic components in Trinidad-New York round trip under daytime conditions with $M \cos \chi$ effects removed.

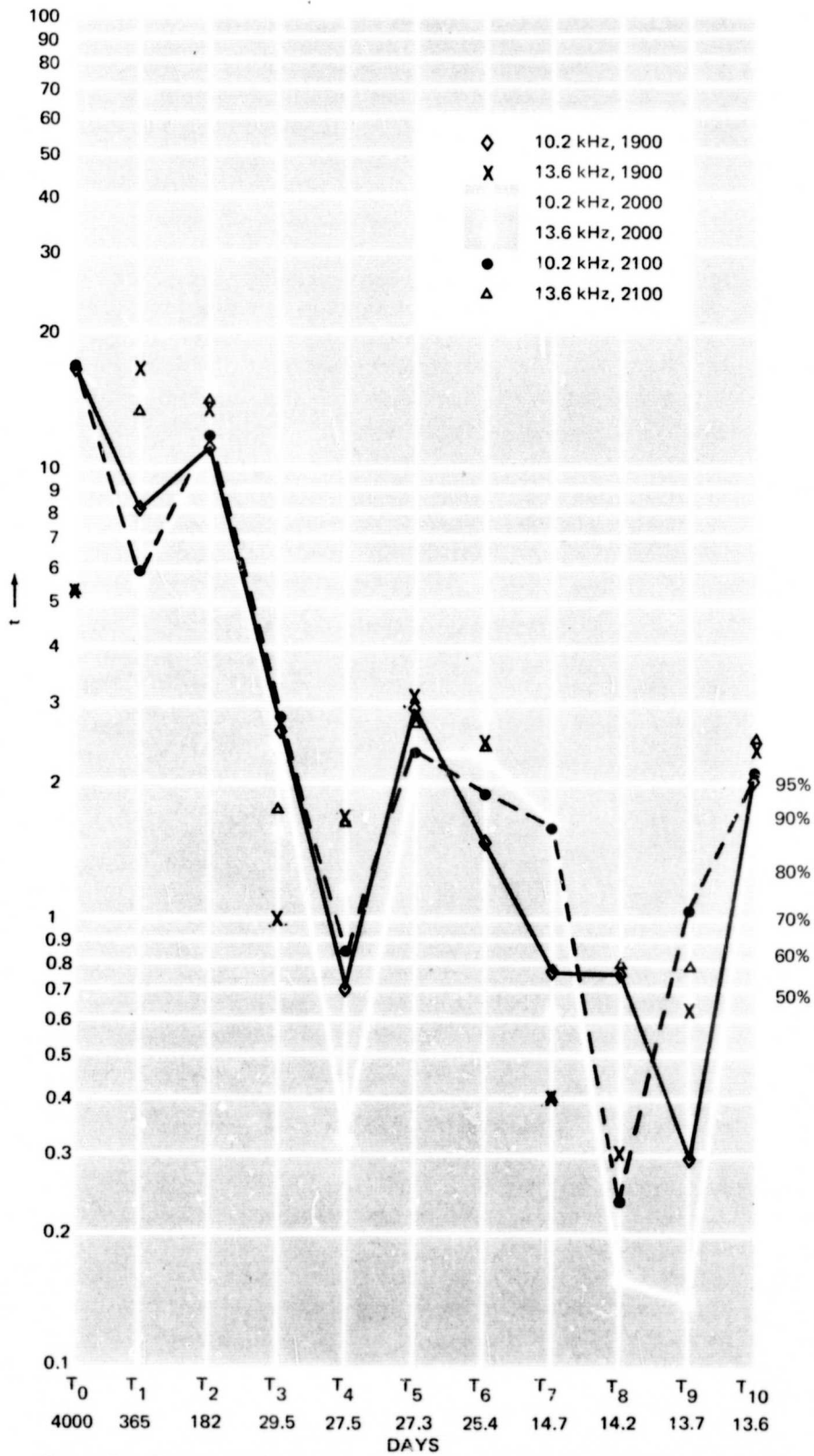


Figure E6. T statistics for periodic components in Trinidad-New York round trip under nighttime conditions.

CONCLUSIONS

A number of statistically significant periodicities were discovered in the Omega measurements studied. However, all have an amplitude of less than 3 cec. Principal periodicities were at the annual, semiannual, and solar cycle periods. Periodicities related to lunar tides all had amplitudes less than 0.8 μsec and, hence, are of little practical concern, although the components can, of course, add disadvantageously under certain circumstances.

A major effect of the periodicities for timing would be in the case of precise frequency determination based on processing phase comparison measurement with a precision standard over periods of a month or more. In principle, such comparisons have a capability to allow frequency comparison to better than one part in 10^{12} (table 3 of report proper). In practice, periodic phase changes will be occurring throughout the measurements. Considering only the semi-annual component of most importance, the effect on frequency determination to be expected from the presence of one component can be found from:

$$\delta f = \frac{d\phi}{dt} = \frac{d}{dt} \left\{ \bar{\phi} + R \cos \left(\frac{2\pi t}{T} + \theta \right) \right\}$$
$$\delta f = -\frac{2\pi R}{T} \sin \left(\frac{2\pi t}{T} + \theta \right)$$

Using a maximum amplitude obtained for 10.2-kHz propagation between Hawaii and New York during the day:

$$\delta f_{\max} = \frac{2\pi (2.8 \text{ cec})}{182 \text{ days}} = \frac{2\pi (2.8 \mu\text{sec})}{1.57 \times 10^{13} (\mu\text{sec})}$$
$$\delta f_{\max} = 1.12 \times 10^{-12}$$

The annual periodicity can also contribute to frequency error but only about half as much as indicated above. Thus, in the most precise applications, frequency accuracy would be limited to about one or two parts in 10^{12} in the case of the Hawaii-New York path, unless care were taken to remove the annual and semi-annual components left after skywave corrections had been used for primary correction. However, frequency biases introduced through periodic components were much less on the Trinidad-New York path and would not have introduced a serious inaccuracy compared with the ability of present frequency standards to maintain frequency.

Another consideration is the calibration of site epoch and propagation paths through transfer of a flying clock. The various periodicities all constitute temporal variations which will cause the path calibration to change from conditions existing at the time of the clock transfer. If the clock transfer were made at the worst possible time, it is possible that all periodic influences would be at peaks in the same sense. The possibility of such an error can, however, easily be

reduced by averaging the reference data base over a month's observations, thus causing the effects of all shorter periodicities to cancel. The annual and semiannual periodicities cannot readily be removed in this way. The maximum inaccuracy indicated was for Hawaii-New York at 10.2 kHz during the day. If calibration occurred when both annual and semiannual variations were at maximums in the same sense, then the average site epoch throughout the year would be in error by 5.3 μ sec, and a peak error of 10.6 μ sec would occur at opposite phasing. The actual phasing of the annual and semiannual periodicities is not, however, such that scalar addition occurs. In addition, the magnitudes are much less on the Trinidad-New York path.

REFERENCES

1. Naval Electronics Laboratory Center Technical Report 1806, *Seasonal Periodic Changes in the Phase of 10.2-kHz Signals*, by V. R. Noonkester, 22 November 1971
2. Naval Electronics Laboratory Center Technical Report 1781, *Diurnal Phase Variation at 10.2 kHz*, by E. R. Swanson and W. R. Bradford, 11 August 1971
3. Svennesson, J., Reder, F., and Crouchley, J., "Effects of X-ray Stars on VLF Signal Phase," *Journal of Atmospheric and Terrestrial Physics*, 34, p. 49-72, Pergamon Press, 1972

BIBLIOGRAPHY

- Brier, G. W., "Long-Range Prediction of the Zonal Westerlies and Some Problems in Data Analysis," *Reviews of Geophysics*, v. 6, no. 4, p. 525-551, November 1968
- Brady, A. H., and Crombie, D. D., "Studying the Lunar Tidal Variations in the D-Region of the Ionosphere by Means of Very-Low-Frequency Phase Observations," *Journal of Geophysical Research*, v. 69, no. 19, p. 5437-5442, October 1963
- Danby, J. M. A., *Fundamentals of Celestial Mechanics*, MacMillan, 1962
- Darwin, G. H., *The Tides and Kindred Phenomena in the Solar System*, W. H. Freeman and Co., 1962
- Doodson, A. T., "The Harmonic Development of the Tide-Generating Potential," *Proceedings of the Royal Society of London, Series A*, v. C, p. 305-329, 1922
- Goldman, S., *Frequency Analysis, Modulation and Noise*, McGraw-Hill, 1948
- Mitra, J. K., *The Upper Atmosphere*, 2nd ed., The Asiatic Society, Calcutta, India, Monograph Series, v. V, 1952
- Siebert, M., "Atmospheric Tides," *Advances in Geophysics*, v. 7, p. 105-187, 1961
- Nautical Almanac Office, *The American Ephemeris and Nautical Almanac*, U.S. Government Printing Office, Washington, D.C., 1968
- U.S. NAVOCEANO H. O. Publication 9, *American Practical Navigator*, by Nathaniel Bowditch, 1962
- Warburg, H. D., *Tides and Tidal Streams*, Cambridge University Press, 1922

APPENDIX F: EFFECTS OF TEMPORAL VARIATIONS AND DISTURBANCES ON PRECISE TIMING

INTRODUCTION

Previous sections and appendices have developed nominal timing capability based on typical results obtained over the 24-hour day and also for daytime hours, including disturbances such as Sudden Ionospheric Disturbances (SID's). Appendix E investigated periodicities contained in repeated vlf measurements. This appendix addresses the optimum performance to be expected from vlf timing if anomalous or periodic influences are removed.

DISTURBANCES

There are two principal types of random disturbances affecting vlf: Polar Cap Absorptions (PCA's) and SID's (also sometimes referred to as Sudden Phase Anomalies (SPA's)). PCA's do not affect signals propagating in the midtemperate latitudes and are principally important for signals propagating into or through the arctic. They may cause very large phase perturbations persisting for from several days to a week; they dominate the phase distribution function above the 95th percentile.¹ However, because of the extreme variations sometimes associated with PCA's, their limited geographic effects, and the fact that normal daily variation is the governing phenomenon 95% of the time, their influence on timing can simply be removed by disregarding perturbed observations. The probability of obtaining perturbed observations for several consecutive days is on the order of several percent for arctic paths, and some consideration of the effects of extended periods of degraded information should be given when using paths susceptible to PCA influences. Depending on solar activity, SID's may cause perturbations in the phase distribution function which exceed nominal scatter about 5% of the time at solar maximum and practically never near solar minimum. Since the effects typically persist for only about 1/2 hour, undisturbed measurements may be expected to be available at some time during most days. Since SID's do not affect propagation at night, night observations will always be undisturbed by them.

Using the disturbance flags with the data of appendix E, an analysis was conducted to determine the percentage of time which might be unusable for timing applications due to the existence of propagation disturbances. This study had two distinct aspects. The first concerned the relative merits of particular hours with regard to the probability of disturbance, while the second concerned the probability of finding at least one good hour in the 3-hour strings being studied. Table F1 summarizes the results of this analysis.

¹Naval Electronics Laboratory Center TR 1835, *Omega Phase Variations during PCA Events*, by J. N. Martin, 17 August 1972.

TABLE F1. MINIMUM AVAILABILITY OF UNDISTURBED SIGNALS.

f →		10.2 kHz					13.6 kHz				
		N	N _F	% _F	% _{1,2}	% _{1,2,3}	N	N _F	% _F	% _{1,2}	% _{1,2,3}
Hawaii↔New York Day	1900Z	1546	424	72.6	—	—	1562	440	71.8	—	—
	2000Z	1556	444	71.5	80.7	—	1558	443	71.6	80.1	—
	2100Z	1542	458	70.4	—	86.9	1548	461	70.2	—	86.8
Trinidad↔New York Day	1600Z	1617	318	80.3	—	—	1589	301	80.1	—	—
	1700Z	1604	327	80.6	89.7	—	1583	312	80.3	89.9	—
	1800Z	1611	343	78.8	—	95.8	1601	327	79.6	—	95.8
HA↔NY Night	0700Z	1639	134	91.8	—	—	1651	135	91.8	—	—
	0800Z	1641	126	92.3	93.6	—	1653	129	92.2	93.8	—
	0900Z	1648	126	92.4	—	94.3	1664	132	92.1	—	94.1
TD↔NY Night	0400Z	1694	86	94.9	—	—	1687	85	95.0	—	—
	0500Z	1691	69	95.9	98.5	—	1683	69	95.9	98.3	—
	0600Z	1692	48	97.2	—	100	1678	48	97.1	—	100

N = sample size

N_F = number of disturbed days

%_F = percentage of undisturbed days at each hour

%_{1,2} = percentage of undisturbed days at the second hour when the first is disturbed

%_{1,2,3} = percentage of undisturbed days at the third hour when the first two are disturbed

The comparable results at 10.2 and 13.6 kHz are not surprising, since the data flags normally are made to agree on all frequencies for standard processing purposes. Although one would expect the same number of disturbed days for all daylight hours, the significantly different values between the Trinidad-Hawaii paths indicate that the SID reporting procedures have led to more flags at the later daylight hours. This, too, is not surprising when the geographic location of the reporting monitor sites is considered. The large number of flags at night is due mainly to PCA's, which were included as a safeguard in the standard processing procedure but which would not have very significant effects on the present analysis. A most encouraging result is that over the 5-year string studied (a period of very high solar activity), there is a 100% chance of finding an undisturbed time during the night on the Trinidad-New York path. Because of the flagging procedure, the other probabilities will all be somewhat pessimistic. In particular, the 1600Z TD↔NY measurements were noted as disturbed almost 20% of the time, while the magnitude of the disturbance will exceed nominal scatter less than 5% of the time. Hence, a number of very small SID's have been flagged. Although the results shown in table F1 need to be further derated by station outages, it is clear that undisturbed information is available almost every day over the Trinidad-New York path.

PERIODIC VARIATIONS

The optimum timing capability after the influences of periodic variations and disturbances are removed can be determined for the data of appendix E through a reduction of variance analysis based on the computed variance for each data string and the contributed variance from the independent periodicities deduced. This was done for the various data strings under the following conditions:

1. Raw Data (unflagged for disturbances and unfiltered for $M \cos X$ or tidal effects)
2. Flagged data (flagged for recognized propagation disturbances but unfiltered for $M \cos X$ or tidal effects)
3. Flagged and partially filtered data (same as (b) except with $M \cos X$ effects removed)
4. Flagged and 'totally' filtered data (same as (c) except with tidal effects removed)

The analysis procedure consisted of computing the variance of the raw data, the variance with disturbed data removed, the variance with $M \cos X$ removed, and the explained variance due to tidal periodicities for the latter two cases. Table F2 lists the relevant results.

TABLE F2. REDUCTION OF VARIANCE (cec^2).

f →		10.2 kHz			13.6 kHz		
		Raw Data	Flagged Data	M cos X Filtered Data	Raw Data	Flagged Data	M cos X Filtered Data
HA ↔ NY Day (1900Z)	V	59.4	49.6	19.0	39.2	30.5	15.6
	EV	--	40.4	7.2	--	22.7	5.7
	V _R	--	9.2	11.8	--	7.8	9.9
TR ↔ NY Day (1600Z)	V	9.2	6.3	2.8	4.7	3.0	3.1
	EV	--	3.8	0.8	--	2.1	1.7
	V _R	--	2.5	2.0	--	0.9	1.4
HA ↔ NY Night (0800Z)	V	29.2	23.3	--	28.3	23.7	--
	EV	--	4.1	--	--	3.1	--
	V _R	--	19.2	--	--	20.6	--
TR ↔ NY Night (0400Z)	V	13.7	13.5	--	15.8	15.6	--
	EV	--	3.8	--	--	4.4	--
	V _R	--	9.7	--	--	11.2	--
Med. V _R (cec^2)			9.5	6.4		9.5	5.7
Med. σ_R (cec)			3.1	2.5		3.1	2.4
Med. σ_R (μsec)			3.1	2.5		2.3	1.8
Med. σ_R (μsec) over all paths						2.4	

The raw data were not analyzed for tidal periodicities, so no reduced variance is tabulated in those columns. Also, no $M \cos X$ correction is applied at night, so those columns also are unused.

For the raw data, especially on Hawaii to New York day, the indicated value of V is probably too conservative due to the inability of the analysis program to properly handle disturbances of greater than 50 cec. As such disturbances normally would be easily detected by a timing site, the indicated value probably is not too far from a practical value. As has been noted elsewhere, stabilities are greater at 13.6 kHz in the daytime and at 10.2 kHz at night. In all cases, elimination of disturbed data has reduced the observed variance. The significantly larger values of EV for the flagged data relative to the $M \cos X$ filtered data are due to the fact that the annual period of 365 days is one of the tidal periodicities being looked for and is the main constituent of the $M \cos X$ variation which has not yet been removed from the flagged data. In all cases, the total EV produced by the tidal periodicities has been tabulated.

Several gross features are apparent in table F2:

1. The quality of the information varies significantly between the various paths and diurnal periods. The worst filtered information exhibits a scatter of $(19.2 \text{ cec}^2)^{1/2}$ at 10.2 kHz ($\sigma \sim 4.3 \mu\text{sec}$), while the best information has a scatter of only $(1.4 \text{ cec}^2)^{1/2}$ at 13.6 kHz ($\sigma \sim 0.9 \mu\text{sec}$).
2. The principal variance reduction usually occurs in removing the expected solar zenith angle variation equivalent to practical application of published skywave corrections. The reduction in variance from this source is usually more significant than removal of perturbed information.
3. A typical timing capability of $2.4 \mu\text{sec}$ is obtained after removal of disturbances and periodicities. (This may be compared with the results indicated in table 2 of the report proper.) Although not shown in the table, it was apparent from the residuals that phase stability is markedly better in summer than in winter.

OPTIMUM SYNTHESIS

For precise timing, we wish to combine all available information from various paths, diurnal periods, and frequencies in an optimum manner. From table F2, however, it is clear that the 13.6-kHz daytime information between Trinidad and New York is markedly superior to any other available information except possibly the corresponding 10.2-kHz information. The superiority of this information may be due to frequency, path length, received signal-to-noise ratio, or other factors. While it is normally true that 13.6 kHz has higher temporal stability than 10.2 kHz and also true that undisturbed daytime measurements tend to be more repeatable than night readings, the precise cause for the high stability in this case cannot be determined unambiguously. It may, however, be indicative that in typical operation one path may exhibit obviously better stability than others. If the superiority is as significant as indicated in table F2,

there is little advantage in performing an optimum combination. In essence, the quality of the optimum combination will be derived primarily from the 13.6-kHz Trinidad-New York day results and will be insignificantly better than those results. Accordingly, an optimum weighting for table F2 will essentially place unity weighting on the best information regardless of how the various phase fluctuations may correlate.

One area of improvement to consider is the synthesis of measurements from the several hours generally available for any particular frequency, path, and diurnal period, since table F2 shows only typical results. The gain to be obtained by averaging will depend on the autocorrelation of the fluctuations over a period of several hours. The improvement possible by averaging several hours can be estimated by forming the average and comparing with one of the component hours or by comparing the difference in phase between subsequent hours. For the variance in the difference in phase between measurements taken on subsequent hours, we have:

$$\text{Var} (x - y) = \text{Var} x + \text{Var} y - 2\rho \sqrt{\text{Var} x \text{Var} y} \quad (\text{F1})$$

where x is the measurement at the first hour and y is the measurement at the second hour. Since $\text{Var} x \approx \text{Var} y$, equation (F1) takes the simplified form:

$$\text{Var} (x - y)/\text{Var} x = 2(1 - \rho) \quad (\text{F2})$$

so that the correlation between subsequent hours may be deduced by computing the fractional reduction in variance, $\text{Var} (x - y)/\text{Var} x$. Since $\text{Var} x$ is known, and since periodic influences affect adjacent hours similarly, ρ is readily obtained by simply computing $\text{Var} (x - y)$, which may be done without removing periodicities. Such computations were performed for each subsequent hour pair for each frequency, path, and diurnal period. All 16 autocorrelation coefficients so determined are narrowly grouped between 0.85 and 0.93. Correlations of this magnitude indicate that information available from each of the three hours sampled within each grouping is essentially redundant, and no useful advantage will result from averaging.

The optimum combination of information for the case studied is thus well approximated by using the daytime measurements at a particular hour on the Trinidad path at 13.6 kHz or averaging the 13.6-kHz measurements with corresponding 10.2-kHz measurements. In either case, the temporal stability will be less than 1 μ sec after disturbances and periodicities are removed. These results will be generally applicable whenever one path exhibits substantially better than nominal stability; once the path is calibrated following the techniques of appendix D, nearly complete reliance may be placed on it.